ANALYTICA CHIMICA ACTA

International journal devoted to all branches of analytical chemistry

Scope. *Analytica Chimica Acta* publishes original papers, short communications, and reviews dealing with every aspect of modern chemical analysis, both fundamental and applied. The section on *Computer Techniques and Optimization* is devoted to new developments in chemical analysis by the application of computer techniques and by interdisciplinary approaches, including statistics, systems theory and operation research. The section deals with the following topics: Computerized acquisition, processing and evaluation of data. Computerized methods for the interpretation of analytical data including chemometrics, cluster analysis, and pattern recognition. Storage and retrieval systems. Optimization procedures and their application. Automated analysis for industrial processes and quality control. Organizational problems.

Submission of Papers. Manuscripts (three copies) should be submitted to:
for *Analytica Chimica Acta:* Dr. A. M. G. Macdonald, Department of Chemistry, The University, P.O. Box 363, Birmingham B15 2TT, England;
for the section on *Computer Techniques and Optimization:* Dr. J. T. Clerc, Universität Bern, Pharmazeutisches Institut, Sahlistrasse 10, CH-3012 Bern, Switzerland.

Information for Authors. Papers in English, French and German are published. There are no page charges. Manuscripts should conform in layout and style to the papers published in this Volume. Authors should consult Vol. 102, p. 253 for detailed information. Reprints of this information are available from the Editors or from: Elsevier Editorial Services Ltd., Mayfield House, 256 Banbury Road, Oxford OX2 7DE (Great Britain).

Reprints. Fifty reprints will be supplied free of charge. Additional reprints (minimum 100) can be ordered. An order form containing price quotations will be sent to the authors together with the proofs of their article.

Advertisements. Advertisement rates are available from the publisher.
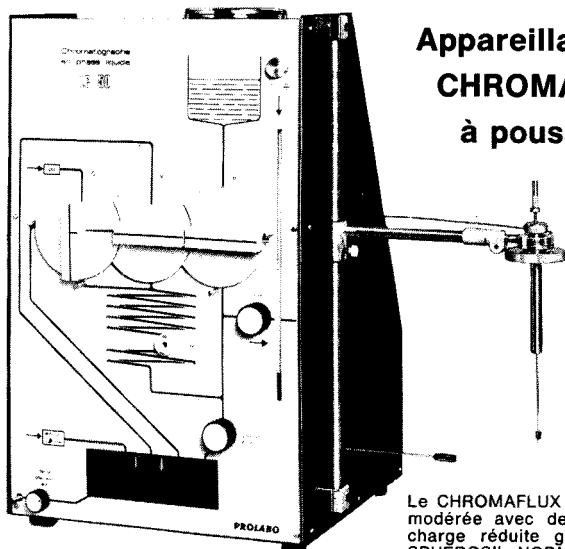
Subscriptions. Subscriptions should be sent to: Elsevier Scientific Publishing Company, P.O. Box 211, 1000 AE Amsterdam, The Netherlands. The section on *Computer Techniques and Optimization* can be subscribed to separately.

Publication. *Analytica Chimica Acta* (including the section on *Computer Techniques and Optimization*) appears in 9 volumes in 1979. The subscription for 1979 (Vols. 104—112) is Dfl. 1179.00 plus Dfl. 135.00 (postage) (Total approx. U.S. $641.00). The subscription for the *Computer Techniques and Optimization* section only (Vol. 112) is Dfl. 131.00 plus Dfl. 15.00 (postage) (Total approx. U.S. $71.20). Journals are sent automatically by air mail to the U.S.A. and Canada at no extra cost and to Japan, Australia and New Zealand for a small additional postal charge. All earlier volumes (Vols. 1—95) except Vols. 23 and 28 are available at Dfl. 144.00 (U.S. $70.20), plus Dfl. 10.00 (U.S. $4.90) postage and handling, per volume.

Claims for issues not received should be made within three months of publication of the issue, otherwise they cannot be honoured free of charge.

Customers in the U.S.A. and Canada who wish to obtain additional bibliographic information on this and other Elsevier journals should contact Elsevier/North Holland Inc., Journal Information Center, 52, Vanderbilt Avenue, New York, NY 10017. Tel: (212) 867-9040.

Inorganic Chemistry in Liquid Ammonia

DAVID NICHOLLS
Donnan Laboratories, University of Liverpool, U.K.

Topics in Inorganic and General Chemistry, Monograph 17

Although numerous review articles have been published, no book on inorgan chemistry in liquid ammonia has appeared in the English language since Franklir classic in 1935. This work, providing a comprehensive treatment of inorgan reactions in liquid ammonia, is intended to fill this gap.

The book consist of eight chapters. It discusses the physical properties of liqu ammonia, practical techniques for the use of liquid ammonia, and the reactio of inorganic substances with liquid ammonia. The reactions of inorganic compoun with liquid ammonia are classified according to reaction type. Separare chapters a devoted to acid-base and oxidation-reduction reactions, reactions of alkali met solutions, and reactions involving metathesis or substitution.

This work will serve not only as a reference book on inorganic reactions i liquid ammonia, but also as a sourcebook for research problems in inorgan chemistry and a practical guide to the use of liquid ammonia. The book will l particularly valuable to researchers in inorganic chemistry. It will also be usef to lecturers teaching senior level undergraduate courses on non-aqueous solvent

Chapter Headings: 1. Introduction to liquid ammonia chemistry. 2. Physical properties of liqu ammonia. 3. Practical techniques in liquid ammonia. 4. Reactions of elements and compounds wit ammonia. 5. Acid-base reactions. 6. Oxidation-reduction reactions. 7. Reactions of alkali metal solution 8. Synthetic reactions involving metathesis or substitution.

Feb. 1979   x + 240 pages   US $49.00/Dfl. 110.00   ISBN 0-444-41774-5

5 Years
f Chromatography
Historical Dialogue

5. ETTRE *and* A. ZLATKIS (Editors).

Irnal of Chromatography Library - Volume 17

the occasion of the 75th anniversary of the invention of chromatography, this book compiles
)ersonal stories of 59 pioneers of the various chromatographic techniques (including five Nobel Prize

laureates). In their contributions to
this volume, these pioneers review
the events which influenced them to
enter the field; explain the back-
ground of their inventions; sum-
marize their activities and results
during their professional lives; and
discuss their interactions with other
scientists and other disciplines.
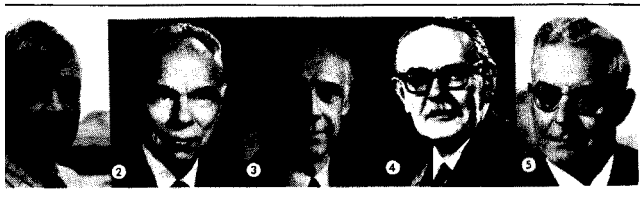
book is more than a nostalgic recollection of the past for those who have been in chro-
)graphy for some time. It also provides, for the younger generation of chromatographers,
ique record of how present-day knowledge was accumulated.
final chapter is devoted to "Those who are no longer with us"

itributors:

Adlard	E. C. Horning	S. R. Lipsky	C. D. Scott
oer	M. G. Horning	J. E. Lovelock	R. P. W. Scott
remer	C. Horváth	* A. J. P. Martin ④	* G. T. Seaborg ②
l. Desty	J. F. K. Huber	* S. Moore ③	M. S. Shraiber
lijkstra	A. T. James	H. W. Patton	L. R. Snyder
Ettre	J. Janák	C. S. G. Phillips	E. Stahl
odin	R. E. Kaiser	J. Porath	* W. H. Stein ⑤
/. Gehrke	A. Karmen	V. Pretorius	H. H. Strain
Giddings	J. G. Kirchner	G. R. Primavesi	F. H. Stross
lueckauf	J. J. Kirkland	N. H. Ray	* R. L. M. Synge ①
. E. Golay	A. V. Kiselev	L. Rohrschneider	R. Teranishi
V. Grant	E. sz. Kováts	K. I. Sakodynskii	J. J. van Deemter
eftmann	E. Lederer	G. Schomburg	A. A. Zhukhovitskii
lesse	M. Lederer	G.-M. Schwab	A. Zlatkis
l. Higgins	A. Liberti	R. D. Schwartz	

)bel Prize laureates)

. 1979   526 pages   *US $49.75/Dfl. 112.00*   *ISBN 0-444-41754-0*   *LC 78-23917*

Review

ANALYTICAL ATOMIC SPECTROSCOPY AT THE CSIRO DIVISION OF CHEMICAL PHYSICS*

J. B. WILLIS

CSIRO Division of Chemical Physics, P.O. Box 160, Clayton, Victoria, 3168 (Australia)

(Received 31st October 1978)

SUMMARY

An account is given of work of interest to analytical chemists carried out in the Spectroscopy Section of the CSIRO Division of Chemical Physics over the past 24 years.

The Commonwealth Scientific and Industrial Research Organization (CSIRO) is a statutory body, established by the Australian Government's Science and Industry Research Act of 1949, and replacing the former Council for Scientific and Industrial Research (CSIR), which was established in 1926. Its principal function is to carry out scientific research in connection with Australian primary and secondary industries and with other matters of national importance. The CSIRO has traditionally interpreted this mandate to mean that research should be carried out at a fundamental level rather than merely on an ad hoc basis. The Chemical Physics Section, which became a Division in 1958, was formed in 1944 as part of the CSIR Division of Industrial Chemistry. It was set up, under the leadership of Dr. A. L. G. Rees, primarily to introduce into Australia a number of major chemico-physical methods which were undergoing rapid development elsewhere at that time. Research in chemical physics is regarded as being the investigation of chemical problems by the methods of modern physics. both theoretical and experimental.

The Spectroscopy Section, led from 1946 by Mr. (now Sir) Alan Walsh, carried out work in the 1940's and 50's on molecular spectroscopy, the interest being in molecular structure and energetics rather than in analytical applications. Walsh himself, who had a background in the spectrochemical analysis of metals from his work at the British Non-Ferrous Metals Research Association during the Second World War, also undertook fundamental studies of emission methods of spectrochemical analysis.

Early in 1952 he realised that atomic absorption spectra appeared to offer many important advantages over atomic emission spectra for spectrochemical

---

*Dedicated to Sir Alan Walsh, F.A.A., F.R.S., Leader, Spectroscopy Section, CSIRO Division of Chemical Physics, 1946—1977.

analysis. He set up simple equipment to demonstrate that, when a sodium vapour-discharge lamp was used with an air—coal gas flame into which a solution of sodium salt was sprayed, it was possible to measure absorption of the sodium resonance lines by sodium atoms in the flame despite the fact that the atomic vapour was also emitting at precisely the same wavelengths.

In an invited lecture at the 1974 Pittsburgh Conference on Analytical Chemistry, Walsh described the reasoning that led him to consider the value of using atomic absorption measurements in chemical analysis, and described how his early experiments led him to develop sealed-off hollow-cathode lamps as intense sharp-line sources that could be used in an instrument to determine a wide range of metals. He then told of the difficulties he encountered in trying to interest analytical chemists in using the technique and instrument manufacturers in making suitable equipment commercially available. This lecture has been published in full [1] and the present review will be restricted to describing subsequent work of analytical interest by the Spectroscopy Section in the field of atomic absorption and related spectroscopic techniques.

EARLY INSTRUMENTATION

Walsh published his basic paper [2] on the principles and potentialities of atomic absorption methods of analysis in 1955. This paper did not deal explicitly with the construction of atomic absorption equipment, though it envisaged the use of both vacuum furnaces and flames as possible means of vaporizing the sample.

The first description of an atomic absorption spectrometer was given by Shelton and Walsh in 1956 at the XVth IUPAC Conference in Lisbon [3, 4] This instrument — shown schematically in Fig. 1(A) — was basically one that had been exhibited in Melbourne in 1954, and used the monochromator from a Beckman model DU u.v.-visible spectrophotometer and a Meker-type air—coal gas flame to atomize the sample solution. The light from a sealed-off hollow-cathode lamp [4] was split into two beams, one beam being chopped at twice the frequency of the other and 90° out of phase with it. Double-beam operation was used because when the work began hollow-cathode lamps were thought to be insufficiently stable to permit their use in a single-beam instrument. By 1957, however, hollow-cathode lamps had been greatly improved, and since then almost all the work on flame atomic absorption spectroscopy has been done with the very much simpler single-beam techniques.

The first single-beam instrument described [5] used hollow-cathode lamps which were electronically modulated at 50 or 100 Hz [6] and the signal from the photomultiplier was fed to a broad-band a.c. amplifier. The sample solution was vaporized in the nebulizer—spray chamber system of an E.E.L. flame photometer and provision was made for either an air—coal gas or air—acetylene burner 2.5—10 cm in length. This instrument is shown diagrammatically in Fig. 1(B).

Gatehouse and Willis [7] replaced the burner of the Box and Walsh instrument [5] by a massive stainless-steel slot burner 10 cm in length, thereby
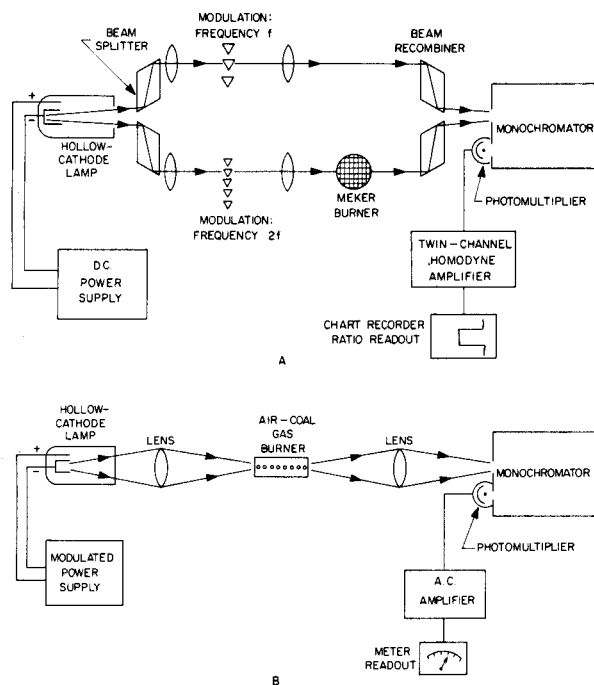
Fig. 1. Schematic diagrams of (A) the original atomic absorption instrument described by Russell, Shelton and Walsh [3, 4] and (B) the instrument described by Box and Walsh [5].

increasing the sensitivity and enabling both air—coal gas and air—acetylene mixtures to be used with greater flame stability and safety. This instrument, with only minor improvements, was used for all the flame atomic absorption work of the Section until about 1965 and formed the basis for the design of the commercially-made Techtron instruments AA-1, AA-2 and AA-3. Gatehouse and Willis measured the characteristic concentrations* for 36 metals using air—coal gas or air—acetylene flames, and it is interesting to note that there has been relatively little improvement in characteristic concentrations since this paper was published. Table 1 shows characteristic concentrations for several metals using instruments of increasing sophistication that have been developed since that time.

Analysis of biological materials by flame atomic absorption

The first published application of atomic absorption spectrometry to a real analytical problem — the determination of magnesium in plant materials and

_____

*Gatehouse and Willis quoted "limits of detection" for different metals on the assumption that the smallest detectable absorption was 1%, which corresponded to the maximum noise level of their instrument. Later [8] the concentration of metal in solution giving an absorption of 1% was referred to as "sensitivity", but the IUPAC-approved term is now "characteristic concentration" [9].

TABLE 1

Typical characteristic concentration values (μg ml^{-1}) found with different atomic absorption instruments, using a 10 cm air—acetylene flame

Metal	Wavelength, (nm)	1961 Gatehouse and Willis [7]	1968 Perkin-Elmer 303 [8]	1977 Varian-Techtron AA375 (manufacturer's literature)
Co	240.73	0.2	0.10	0.06
Cr	357.87	0.15	0.15	0.06
Cu	324.75	0.1	0.1	0.04
Fe	248.33	0.1	0.15	0.05
Pb	283.31	0.5	0.5	0.3[a]
Zn	213.86	0.03	0.04	0.009

[a]Approximate figure calculated from the figure of 0.13 μg ml^{-1} quoted for the 217.00-nm line.

soil extracts — was carried out by Allan in New Zealand [10]. It was followed closely by the determination of zinc in agricultural materials by David [11], at the CSIRO Division of Plant Industry in Canberra, Australia. Despite the success of these two workers in carrying out analyses of great importance in the field of agricultural chemistry, there was still little general interest at this time in the atomic absorption technique. Walsh realized that the usefulness of the new technqiue would have to be demonstrated by developing detailed methods of practical analysis in as many different fields of application as possible.

In April 1958 the author began to study the determination by atomic absorption of calcium and magnesium in blood serum. At that time the determination of calcium was tedious, inaccurate, and required relatively large amounts of serum, while the determination of magnesium was so difficult that it was scarcely ever attempted. Use of the air—acetylene rather than the air—coal gas flame, and the development of methods of overcoming chemical interferences from protein and phosphorus, proved necessary in the development of suitable procedures. For best results, removal of the protein by precipitation was recommended for measuring calcium [12], while for magnesium the only preparatory treatment necessary was the addition of strontium chlorid or EDTA solution [13]. For the first time, rapid and accurate determinations of magnesium on samples of blood serum as small as 0.05 ml became possible. The determination by atomic absorption of magnesium in solutions of ashed muscle tissue made possible a collaborative study of the effect of lipids on the composition of skeletal and cardiac muscle [14].

In the late 1950's, the determination of sodium and potassium in serum was being carried out satisfactorily with the emission flame photometer, but it proved possible to obtain equally good results by atomic absorption [15]. Thus it became possible to determine the four important blood electrolytes, sodium, potassium, calcium and magnesium with one simple instrument.

The analysis of urine is complicated by the presence of varying and sometimes very large concentrations of phosphorus and minerals, particularly sodium, potassium and calcium. The techniques developed for overcoming phosphorus interference on calcium absorption in the analysis of blood serum were successfully extended to the analysis of urine and led to the development of very simple methods for the determination of calcium and magnesium [16].

Knowledge of the concentration of heavy metals, particularly lead, cadmium and mercury, in urine is of great importance in industrial hygiene and in monitoring the progress of chelation therapy in the treatment of heavy metal poisoning. The concentration of heavy metals in the urine of unexposed persons is very low ($\approx 0.02\ \mu$g Pb ml^{-1}), and even in cases of lead poisoning the level may be only a few times greater than this. Thus, it is generally not practicable to measure the absorption of urine sprayed directly into the flame, and some form of concentration is required. Extraction with ammonium pyrrolidine carbodithioate into an immiscible solvent such as 2-heptanone, followed by the spraying of this extract into the flame, was found satisfactory for the determination of several heavy metals in urine [17]. The sensitivity of the atomic absorption technique was sufficiently good to allow the determination of zinc and cadmium, usually by spraying the urine directly into the flame. It was noted, however, that background absorption or scattering by the high concentration of sodium chloride, if not corrected, could cause errors.

The application of atomic absorption methods to the analysis of biological materials was reviewed in 1963 [18].

Analysis of miscellaneous materials by flame atomic absorption

As the usefulness of the atomic absorption technique became more widely realised, the Section was involved in a number of collaborative investigations of analyses of importance to various industries.

The determination of traces of copper in butter and butterfat is important because of the accelerating effect of this metal, even at the 0.1-ppm level, on the development of off-flavours during storage. The high concentration of fat makes the ashing of butter products very difficult, but by shaking the butter with light petroleum and nitric acid it was possible to concentrate the fat into the organic phase and copper into the aqueous phase. The latter was then sprayed into the flame and measured by using the analyte addition technique, a considerable correction being required for background absorption by sodium chloride [19].

In the electroplating industry, contamination of metal-plating solutions by traces of other metals can have adverse effects on the quality of the plating. Flame atomic absorption proved to be a very useful method both for determining traces of zinc, copper and nickel in acid and cyanide plating solutions of various metals, and also for checking the concentration of the major metals in these solutions [20].

The determinations of trace metals in used lubricating oil is important in the monitoring of the wear on various components of internal combustion

engines. Simple methods of determining traces (0—100 ppm) of copper, chromium, iron, lead and silver in the oil from diesel engines were developed [21]; the oil was simply diluted with 2-methyl-4-pentanone and sprayed into the air—acetylene flame. Absorption was measured relative to that produced by reference solutions of organometallic compounds in 2-methyl-4-pentanone containing the appropriate concentration of unused oil.

THE DEVELOPMENT OF HIGH-TEMPERATURE FLAMES

Very early in the development of atomic absorption spectroscopy as an analytical technique it was realized that the low-temperature flames then used to vaporize solutions were unsatisfactory for many metals. Thus, in 1957 [4]: "At the present state of its development, by far the most serious difficulty in the atomic absorption method is due to the difficulty in atomizing various elements. For example, highly oxidizable elements such as aluminium, silicon, hafnium, etc. are not atomized in the air—coal gas flame used in this work and are thus not detectable in absorption. Similarly, many other elements will not be completely atomized, thus decreasing the sensitivity and providing a serious obstacle to accurate absolute analysis".

The introduction of the premixed air—acetylene flame around 1957—58 improved the atomization efficiency for a number of important metals, such as calcium and magnesium, but the problem described above still persisted. It seemed necessary to develop a flame having a higher temperature than air—acetylene and providing a suitable environment in which refractory oxides could be reduced to the metal.

Some success was achieved by other workers [22—24] who used direct-injection burners to aspirate solutions in organic solvents into oxygen—hydrogen or oxygen—acetylene flames. However, direct-injection burners are unpleasantly noisy in operation and give tall narrow flames that are difficult to use in atomic absorption work. It was clearly desirable to develop premixed flames having reasonably long light paths based on burners that could be fitted directly to the spray chamber of a simple atomic absorption instrument.

Different lines of attack on this problem were pursued independently by the two groups in different parts of Australia. Amos and Thomas [25], working at the Sulphide Corporation near Newcastle, N.S.W., developed an oxygen-enriched air—acetylene flame, while Willis [26], in Melbourne, developed the nitrous oxide—acetylene flame . Since the two flames had several-features in common, a detailed paper on these flames [27] was written jointly. The nitrous oxide—acetylene flame proved the safer and more convenient of the two, and is now used everywhere for atomic absorption measurements on metals forming refractory oxides. It is also valuable for obtaining better sensitivity and reduced chemical interference for metals, such as calcium and molybdenum, that are only partially atomized in the air—acetylene flame.

Some typical analytical applications of the nitrous oxide—acetylene flame, including the determination of strontium and barium in rocks, vanadium in

fuel oil, aluminium, silicon and titanium in bauxite, and titanium in steel were then described [28]. For a number of metals, notably hafnium, zirconium, tantalum and titanium, the absorption found in high-temperature flames was greatly increased by the presence of traces of fluoride ion [27]. Other workers [29], while investigating this enhancement as a method for determining fluoride, found that ammonium ion caused a similar enhancement of zirconium atomic absorption in the nitrous oxide—acetylene flame. It was shown [30] that the magnitude of this enhancement could be used to determine ammonia at the 10^{-4}—10^{-2} M level and also to determine other nitrogen compounds that can act as Lewis bases.

During a sabbatical year at the Ames Laboratory of Iowa State University, the author and his colleagues used a line-reversal method to measure the temperature profiles of premixed nitrous oxide—acetylene flames of differing stoichiometries. They showed [31] that the temperature of the region of the fuel-rich flame where atomic emission and absorption measurements are usually made is about 2880 K, which is some 350 K less than the calculated value for the hottest part of a stoichiometric flame. A premixed nitrous oxide—hydrogen flame was also studied [32]; this flame has a temperature only about 150 K less than that of the nitrous oxide—acetylene flame, and at first sight looks attractive as a means of atomizing metals that form stable oxides. The results were very disappointing, though the nitrous oxide—hydrogen flame was thought to show promise for emission measurements on easily atomized metals. It also permitted the reduction of several chemical inter-ferences, such as that of phosphorus on calcium, encountered in cooler flames without at the same time producing the high degree of ionization found for the alkali earth metals in the nitrous oxide—acetylene flame. A review of the use of high-temperature flames in atomic absorption spectrometry was published in 1968 [33].

METAL ATOMIZATION IN THE FLAME

In addition to the development of high-temperature flames for use in the practical determination of metals forming refractory oxides, extended studies were made of the factors affecting the atomization efficiencies for metals in various flames. This work was partly aimed at establishing the efficiency of the various components of a commercially-made atomic absorption instrument and where improvements should be sought. The first step was to study the mode of operation of a typical commercial nebulizer—spray chamber system, used with an air—coal gas or air—acetylene flame [34]. The sensitivity of the instrument and the effect of chemical interferences in the flame were found to be critically dependent on the construction of the nebulizer and particularly on the rate of liquid uptake. Determination of drop-size distribution of the spray entering the flame pointed to the importance of small drop size for the efficient atomization of metals that tend to form refractory compounds in the flame. An essential part of this work was the design and construction of an

adjustable nebulizer [35] that allowed the liquid-uptake rate to be accurately controlled over the range 0.8—8 ml min^{-1}. The next step [36] was to study the profile of metal atom concentration in different parts of the flame, and to show how and why this varied from metal to metal and from one type of flame to another. With the assumption that one metal, usually copper, was completely atomized in the flame, relative atomization efficiencies were obtained for various metals in air—acetylene and nitrous oxide—acetylene flames. Both peak absorbance and integrated absorbance methods were used, but neither method was found to be completely satisfactory.

The integrated absorption method was then used to obtain absolute atomization efficiencies in a flame-shielded Meker-type air—acetylene flame for sodium, copper, silver and gold [37]. Allowance was made for the effect of hyperfine structure of the resonance lines, and it was found that atomization of these metals in this type of flame is virtually complete. It is unfortunate that the results of such experiments depend directly on the values of the oscillator strength (f-values) of the absorption lines, as some of these were not known at the time as accurately as could be desired. For instance, the f-value of the 324.75-nm copper line, based on the data available in 1970, was taken as 0.32, whereas use of the value of 0.43 accepted today [38] would lead to the conclusion that copper is only about 75% instead of 100% atomized in the air—acetylene flame.

All the work so far described was based on the conventional method of sample introduction into the flame, i.e. the spraying of a solution via a nebulizer and spray chamber. More recently, the factors influencing the atomization efficiencies of a number of heavy metals were studied for suspensions of geological materials sprayed into the flame [39]. Only particles below about 12 μm in diameter contributed significantly to the observed atomic absorption, and the atomization efficiency increased rapidly with decrease of particle size. With suspensions of samples ground to 325 mesh (<44 μm) or finer, the atomization efficiency of a given metal varied by a factor of only about two between rocks of very different types. This atomization efficiency, relative to that found for a true solution of the metal, was of the order of 0.2—0.4 for metals such as copper, nickel, cobalt, manganese and zinc in the air—acetylene flame.

In the determination of low concentrations of metals in samples containing large concentrations of other material, there is frequently a contribution to the measured absorption from the matrix material; this effect was first noticed in the determination of traces of zinc and cadmium in urine [16]. A study of the attenuation of the light beam by concentrated solutions of sodium chloride and other inorganic salts showed an approximately λ^{-4} dependence for this attenuation, which suggested that the effect might be due to light scattering of the Rayleigh type by solid salt particles in the flame [18, 19]. Later work by Koirtyohann and Pickett [40] showed that the phenomenon was better explained as due to absorption by undissociated salt molecules in the vapour phase. In a recent paper [41] the author has studied background

attenuation in some detail and identified three types of phenomenon, which may however be superimposed on each other in some cases. These are: (1) continuum absorption by molecular species; (2) sharp-line absorption by atomic and molecular species; and (3) scattering, apparently of the Mie type, by solid particles of refractory compounds. This work should help to identify analytical situations where absorption measurements are likely to be in error because of attenuation of the light beam by matrix materials.

NON-DISPERSIVE FLAME ATOMIC FLUORESCENCE

Winefordner and Vickers [42] first proposed flame atomic fluorescence spectrometry as an analytical technique and demonstrated its potential value, particularly for metals for which strong sharp-line sources such as electrode-less discharge lamps could be constructed. Winefordner and other workers in this field used monochromators to separate a resonance line of the analyte metal from the radiation emitted by the flame. Walsh, however, proposed [43, 44] the use of a solar-blind photomultiplier, i.e. a photomultipler giving virtually no signal from radiation above a wavelength of about 320 nm, to enable the detection of metal fluorescence lines below this wavelength without the need for using a monochromator. This technique permits collection of fluorescence radiation over a wider angle than is possible when a monochromator is used and also has the advantage of recording the total fluorescence signal of all the lines lying within the sensitivity curve of the detector, thus enhancing the sensitivity of the method.

More detailed work by Larkins [45], who used the very simple equipment shown in Fig. 2, which incorporated a nitrogen-sheathed air—acetylene flame, showed that the non-dispersive flame fluorescence technique was useful for the determination of many elements having resonance lines below 300 nm. The performance achieved was comparable with, and in many cases better than, that obtainable with a monochromator. The few metals that have their resonance lines in the 300—400 nm region, such as copper, chromium and
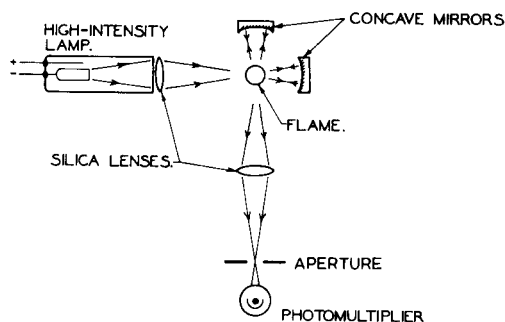

Fig. 2. Schematic diagram of the optical system of a non-dispersive flame atomic fluorescence spectrometer [45].

silver, could be determined merely by replacing the solar-blind photomultiplier with one sensitive in the 300—400-nm region and a simple absorption filter. To obtain the best limits of detection in non-dispersive flame atomic fluorescence, boosted-output hollow-cathode lamps or vapour-discharge lamps were necessary.

For metals that are difficult or impossible to atomize in the air—acetylene flame, Larkins and Willis [46] showed that a nitrogen-sheathed nitrous oxide—acetylene flame was useful, at any rate in the wavelength region below 300 nm. They found, however, that the nitrous oxide—hydrogen flame was no more useful in atomic fluorescence than in atomic absorption.

In analysis for trace metals in sample solutions containing high concentrations of matrix material, the usefulness of the atomic fluorescence technique may be limited by the scatter signal from particulate matter in the flame. Larkins and Willis [47] investigated this phenomenon and discussed various methods of correction for it, the most useful being measurement of the scatter signal alone by use of a suitable line source not containing the analyte metal. They demonstrated how the non-dispersive atomic fluorescence system could be used in practical analyses of plant materials, soil samples and high-purity metals.

SAMPLE ATOMIZATION BY THE CATHODIC SPUTTERING TECHNIQUE

Walsh realized early in the development of analytical atomic absorption spectrometry that the flame has serious drawbacks as a means of sample atomization. First, several important metals such as aluminium, titanium, vanadium and zirconium are not appreciably atomized in low-temperature flames, because of the formation of refractory compounds. Secondly, many other metals are only partially atomized and suffer chemical interferences in the flame. Thirdly, elements such as carbon, whose strongest resonance lines lie in the vacuum ultraviolet, cannot be determined in the flame owing to absorption at these wavelengths by the flame gases. Finally, for reasons of speed and convenience, it is obviously desirable to be able to analyze alloys directly, without the need for prior dissolution of the sample.

Russell and Walsh [48] showed that the cathodic sputtering process was a very convenient and efficient method of producing an atomic vapour directly from a metallic sample. Their preliminary experiments showed that the use of a sputtering chamber as an absorption cell might prove valuable for the direct analysis of metals, particularly for analyses requiring very high sensitivity. Gatehouse and Walsh [49] described a sputtering cell in which the sample for analysis was in the form of a cylindrical hollow cathode, 40 mm long and 12 mm internal diameter (Fig. 3). The cell was filled with argon at a pressure of 1 torr, and the sample surface was "cleaned" by passage of a 60-mA discharge for 4 min. The chamber was then evacuated, refilled with argon, and the discharge passed for another 3 min, after which the absorption of the sputtered vapour was measured. The sputtering cell simply replaced the flame
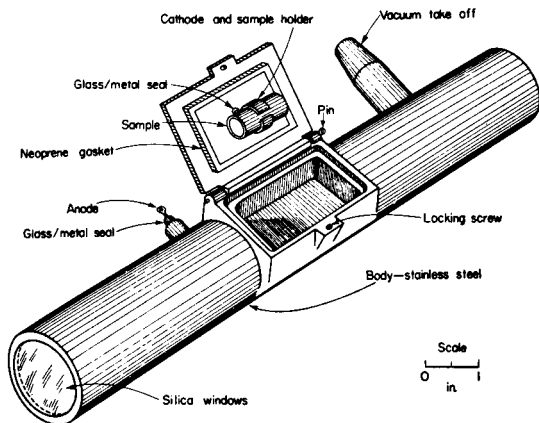
Fig. 3. Sputtering cell used by Gatehouse and Walsh [49].

in the single-beam instrument of Box and Walsh [5]. The determination of silver at the 0.005—0.05% level in copper was carried out with standard deviations of 0.001—0.0035% over this range. It must be remembered that the determination of silver in copper is one of the most favourable measurements as far as sensitivity is concerned, as the sputtering yields are high. Sullivan [50], introducing improvements such as a flow-through gas system and water-cooling of the sample, obtained calibration curves for silicon in steel and in aluminium and, using the P 177.5-nm line, for phosphorus at the 0.1—0.5% level in copper.

This work was then abandoned for some time because other applications of the sputtering technique appeared to be more interesting. With the increased understanding of glow discharges thus obtained, and the development of more sophisticated electronics to achieve better signal-to-noise ratios, it proved possible to resume the work in a form that showed greater promise for routine metallurgical analysis.

Thus, in more recent work the cathode specimen, in the form of a flat metal disc, is clamped between a water-jacket and a hollow silica annulus. A gas inlet tube fits into the annulus, so that the argon flows through a small gap and across the face of the specimen, thus sweeping away gaseous impurities and reducing the reaction with readily-oxidized elements such as aluminium. The top surface of the annulus has a small recess less in depth than the width of the cathode dark space in the glow discharge (Fig. 4). An argon flow of 0.2—0.3 1 min^{-1}, at a pressure of 5 torr, is used, the gas being supplied by a special control unit designed by Larkins [51]. In this unit a simple push-button activates a set of solenoids which control the pumping-down of the cell and the establishment of a pre-set pressure and flow rate of argon.

In the first cell of this type described by Gough et al. [52]. the concentrations of metals in the vapour of the sputtered sample were measured by
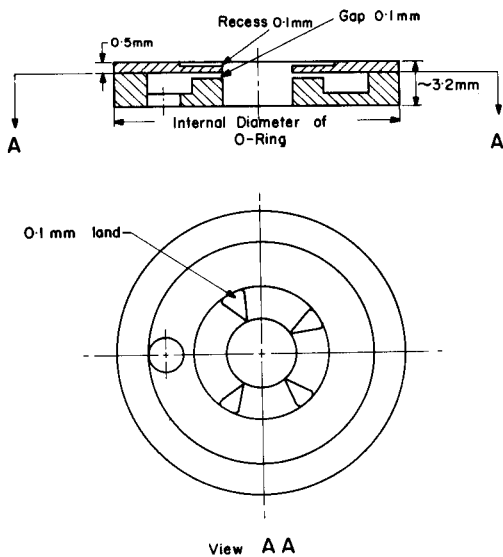
ห้องสมุด กรมวิทยาศาสตร์บริการ

Fig. 4. Schematic diagram of the hollow silica annulus admitting gas into the sputtering chamber [54]. The diagram is not to scale, as the gap and recess dimensions have been enlarged for clarity.

non-dispersive atomic fluorescence spectrometry. Modulated radiation from boosted hollow-cathode lamps of the type described by Lowe [53] was used, the sample was sputtered with a d.c. current, and the modulated fluorescence signal was separated by synchronous demodulation from the d.c. emission produced by the sputtering discharge. Nickel, chromium, copper, manganese and silicon in iron-base alloys were measured and linear calibration curves were obtained for each metal over the range of concentrations studied (0—2%). The limits of detection found are shown in Table 2. It was also possible [52]

TABLE 2

Limits of detection of impurities in iron based on non-dispersive fluorescence measurements on a sputtered vapour [52]

Element	Concentration in iron (%)	Signal-to-noise ratio (time constant 1 s)	Approximate detection limit[a] (ppm in iron)
Cr	0.08	26	30
Cu	0.15	32	5
Mn	0.13	20	70
Ni	0.12	70	20
Si	0.08	1.7	400

[a]The detection limit is defined here as the concentration required to give a signal-to-noise ratio of one when the output is read on a chart recorder.

to measure the iron, chromium and nickel fluorescence simultaneously from sputtered vapours of various stainless steels. The three light sources were modulated at slightly different frequencies and the atomic fluorescence detected by a single R106 photomultipler fitted with a UG5 glass filter. The signals were separated by three phase-sensitive amplifiers synchronized with the modulation of the sources.

Gough [54] analyzed metal samples by atomic absorption, using a sputtering cell rather similar to that of Gough et al. [52] but designed for measurement of the transmitted radiation from the atomic spectral lamp (Fig. 5). This cell could be easily interchanged with the flame atomizer of a conventional atomic absorption instrument. A dual-modulation amplifer provided automatic compensation for background absorption by metal paricles and for any variation in the intensity of the spectral lamp. Gough successfully analyzed alloys of iron, aluminium, copper and zinc for some 16 metals, the time required per analysis being 2—3 min for brasses, 5 min for zinc, and 10 min for aluminium alloys. Reproducibility was typically ±1% for iron- and copper-base alloys, ±2% for aluminium-base and ±3% for zinc-base alloys. Detection limits were in the range 3—400 ppm.

In all the foregoing work on the analysis of metals and alloys vaporized by cathodic sputtering, it was necessary to have reference samples with similar sputtering rates to the analytical samples. Changes in sputtering rate may occur when different matrices are sputtered or when there is a change in the energy or flux of the bombarding ions.

McDonald [55] overcame this difficulty by using an internal standard together with a reference sample of known analyte concentration. He showed that in the atomic absorption analysis of materials such as low-alloy steel the major constituent, in this case iron, may often be used as the internal standard for the determination of other metals. He also extended the technique to the
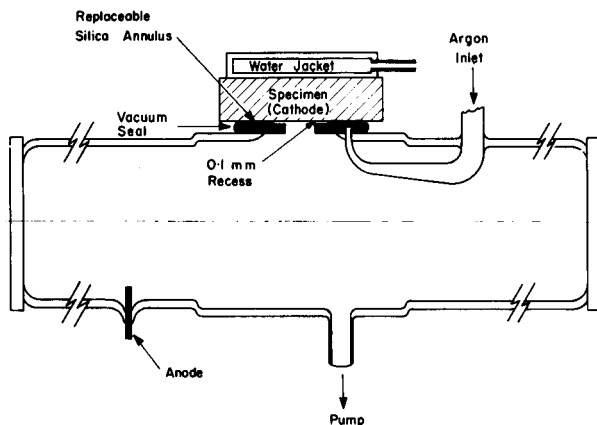

Fig. 5. Schematic diagram of sputtering chamber used by Gough [54] for atomic absorption measurements.

analysis of finely-divided metals and non-metallic materials by pressing the powdered sample into a pellet with copper or silver powder. The internal standard used was either the copper powder itself or an element such as nickel, added in powdered form at a concentration of 1%. McDonald found that, in the determination of copper in slag samples incorporated in silver discs, the use of nickel as internal standard allowed accurate determination of copper in slags whose copper content ranged from 0.4% to 73%. This was so despite the fact that the relative sputtering rate of copper, for a given concentration of this metal, varied over a five-fold range between one sample and another.

McDonald's results suggest the preferential sputtering, ionization and agglomeration effects do not occur in this type of discharge. This raises again the possibility of absolute analysis, i.e. analysis without a reference sample, first proposed by Walsh [2] in 1955.

A detailed description of the development of the cathodic sputtering technique for the direct analysis of metals and alloys up to 1972 was given by Walsh in his Hasler Award Address of that year [56].

DEVELOPMENT OF IMPROVED ATOMIC SPECTRAL LAMPS

As mentioned earlier, Walsh has described [1] how the development of the sealed-off hollow-cathode lamp played an essential part in establishing the atomic absorption technique as a practical means of chemical analysis. Following the early work of Jones and Walsh [6], the Spectroscopy Section has devoted a continuing effort to the improvement of lamps for use in atomic absorption and atomic fluorescence spectroscopy.

For some elements the early hollow-cathode lamps showed relatively poor resonance-line emission intensity. Improvement in this intensity was highly desirable, particularly for lamps that were to be used with double-beam instruments, whose optical paths have many reflecting surfaces and thus cause considerable loss of energy.

In 1962 Sullivan and Walsh [57] developed a "high-intensity" hollow-cathode lamp. (The term "high-intensity" is better replaced by the term "boosted-output", which describes more accurately the mode of operation of the lamp.) In this lamp (Fig. 6) the functions involving the formation and excitation of atomic vapour were separated. One electrical discharge was used to produce by cathodic sputtering the optimum pressure of atomic vapour, and a second ("booster") discharge, electrically isolated from the first, produced the necessary excitation. In this manner increasing the excitation of the vapour by increasing the current through the second discharge did not affect the vapour pressure and did not lead to any increase in self-absorption or self-reversal.

The new lamps frequently gave resonance line intensities of 50—100 times those of conventional hollow-cathode lamps without any increase in line-width. A pleasing feature was that the enhancement of intensity was largely confined to the resonance lines (Fig. 7).
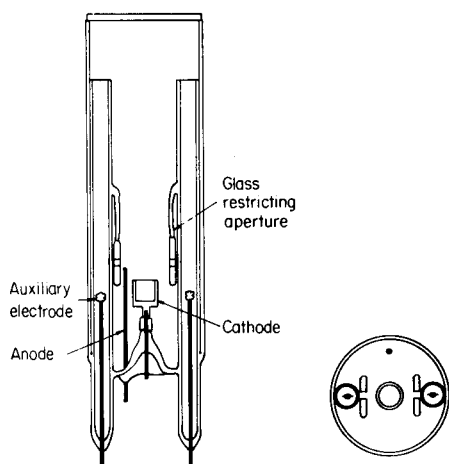
Fig. 6. Boosted-output hollow-cathode lamp as described by Sullivan and Walsh [57].
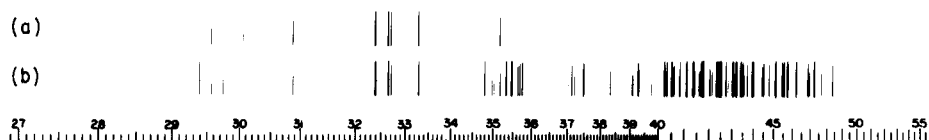
Fig. 7. Spectrum of a Sullivan—Walsh type boosted-output copper hollow-cathode lamp compared with that of a conventional copper hollow-cathode lamp [57]. (a) Boosted-output lamp, exposure 2 s. (b) Conventional lamp, exposure 5 min.

With the advent in 1964 of atomic fluorescence spectrometry as an analytical technique [42], the need for high-intensity line sources became more acute, since in atomic fluorescence, unlike atomic absorption spectrometry, the sensitivity of the method is directly proportional to the intensity of the light source. In 1969—70, Lowe [53] developed a modified version of the Sullivan—Walsh lamp in which an open-ended cylinder was used as the cathode for the hollow-cathode discharge. The boosting discharge was directed through the centre of the cathode cylinder instead of across its open end (Fig. 8).

Fig. 8. Lowe-type boosted-output hollow-cathode lamp [53].

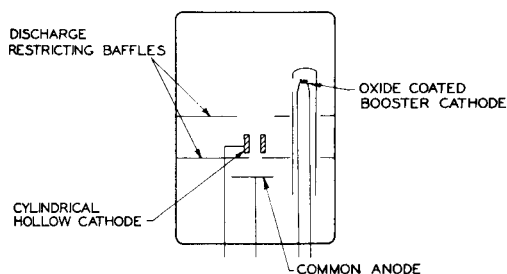Greater emission intensities of the resonance lines were achieved than with the Sullivan—Walsh type of lamp, though this was accompanied in some cases by some broadening of the lines.

Lowe compared his lamps with the Sullivan—Walsh type and with conventional hollow-cathode lamps, using them as light sources in the simple non-dispersive flame atomic fluorescence system shown in Fig. 2. The results, shown in Table 3, demonstrate the merits of his boosted-output hollow-cathode lamps as sources in atomic fluorescence spectrometry.

Following the development of the technique of vaporizing analytical samples by cathodic sputtering in a stream of argon, several new types of boosted-output lamp with argon flow-through have been developed. The flow of argon through the lamp is readily controlled by use of the Larkins gas-control unit, and the lamps are demountable so that the cathode can readily be replaced by one of another element. Unlike the sealed-off type of lamp, these lamps require no tedious processing before use. The lamp shown in Fig. 9, described by Sullivan and Van Loon [58], is a modification of the boosted glow-discharge source developed by Lowe [59] for spectrochemical emission measurements. The cathode of the element whose resonance lines are to be excited is in the the form of a disc pressed from the appropriate powder or machined from rod and is press-fitted into a water-cooled aluminium block. This lamp, which is best suited for relatively non-volatile elements, gives more intense resonance line emission and narrower lines than do conventional hollow-cathode lamps. The smaller line-width results in better sensitivity and greater linearity of calibration curve when the lamp is used as a source in atomic absorption (Fig. 10). The high intensity of emission makes the lamp suitable as a light source for atomic fluorescence, and Table 4 shows that in non-dispersive flame atomic fluorescence at least as good limits of detection can be obtained with this lamp as with the sealed-off boosted hollow-cathode lamp of the Sullivan—Walsh or Lowe type.

Sullivan and Van Loon used their lamps in the determination of nickel, cadmium, zinc and copper at the 1—10 ppb level directly in river water by

TABLE 3

Comparative intensities of signals from 1 μg ml^{-1} solutions measured by non-dispersive flame fluorescence with different types of lamp [53]

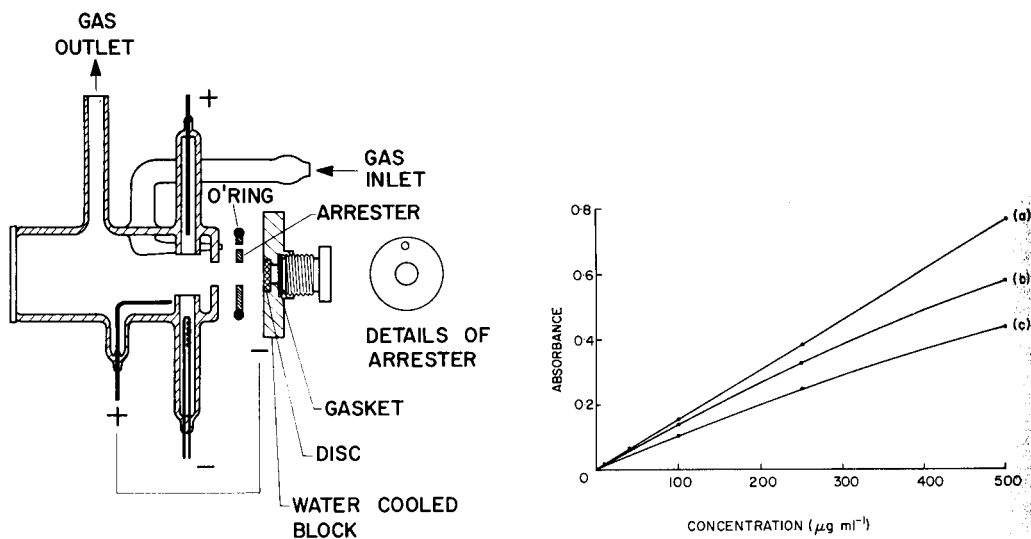| Metal	Hollow-cathode lamp	Commercial Sullivan—Walsh type lamp	Lowe type boosted-output lamp
Ag	1	17	119
Au	1	12	50
Co	1	0.75	15
Cr	1	—	12
Cu	1	11	44
Fe	1	4	50
Ni	1	4	50

Fig. 9. Sullivan—Van Loon type of demountable boosted-output spectral lamp [58].

Fig. 10. Atomic absorption calibration curves for tin, with the Sullivan—Van Loon demountable lamp [58] and an air—hydrogen flame. All the curves were obtained at 224.6 nm, bandpass 0.2 nm: (a) demountable lamp, lamp current 500 mA (booster) and 20 mA; (b) demountable lamp, lamp currents 500 mA and 30 mA; (c) hollow-cathode lamp, lamp current 7 mA.

non-dispersive flame fluorescence and obtained results in good agreement with those obtained by a.a.s. after pre-concentration of the metals by chelation into an organic solvent. The total dissolved solid levels of the samples lay in the range 60—300 mg l^{-1} and presented no problem except with nickel, when a scattering correction had to be made in the manner described by Larkins and Willis [47].

Another type of boosted-output spectral lamp with an interchangeable cathode [60] is shown in Fig. 11. It is particularly suitable for relatively volatile elements such as arsenic and selenium, because the argon flow takes place transversely between the cathode and the window, thereby avoiding any risk of depositing the volatile element on the latter. The lamp has a high numerical aperture, which is a great advantage in atomic fluorescence work.

This lamp was compared with commercially-available electrodeless-discharge lamps for arsenic, selenium, cadmium, lead and antimony and found to be superior with respect both to warm-up time and to sensitivity when used as the light source in non-dispersive flame atomic fluorescence. Table 4 compares the limits of detection found with the different types of lamp.

Recently, Sullivan [61] has described a simple sealed-off lamp designed for elements such as sulphur, selenium and phosphorus, the characteristic feature of this lamp being that a controlled temperature gradient is maintained

TABLE 4

Limits of detection in non-dispersive flame atomic fluorescence[a]

Element	Demountable boosted-output lamps		EDL's Sullivan [60] (ng ml^{-1})	Sealed-off conventional and boosted hollow-cathode lamps Larkins [45] (ng ml^{-1})
	Sullivan and Van Loon [58] (ng ml^{-1})	Sullivan [60] (ng ml^{-1})		
Ni	1.5	—	—	2[b]
Cu	0.2	—	—	1[b]
Ag	0.1	—	—	0.15[b]
Zn	0.1	—	—	0.3[c]
Cd	0.1	0.1	0.2	4[d,e]
As	—	100	400[f]	6000[d]
Se	—	150	650[f]	6000[d]
Pb	—	10	50	150[c]
Sb	—	10	50	40[b]

[a]The limits of detection follow the very conservative definition used by Larkins [45], namely the concentration giving a signal equal to twice the peak-to-peak fluctuation when only water or dilute acid is aspirated.
[b]Lowe type [53] boosted hollow-cathode lamp.
[c]Sullivan—Walsh type [57] boosted hollow-cathode lamp.
[d]Conventional hollow-cathode lamp.
[e]Using a vapour-discharge lamp, Larkins obtained a limit of detection of 0.2 ng ml^{-1}.
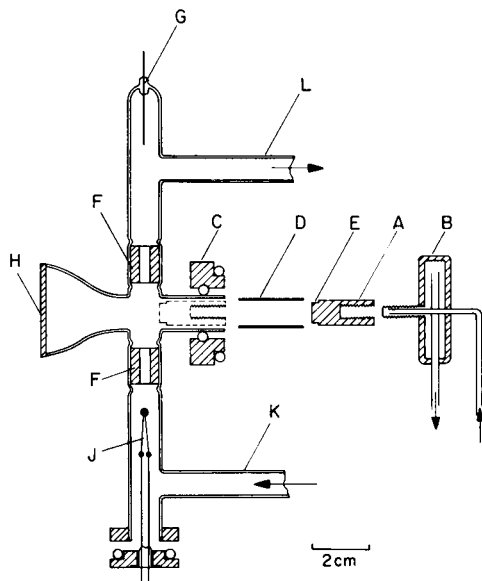[f]These figures are somewhat uncertain, as the mechanical chopper used led to flame instability.

Fig. 11. Boosted-output spectral lamp with interchangeable cathode [60].

between the anode and the cathode (Fig. 12). With this lamp atomic fluorescence measurements can be made on elements having their resonance lines below 200 nm, the sample being vaporized by cathodic sputtering in a cell resembling that used by Gough et al. [52].

Boosted glow-discharge sources for spectrochemical analysis

The lamps so far described were developed specifically to give the spectra of pure elements for use as light sources in atomic absorption and fluorescence spectrometry. However, the principles of construction of the demountable boosted-output lamp had already been applied by Lowe [59] to the construction of a boosted-output glow-discharge source for use in spectrochemical emission. This source was based on the glow-discharge source developed in Germany by Grimm [62, 63], but incorporated also a pair of booster electrodes. The cathode was a roughly polished block of the metal or alloy to be analyzed. The emission spectra were simpler than those produced by the Grimm lamp, since preferential enhancement of the resonance lines occurred. The signal-to-noise ratio was also improved (Fig. 13).

Lowe's design was modified somewhat by Gough and Sullivan [64], whose all-metal emission source is shown in Fig. 14. Its use in spectrochemical analysis was demonstrated in the simultaneous determination of nine elements in aluminium-base alloys, low-alloy steels, cartridge brass and zinc-base die-casting
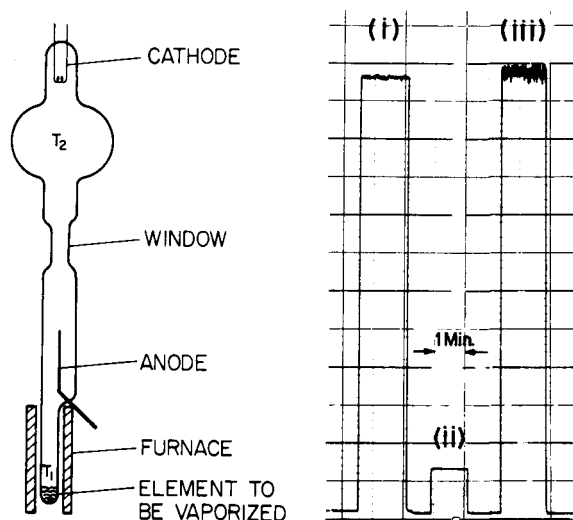

Fig. 12. Controlled temperature-gradient atomic spectral lamp [61].

Fig. 13. Typical recorder traces from Lowe's boosted glow-discharge source [59]. The 285.2-nm line of magnesium is being measured for an aluminium alloy containing 0.051% magnesium. Recorder time constant, 1 s. (i) Glow discharge 30 mA, plus booster discharge 750 mA; (ii) glow discharge alone 30 mA, same gain as (i); (iii) glow discharge alone 30 mA, expanded gain.
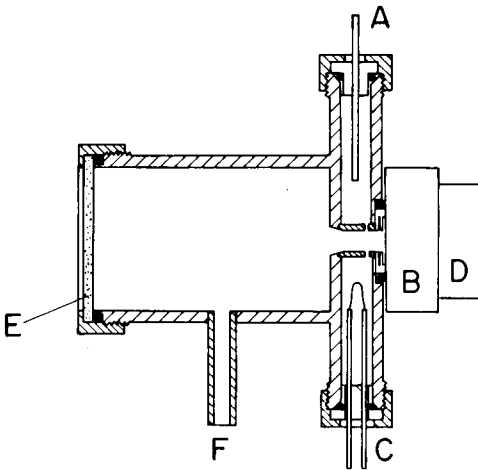
Fig. 14. Boosted glow-discharge source, Gough—Sullivan type [64].

alloys. The source was used in conjunction with a polychromator which had direct readout facilities. The intensities of the resonance lines emitted by the source were sufficiently high to permit detection of metals at concentrations of a few parts per million, and the precision (r.s.d.) of measurement of major, minor and often trace constituents in alloys was approximately 1%.

Selective modulation of resonance lines from lamps

All the atomic spectral lamps described up to this point emit not only the resonance lines of the element forming the cathode but also, to a greater or lesser extent, other lines in the spectrum of the element. If the output of these other lines could be suppressed it would be possible, in some instances at least, to make atomic absorption measurements without the need for a monochromator.

Bowman et al. [65] showed that the resonance lines can effectively be "isolated" by periodic interposition of a cloud of absorbing atoms in the light beam of a d.c.-operated boosted-output hollow-cathode lamp. The resonance lines, but not the other lines from the lamp, are absorbed by this pulsating cloud of atoms, and if the photodetector feeds an a.c. amplifier the signal at the output of this amplifier will be due to the resonance lines alone. The non-resonance lines, which are not absorbed by the atomic cloud, will give rise to a d.c. signal at the detector, but this will merely contribute noise at the out-put of the a.c. amplifier.

A convenient way of achieving this result is to incorporate a modulating, i.e., a.c.-operated, electrode of the same metal in front of the hollow cathode. In practice, in order to avoid excessive noise from unmodulated lines, it proved necessary to use a boosted-output rather than a conventional-type hollow-cathode lamp. It was also found that a monochromator, though not one of

very high resolution, was necessary. Figure 15 shows that considerable simplification of the spectrum of nickel near the 232.0-nm resonance line is achieved with a selectively-modulated lamp, and Fig. 16 shows that this leads to greatly improved linearity in the calibration curve for this metal, even when a monochromator of relatively poor resolution is used.

Lowe [66] described a simple technique for selectively modulating the resonance lines from a standard hollow-cathode spectral lamp without using any extra modulator electrode. The lamp is operated at a steady d.c. level and short, high-current pulses are superimposed on it. The increased sputtering from each pulse causes a cloud of atoms of the cathode material to be formed inside and in front of the hollow cathode, and by adjusting the pulse height and width it is possible to make the vapour cloud large enough to cause almost complete absorption of the resonance lines. As the vapour cloud decays between pulses the output intensity of the resonance lines rises again to that of the d.c. level. Suitable gating techniques have been described [67] for the amplification of the modulated signal. Figure 17 shows how effectively the resonance lines of copper can be isolated in this way.

The principle of selective modulation of atomic resonance lines has been put to practical use in the field of molecular spectrophotometry. Bennett et al. [68] described a simple instrument for the continuous monitoring of proteins
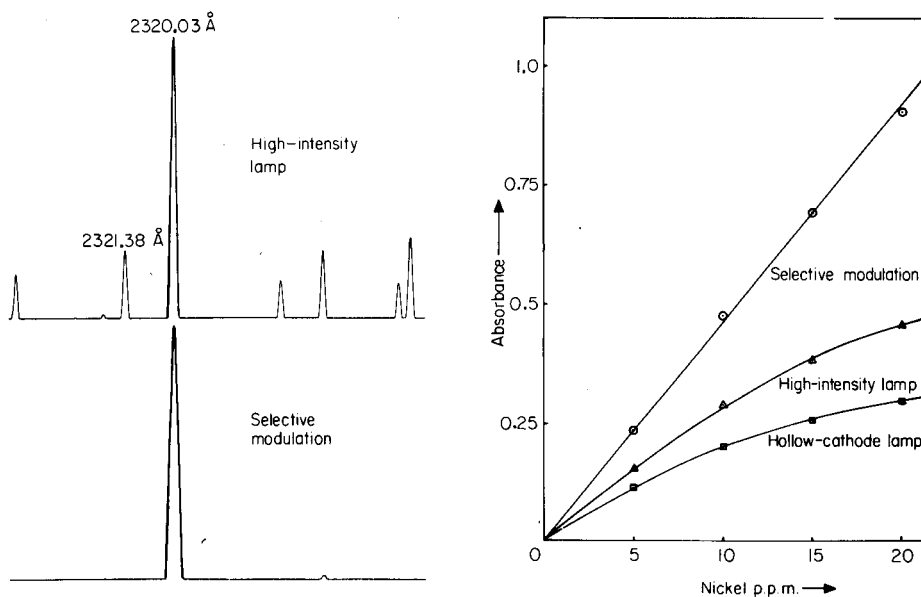

Fig. 15. Spectra showing isolation of the nickel resonance line at 232.003 nm by selective modulation [65]. Modulator, 20 mA; lamp primary discharge, 30 mA; lamp booster discharge, 400 mA.

Fig. 16. Calibration curves showing the application of the selective modulation technique to the determination of nickel by a.a.s. [65]. Spectral bandpass, 0.7 nm.
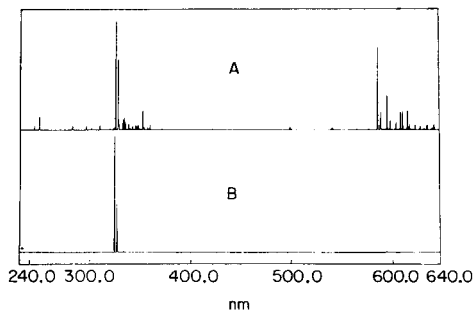
Fig. 17. Spectra recorded from a copper—neon hollow-cathode lamp. (A) D.c. operation; (B) pulsed current operation to produce selective modulation [67].

in solution, using the well-known protein absorption band in the neighbour-hood of 280 nm ascribed to aromatic amino acids, especially tyrosine and tryptophan. Radiation from a selectively modulated magnesium hollow-cathode lamp, having a wavelength of 285.2 nm, traversed the solution, which was contained in a small cell (10 mm × 3 mm diameter), and then fell on a photo-detector whose output was fed to a gated amplifier.

RESONANCE SPECTROMETERS*

Sullivan and Walsh [69] used the cloud of atomic vapour produced by cathodic sputtering in a conventional hollow-cathode lamp to absorb and re-emit the resonance lines in the radiation emitted by a boosted hollow-cathode lamp of the same element run on modulated current. By viewing the re-emitted lines with a photomultiplier whose output was fed to an a.c. amplifier, it was possible to record only the signal from the resonance lines of the element. This "resonance detector" thus functioned as a spectrometer for isolating the resonance lines of the element, and flame atomic absorption measurements could be made merely by interposing the flame between the boosted-output lamp and the resonance spectrometer.

The particular advantage of the "sputtering-type" resonance spectrometer just described is that it is, in principle, applicable to all metallic elements, irrespective of melting point, because the atomic vapour is produced without the necessity of heating the metal. The main disadvantage of the sputtering technique is that the electrical discharge necessarily results in the emission of radiation in the visible and ultraviolet regions of the spectrum, which leads to a serious reduction in the signal-to-noise ratio of the output signal. In a later paper [70] Sullivan and Walsh described a "thermal-type" resonance spectro-meter for low melting-point metals such as calcium, magnesium, sodium, pot-assium and lead. Here the atomic vapour does not generate any appreciable

*The devices described in this section have traditionally been referred to as "resonance detectors"; the term "resonance spectrometer" is preferred by IUPAC [9].

radiation, and such resonance spectrometers can be used with conventional, instead of boosted, hollow-cathode lamps. Figure 18 shows a diagram of an atomic absorption instrument employing a thermal-type resonance spectrometer.

When a resonance spectrometer is used, the width of the resonance lines emitted by the light source is not critical, because only the centre of the line(s) can be absorbed by the atomic vapour in the resonance lamp and produce an output signal.

Several applications of resonance spectrometers in practical analysis have been described. Bowman [71] determined lithium in blood serum (diluted 1:10 with water), using a conventional lithium hollow-cathode lamp and a thermal-type resonance spectrometer. In order to make use of the high aperture of the resonance spectrometer, an air—coal gas flame was used with a burner having two parallel slots, 5 mm apart and 75 mm long. The lithium reference solutions were matched in sodium and potassium content to an average blood serum, and the measured lithium concentrations were reproducible to $\pm 0.2 \, \mu g \, ml^{-1}$ in the serum. The limit of detection was $0.6 \, \mu g \, ml^{-1}$ in the serum with the resonance spectrometer, and $0.3 \, \mu g \, ml^{-1}$ with a conventional monochromator.

Boar and Sullivan used conventional hollow-cathode lamps and thermal-type resonance spectrometers in the determination of calcium [72] and magnesium [73] in brown-coal ash. Both air—acetylene and nitrous oxide—acetylene flames were used for calcium; in the latter flame the sensitivity was improved and chemical interferences were eliminated. Figure 19 shows typical calibration curves for calcium.

Sullivan et al. [74] used a boosted-output hollow-cathode lamp, a sputtering-type resonance spectrometer and an air—propane flame at a burner having two parallel rows of holes, for the determination of nickel in ores. They showed that, within the range 0.5—1.6% nickel, the method gave an accuracy for a single determination of ±5.1% of the mean at the 0.95 confidence level.

Sullivan and Walsh [75] have described the use of resonance spectrometers for the measurement of the ultraviolet absorption by solutions. Light from an atomic spectral lamp emitting the spectrum of a suitable element passes into a resonance spectrometer containing an atomic vapour of the same element. This vapour selectively absorbs the resonance lines, which are
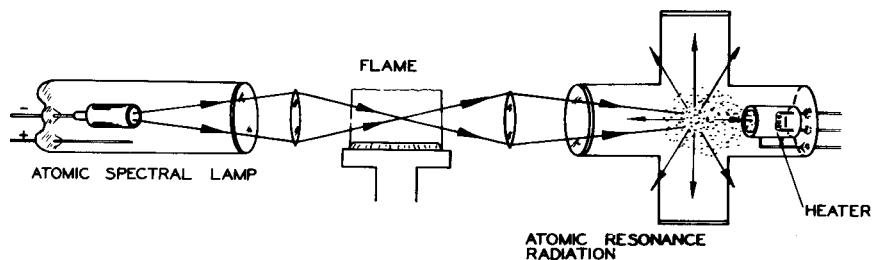

Fig. 18. Diagram of an atomic absorption instrument employing a thermal-type resonance spectrometer [70].
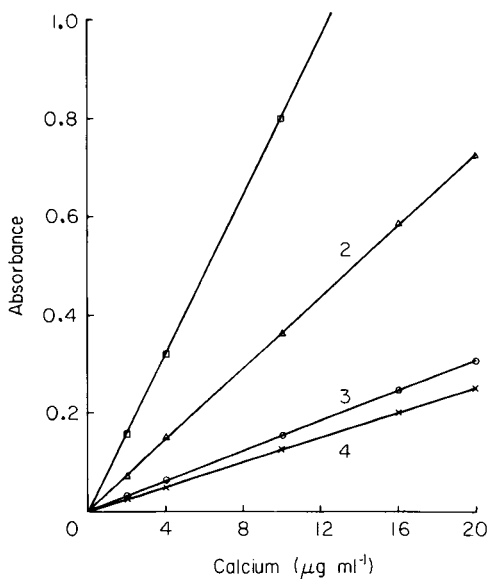
Fig. 19. Calibration curves for the determination of calcium in brown coal [72]. (1) Conventional monochromator, N_2O–C_2H_2 flame; (2) resonance spectrometer, N_2O–C_2H_2 flame; (3) resonance spectrometer, air–C_2H_2 flame; (4) conventional monochromator, air–C_2H_2 flame. A 50 mm single-slot burner was used in (1), (2) and (4), and a 50-mm double-slot burner in (3).

subsequently re-emitted in all directions. The intensity of the resonance radiation after passage through the solution whose absorption is to be determined is measured photoelectrically. Table 5 shows the wavelengths of the resonance lines that can be isolated by this technique. Sullivan and Walsh found that proteins in solution could be determined by measuring their characteristic absorption in the 280-nm region with a magnesium resonance spectrometer used at 285.2 nm.

The isolation and detection of atomic resonance lines by the techniques of selective modulation and resonance detection have been reviewed by Sullivan and Walsh [76]. They pointed out the relative advantages and disadvantages of the resonance spectrometer compared with the conventional monochromator.

More recently, Walsh has shown [77] that a separated flame can be used as a resonance spectrometer for a given element by spraying into it a pure solution of the element. When this flame is illuminated, the fluorescence signal can only be due to radiation of wavelength(s) corresponding to the absorption line(s) of that element. A non-dispersive flame-fluorescence spectrometer can thus be converted to an atomic absorption spectrometer by interposing a second flame, into which is sprayed the solution for analysis. The separated flame has the outstanding advantage over previous types of resonance spectrometer in the ease with which it can be changed from the detection of one element to another: it is only necessary to spray the appropriate solution into the flame.

TABLE 5

Wavelengths isolated by resonance spectrometers [75]

Element	Light source[a]	Type of resonance spectrometer	Wavelength(s) of resonance radiation, (nm)
Zn	BOHC or VDL	Thermal	213.86
Cd	BOHC or VDL	Thermal	228.80
Be	BOHC	Sputtering	234.86
Hg	VDL	Thermal	253.65
Pb	HC	Thermal	283.31
Mg	HC	Thermal	285.21
Cu	HC or BOHC	Sputtering	324.75 ⎫ 327.40 ⎭
Ag	HC or BOHC	Sputtering	328.07 ⎫ 338.29 ⎭
Tl	HC or VDL	Thermal	377.57
Ca	HC	Thermal	422.67
Sr	HC	Thermal	460.73
Ba	HC	Thermal	553.55
Na	VDL	Thermal	589.00 ⎫ 589.59 ⎭
Li	HC	Thermal	670.78
K	VDL	Thermal	764.49 ⎫ 769.90 ⎭

[a]HC: hollow-cathode lamp. BOHC: boosted-output hollow-cathode lamp. VDL: vapour discharge lamp.

Larkins and Walsh [78] have described the performance of such an instrument for eight metals. Figure 20 shows typical calibration curves obtained with the flame resonance spectrometer and with a conventional monochromator. The flame resonance spectrometer can also be used in a number of other ways; for instance with some elements the atomic spectral lamp can be replaced by a continuum source. Again, the flame resonance spectrometer can be used as a wavelength-selective detector in emission measurements, with the sample to be analyzed being made the cathode of a boosted glow-discharge source of the type described earlier [59, 64]. Manganese can be determined in low-alloy steels by this technique [78]; calibration graphs are linear over the range 0—1.5% manganese. Other ways of using flame- and sputtering-type resonance spectrometers in building general-purpose atomic spectrometers have also been described [79].

FUNDAMENTAL STUDIES ON ATOMIC SPECTRAL LINES

Hollow-cathode lamps were first proposed as suitable light sources for analytical atomic absorption spectrometry [2] on the basis that their emission lines are sharper than the absorption lines of atoms in flames. Under these
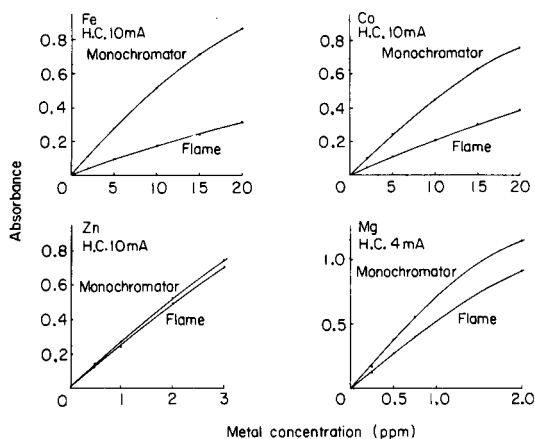
Fig. 20. Comparison of calibration curves obtained with a flame-type resonance spectro-meter and with a conventional monochromator. H.C. indicates the use of a hollow-cathode lamp square-wave modulated at the average current indicated [78].

conditions the measured absorbance of a flame is directly proportional to the (peak) absorption coefficient at the centre of the absorption line and hence to the concentration of absorbing atoms. Thus knowledge of the profiles of the lines emitted by hollow-cathode lamps is necessary for any quantitative understanding of the absorption process.

In 1966—68, Yasuda in Japan [80, 81] made interferometric measurements on the calcium 422.673-nm resonance line, which is almost completely free from hyperfine structure. He obtained Doppler widths corresponding to atomic vapour temperatures of 1200—2700 K for hollow-cathode lamp currents of 20—90 mA. These widths seemed anomalously high, and Bruce and Hannaford [82] re-investigated the problem, using an interference filter instead of a monochromator to separate the calcium resonance line. They were able to measure interferometrically the profile of the line for hollow-cathode lamp currents close to those used in analytical atomic absorption work, and for currents in the range 5—15 mA d.c. found that the half-intensity width varied from 0.00092 to 0.00154 nm. These values could be accounted for satisfac-torily in terms of Doppler broadening corresponding to the temperatures of the hollow cathode as measured with a thermocouple (347—429 K), self-absorption broadening, and (to a lesser extent) Lorentz pressure broadening and natural broadening.

It was noticed a few years ago by several workers that replacement of the neon fill gas by argon in a boron hollow-cathode lamp reduced the absorbance for this element, measured in a flame, by a factor of up to four. As the measured absorbance depends on the width of the emission line, these results suggested that the change from neon to argon may cause unexpected broadening of the boron emission lines. Hannaford and Lowe [83], using a 3.8-m Czerny—

Turner monochromator with a resolution of 0.0048 nm, measured the profiles of the resonance lines near 249.7 nm and 208.9 nm from boron hollow-cathode lamps filled with different rare gases. They found that for discharges operated in argon, krypton or xenon the lines are extremely broad (half-widths 0.013—0.027 nm) and are emitted very close to the cathode surface with unusually high intensity, whereas in neon the line-width was found interferometrically to be 0.0020 nm. The abnormal line-widths are due to Doppler broadening, which was shown to be unusually large because of preferential excitation of those sputtered boron atoms having high kinetic energies of ejection. Hannaford and Lowe interpreted the high excitation efficiency at relatively low collision energies in terms of curve crossings, which appear to be particularly favourable for some boron—rare gas systems. They then showed that the ratio of fluorescence intensities of the boron 208.9- and 249.7-nm lines in a cathodic-sputtering discharge depends on rare-gas pressure for both xenon and krypton [84]. They interpreted this as evidence of rare-gas quenching of the boron resonance radiation and the occurrence of curve crossings at large internuclear separation in some boron—rare gas systems.

A useful practical application arose from this fundamental work on the widths of boron lines excited in various rare gases. Hannaford and Lowe [85] found that it was possible to determine boron isotope ratios by atomic absorption spectrometry, with neon-filled (but not argon-, krypton- or xenon-filled) discharge lamps as the source of boron resonance lines. For accurate measurement of the $^{10}B/^{11}B$ ratio, it is advantageous to use enriched isotope sources and a sharp-line absorber, such as a water-cooled sputtering cell, and to make the absorption measurements on the 208.89/208.96-nm doublet, which has a considerably larger isotope shift than the main 249.68/249.77-nm resonance-line doublet. A less accurate determination of boron isotope ratios is possible if enriched isotope sources are used to measure absorption in a nitrous oxide--acetylene flame. A very simple approximate method uses a commercial natural-boron source and the nitrous oxide—acetylene flame.

A quantity of fundamental importance in the quantitative understanding of atomic absorption is the oscillator strength, f. The literature values of f for most elements show great discrepancies, and it is highly desirable that reliable values should be available, particularly for metals such as copper, whose efficiency of atomization in the flame has been widely discussed [36, 37] and which is potentially a suitable element for use as an internal standard in chemical analysis [55]. Hannaford and McDonald [38] measured the relative oscillator-strength values of eleven resonance lines of this metal, making allowance for the effect of differences in the hyperfine structure of the lines, from atomic absorption measurements on copper vapour produced in a low-pressure glow-discharge. The relative f-values thus obtained were placed on an absolute scale by normalizing with respect to the currently-accepted value (0.43) for the main 324.8-nm copper resonance line.

DEVELOPMENT OF SIMPLE ANALYTICAL INSTRUMENTS BASED ON MEASUREMENT OF MOLECULAR ABSORPTION

Experience gained in the design of various types of atomic absorption and fluorescence spectrometer led to the development of simple instruments for the determination of several substances by measurement of their molecular absorption.

Sullivan and Woodcock [86] described a simple double-beam instrument for the on-stream determination of xanthate in mineral flotation liquors, using the xanthate absorption band centred on 301 nm. A mercury lamp was used as the light source with a composite filter of UG11 glass and chromate solution to isolate the lines at 312.6 nm and 313.2 nm. The light beam was split into two components of approximately equal intensity, one being passed through the xanthate solution to a photosensitive diode detector and the other through a reference cell containing water to a second detector. The reference signal controlled amplifier gain to eliminate effects of lamp intensity changes, and the amplified sample signal was used to measure xanthate concentration. The detector—amplifier—indicator system, described by Box and Meldrum [87], was capable of maintaining an output indication constant to within 0.5% over a 24-h period despite mains fluctuations of ±10% and lamp-intensity variations of 50%. The long-term drift, measured over a 1-week period, was ±0.25% of full-scale deflection.

Larkins and Meldrum [88] described a simple interference-filter instrument for the determination of proteins in solution, based on absorption of the 285.2-nm line from a magnesium hollow-cathode lamp. No beam-splitter or lenses were used and the two photodetectors merely viewed the lamp, through the sample and reference solutions, from two slightly different positions. The performance of this simple instrument was comparable to that of a more sophisticated dual-beam system based on a selectively-modulated magnesium hollow-cathode lamp and a special low-noise amplifying system [89].

The performance of an instrument without a filter, but with a solar-blind photocell detector, was not as good, but appeared to be adequate for qualitative column monitoring work. Figure 21 shows calibration curves for serum albumin solutions obtained with different wavelength-isolation systems.

Loss of sulphur dioxide by permeation occurs when foods containing this preservative are packaged in polymer films. However, the partial pressures of sulphur dioxide in the headspace of packages of these foods are less then ≈ 20 Pa [200 ppm v/v], which calls for the development of a very sensitive method of measuring the permeability of such films. Davis et al. [90] developed an apparatus based on the absorption by sulphur dioxide at the wavelength of the zinc resonance line, namely 213.8 nm. The light beam, after passage through an interference filter, was split by prismatic mirror into two beams which traversed two cells, of length 500 mm, one containing the sulphur dioxide—nitrogen mixture and the other pure nitrogen to serve as a reference.
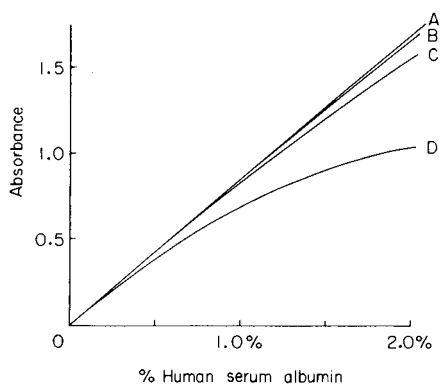
Fig. 21. Absorbance of human serum albumin solutions for radiation from a magnesium hollow-cathode lamp with various wavelength isolation systems [88]. (A) Monochromator set on 285.2-nm line; (B) selective modulation; (C) interference filter, peak wavelength 285.2 nm, half-intensity bandpass 2.1 nm; (D) solar-blind photocell, effective spectral range 200—320 nm.

The light emerging from the absorption tubes was detected by a pair of matched solar-blind photocells whose output was amplified and fed to a potentiometric recorder. With this apparatus, the permeabilities of eleven types of polymer film to sulphur dioxide were measured at partial pressures of 2.4—60 Pa.

ASSISTANCE TO THE AUSTRALIAN SCIENTIFIC INSTRUMENT INDUSTRY

One of the aims of the Division of Chemical Physics has been to foster the development of an Australian-based scientific instrument industry. It has already been mentioned that the single-beam instrument developed by the Spectroscopy Section in the late 1950's became the prototype of the first atomic absorption spectrometer produced commercially in Australia. A suitable dispersing element was needed for the monochromator of this instrument, and it was fortunate that facilities for the ruling of diffraction gratings had been developed in the Division by D. A. Davies and G. M. Stiff. An account of their work has been given by McNeill [91].

CURRENT WORK IN THE SPECTROSCOPY SECTION

The present research work of the Section includes:
(1) development of improved types of atomic spectral lamp;
(2) improvement of the techniques for the analysis of atomic vapours produced by cathodic sputtering, based on atomic fluorescence rather than atomic absorption measurements;
(3) further studies on the possibility of absolute analysis of sputtered vapours;
(4) development of sputtering-type resonance spectrometers for use in emission spectroscopy;

(5) studies of fluorescence yields and collisional quenching rates of atoms in the flames commonly used in analytical atomic spectroscopy.

REFERENCES

1 A. Walsh, Anal. Chem., 46 (1974) 698A.
2 A. Walsh, Spectrochim. Acta, 7 (1955) 108; erratum ibid. p. 252.
3 J. P. Shelton and A. Walsh, XVth Congress IUPAC, 2 (1956) IV-50, p. 403.
4 B. J. Russell, J. P. Shelton and A. Walsh, Spectrochim. Acta, 8 (1957) 317.
5 G. F. Box and A. Walsh, Spectrochim. Acta, 16 (1960) 255.
6 W. G. Jones and A. Walsh, Spectrochim. Acta, 16 (1960) 249.
7 B. M. Gatehouse and J. B. Willis, Spectrochim. Acta, 17 (1961) 710.
8 W. Slavin, At. Absorpt. Newsl., 10 (1963) 1; Atomic Absorption Spectroscopy, Inter-science, New York, 1968.
9 IUPAC Compendium of Analytical Nomenclature, Pergamon Press, Oxford, 1978, p. 131
10 J. E. Allan, Analyst, 83 (1958) 466.
11 D. J. David, Analyst, 83 (1958) 655.
12 J. B. Willis, Nature, 186 (1960) 249; Spectrochim. Acta, 16 (1960) 259.
13 J. B. Willis, Nature, 184 (1959) 186; Spectrochim. Acta, 16 (1960) 273.
14 D. B. Cheek, J. E. Graystone, J. B. Willis and A. B. Holt, Clin. Sci., 23 (1962) 169.
15 J. B. Willis, Spectrochim. Acta, 16 (1960) 551.
16 J. B. Willis, Anal. Chem., 33 (1961) 556.
17 J. B. Willis, Nature, 191 (1961) 381; Anal. Chem., 34 (1962) 614.
18 J. B. Willis, in D. Glick (Ed.), Methods of Biochemical Analysis, Vol. 11, Interscience, New York 1963.
19 J. B. Willis, Aust. J. Dairy Technol., 19 (1964) 70.
20 C. M. Whittington and J. B. Willis, Plating, 51 (1964) 767.
21 J. A. Burrows, J. C. Heerdt and J. B. Willis, Anal. Chem., 37 (1965) 579.
22 V. A. Fassel and V. G. Mossotti, Anal. Chem., 35 (1963) 252.
23 W. Slavin and D. C. Manning, Anal. Chem., 35 (1963) 253.
24 F. B. Dowling, C. L. Chakrabarti and G. R. Lyles, Anal. Chim. Acta, 28 (1963) 392; 29 (1963) 489.
25 M. D. Amos and P. E. Thomas, Anal. Chim. Acta, 32 (1965) 139.
26 J. B. Willis, Nature, 207 (1965) 715.
27 M. D. Amos and J. B. Willis, Spectrochim. Acta, 22 (1966) 1325; errata ibid. p. 2128.
28 J. A. Bowman and J. B. Willis, Anal. Chem., 39 (1967) 1210.
29 A. M. Bond and T. A. O'Donnell, Anal. Chem., 40 (1968) 560.
30 A. M. Bond and J. B. Willis, Anal. Chem., 40 (1968) 2087.
31 J. B. Willis, J. O. Rasmuson, R. N. Kniseley and V. A. Fassel, Spectrochim. Acta, Part B, 23 (1968) 725; addendum, Spectrochim. Acta, Part B, 24 (1969) 155.
32 J. B. Willis, V. A. Fassel and J. A. Fiorino, Spectrochim. Acta, Part B, 24 (1969) 157.
33 J. B. Willis, Appl. Optics, 7 (1968) 1295.
34 J. B. Willis, Spectrochim. Acta, Part A, 23 (1967) 811.
35 D. A. Davies, R. Venn and J. B. Willis, J. Sci. Instrum., 42 (1965) 816; addendum, J. Sci. Instrum., 43 (1966) 406.
36 J. B. Willis, Spectrochim. Acta, Part B, 25 (1970) 487; erratum ibid. 27B (1972) 430.
37 J. B. Willis, Spectrochim. Acta, Part B, 26 (1971) 177.
38 P. Hannaford and D. C. McDonald, J. Phys. B, 11 (1978) 1177.
39 J. B. Willis, Anal. Chem., 47 (1975) 1752.
40 S. R. Koirtyohann and E. E. Pickett, Anal. Chem., 37 (1965) 601; 38 (1966) 585, 1087.
41 J. B. Willis, Proc. 7th Int. Conf. Atom. Spectrosc., (Prague, 1977), Statni Pedagogicke Nakladatelstvi, Prague, 1977, Vol. 1, p. 139.
42 J. D. Winefordner and T. J. Vickers, Anal. Chem., 36 (1964) 161.

43 A. Walsh, paper presented at ASTM meeting, San Francisco, June 1968; ASTM Special Technical Publication No. 443, p. 3.

44 P. L. Larkins, R. M. Lowe, J. V. Sullivan and A. Walsh, Spectrochim. Acta, Part B, 24 (1969) 187.

45 P. L. Larkins, Spectrochim. Acta, Part B, 26 (1971) 477.

46 P. L. Larkins and J. B. Willis, Spectrochim. Acta, Part B, 26 (1971) 491.

47 P. L. Larkins and J. B. Willis, Spectrochim. Acta, Part B, 29 (1974) 319.

48 B. J. Russell and A. Walsh, Spectrochim. Acta, 15 (1969) 883.

49 B. M. Gatehouse and A. Walsh, Spectrochim. Acta, 16 (1950) 602.

50 J. V. Sullivan, unpublished work quoted by A. Walsh, in E. R. Lipincott and M. Margoshes (Eds.), Proc. Xth Colloquium Spectroscopicum Internationale (Washington, 1962), Spartan Books, Washington, 1963, p. 127.

51 P. L. Larkins, Anal. Chim. Acta, submitted.

52 D. S. Gough, P. Hannaford and A. Walsh, Spectrochim. Acta, Part B, 28 (1973) 197.

53 R. M. Lowe, Spectrochim. Acta, Part B, 26 (1971) 201.

54 D. S. Gough, Anal. Chem., 48 (1976) 1926.

55 D. C. McDonald, Anal. Chem., 49 (1977) 1336.

56 A. Walsh, Appl. Spectrosc., 27 (1973) 335.

57 J. V. Sullivan and A. Walsh, Spectrochim. Acta, 21 (1965) 721.

58 J. V. Sullivan and J. C. Van Loon, Anal. Chim. Acta, 102 (1978) 25.

59 R. M. Lowe, Spectrochim. Acta, Part B, 31 (1976) 257.

60 J. V. Sullivan, Anal. Chim. Acta, 105 (1979) 213.

61 J. V. Sullivan, Anal. Chim. Acta, in press.

62 W. Grimm, Naturwissenschaften, 54 (1967) 586.

63 W. Grimm, Spectrochim. Acta, Part B, 23 (1968) 443.

64 D. S. Gough and J. V. Sullivan, Analyst, 103 (1978) 887.

65 J. A. Bowman, J. V. Sullivan and A. Walsh, Spectrochim. Acta, 22 (1966) 205.

66 R. M. Lowe, Spectrochim. Acta, Part B, 24 (1969) 191.

67 P. D. Lloyd and R. M. Lowe, Spectrochim. Acta Part B, 27 (1972) 23.

68 P. A. Bennett, J. V. Sullivan and A. Walsh, Anal. Biochem., 36 (1970) 123.

69 J. V. Sullivan and A. Walsh, Spectrochim. Acta, 21 (1965) 727.

70 J. V. Sullivan and A. Walsh, Spectrochim. Acta, 22 (1966) 1843.

71 J. A. Bowman, Anal. Chim. Acta, 37 (1967) 465.

72 P. L. Boar and J. V. Sullivan, Fuel, 46 (1967) 47.

73 P. L. Boar and J. V. Sullivan, Fuel, 46 (1967) 230.

74 J. V. Sullivan, A. B. Timms and P. A. Young, Proc. Aust. Inst. Mining Metall., No. 226, Part 1 (1968) 31.

75 J. V. Sullivan and A. Walsh, Spectrochim. Acta, Part B, 23 (1967) 131.

76 J. V. Sullivan and A. Walsh, Appl. Opt., 7 (1968) 1271.

77 A. Walsh, Analyst, 100 (1975) 764.

78 P. L. Larkins and A. Walsh, Proc. Int. Conf. on Heavy Metals in the Environment, (Toronto, 1975), Vol. 1, p. 249.

79 A. Walsh, Pure Appl. Chem., 49 (1977) 1621.

80 K. Yasuda, Anal. Chem., 38 (1966) 592.

81 K. Yasuda, Jpn. Anal., 17 (1968) 289.

82 C. F. Bruce and P. Hannaford, Spectrochim. Acta, Part B, 26 (1971) 207.

83 P. Hannaford and R. M. Lowe, J. Phys. B, 9 (1976) 2595.

84 P. Hannaford and R. M. Lowe, Phys. Rev. Lett., 38 (1977) 650.

85 P. Hannaford and R. M. Lowe, Anal. Chem., 49 (1977) 1852.

86 J. V. Sullivan and J. T. Woodcock, Proc. Aust. Inst. Mining Metall., No. 248 (1973) 1.

87 G. F. Box and J. R. Meldrum, Aust. J. Instrum. Control, 29 (3) (1973) 74.

88 P. L. Larkins and J. R. Meldrum, Anal. Biochem., 63 (1975) 255.

89 P. L. Larkins and J. R. Meldrum, Aust. J. Instrum. Control, 30 (5) (1974) 12.

90 E. G. Davis, M. L. Rooney and P. L. Larkins, J. Appl. Polym. Sci., 19 (1975) 1829.

91 J. J. McNeill, Records Aust. Acad. Sci., 3 (1) (1974) 30.

STOPPED FLOW AND MERGING ZONES — A NEW APPROACH TO ENZYMATIC ASSAY BY FLOW INJECTION ANALYSIS

J. RŮŽIČKA* and E. H. HANSEN

Chemistry Department A, The Technical University of Denmark, Building 207, DK-2800 Lyngby (Denmark)

(Received 1st December 1978)

SUMMARY

Four alternative flow injection methods based on the concept of merging zones have been developed for the assay of glucose in serum with glucose dehydrogenase. Special attention has been paid to the dispersion and synchronization of the merging zones and to methods of measuring the blank value of serum. The optimal procedure, based on rate measurements, allows the assay of glucose to be done at a rate of 100 determinations per hour, with the analytical readout available 30 s after sample injection. The assay requires less than one unit of enzyme per sample.

Flow injection analysis has so far been performed by injecting a defined sample zone into a continuously moving stream of reagent [1, 2]. The concentration profiles formed on the interface between the sample zone and the reagent-containing carrier stream have been exploited for a variety of analytical purposes, with a number of flow-through detectors [3]. It has also been recognized that the dispersion of the sample zone on its way towards the detector is due to the forward movement of the fluid as it flows through the open narrow tubes. Depending on the intended analytical application, limited, medium, or large dispersion of the sample zone can be achieved by an appropriate design of the flow injection system. For theoretical reasons [2], it was decided to define the dispersion in the system, D_t, as the ratio of the concentrations of the sample solution before (C_0^0) and after (C^{max}) the dispersion process has taken place in those elements of fluid which correspond to the maximum on the dispersion curve (Fig. 1):

$$D_t = C_0^0/C^{max} = H_0^0/H^{max}$$

Thus, after appropriate calibration, simply the peak height H^{max} can be used to measure dispersion.

As long as the carrier stream moves forward, the dispersion for a given flow rate and a given tube diameter is a function of either tube length L or residence time T:

$$D_t = D_i \, const_1 \, L^{1/2} \text{ or } D_t = D_i \, const_2 \, T^{1/2}$$

(D_i being the dispersion associated with the process of injecting the sample volume and $const_1$ and $const_2$ being the system constants describing the mixing intensity [2]). Should, however, the carrier stream cease to move, dispersion of the sample zone will stop and D_t will thus remain constant, i.e., independent of T. It was indeed proved that the movement of the carrier stream can be controlled exactly down to complete standstill, so that any desired portion of the sample zone can be held within the flow cell (Fig. 2). Such a stop-flow approach has obvious implications for performing kinetic assays, as the course of the chemical reaction can be continuously monitored in a single flow-through detector [2].

In contrast to conventional stopped-flow systems [4, 5] in which sample and reagent solutions are completely mixed by force in a special chamber, the stopped-flow injection method exploits the concentration profiles formed along the sample zone in order to obtain the optimum degree of the dispersion. Therefore, as the mixing takes place in ordinary tubing without any special auxiliaries, the apparatus is simple to construct. The working cycle, flow-stop-flow, may be as short as 30 s, of which little more than half is the stop period during which the reaction rate is being measured. As no reagent is pumped during the stop period, the stop-flow injection method is less demanding on reagent consumption — an important aspect in enzymatic assays.

A further reduction of reagent consumption can be achieved by applying the merging-zone principle, recently proposed independently by Bergamin et al. [6] and Mindegaard [7]. Potential applications of this principle are numerous:
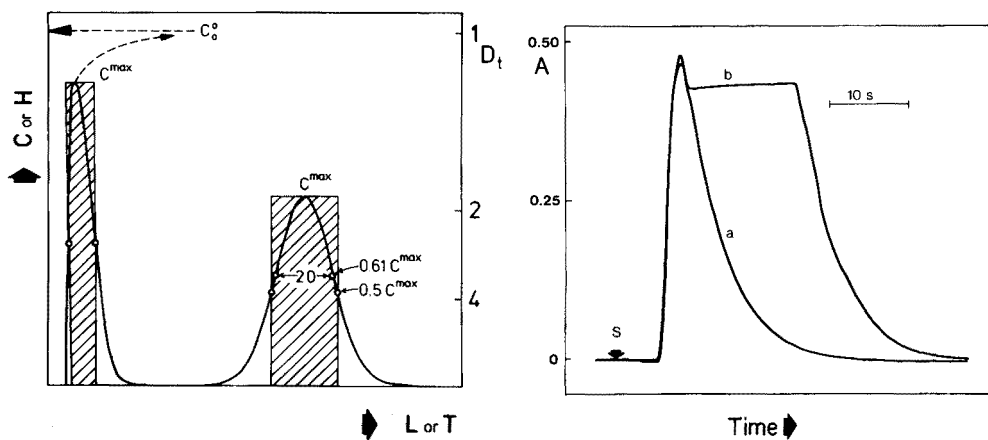

Fig. 1. The total dispersion D_t of the sample, of original concentration C_0^0, is a function of the tube length L or of the residence time T, and can be computed from C^{max} or peak height H^{max}.

Fig. 2. Dispersion of the sample zone during a 40-s flow/stop/flow cycle. S, sample injection; A, absorbance recorded as the colourless carrier stream and the blue sample zone (26.5 μl) pass through the flow cell (cf. manifold Fig. 13). (a) Continuous flow; (b) stopped flow (T = 7.6 s, stop delay time 2.0 s, stop time 15 s).

while Bergamin et al. [6] suggested this approach to reduce the consumption of the lanthanum reagent required for assaying calcium by atomic absorption spectrometry [8], Mindegaard [7] applied unsynchronized merging zones for the analysis of highly concentrated samples of albumin to avoid their manual predilution prior to reaction with bromocresol green.

In conventional flow injection analysis, the sample zone is injected into a continuous stream of reagent which fills the entire system except for the sample zone. In contrast, the merging zone principle is based on the simultaneous injection of the sample and the reagent zones into two separate carrier streams which then meet in a controlled manner (Fig. 3). As distilled water (or a dilute buffer-detergent mixture) is used as carrier, reagent is consumed only during actual analyses and the reagent volume may be as small as that of the sample, i.e. 30 μl or less.

Successful combination of the above two principles — stopped-flow injection with merging zones — should lead to a revision of the present concept of performing enzymatic assays, as the new method would combine the inherent advantages of both the continuous and the batch approaches, having none of their drawbacks. It would also influence current views on the use of insolubilized enzymes in continuous flow analysis, where one of the important arguments is reagent economy.

The specific reaction of glucose dehydrogenase with β-D-glucose was used as a model system to investigate various ways in which merging zones and stopped-flow methods may be combined so that a practical as well as an economical assay of glucose in serum could be developed. Special attention was given to the interferences from the variable blanks commonly encountered in clinical assays.

EXPERIMENTAL

Apparatus

The flow injection systems used were essentially the same as those described previously [2]. Reagents were pumped by a four-channel peristaltic pump (ISMATEC Minipuls, type 840). The spectrophotometer (Corning Model 256) was furnished with a Hellma flow-cell (Type 178.13, 8-μl volume, 10-mm optical path). The coils and the injection valve were assembled from the modular block system described previously [2].

Reagents

The carrier stream in all enzymatic measurements consisted of 0.12 M diammonium hydrogenphosphate, pH 7.62, containing 0.14 M NaCl. All glucose standards were prepared from an aqueous glucose stock solution (100 mmol l^{-1}) by diluting to the desired concentrations with the carrier solution. Serum samples and Monitrol serum standards were diluted (1 + 1) with the carrier solution prior to injection.

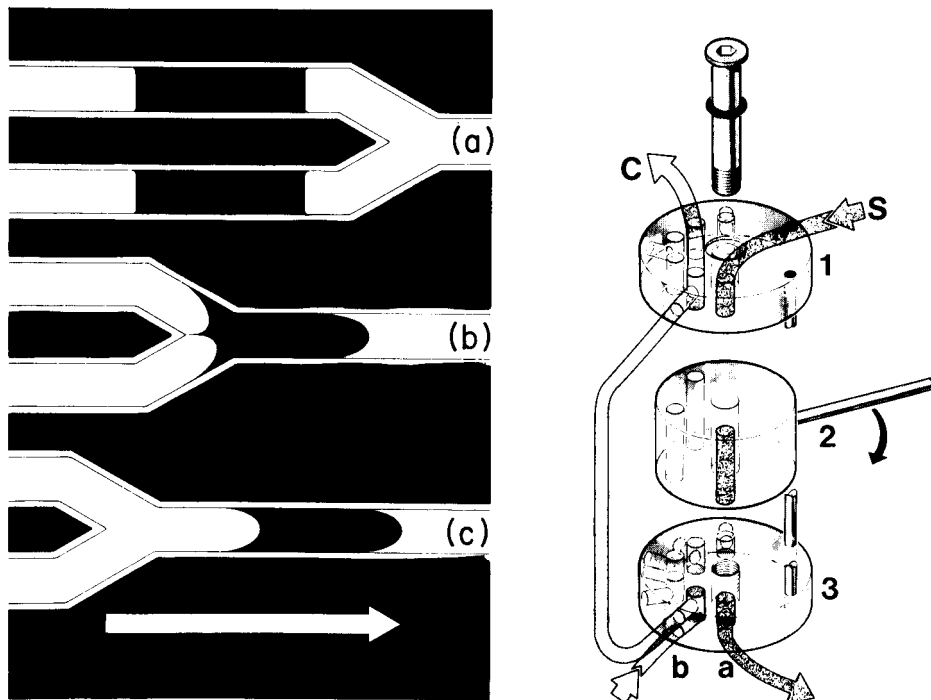The enzyme solution, containing glucose dehydrogenase, mutarotase and

Fig. 3. The synchronous merging of two zones in a symmetrical system: (from top) (a) equal sample and reagent volumes are injected, (b) merge with identical velocities after passing through equal lengths of tubing, and (c) continue downstream while being mixed and dispersed into the carrier stream.

Fig. 4. Multi-injection valve consisting of a rotor (2) sandwiched between two stators (1 and 3), the whole system being clamped together by a bolt when assembled. The rotor (20 mm high) has three volumetric bores of which one is shown filled by sample solution S, the excess of which is drained through the bottom stator at (a). In the rotor position shown, the carrier stream C bypasses the rotor through a shunt, entering the valve through the bottom stator at (b). Thus, after turning the rotor (as indicated by the arrow), the precisely measured sample zone is swept by the carrier stream into the system, because the bypass conduit has a higher hydrodynamic flow resistance [2, 7].

NADH reagent, was prepared by dissolving the components of the Merck Glucose System (Kit 14055) in the carrier solution so that the enzyme solution contained 20 kU of glucose dehydrogenase per litre. As only 10 ml of this solution was needed for the enzyme supply circuit used, only one 25-ml portion was prepared weekly by weighing out the appropriate amount of solid components from the enzyme kit. In accordance with the manufacturer's information, the components of the Glucose System were found stable in solution for at least two months. All spectrophotometric measurements were made at 340 nm.

The serum standards, Monitrol I and II (Dade) were dissolved and handled as recommended by the manufacturer.

The carrier stream for the dispersion experiments was 0.1 M sodium tetraborate. The bromothymol blue dye used for injections was dissolved in the borate carrier solution and all measurements were made at 600 nm.

DISPERSION OF ZONES AND THEIR SYNCHRONIZATION

Though the results of Bergamin [6, 8] and Mindegaard [7] demonstrated that excellent reproducibility can be obtained in a system where reagent and sample zones merge, it was decided first to perform a series of dispersion experiments in order to confirm the feasibility of synchronization of two, or several, injected zones and to compare the dispersion patterns of merging zones of equal or different volumes. For that purpose a triple injector of the sandwich type was made (Fig. 4) in which the injected volumes could be altered by using interchangeable rotors (2) with volumetric bores of different diameters (0.4—1.3 mm). The valve stators (1 and 3) are made of perspex and accommodate three groups of paired holes, of which one pair is shown on Fig. 4 to carry sample (a) and carrier stream (b). Thus, in the "sampling" position (Fig. 4) the carrier stream flows uninterruptedly through a bypass (which has approximately 500 times higher hydrodynamic flow resistance than the volumetric bore), and after the rotor (2) has been turned, the exactly measured section of the sample stream is swept by the diverted carrier stream into the system. For double and triple injection of reagent (or sample zones) the other two rotor bores are used similarly. Although it was not used for the purpose in the present work, the triple injector could very well be employed to inject the same sample material into three independent manifolds for performing multiple analyses on one sample.

The dispersion tests were made as described previously [2], i.e., by injecting a dye (bromothymol blue) into a colourless carrier stream (borate buffer) and measuring the absorbance recorded with a flow-through spectrophotometer at 600 nm. The manifold is shown in Fig. 5 where the multiple valve is used to inject "sample" through position A and "enzyme" through position B. The additional valve C, to be used later in the actual analysis, was kept open (see *Enzyme supply circuit* below). At first, 26.5 μl of a dye solution of a concentration which was denoted $C = 1$ was injected through the sample valve A, while the colourless carrier solution was pumped through all lines. The recorded curve (with the shaded area on Fig. 6) shows the shape of the concentration profile of the sample zone, the maximum of which appears at $T = 16$ s after injection. The dispersion for this "sample curve" was found to be $D_t = 10$. In the next run, a colourless solution was injected as sample (through A) while 26.5 μl of a dye solution of twice the previous concentration (i.e., $C = 2$) was injected through the "reagent valve" (B). This concentration profile of the "reagent" zone (R_2, Fig. 6) was recorded from the same starting point S as the first run. Because the flow paths (a—c—d and b—c—d), the injected volumes (26.5 μl), and the pumping rates (x and y) are equal, the residence times and the dispersions of the sample and of the
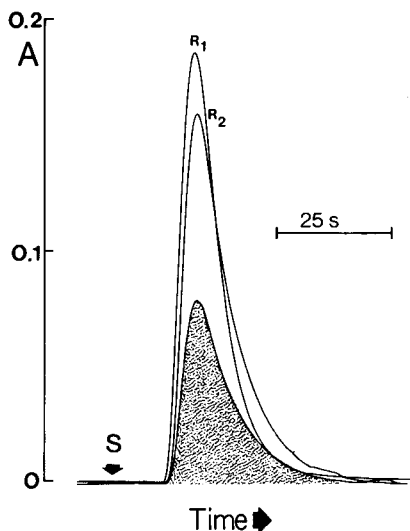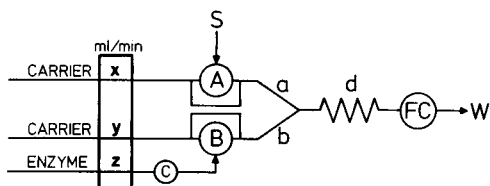
Fig. 5. Symmetrical manifold for the synchronous merging of two zones where the sample zone (S, injected at A) and the enzyme zone (injected at B) merge in the carrier stream pumped at equal rates in both channels ($x = y = 1.0$ ml min^{-1}). Tube internal diameter, 0.5 mm; tube lengths, a = b = 10 cm, and d = 30 cm (tube i.d. 0.75 mm). FC, flow cell (8 μl); W, waste; C, a separate valve used for blank experiments (see text).

Fig. 6. The synchronous merging of zones of various volumes and concentrations. S, sample injection; A, absorbance recorded as the colourless carrier solution and the coloured sample reagent zone(s) pass through the flow cell. (R_1) 10.0-μl reagent zone, concentration $C = 8$; (R_2) 26.5-μl reagent zone of concentration $C = 2$ (see text). D_t was 36 for R_1, and 10 for R_2 and the shaded sample peak (concentration $C = 1$).

reagent zones (R_2) are identical ($D_t = 10$). Further, Fig. 6 shows that when the reagent concentration is twice as high as that of the sample, a double excess of reagent to sample is present at any point of the concentration profile. It follows from flow injection theory [2] that while the concentration ratio of reagent/sample will always remain constant in the case of merging zones (except for the consumption in the required chemical reaction) and, indeed, regardless of how far the zones have travelled — this reagent/sample ratio will increase because of increasing dispersion of the sample zone alone when the sample zone is injected into a continuous carrier stream of reagent. Thus, while in the latter case the reaction is being promoted with increasing dispersion and residence time, dispersion should be minimized in the case of merging zones and the necessary reaction time should be achieved by slow pumping or by stopping the flow.

The implications of using a smaller volume of a more concentrated reagent can be seen by comparing the shaded "sample" curve with the "reagent" curve R_1 (Fig. 6) which was obtained by injecting 10 μl of a dye solution of concentration $C = 8$. Although both injected zones are carried forward at the

same speed ($x = y$), the residence times are not exactly the same ($T_{R_1} < T_{R_2} = T_S$), and the dispersion for R_1 is much higher ($D_t = 36$ for R_1 and $D_t = 10$ for R_2), because the injected volume is smaller. Close examination of the concentration profiles of curves R_1 and R_2 shows an intersection point on the falling parts of the peaks; this is due to the differences in the dispersion patterns. It was suggested [9] that these variable interface concentration gradients could be applied to develop a titration technique which would not rely on the use of a mixing chamber to obtain a concentration gradient [10].

Simultaneous injection of three separate zones into a system with one flow-through cell could conceivably be exploited for a variety of purposes. Separate blank determinations might be useful in clinical applications, where individual samples exhibit different blanks because of turbidity and the presence of various substances of natural origin as well as from drugs used medicinally. Such a system in which three zones are injected simultaneously is shown in Fig. 7 where equal volumes of sample and reagent solutions (26.5 μl) were injected by a triple valve in positions B and C (reagent) while 10 μl of sample solution were injected through the blank position A. The carrier streams (y and z) were pumped at equal rates while the blank stream was pumped twice as fast (i.e., $x = 2y = 2z$). Because the same dye concentration was used in all experiments, the same dispersion scale could be plotted (Fig. 8) for all recordings. At first the dye solution was injected through position A (Fig. 7) while the colourless carrier solution was pumped through all the lines. The recorded curve (Fig. 8 A; $D_t = 12$, $T = 5$ s) exhibits the smallest dispersion as the injected sample has passed through the shortest line. Next, curve B was recorded by injecting the dye solution through position B while colourless solution was injected through position A. The resulting concentration profile corresponds to a peak with $D_t = 19$ and $T = 20$ s. Thereupon dye was injected through both positions A and B resulting in a composite curve with two maxima. This injection experiment was repeated three times from the same starting point, and the concentration profiles were so well reproduced that the three tracks
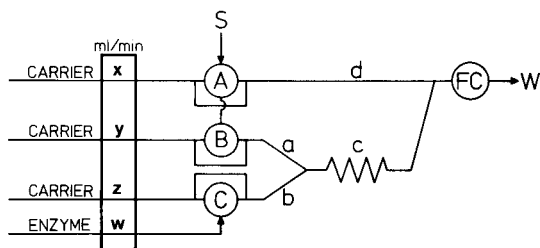

Fig. 7. Symmetrical manifold for the synchronous merging of sample (S, injected at B) and enzyme (injected at C) zones, with an asymmetrical part for the non-synchronous injection of sample S at A for blank readout. FC, flow cell; W, waste; $y = z = 1$ ml min^{-1}; $x = 2$ ml min$^-$ a = b = 10 cm (0.5 mm i.d.); c = 30 cm (0.75 mm i.d.); d = 2 cm (0.4 mm i.d.). Between the flow cell and the T-type connector (combining lines c and d) 15 cm of 0.4-mm i.d. tubing was used.
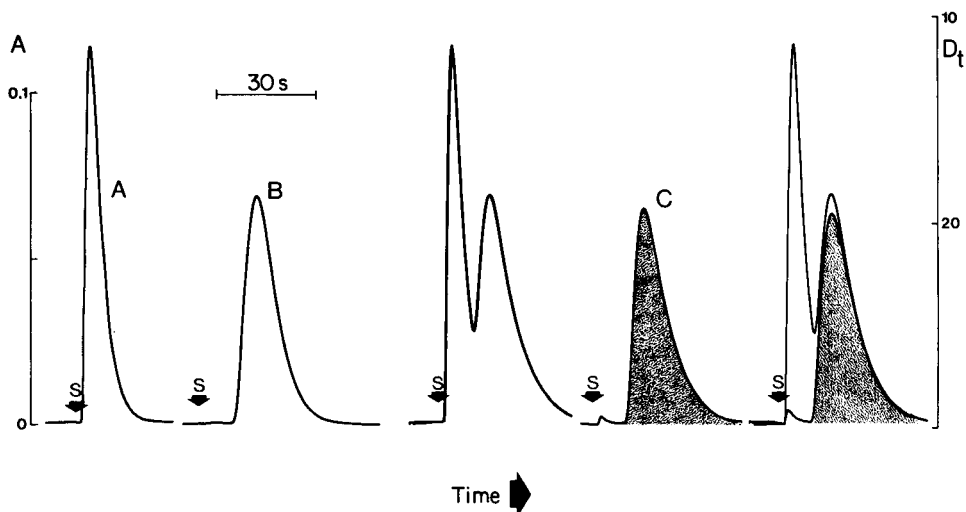
Fig. 8. Dispersion and merging of three simultaneously injected zones (manifold Fig. 7), recorded when a colourless carrier solution and a coloured sample and/or a reagent zone pass through the flow cell. (A) 10.0 μl of dye injected through the A-position, thus depicting the "blank" peak (S is the point of injection). (B) 26.5 μl of dye injected through position B, depicting the "sample" peak. The following double peak was obtained by injecting dye in positions A and B simultaneously. To demonstrate the reproducibility, this injection was repeated three times and the curves were recorded atop each other from the same starting point S in the runs shown. (C) 26.5 μl of dye injected through position C, depicting the "enzyme" peak (shaded). The last run on the right shows all three previous experiments combined in two recordings (A + B and C), which demonstrates that there is no enzyme present when the blank peak is recorded.

are practically identical (Fig. 8). The "reagent" profile was recorded by injecting the dye solution through position C and colourless solution through sample positions A and B. The resulting "reagent" profile (shaded curve C, Fig. 8) is, as one would expect, identical with "sample" curve B. The final two runs, composed of two "sample" and one "reagent" dye injections, recorded from the same injection point, demonstrate perfect synchronization of the respective concentration zones, of which the first (blank) passes through the detector without being mixed with the reagent zone (shaded), while the second exactly coincides with the reagent zone.

THE ENZYMATIC ASSAY OF GLUCOSE IN SERUM

The specific reaction of glucose dehydrogenase (GDH) with β-D-glucose as described by Banauch et al. [11]:

$$\alpha\text{-D-glucose} \xrightarrow{\text{mutarotase}} \beta\text{-D-glucose} \xrightarrow[\text{NAD}^+]{\text{GDH}} \text{D-glucono-}\delta\text{-lactone} + \text{NADH} + \text{H}^+$$

has been successfully used for the determination of glucose in serum by manual methods [11—13] with deproteinization, by an AutoAnalyzer procedure with dialysis [12], and by an f.i.a. method based on two detectors for two-point kinetic assay [14]. The glucose dehydrogenase used here is commercially available in an enzyme kit [13], in which nicotinamide adenine dinucleotide (NADH) acts as the indicator. Spectrophotometry of NADH at 340 nm is widely used in clinical enzymatic assays, hence any blanking and detection problems associated with the use of NADH should be of general interest.

As the enzyme solution was intended only to be injected intermittently, an enzyme supply circuit (Fig. 9) was designed. For each injection of 26.5 μl of enzyme solution 26.5 μl of the carrier solution is added to the enzyme supply. This is a mere dilution of the enzyme stock solution as the carrier stream consists of the same buffer as that in which the enzyme is dissolved. The enzyme solution can, therefore, be either circulated or saved in the collecting container (Fig. 9), which then is intermittently exchanged for the supply container.

Single point determination with separate blanking

In the previous work with glucose dehydrogenase [14], 50% of the maximum signal achievable in the f.i.a. system was reached at $T = 17$ s. The manifold (Fig. 5) used in the dispersion and synchronization tests was designed with this in mind and it is therefore directly suitable for the assay of glucose. The sample and the reagent volumes were chosen equal, i.e., 26.5 μl, and because the travel paths of sample and reagent zones are identical, the same dispersion (D_t) is obtained for both merging zones, which are also identical in shape. The concentration of enzyme in the previous f.i.a. method [14], where the solution was continuously pumped, was 5 kU l^{-1}. In the present case, however, where the enzyme zone is diluted ten times by dispersion ($D_t = 10$, cf. Fig. 6) when it reaches the detector, it was necessary to increase the enzyme concentration to 20 kU l^{-1}; at lower enzyme concentrations a deviation from linearity was observed for the high glucose standards.

The calibration run (Fig. 10, left) confirms the reproducibility of the assay,
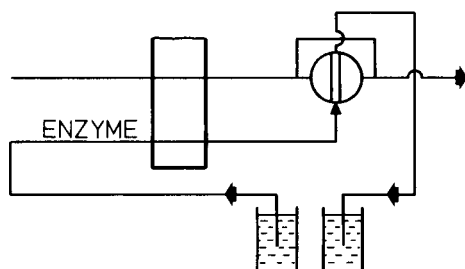

Fig. 9. The enzyme supply circuit used. The pumping rate of enzyme was 0.5 ml min^{-1}. The volume of injected enzyme solution was 26.5 μl, the total volume of the circulating enzyme solution being 10 ml. The carrier stream was pumped through the unmarked pump tube.

which can be carried out at a rate of 120 injections per hour with a linear response for glucose up to 15 mmol l^{-1}. For serum analysis, however, it was necessary to measure a blank value in the absence of enzyme. This was done by injecting the sample while valve C (Fig. 5) was closed. This separate blanking procedure yielded values within the expected range for the Monitrol I and Monitrol II standards (Table 1). Although the observed blank values were
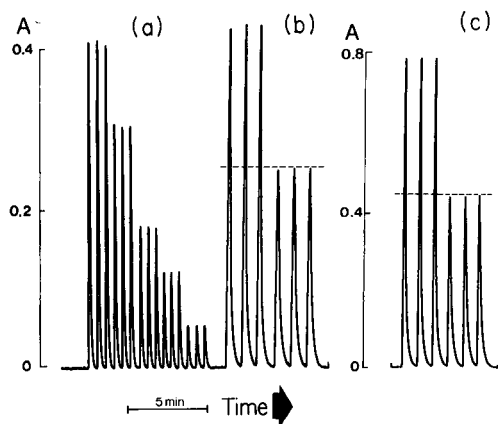

Fig. 10. Determination of glucose with separate blank runs in the manifold shown in Fig. 5. The three groups of peaks show, from left to right, the analysis of: (a) aqueous glucose standards containing 15.0, 10.0, 5.0, 3.0, and 1.0 mmol l^{-1}; (b) Monitrol I serum standards (diluted 1 + 1 with carrier stream solution prior to injection), injected in the presence and then in the absence of enzyme (valve C, Fig. 5, closed) so that the dotted line depicts the blank value; (c) Monitrol II serum standards analysed in the same manner as Monitrol I. All samples injected in triplicate.

TABLE 1

Determination of the glucose contents in standard serum samples with glucose dehydrogenase by four different flow-injection procedures based on the merging zones principle (All values are expressed in mmol l^{-1}, as the means of three measurements; all Monitrol serum standards were diluted 1 + 1 prior to injection.)

Method	Sample				Note
	Monitrol I		Monitrol II		
	Found	Assigned	Found	Assigned	
Continuous flow					
Separate blank	5.0	5.55[a]	11.3	12.4[a]	Fig. 10
Simultaneous blank	4.4	(4.55—6.55)[b]	11.2	(11.4—13.4)[b]	Fig. 12
Stopped flow					
Peak maximum	4.6		12.4		Fig. 14
Fixed time	4.3		13.0		Fig. 16

[a] Values stated by the manufacturer based on the Merck glucose dehydrogenase reaction.
[b] Confidence limits.

nearly as high as the signal resulting from the enzymatic reaction (Fig. 10, right), the single-point assay with separate blank runs yielded reliable results with an enzyme consumption of less than one unit per determination.

The above approach requires each sample to be injected twice and thus the effective sampling rate is decreased to 60 determinations per hour (with a total serum consumption of 26.5 μl per assay as the sample material is diluted $(1 + 1)$ prior to injection). Attempts were therefore made to perform the same type of analysis with a single injection of sample solution by employing the triple valve as indicated in Fig. 7. Comparison of Figs. 5 and 7 shows that only the blanking part of the manifold, with injecting position A (10 μl), has been added to the previous system. Yet, as the blank carrier stream is pumped at a rate of 2 ml min^{-1} ($x = 2y = 2z$) and all streams are mixed before the flow cell, the reagent and sample zones have nearly twice as high dispersions ($D_t = 19$) as in the double-injection method so that the peak heights are correspondingly reduced (compare Fig. 10 and 11). Furthermore, as the blank passes through a shorter line than the sample, these two zones disperse in different ways so that their peak ratio has to be measured by a dispersion experiment. Although this value reflects the ratio of the respective D_t values of the blank and the sample zones, it does not exactly correspond to the separately measured peaks heights (Fig. 8, A and B) for which were found D_t (blank) = 12 and D_t (sample) = 19 yielding a ratio of 0.63, whereas the corresponding ratio is
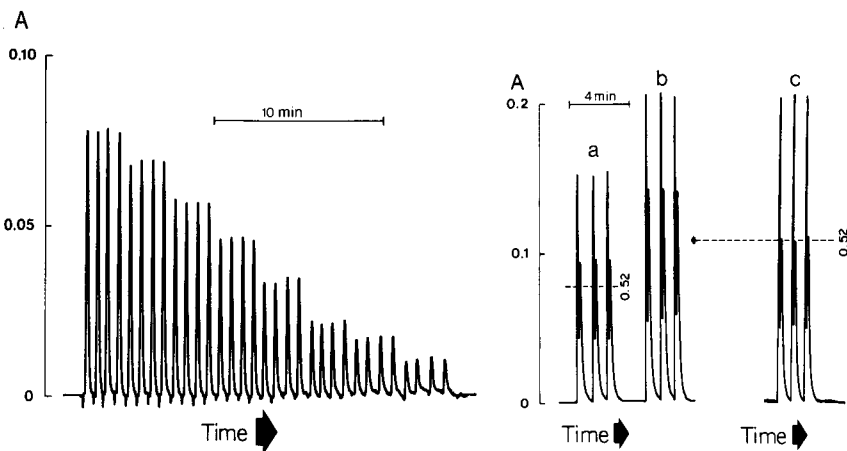

Fig. 11. The calibration graph for the determination of glucose with simultaneous blank runs in the manifold shown in Fig. 7 (dispersion tests, Fig. 8) obtained by injecting (in quadruplicate) aqueous glucose standards containing 15.0, 12.5, 10.0, 7.5, 5.0, 2.5, 1.5, and 0.5 mmol l^{-1}. Note the absence of blank peaks.

Fig. 12. Determination of glucose in standard serum samples Monitrol I (a) and Monitrol II (b) with simultaneous blank runs. Group (c) shows Monitrol II injected in the absence of enzyme, thus yielding the blank correction coefficient of 0.52 between the first and the second sample peak. All injections performed in triplicate.

0.60 for the single simultaneous injection method because of a small carry-over from blank to sample zone, and a value of 0.52 for sera of different viscosity (cf. Fig. 12).

The calibration traces obtained with the triple injection system (Fig. 11) show only one peak per injection, as the aqueous glucose standards do not exhibit any blank value. (There is, for unknown reasons, a very small negative peak instead of a blank for the highest glucose standards.) The actual serum analyses (Fig. 12), shown for Monitrol I (curves a) and Monitrol II (curves b), yielded for each injection a double peak, the first maximum always being the serum blank. After correction for the difference between the blank and sample zone dispersions by a factor of 0.52, which was obtained by injecting Monitrol II in the absence of enzyme (Fig. 12, curve c), the difference between the heights of the first and second maxima on each double peak was used to read out the glucose content from the calibration graph (Table 1). Although the glucose contents in the serum samples, as obtained by the triple-injection method, yielded results within the expected range, it is obvious that the analytical readout is far from reliable because of the inherently unfavourable blank/sample ratio. Though this ratio conceivably could be improved by further decreasing the volume of serum injected in the blank line and by changing the pumping ratios in favour of the reaction lines (e.g. $x = y = z$), it was decided that for serum analyses, where at 340 nm the blanks on clinical samples are often even higher than those found for Monitrol standards, this approach is not feasible. Thus, instead of separate blank runs, simultaneous blanking with a single sample zone was attempted by a stopped-flow method.

Multipoint determination with simultaneous blanking

Regardless of whether the stopped-flow injection assay is done with a continuous stream of enzyme solution [2] or by the use of the merging zones principle, it ought to be designed in such a way that the recorded curve will reflect a suitable portion of the reaction rate curve monitored while the sample zone is being held within the flow cell. In order to obtain a maximum signal/blank ratio, as much as possible of the enzymatic reaction should take place within the flow cell, and therefore the merged zones should pass to the flow cell through a very short length of tubing (Fig. 13, line c). In the system
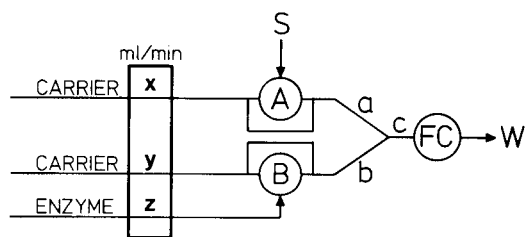

Fig. 13. Manifold for the stopped-flow injection analysis of glucose. S, sample injection through position A (26.5 or 10.0 μl); B, enzyme injection (26.5 μl); a = b = 10 cm; c = 20 cm; all tubes 0.5 mm i.d. $x = y = 1.0$ ml min^{-1}.; FC, 8-μl flow cell; W, waste.

depicted, the sample zone reaches the flow cell ca. 8 s after injection, and is held there for 20 s during which the reaction rate is recorded; the measuring cycle is concluded by a washout period of 12 s (Fig. 2), thus permitting a sampling rate of 120 determinations per hour.

Although the manifold for the merging zones method is simple to assemble, the obvious difficulty is to stop reproducibly always at the same section of the sample zone within the flow cell. Exact timing is essential because dispersion gives a concentration profile in which the sample/enzyme or sample/enzyme/carrier stream ratio changes continuously along the sample zone. The slope of the reaction-rate curve would therefore change correspondingly, yielding its maximum value when the zone is stopped in the detector atop a peak. Accordingly, the feasibility of the stopped-flow method depends on how this variable can be fixed, i.e., on locating and stopping precisely the same segment of the dispersed zone in the flow cell on each run. Two approaches were tested and compared, one based on electronic identification of the peak maximum — subsequently referred to as the peak maximum method — and the other on fixing the exact time interval between sample injection and arrival of the zone into the detector — the fixed time method.

Peak maximum method. This was investigated with the help of the peak maximum location electronic device described earlier [15] in connection with the use of ion-selective electrodes in the f.i.a. system, where the digital readout of the maximum peak height was needed. Such a device was coupled to the peristaltic pump via a time delay/stop/start switch so that the pump could be stopped for any period between 5 s and 25 s at any chosen time delay (0.1—5 s) after the peak maximum had passed through the detector. A set of analyses carried out with this set-up is shown in Fig. 14, which depicts a series of aqueous glucose standards, followed by Monitrol I and Monitrol II serum standards. In this run, where the time from the starting point to the peak maximum plus the stop delay time was 8 + 1 s and the measuring—stop period was 20 s — identical with the dispersion experiment shown in Fig. 2 — the recorder chart movement was electronically stopped whenever the colorimeter output signal was lower than the level indicated by the dotted line. The dotted line also indicates the minimum detector output which had to be exceeded so that the electronic device would recognise the transformation of the output signal as approaching a peak; otherwise any large fluctuations of the baseline could be mistaken for a maximum. This electronic function eventually proved to be a weakness of the system, because some serum samples caused unexpected negative deviations of the baseline, which were so large that the detector output even at peak maximum did not exceed the critical trigger level and the pump did not stop. Although only occasional samples caused the stop system to fail in this way, it was decided to turn to another system based on the fixed time interval.

Fixed time method. This is based on exact measurement of the residence time T while the system pumps continuously, and on subsequent adjustments of the electronic timer to stop the pump either to the exact T-value (peak maximum)
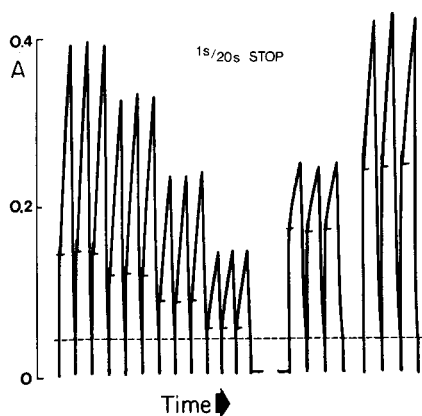
Fig. 14. Stopped-flow injection analysis of glucose by the peak maximum location device. The pump was stopped 1.2 s after the peak maximum appeared in the flow cell and the stop period lasted for 20 s. The dotted line indicates the threshold level of the output signal (see text). All samples (26.5 μl) were injected in triplicate. From left to right: aqueous glucose standards containing 10.0, 7.5, 5.0, and 2.5 mmol l^{-1}, followed by Monitrol I and Monitrol II standard serum samples (diluted 1 + 1 by carrier stream prior to injection).
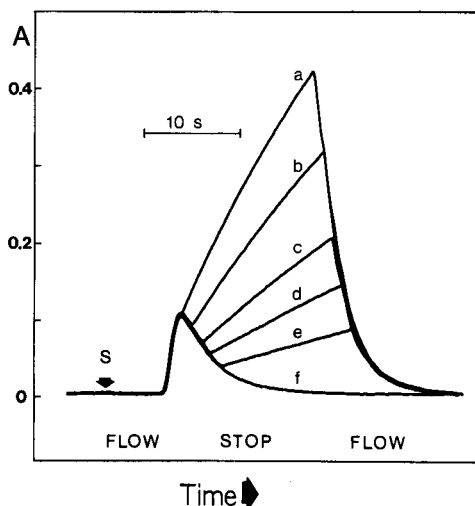
Fig. 15. Stopped-flow analysis of glucose by the fixed-time method showing the influence of increasing stop delay time on the slope of the reaction-rate curve. With a residence time T = 7.6 s, and stop delay times of 0.2, 1.2, 2.2, 3.2, and 4.2 s, followed in each case by a stop period of 15 s, curves a to e — as well as a continuous run (curve f) — were recorded on the same chart from the same starting point S. An aqueous glucose standard containing 10 mmol l^{-1} was injected. The manifold was that shown in Fig. 13; sample volume and enzyme volume were each 26.5 μl.

or to T plus a delay. This simple approach proved to be far more reliable, as the stopping of the zone is affected neither by changes in the baseline level nor by unusually high (or negative) blank values of individual samples. As this approach relies on the constancy of the flow rate it was feared, however, that the flow generated by a peristaltic pump would change so rapidly that frequent recalibration of the instrument would be needed. Fortunately, it was found that the increase of the residence time T was so slow and gradual that after an initial calibration a check with two standard solutions about twice an hour was satisfactory.

For the assay of glucose the system used (Fig. 13) had the flow rates $x = y = 1$ ml min^{-1}, and tube lengths $a = b = 10$ cm of 0.5-mm i.d. tubing linked via a T-connector to $c = 20$ cm (0.5 mm i.d. tubing). When 26.5 μl of enzyme solution and 26.5 μl of glucose solution (10 mmol l^{-1}) were injected, the residence time was found to be 7.6 s (Fig. 15, curve f). If the flow was stopped, the slope of the rate curve obtained depended on which section of the dispersed

sample zone was held within the flow cell for the measurement. Thus, by increasing the stop delay time from 0.2 s (curve a) to 4.2 s (curve e), a series of curves was recorded on top of each other from the same starting point (S) with the stop delay time increasing in steps of 1.0 s, the stop for each curve lasting 15 s. It follows from Fig. 14 that a measuring cycle, i.e., flow—stop—wash, is completed within 32 s, which permits a sampling frequency of 110 determinations per hour. Further, the mixing ratio between the sample, enzyme and carrier streams can be finely adjusted by appropriate choice of the stop delay time as reflected by the changing slope of the rate curve. Although this is not an important variable when aqueous samples of glucose are analyzed, it proved to be crucial in serum analyses.

The higher the viscosity of the injected sample, the lower its dispersion will be [16], and therefore the sample zone will be less effectively mixed with the carrier stream and with the merging reagent zone. This is why the viscosity of the serum samples has to be decreased before analysis by dilution with a buffer (or another aqueous solution) so that differences in viscosities between sera and aqueous standards do not influence the analytical result. Some combination of manual pre-dilution (1 + 1 or 1 + 2), which saves serum material, and auto-matic dilution, by a suitably chosen dispersion of the sample zone in the f.i.a. system, is necessary, otherwise the aqueous and serum standards will not yield comparable results. In the stopped-flow method, the sample zone should reach the flow cell as rapidly as possible; yet that portion of it which is to be measured must be sufficiently well mixed with the enzyme zone. Therefore, when 26.5-μl serum samples were injected into the stopped-flow system (Fig. 13) and the flow was stopped 7.8 s after injection, i.e. a stop delay time of 0.2 s (Fig. 15, curve a), it was not possible to obtain agreement between the aqueous glucose standards and the serum standards Monitrol I and Monitrol II, although the precision of measurement on all three sample materials was satisfactory. When the stop delay time was increased to 1.2 s, better agreement was found; when the zone was stopped 3.2 s after T, the analyses of the serum standards were both accurate and precise because the original difference in the viscosities of the mixed fluids was no longer reflected in the portion of the sample zone which was stopped in the flow cell. However, the theory of dispersion [2] indicates that the dilution of sample material is preferably achieved by reducing the sample volume and therefore for the final approach the sample volume was reduced to 10 μl. This allowed a slight decrease of the stop delay time to 2.0 s, and with a stop period of 20 s and a wash period of 5 s the total working cycle, including $T = 7.6$ s, became 35 s. The calibration curve and the analyses of Monitrol I and II, performed at a rate of 100 samples per hour, is shown in Fig. 16, while the results of these analyses are given in Table 1.

DISCUSSION AND CONCLUSION

The merging zone principle allows enzymatic assays to be done either on a continuous (single point) or a stopped-flow basis (rate measurement) with
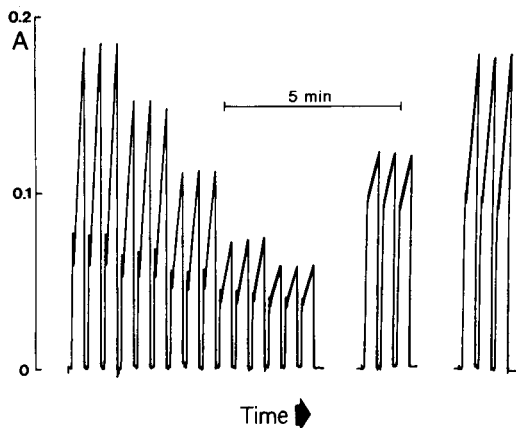
Fig. 16. Stopped-flow analysis of glucose in serum by the fixed-time method. Sample volume, 10.0 μl; enzyme volume, 26.5 μl; all samples injected in triplicate. From left to right is shown a series of aqueous glucose standards containing 10.0, 7.5, 5.0, 2.5, and 1.5 mmol l^{-1}, Monitrol I and Monitrol II. The stop delay time was 2.0 s and the stop period was 20 s, yielding a sampling cycle of 35 s, i.e., a sampling rate of 100 determinations per hour.

minimum reagent consumption. Thus, in the present work, less than one unit of glucose dehydrogenase was used per determination. With the stopped-flow method, analyses were possible at a rate of 100 determinations per hour, with the analytical readout available ca. 30 s after sample injection. Surprisingly, the greatest difficulty in developing the methods for glucose determination in serum was not associated with synchronization of the reagent and sample zones or the exactness of injecting these solutions reproducibly, but difficulties in eliminating the relatively high (and variable) blanks encountered with serum samples when monitoring the NAD-NADH indicator system at 340 nm. As the serum samples are more viscous than the aqueous standards, it was necessary to predilute them manually at least 1 + 1 with the carrier stream buffer, and to design the manifold so that at least D_t = 5 was obtained before the sample zone reached the flow cell. As far as the various procedures are concerned, the first method with separate blank runs requires the simplest experimental set-up, but two separate injections have to be made if the blank value is significant in the assayed material. The fixed-time stopped-flow method is the best choice as it yields the blank value, the analytical read-out and information on the reaction rate curve on one sample injection within less than 30 s.

Immobilized enzymes have been very widely studied for analytical work since Updike and Hicks [17] published their pioneering work on "reagentless" systems. There are several reasons for the use of immobilized enzymes in columns [18, 19] or as inner coatings of tubes [20] which serve as reactors in continuous flow systems. Better selectivity and time stability of the insolubilized enzymes are often quoted [19—21], but the main reason is undoubtedly the enzyme economy. However, there are various drawbacks to this approach:

loss of activity caused by loss of enzyme from the column [19, 20], gradual occlusion of the active surfaces and blocking of the column by particulate matter (invariably present in serum), and compressibility of column material which causes increase of the back-pressure and eventual decrease of the flow [19]. Furthermore, there is a difficulty in obtaining a blank measurement (for which an inactive column must be connected in parallel [18]), and the impossibility of performing multipoint rate measurements. Thus, although the enzyme is not consumed in the chemical reaction, losses are inevitable, and in order to have sufficient activity in reserve, large amounts of enzyme must be used in preparing reactors. Since the exact enzyme balance is difficult to assess, only an estimate can be made. From this it appears that on a normal column the enzyme consumption is about the same as in the present work, because usually several hundreds [18] up to a thousand [19] enzyme units are immobilized on a column which allows several hundred assays to be done [18, 19]. Besides, the maximum attainable sampling frequency on a column system (e.g. ca. 40 samples per hour [19]) will always be lower than in an open-tube system because contact between all volume elements of the sample zone with the solid surfaces has to be established; adequate mixing of two liquid zones in the flow injection system is rapidly accomplished with low dispersion.

The present paper describes a model system which indicates the advantages and drawbacks of the merging zone concept combined with the stopped flow method; obviously, the system could also be used for the measurement of enzymatic activity.

The flow injection method allows the concentration gradients formed between the sample, reagent and carrier streams to be exploited. In the example given here, stopping the stream with a suitable time delay makes it possible to select for measurement a section of the sample zone in which the ratio between the reacting components is at an optimum. The multitude of means by which dispersion and timing can be manipulated and the different concentration profiles that can be created makes the flow injection method very flexible. Furthermore, exactness of timing and well-controlled movement of the unsegmented streams makes these measurements reproducible. The greatest experimental difficulty in the present work was to overcome the difference in viscosities between sample and standard solutions for D_t values smaller than about five. The limitation of the flow injection method for rate measurements appears to be the speed of mixing which, for very fast reaction rates, would impede the measurement. The theory of mixing within the zone itself has still to be worked out. Little is known about the mixing pattern when two zones merge although it is certain that the zones are not mixed homogeneously. Though the influence of the geometry of the confluence point at which the two streams meet cannot be seen on the peak shapes if a mixing coil is placed between the mixing point and the detector, there is marked difference between T, Y, and F-shaped confluence points on the peak shape when the mixing coil is omitted. There are several ways in which reagent and sample zones can be

made to merge: synchronously as used above, non-synchronously as suggested by Mindegaard [7], or even by injecting them in the same tube and letting them "chase" each other — an approach employed most recently by Krugg [22] in turbidimetry, (cf. Fig. 21 of [2]). The stopped-flow approach has implications far beyond enzymatic assays as it is useful not only for rate measurements, but also if flow injection should be considered for the automation of chemistries involving very slowly reacting components.

REFERENCES

1 J. Růžička and E. H. Hansen, Anal. Chim. Acta, 78 (1975) 145.
2 J. Růžička and E. H. Hansen, Anal. Chim. Acta, 99 (1978) 37.
3 D. Betteridge, Anal. Chem., 50 (1978) 832 A.
4 A. C. Javier, S. R. Crouch and H. W. Malmstadt, Anal. Chem., 41 (1969) 239.
5 P. M. Beckwith and S. R. Crouch, Anal. Chem., 44 (1972) 221.
6 H. Bergamin F°, E. A. G. Zagatto, F. J. Krugg and B. F. Reis, Anal. Chim. Acta, 101 (1978) 17.
7 J. Mindegaard, Anal. Chim. Acta, 104 (1979) 185.
8 E. A. G. Zagatto, F. J. Krugg, H. Bergamin F°, S. S. Jorgensen and B. F. Reis, Anal. Chim. Acta, 104 (1979) 279.
9 A. Ramsing, private communication.
10 J. Růžička, E. H. Hansen and H. Mosbæk, Anal. Chim. Acta, 92 (1977) 235.
11 D. Banauch, W. Brümmer, W. Ebeling, H. Metz, H. Rindfrey, H. Lang, K. Leybold and W. Rick, Z. Klin. Chem. Klin. Biochem., 13 (1975) 101.
12 A. Scholer and A. Pianezzi, J. Clin. Chem. Clin. Biochem., 14 (1976) 189.
13 W. Brümmer and W. Ebeling, Kontakte, No. 2 (1976) 3.
14 E. H. Hansen, J. Růžička and B. Rietz, Anal. Chim. Acta, 89 (1977) 241.
15 J. Růžička, E. H. Hansen and E. A. Zagatto, Anal. Chim. Acta, 88 (1977) 241.
16 D. Betteridge and J. Růžička, Talanta, 23 (1976) 409.
17 S. J. Updike and G. P. Hicks, Science, 158 (1967) 270.
18 B. Mattiasson, B. Danielsson and K. Mosbach, Anal. Lett., 9 (1976) 867.
19 R. S. Schifreen, D. A. Hanna, L. D. Bowers and P. W. Carr, Anal. Chem., 49 (1977) 1929.
20 B. Watson and M. H. Keyes, Anal. Lett., 9 (1976) 713.
21 D. N. Gray, M. H. Keyes and B. Watson, Anal. Chem., 49 (1977) 1067 A.
22 F. J. Krugg, private communication.

BIAMPEROMETRIC DETERMINATION OF GLYCEROL AND TRIGLYCERIDES WITH OPEN TUBULAR CARBON ELECTRODES IN FLOW STREAMS

ABDULRAHMAN S. ATTIYAT and GARY D. CHRISTIAN*

Department of Chemistry, University of Washington, Seattle, WA 98195 (U.S.A.)
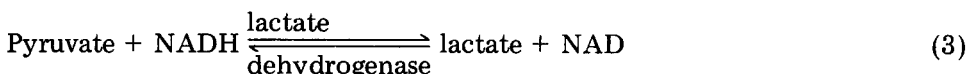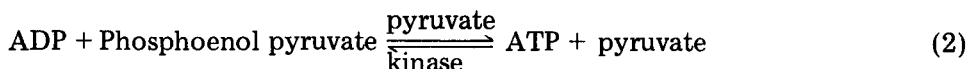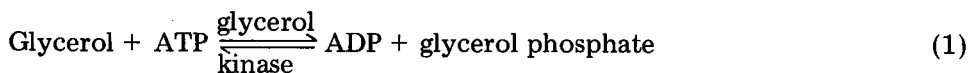
(Received 11th September 1978)

SUMMARY

Biamperometric measurements, with open tubular carbon electrodes in flowing streams, are used to monitor the concentration of hexacyanoferrate(II) produced by the diaphorase-catalyzed reaction between NADH and hexacyanoferrate(III). NADH produced by the glycerol dehydrogenase-catalyzed reaction between glycerol and NAD can be measured in this manner to determine glycerol concentrations; linear calibration plots are obtained in the range 5×10^{-5}—6×10^{-4} M glycerol. Triglycerides are hydrolyzed by lipase and the glycerol liberated is measured similarly. Glycerol and triglycerides are determined in serum control samples by the standard addition technique.
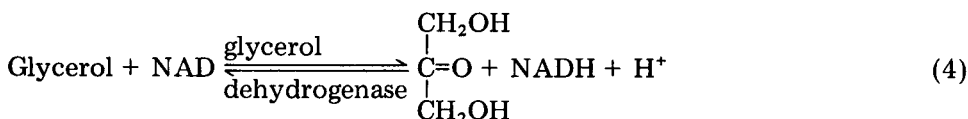
Many methods have been reported for the determination of triglycerides in biological samples and in industrial and natural products. Triglycerides in food oils have been determined by chemical-ionization mass spectrometry (c.i.m.s.) [1, 2] and gas chromatography-c.i.m.s. [3, 4]. High-pressure liquid chromatography has been used for the determination of glycerides in lubricants [5].

In biological samples, the triglyceride level is of clinical importance [6, 7] and numerous chemical and enzymatic determinations have been reported [8—12]. Chemical methods include gravimetric determination of triglycerides by difference: triglycerides = total lipids — phospholipids — cholesterol — cholesterol esters [8]. Other methods employ extraction and saponification or transesterification to free glycerol and determine the glycerol by oxidation with periodic acid to formaldehyde which is measured photometrically with chromotropic acid [8]. An automatic Autoanalyzer method measures the fluorescence of the formaldehyde with diacetylacetone and ammonia [8, 13, 14]. Other chemical methods employ lipase for hydrolysis of triglycerides and chemical determination of the liberated glycerol [13, 14].

Enzymatic methods involve either saponification [8] or lipase hydrolysis [15] to liberate glycerol, and then determination of glycerol through a series of enzyme reactions. One method uses the following reactions [8].

$$\text{Glycerol} + \text{ATP} \underset{\text{kinase}}{\overset{\text{glycerol}}{\rightleftharpoons}} \text{ADP} + \text{glycerol phosphate} \qquad (1)$$

$$\text{ADP} + \text{Phosphoenol pyruvate} \underset{\text{kinase}}{\overset{\text{pyruvate}}{\rightleftharpoons}} \text{ATP} + \text{pyruvate} \qquad (2)$$

$$\text{Pyruvate} + \text{NADH} \underset{\text{dehydrogenase}}{\overset{\text{lactate}}{\rightleftharpoons}} \text{lactate} + \text{NAD} \qquad (3)$$

The amount of glycerol present is proportional to the decrease in the absorbance of NADH at 340 nm. Commercial kits are available for this method, and evaluations of the method and the kits have been reported [16]. Another method uses glycerol dehydrogenase, after lipase hydrolysis, to measure the glycerol [9—12, 15, 17—19].

$$\text{Glycerol} + \text{NAD} \underset{\text{dehydrogenase}}{\overset{\text{glycerol}}{\rightleftharpoons}} \begin{array}{c} \text{CH}_2\text{OH} \\ | \\ \text{C=O} \\ | \\ \text{CH}_2\text{OH} \end{array} + \text{NADH} + \text{H}^+ \qquad (4)$$

Either absorbance at 340 nm [9] or excitation of NADH at 340 nm and measurement of its fluorescence at 450 nm [11, 12] is used to detect the NADH. Fluorimetric measurement of NAD after addition of methyl ethyl ketone has been reported [20].

Electrochemical methods have been applied to the measurement of enzyme reactions with success [12, 21—30]. These methods have the advantage of being inexpensive, unaffected by other absorbing species, and are readily automated [16, 23]. Turbidity, which is a problem in triglyceride determination because of the insoluble fatty acids produced by hydrolysis [8], does not affect the electrochemical measurements.

NADH can be monitored electrochemically by reacting with hexacyanoferrate(III) in the presence of diaphorase, with biamperometric measurement of the hexacyanoferrate(II) produced [23]. This system has been utilized in a flowing stream with two identical open tubular carbon electrodes for monitoring NADH produced in an enzyme reaction [31]. The feasibility of the flow system was demonstrated in the measurement of ethanol concentrations [31], and lactate or LDH in blood [32].

This paper describes a study in which open tubular electrodes were used to determine glycerol and triglycerides in flowing streams. Lipase is used to hydrolyze triglycerides to glycerol, which in turn reacts with NAD in the presence of glycerol dehydrogenase. The produced NADH is treated with hexacyanoferrate(III) ion in the presence of diaphorase and the produced hexacyanoferrate(II) ion is measured biamperometrically. The measurement of glycerol or triglycerides added to buffered solutions or serum control samples is demonstrated.

EXPERIMENTAL

Reagents

Glycine buffer, pH 8.0. A solution 0.05 M in glycine and 0.1 M in NH_4Cl was prepared and adjusted to pH 8.0 with KOH and HCl. All buffered solutions in this study were prepared with this buffer unless otherwise stated.

Hexacyanoferrate(III) solution. Reagent-grade $K_3Fe(CN)_6$ gave a high biamperometric background current when dissolved in the above buffer, so a stock 0.01 M hexacyanoferrate(III) solution in buffer was pre-electrolyzed at a platinum gauze anode at a potential of +0.6 V vs. SCE for 24 h. This was diluted to 0.001 M with buffer before use.

Triglyceride standards. Tristearin was used as a source for triglycerides. A 0.001 M suspension was prepared in a volumetric flask to which was also added 0.5 ml of lipase (3,000 units; 1 unit hydrolyzes 1 μmol of olive oil per hour) suspended in 0.005 M $CaCl_2$ solution. The mixture was diluted to volume with glycine buffer pH 8.0. The flask was incubated for 15 min in a waterbath at 37°C with occasional shaking to ensure complete hydrolysis before analysis. A series of standards was then prepared by dilution of this stock solution with buffer.

Enzymes and coenzymes. NAD was obtained from ICN Pharmaceutical, Inc., and diaphorase, glycerol dehydrogenase (GDH) and lipase from Sigma Chemical Company.

NAD, diaphorase, and glycerol dehydrogenase solutions were prepared in the above buffer pH 8.0.

Instrumentation

Tubing and pump. All tubing, tees, crosses, tube connections and tube ending adaptors were obtained from Gilson Medical Electronics. An electric flanger was used to prepare tube ending for connectors (Gilson Medical Electronics). The tubing for introduction of reagents and samples was of 0.08 mm i.d., while tubing following mixing was of 0.125 mm i.d.

A Gilson Minipulse II 4-channel peristaltic pump was used throughout.

Flow cell. A carbon rod from a standard 1.5-V battery approximately 8 mm in diameter was cut into 2-cm lengths, and a 0.8-mm hole was drilled down the axis of each rod. Indentations of 3-mm diameter were then drilled into the ends of the electrodes and the Tygon tubes were glued into these openings. The electrodes were separated by a 2-cm length of tubing. The emptying end of the flow tubing was kept well down stream from the second electrode to avoid pulsations from pressure changes in the tubes.

Voltage source. A PAR-174 Polarographic Analyzer was used to set the voltage between the electrodes at 200 mV and to measure the current. An x—y recorder was used to monitor the current.

Determination of glycerol

Standards of glycerol in aqueous buffer solutions, pH 8.0, or in serum

control samples which had been diluted tenfold with buffer, were determined by mixing with 0.001 M $K_3Fe(CN)_6$ and 0.01 M NAD in the same buffer. The NAD solution contained also GDH (1 U ml^{-1}) and diaphorase (1 U ml^{-1}). These three solutions were mixed at the cross in the flow stream. Both the pump speed and the length of the mixing tube were adjusted to allow a reaction time of 5 min before the electrodes were reached. Sample consumption was 100 μl min^{-1} and sampling was for 2 min.

Determination of triglycerides

Triglyceride standards in buffer or serum control samples diluted ten-fold with buffer were analyzed. A solution (10 μl) of lipase (600 U) was added to 5 ml of diluted serum samples, which were then incubated for 10 min at 37° C for hydrolysis. Hydrolyzed aqueous or serum samples were analyzed by the procedure described for glycerol.

Correction for free glycerol in the serum samples was corrected for by using a similar measurement without hydrolysis.

RESULTS AND DISCUSSION

Enzyme reactions

Glycerol dehydrogenase catalyzes reaction (4). The optimum pH has been reported to be 9.0 [9] and 8—10 [33]. At pH 11, the enzyme is nearly inactive [9]. The K_m value for glycerol is 1.7×10^{-2} M and 5.6×10^{-3} M in the presence of 3.3×10^{-3} M and 3.3×10^{-2} M NH$_4$Cl, respectively [9]. V_{max} is increased by NH$_4^+$, K$^+$ and Rb$^+$, whereas Zn^{2+}, Li$^+$ and Na$^+$ inhibit the enzyme, as does high ionic strength [9, 33, 34]. The use of sodium salts in reagents was therefore avoided and the pH of all the solutions was adjusted with KOH where necessary.

Lipase catalyzes the hydrolysis of triglycerides to glycerol and fatty acids [9, 10, 15, 17—19]. The optimum pH has been reported to be different with the different isoenzymes, with activity demonstrated over the pH range 3—9 [9]. The activity is inhibited by Zn^{2+}, Cu^{2+}, Hg^{2+} and iodine, but enhanced by Ca^{2+} and, to a lesser extent, by Sr^{2+} and Mg^{2+}. Emulsifiers have been used to increase the activity by increasing the surface area [15].

The calibration curve for the determination of glycerol in buffer was linear up to about 6×10^{-4} M glycerol and then leveled off; the relative standard deviation at the 10^{-4} M level was about 5% ($n = 6$). The lowest limit detected was 5×10^{-5} M. The reaction time was 5 min and a well resolved and reproducible signal was obtained after introducing sample for 1 min. Figure 1 shows the calibration curve for the determination of glycerol in serum control solution. The signal was plotted after subtraction of the background, which is due to impurities of hexacyanoferrate(II) in the hexacyanoferrate(III) solution [31], NADH impurities in the NAD solution, and the high ionic strength (see below). The non-zero intercept is due to glycerol present in the serum control sample.
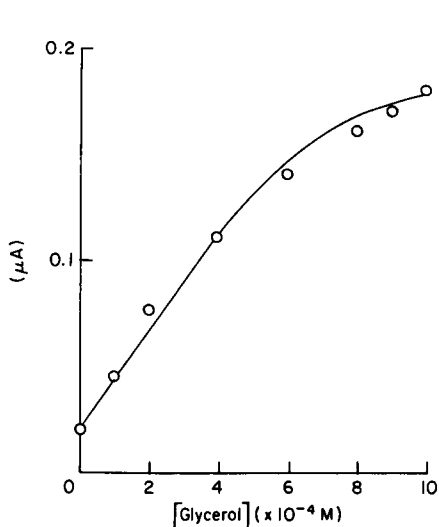
Fig. 1. Calibration curve for the determination of glycerol in serum control samples. The non-zero intercept is due to glycerol in sample.
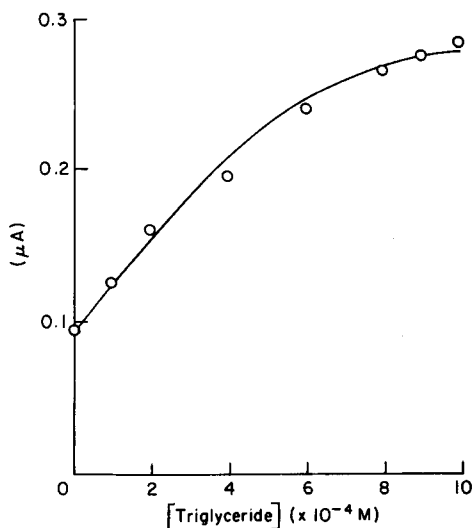
Fig. 2. The calibration curve for the determination of triglycerides in a serum control sample. The non-zero intercept is due to triglycerides in the control sample.

The calibration curve for the determination of triglycerides in buffer solution was similar to that for glycerol, with a similar detection limit. Figure 2 shows the calibration curve for the determination of triglycerides in serum control solutions. The signal was plotted after subtraction of the background obtained with the sample before hydrolysis; this corrects for the free glycerol in the sample. The non-zero intercept is due to triglycerides in the serum control sample. The curve shows that the sample contains 230 mg/100 ml calculated as triolein, which is within the reported limits for the sample (197—247 mg/100 ml as triolein) [35].

Duration of reaction

The time of the above reactions can be varied by changing the pumping rate and/or the length of tubing following the mixing T or cross. Also the ratio of reagent to sample can be varied by changing the relative sampling tube diameters. For the tube diameters given under Experimental, the optimum length of mixing coil was 60 cm; the optimum flow rates were 0.1 and 0.1 ml min^{-1} for the hexacyanoferrate(III) and NAD solutions, respectively.

Effect of ionic strength, ammonium ion and pH

Figure 3 shows the effect of ionic strength of the solution on the background current. The current increases rapidly by the increase of ionic strength
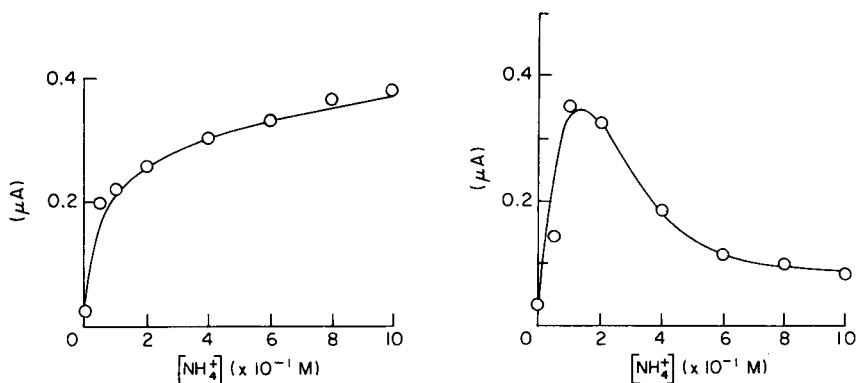
Fig. 3. The effect of ionic strength of the solution on the background signal.

Fig. 4. The effect of ammonium ion concentration on the overall signal for 6×10^{-4} M glycerol (corrected for background).

up to 0.2 M, then levels. The experiment was performed with ammonium chloride solution, and similar results were obtained when potassium nitrate solution was used.

Figure 4 shows the effect of ammonium ion concentration on the diamperometric signal of the overall reaction, which arises from its activating influence on glycerol dehydrogenase [9, 33, 34]. The signal increases rapidly with concentration of ammonium ion until it reaches maximum at 0.1 M; the signal then decreases, because of the inhibition of glycerol dehydrogenase by high ionic strength [9]. The signal was plotted after subtraction of background at each point.
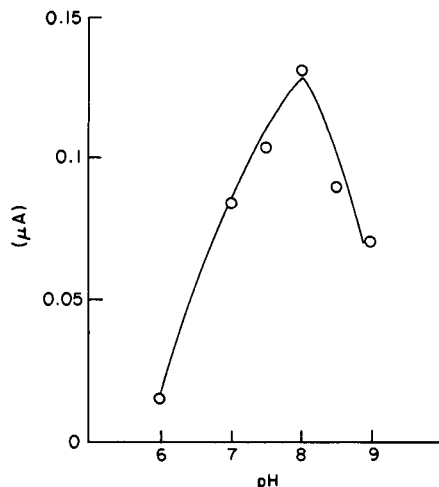

Fig. 5. The effect of pH on the net signal for 6×10^{-4} M glycerol.

The biamperometric signal of hexacyanoferrate(II) ion is pH-dependent, increasing in acidic solutions [31], so that the optimum pH of the reactions will be a trade off between this dependence and the optimum pH for the enzyme reactions involved in the determinations. The pH dependence of the overall reaction showed a sharp maximum at pH 8 when background subtraction was plotted (Fig. 5).

REFERENCES

1 T. Marata and S. Takahashi, Anal. Chem., 49 (1977) 728.
2 H. M. Fales, G. W. A. Milne, H. U. Winklen, H. D. Beckey, J. N. Damico and R. Barron, Anal. Chem., 47 (1975) 207.
3 T. Murata, Anal. Chem., 49 (1977) 2209.
4 T. Murata and S. Takahashi, Anal. Chem., 45 (1973) 1916.
5 J. A. Sinsel, B. M. La Rue and L. D. McGraw, Anal. Chem., 47 (1975) 1987.
6 J. W. Winkelman and D. R. Wybenga, in R. J. Henry, D. C. Cannon and J. W. Winkelman (Eds.), Clinical Chemistry, Principles and Techniques, Harper and Row, New York, 1974.
7 R. D. Ellefson and W. T. Caraway, in N. W. Tietz (Ed.), Fundamentals of Clinical Chemistry, Saunders, Philadephia, 1976.
8 D. R. Wybenga and J. A. Inkpen, in R. J. Henry, D. C. Cannon and J. W. Winkelman (Eds.), Clinical Chemistry, Principles and Techniques, Harper and Row, New York, 1974.
9 L. A. Decker (Ed.), Worthington Enzyme Manual, Freehold, N. J., 1977.
10 S. H. Grossman, E. Mollo and G. Ertingshausen, Clin. Chem., 22 (1976) 1310.
11 M. G. Gore, Anal. Biochem., 75 (1976) 604.
12 M. M. Fishman, Anal. Chem., 50 (1978) 206 R.
13 H. J. Boehme and H. Dost, Fresenius Z. Anal. Chem., 259 (1972) 363.
14 M. M. Fishman and H. F. Schiff, Anal. Chem., 46 (1974) 367R.
15 P. Desnuelle and P. Savary, J. Lipid Res., 4 (1963) 369.
16 See, e.g., G. Lehnus and L. Smith, Clin. Chem., 24 (1978) 27.
17 A. M. Seligman and M. M. Nachlas, J. Clin. Invest., 29 (1950) 31.
18 J. F. Kochmar and D. W. Moss, in N. W. Tietz (Ed.), Fundamentals of Clinical Chemistry, Saunders, Philadelphia, 1976.
19 A. Cantarow and B. Schepartz, Biochemistry, Saunders, Philadelphia, 1962.
20 J. A. Demtriaus, P. A. Drewes and J. B. Gin, in R. J. Henry, D. C. Cannon and J. W. Winkelman (Eds.), Clinical Chemistry, Principles and Techniques, Harper and Row, New York, 1974.
21 G. D. Christian, Adv. Biomed. Engineering Med. Physics, 4 (1971) 95.
22 G. D. Christian, in M. Kessler (Ed.), Ion and Enzyme Electrodes in Biology and Medicine, Urban and Schwarzenberg, Munchen, 1976.
23 L. C. Thomas and G. D. Christian, Anal. Chim. Acta, 82 (1976) 265.
24 F. S. Cheng and G. D. Christian, Anal. Chem., 49 (1977) 1785.
25 F. S. Cheng, Ph.D. Thesis, University of Washington, 1977.
26 L. C. Thomas and G. D. Christian, Anal. Chim. Acta, 58 (1975) 271.
27 S. J. Leach, J. H. Boxendale and M. G. Evans, Aust. J. Chem., 6 (1953) 395.
28 M. D. Smith and C. L. Olsen, Anal. Chem., 46 (1974) 1544; 47 (1975) 1074.
29 W. J. Blaedel and R. C. Engstrom, Anal. Chem., 50 (1978) 476.
30 W. J. Blaedel and G. W. Schieffer, Anal. Chem., 46 (1974) 1564.
31 A. S. Attiyat, E. L. Gulberg and G. D. Christian, unpublished results.
32 A. S. Attiyat and G. D. Christian, unpublished results.
33 J. E. Strickland and D. N. Millen, Biochim. Biophys. Acta, 159 (1968) 221.
34 W. G. McGregor, J. Phillips and C. H. Suelter, J. Biol. Chem., 249 (1974) 3132.
35 MONI-TROL II Chemistry Control, lot number PTD-50, DADE (1977).

DEVELOPMENT OF A GLUCOSE ANALYZER BASED ON IMMOBILIZED GLUCOSE OXIDASE

B. WATSON, D. N. STIFEL and F. E. SEMERSKY*

North Technical Center, Owens-Illinois, Toledo, Ohio 43666 (U.S.A.)

(Received 11th September 1978)

SUMMARY

A dedicated instrument for the determination of glucose in serum or plasma is described. The flow system includes an amperometric sensor to measure the hydrogen peroxide liberated from the total conversion of a 2-μl sample injected into a column of immobilized glucose oxidase covalently coupled to a porous alumina substrate. The instrument digitally displays the glucose concentration and is capable of testing 60 samples/h. No sample or reagent preparation is necessary. The accuracy, precision, and selectivity are discussed.

Glucose oxidase (E.C. 1.1.3.4.β-D-glucose: oxygen oxidoreductase) catalyzes the reaction:

D-glucose + O_2 → D-gluconic acid + H_2O_2
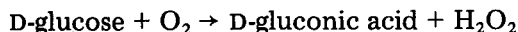
and is frequently employed for glucose determinations because of its high selectivity for β-D-glucopyranose [1—3]. Immobilization of glucose oxidase provides a reagent that combines this high selectivity with increased stability and since reactants and products are separated, the enzyme can be re-used [4]. Sufficient glucose oxidase can be immobilized on porous alumina to catalyze complete reaction of small aliquots of glucose.

Unlike many wet chemical techniques based on soluble glucose oxidase, the hydrogen peroxide generated from the enzymatic reaction is not coupled to the color development of a chromogen; these often require the use of a second enzyme, peroxidase, and for better accuracy a deproteinization step with carefully prepared reagents [5]. In the present case, the hydrogen peroxide is measured directly by an amperometric sensor, such as has frequently been used in glucose assays. The electric current associated with the 2-e reaction of hydrogen peroxide is linearly related to the glucose concentration, and the specially designed sensor provides reliability.

EXPERIMENTAL

Reagents

The buffer consists of 0.20 M sodium acetate, 0.018 M acetic acid, 0.1 M KCl and 50 ppm BioBan P 1487 (Commercial Solvents Corp., 245 Park Avenue, N.Y.).

The glucose standard contains 1.11×10^{-2} M D-glucose (National Bureau of Standards, Standard Reference Material 917) [6], 0.1 M KCl and 8.2 mM benzoic acid.

The hydrogen peroxide standard consists of 7.22 mM H_2O_2 with 75 μM $Na_2SnO_3 \cdot 3H_2O$, 90 μM $Na_4P_2O_7 \cdot 10H_2O$ and 0.86 mM adipic acid.

All reagents were of analytical grade unless otherwise indicated. Distilled, deionized water was used in all formulations.

Fresh human serum samples were frozen immediately after preparation and thawed immediately before use. An aliquot of the normal pooled sample was spiked with glucose (National Bureau of Standards, SRM 917) to achieve an elevated glucose concentration (abnormally high pool).

Enzyme

Immobilized glucose oxidase must meet certain stringent requirements for use in a flow-through system. The flow rate of the buffer through the column must remain constant; therefore the support material must resist breakage and the tendency to pack. A porous alumina was developed to meet these requirements. Sufficient enzyme must be immobilized to ensure that the reaction proceeds to completion so that the analysis is independent of the rate of reaction and, therefore, requires no elaborate temperature control. Also, the immobilized enzyme must be sufficiently stable to support the total conversion of glucose for many hundreds of assays. The development of a means of immobilization satisfying these requirements has been reported elsewhere [7].

Instrumentation

A schematic diagram of the flow system is shown in Fig. 1.

The buffer is delivered at a constant rate of approximately 1 ml min^{-1}. The reagent delivery system previously reported [8] assures virtually pulse-free flow.

A repeating syringe capable of consistently delivering 2-μl samples was specially designed for this purpose jointly with Unimetrics, Inc., Anaheim, California 92801.

Electrodes. The main features of the electrode system are shown in Fig. 2. A three-electrode system was used to negate the effects of current passing through the reference electrode common to two electrode systems [9]. Platinum was used for the indicator and counter electrodes and silver—silver chloride as the reference electrodes. Electrodes were activated by polishing the surface with loose abrasives (alumina) (particle size 0.5—22.5 μm), and re-activated as required (after several months).

The voltammetric curves for the oxidation of electroactive species (Fig. 3) were established from current—potential curves generated by using steady-state voltammetry with the electrode designed for the instrument. The traditional method of sweeping anodic potentials while simultaneously measuring electrolysis current is not considered the best way to generate
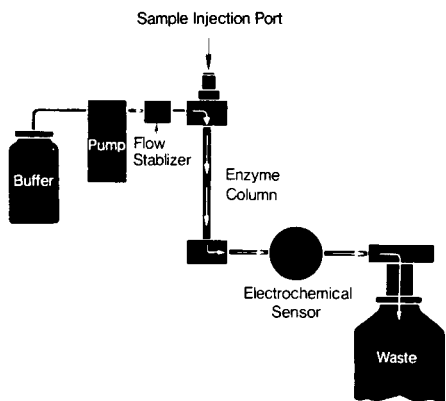
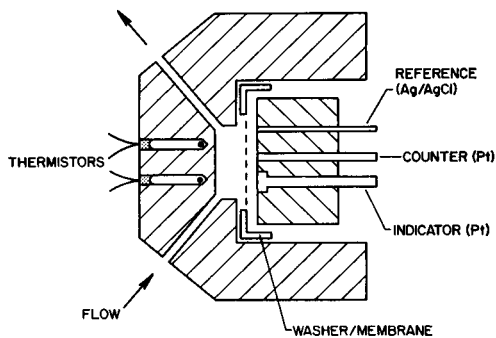Fig. 1. Flow diagram of the glucose system.
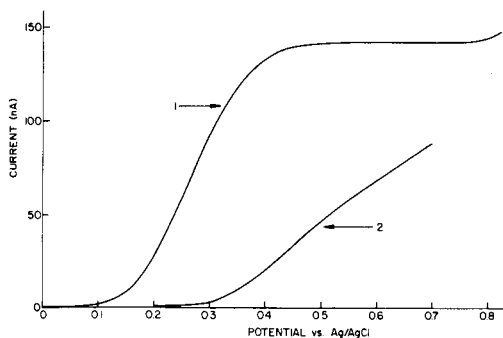
Fig. 2. Cross-section of the electrode.

Fig. 3. Current—potential curves for (1) glucose; (2) uric acid in 0.2 M acetate buffer pH 5.6 with 0.1 M KCl supporting electrolyte.

i—E curves at solid electrodes [10, 11]; the steady-state technique permits the generation of more reproducible and reversible curves. Curve 1 (Fig. 3) shows a well-defined plateau in the range 0.5—0.7 V (vs. Ag/AgCl), and the optimum applied potential is 0.5 V (see below).

Membranes. Several commercially available membranes were used. Maximum performance was obtained with cellulose dialysis membranes (Spectrapor, T. M. Spectrum Medical Industries, Los Angeles, California 90052). The nominal molecular weight exclusion limits given for the types used are: Spectrapor 1, 6000—8000; Spectrapor 2, 12,000—14,000; Spectrapor 3, 3500.

Electronics. A typical response curve from the glucose electrode is shown in Fig. 4a, which illustrates the current changes which take place as a sample passes through the electrode. The difference between the peak current (i_p) and the baseline or residual current (i_r) is used to determine the glucose concentration, as this method corrects for any change in baseline during a series of measurements.
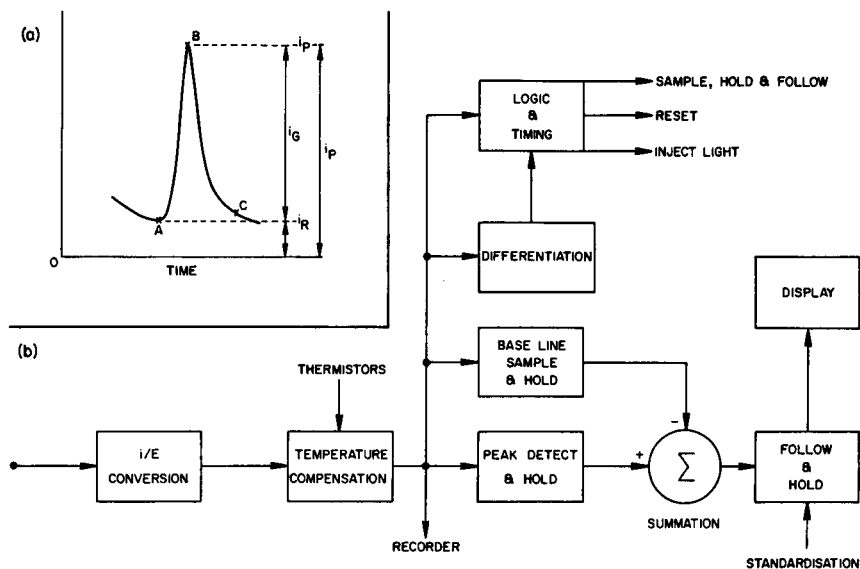
Fig. 4. Typical response curve (a) and schematic circuit (b).

Figure 4b shows a simplified block diagram of the electronic circuit functions. The electrode outputs are constantly tracked and points A and B are selected. The value $i_g = i_p - i_r$ is determined which is related to the concentration of glucose in the standard. After a one-point mid-range calibration, the glucose values of the samples are directly displayed in milligrams per deciliter (common clinical units). When point C on the response curve is reached (determined by the rate of change of current falling below some preset level), an INJECT SAMPLE light on the instrument panel is activated, directing the user to inject the next sample.

The electronics prevent the display of any glucose value exceeding 400 mg/dl (2.22×10^{-2} M), the upper range of linearity. Any sample having a concentration greater than this requires dilution and the user is so informed by a DILUTE SAMPLE light which appears on the front instrument panel.

During periods of prolonged use, the pumping system can cause an increase in temperature of the reagent stream. Since the electrodes are temperature-sensitive, this is manifested by a slow upward drift in response. The effect of this drift is negated by a temperature compensation circuit controlled by a pair of thermistors situated close to the electrode cavity/ sensing area.

Anodization of the reference electrode can be performed in situ by a switch on the rear of the instrument.

Evaluation

An evaluation of the precision, accuracy and selectivity of the glucose analyzer was performed by essentially following the test protocol of Barnett

and Youden [12]. For twenty consecutive days three aqueous standards, 50 mg/dl (2.77 mM), 100 mg/dl (5.55 mM) and 350 mg/dl (19.4 mM), were run in random order. These were followed by three pooled sera whose nominal values represented abnormally low, normal and abnormally high concentrations of glucose in serum and were also run in random order. These were followed by five patient samples. The reference method used was similar to the hexokinase/glucose-6-phosphate dehydrogenase procedure of Neese et al. [13].

The effects of interferences were determined by alternately injecting a pooled serum sample and a spiked pool serum sample until five of each had been run. This method of alternation decreased any effects caused by baseline drift that could have become apparent had the samples been run in successive groups of five. The list of interfering substances, their formulations and suppliers, and the means of preparation have been given by Passey et al. [14].

Instrument-to-instrument variability was assessed by running the protocol simultaneously on two instruments.

RESULTS AND DISCUSSION

The buffer was formulated to perform three separate functions. The acetate buffer maintains a constant pH 5.6 in the optimum range of the immobilized glucose oxidase. The potassium chloride serves as a supporting electrolyte for the electrolysis reaction and provides a stable potential for the silver—silver chloride reference electrode. The BioBan P 1487 is added to prevent the growth of microorganisms in the buffer. The growth of aerobic organisms, especially yeasts, was found to deplete the dissolved oxygen supply and reduce the linear range of response.

The instrument calibration requires a single glucose standard at the midpoint of the linear range; potassium chloride maintains a constant ionic strength, and benzoic acid acts as a preservative.

The hydrogen peroxide standard has a concentration equivalent to a 200 mg/dl (1.11×10^{-2} M) D-glucose solution. The difference in absolute concentration reflects the fact that at room temperature, about 65% of D-glucose exists in the β-form, the isomer of D-glucose oxidized by glucose oxidase. The rate of mutarotation of the residual α-D-glucose to the β-D form after complete oxidation of the β-D-glucose by glucose oxidase is slow [15, 16] compared to the residence time of the sample in the immobilized glucose oxidase, which is of the order of 15 s. A hydrogen peroxide standard is necessary to determine if the glucose oxidase is still converting at a 100% rate. Any reduction in conversion rate implies that the final method of determination no longer corresponds to 100% conversion and the instrument is then subject to errors from temperature fluctuations and interferences. The adipic acid controls the pH of the solution in the acidic region where hydrogen peroxide is more stable, and the two sodium salts effectively

chelate heavy metals which catalyse the destruction of hydrogen peroxide [17]. The peroxide standard is stable at room temperature for more than six months.

Minimization of interferences

Curve 2 in Fig. 3 was produced by the steady-state $i—E$ method for uric acid (40 mg/dl). Unfortunately, uric acid is oxidized at the same potential as is optimal for hydrogen peroxide determination. The $i—E$ curves for ascorbic acid and L-cysteine are similar to that of uric acid. Since all three of these substances may be present in significant amounts in serum samples, any attempt to measure glucose at the optimum potential would be subject to severe interferences from the other three compounds.

A partial solution to the problem can be seen in Fig. 3. If the applied potential were reduced to 0.3 V, the current generated by the interfering substances would be reduced to acceptable levels. However, regardless of the polishing methods employed, the platinum electrode is not sufficiently active for continuous use at a potential of 0.3 V. An electrode may be held at a more anodic potential (0.7 V) for several hours and then adjusted to 0.3 V with some success. A considerable time delay before the electrode achieves a steady state is required and, after the steady state is maintained, the signal decays to an unusable level quite rapidly. It has been reported [8] that "oxide" layers are stripped from platinum anodes at less anodic potentials which may account for the signal loss and implies that the working electrode functions best when in an "oxidized" state. This was confirmed by the fact that the treatment of the working electrode with chromic acid gave a much larger signal at 0.3 V, but this signal was also subject to rapid decay. Neither electrolytic nor chemical activation techniques are solutions to the problem of interferences. A compromise voltage, 0.5 V, is selected, being high enough to minimize stripping but low enough to reduce the effects of interfering substances.

Effective interference control can be achieved by imposing a membrane between the electrode and the flow chamber. Obviously, given the nominal molecular weight exclusion limits of the membranes employed, the exclusion of the interfering substances mentioned above, having molecular weights ranging from 121 for L-cysteine to 176 for ascorbic acid, is not one of ultrafiltration or molecular exclusion. It is suggested that the rate of diffusion of the larger molecules through the membrane is significantly slower than that of the much smaller H_2O_2 molecule. Therefore, as a reacted sample containing both hydrogen peroxide and interferences enters the electrode cavity, the concentration of all electroactive species increases. This increase creates a concentration gradient across the membrane driving the molecules toward the electrode. This concentration gradient peaks as the entire sample fills the electrode cavity, then decreases as fresh buffer washes the sample out of the cavity, thus reversing the gradient. During the period of time when the gradient is positive (i.e. molecules diffusing toward the electrodes),

TABLE 1

Interference study

Substance added (mg/dl)	Bias (mg/dl)		Substance added (mg/dl)	Bias (mg/dl)	
	Instrument 1	Instrument 2		Instrument 1	Instrument 2
Endogenous substances			*Exogenous substances*		
Fructose (150)	+1.6	0	L-Dopa (10)	+1.0	+2.2
Mannose (300)	+2.8	+4.1	Xylose (150)	+1.8	+0.2
Galactose (300)	+1.2	+0.3	Ribose (150)	+1.2	+0.8
Ascorbic acid (25)	+3.4	+1.8	Na salicylate (50)	+1.0	+0.2
Creatinine (25)	+0.4	−0.2	Na diatrizoate (5% v/v)	+0.6	+0.6
Glutathione (50)	+1.8	+1.6	Meglumine diatrizoate	+1.6	+0.8
Citric acid (1500)	−3.8	−4.4	(5% v/v)		
Hemoglobin (5000)[a]	−4.8	−2.6	Tolbutamide (25)	−0.8	0
NH$_4$Cl (1)	−1.2	+0.6	Methyl dopa (25)	+3.0	+2.8
Bilirubin (25)	0	0	Streptomycin (30)	−0.6	+1.0
Uric acid (25)	+1.0	+3.4	Sulfadiazine (50)	+2.2	+1.0
Cysteine (40)	+2.0	+3.6	Dextran (100% of	+2.4	+1.6
Lipid (600)		+1.6	plasma volume)		
			Acetylsalicylic acid (30)	+0.2	0
Anticoagulants and preservatives					
Na fluoride (750)	+2.4	+2.5			
Na heparin (7000 U/dl)	−0.6	+0.4			
Thymol (500)[b]	−4.8	−2.8			
EDTA (550)	+0.2	+1.2			
Na oxalate (800)		+1.0			
Na citrate (2100)	+2.2	+3.8			

[a]Obtained from lysed red cells; the negative interference is more likely due to the presence of catalase than hemoglobin itself. Catalase activity was found to be 6800 U ml^{-1}.
[b]Not recommended as additive, as it causes poor baseline definition, and is probably detrimental to membrane.

hydrogen peroxide is the only species which has a diffusion rate sufficiently high to permit penetration across the membrane distance. The interferences diffuse into the membrane but before completing the transit across the membrane the gradient reverses as does the direction of the diffusion.

The use of a membrane also prevents protein molecules from coming into contact with the electrodes, thus minimizing fouling.

The results of a full interference study are shown in Table 1. In every case, the interference is less than 5 mg/dl at the level tested.

DISCUSSION

Precision

Day-to-day precision evaluated from results on aqueous standards and stable serum pools is shown in Table 2. In every case, reproducibility expressed as the coefficient of variation (c.v.) is less than 2%. As far as clinical significance is concerned up to 5% is acceptable [9]. A measure of instrument-to-instrument variability is provided by the analysis of variance (F

TABLE 2

Precision (all values in mg/dl except where indicated)

	Instrument 1			Instrument 2		
	Mean	S.d.	C.v. (%)	Mean	S.d.	C.v. (%)
Aqueous standards prepared from NBS SRM 917						
50	49.3	0.66	1.3	50.0	0.73	1.5
100	99.7	1.38	1.4	99.6	0.69	0.7
350	345.7	2.90	0.8	345.4	2.7	0.8
Serum pools						
Low	51.6	0.95	1.8	51.6	0.76	1.5
Normal	125.5	2.04	1.6	124.1	1.59	1.3
High	336.9	3.88	1.2	333.5	2.40	0.7

Statistical analysis

Sample	Paired t (vs. true value)		(F test)
	Instrument 1	Instrument 2	
50 (aq.)	4.74*	0	1.22
100 (aq.)	0.97	2.59*	4.0*
350 (aq.)	6.63*	7.6*	1.22
Low (Serum)			1.56
Normal (Serum)			1.65
High (Serum)			2.61*

test) in Table 2. Two pairs of results (asterisked) show statistically significant differences (at the 5% critical level, $F = 2.15$), although clinically this is of no significance, and the precision of both instruments is judged to be extremely good.

Accuracy

Results obtained with aqueous standards can be used to assess the accuracy of the method, because these are the only samples analyzed where the true value is known. Some of the results in Table 2 (asterisked) indicate statistically significant differences from the true value. It is important to note that this occurs not because of significant bias, but rather because of the excellent precision of the method shown by the small values of the standard deviation. In no case does the measured value differ from the true value by more than 1.4%.

Comparison with hexokinase reference method. Table 3 summarizes the statistical analysis of the data for both instruments. According to the *t*-test, the results are significantly different from the reference method at the 5% level (critical $t = 2.0$). A breakdown of the raw data indicates that the main contribution to the bias comes from values in excess of 250 mg/dl. In this range the glucose analyzer tends to give results which are lower than the

TABLE 3

Accuracy estimated by comparison with the hexokinase reference method

Statistical parameter	Instrument 1	Instrument 2
No. of samples	72	72
Bias	+1.4	+3.0
Paired t	2.67	5.09
Y-intercept (mg/dl)	4.141	3.561
Slope	0.958	0.951
$Sx.y$ (mg/dl)	2.64	2.66
Correlation(r)	0.9995	0.9995

reference method. This, coupled with the small $S_{x.y}$ values (good precision), yields the high "t" values.

The calculated regression lines shown in Fig. 5 illustrate the good correlation suggested by the $S_{x.y}$ and r values. The differences between the two instruments are statistically insignificant ($t = 1.45$).
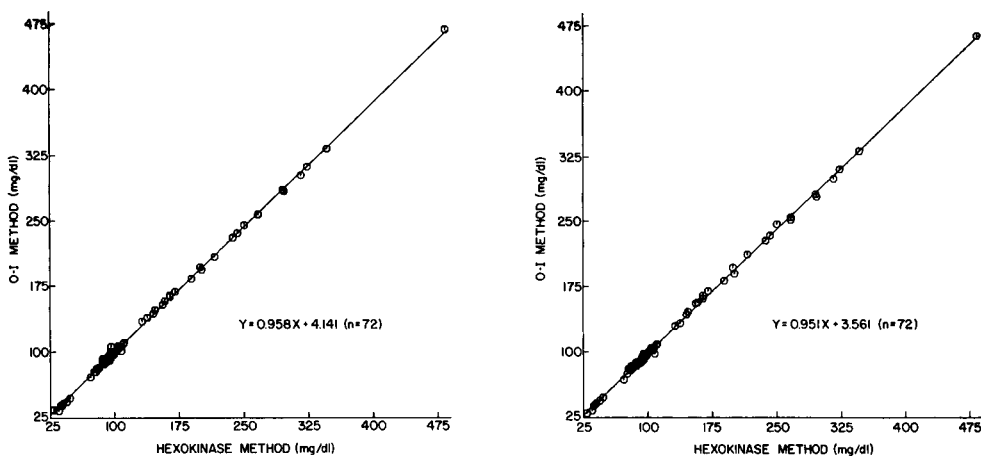
Fig. 5. Comparison of the hexokinase/G-6-PDH reference method to (a) Instrument 1 and (b) Instrument 2.

REFERENCES

1 P. Trinder, Anal. Clin. Biochem., 6 (1969) 24.
2 R. G. Martinek, J. Am. Med. Technol., 31 (1969) 530.
3 H. J. Kunz and M. Statsny, Clin. Chem., 20 (8) (1974) 1018.
4 D. N. Gray, M. H. Keyes and B. Watson, Anal. Chem., 49 (1977) 1067A.

5 N. Nelson, J. Biol. Chem., 153 (1944) 375.

6 J. P. Cali, Fed. Proc., 34 (12) (1975) 2123.

7 M. H. Keyes, U.S. Patent 3,933,589.

8 B. Watson and M. H. Keyes, Anal. Lett., 9 (1976) 713.

9 J. B. Flato, Anal. Chem., 44 (1972) 75A.

10 W. J. Blaedel and R. A. Jenkins, Anal. Chem., 46 (1974) 1952.

11 G. Charlot, J. Badoz-Lambling and B. Trémillon, Electrochemical Reactions, Elsevier, New York, 1962, p. 138.

12 R. N. Barnett and W. J. Youden, Am. J. Clin. Pathol., 54 (1970) 454.

13 J. Neese, P. Duncan, D. Bayse, M. Robinson, T. Cooper and C. Stewart, Clin. Chem., 20 (1974) 878.

14 R. B. Passey, R. L. Gillum, J. B. Fuller, F. M. Urry and M. L. Giles, Clin. Chem., 23 (1977) 131.

15 J. Okuda and I. Miwa, Anal. Biochem., 39 (1971) 387.

16 J. Okuda and I. Miwa, Anal. Biochem., 43 (1971) 312.

17 W. C. Schumb, C. N. Satterfield and R. L. Wentworth, Hydrogen Peroxide, Reinhold, New York, 1955.

18 R. N. Adams, Electrochemistry at Solid Electrodes, M. Dekker, New York, 1969.

19 R. N. Barnett, Am. J. Clin. Pathol., 50 (1968) 671.

AMPEROMETRIC DETERMINATION OF PHOSPHATIDYL CHOLINE IN SERUM WITH USE OF IMMOBILIZED PHOSPHOLIPASE D AND CHOLINE OXIDASE

ISAO KARUBE*, KENJI HARA, IKUO SATOH and SHUICHI SUZUKI

Research Laboratory of Resources Utilization, Tokyo Institute of Technology, 4259 Nagatsuta-cho, Midori-ku, Yokohama, 227 (Japan)

(Received 18th July 1978)

SUMMARY

Phospholipase D (EC 3.1.4.4.) and choline oxidase (EC 1.1.99.1.) are immobilized together on a hydrophobic agarose gel and used to convert the phospholipid to betaine and hydrogen peroxide, which is measured amperometrically at $+0.60$ V vs. SCE. The response time of the sensor is 2 min, and the calibration curve for 0—3 g l^{-1} of phosphatidyl choline is linear. Different methods of insolubilizing the enzymes are compared.

Determination of phospholipids in serum is important in clinical analysis. Phosphatidyl choline is a main serum phospholipid; various procedures have been described for its determination [1]. To improve the accuracy, selectivity and rapidity of the assay in serum, enzymatic methods involving a combination of phospholipase D and choline oxidase have been proposed [2]. The reactions involved are:

$$\text{Phosphatidyl choline} \xrightarrow{\text{phospholipase D}} \text{phosphatydic acid} + \text{choline} \tag{1}$$

$$\text{Choline} + 2O_2 + H_2O \xrightarrow{\text{choline oxidase}} \text{betaine} + 2H_2O_2 \tag{2}$$
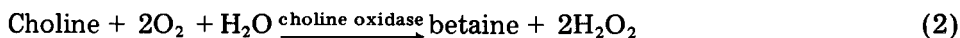
The hydrogen peroxide formed has been measured spectrophotometrically. However, these enzymatic methods require a long incubation time, additional reagents and expensive enzymes. In order to achieve a rapid and simple serum phospholipid assay, electrochemical monitoring of these reactions may have definite advantages [3, 4]. The use of immobilized enzymes with direct amperometric measurement of the hydrogen peroxide liberated appeared to be the best approach.

In this paper, phospholipase D and choline oxidase are immobilized together on cyanogen bromide-activated hydrophobic agarose gel. The measurement system for phosphatidyl choline consists of an immobilized enzyme reactor with the electrodes positioned close to the reactor.

EXPERIMENTAL

Materials

Phospholipase D (EC 3.1.4.4., from *Streptomyces chromofuscus*, 11.3 I.U. mg^{-1}) and choline oxidase (EC 1.1.99.1., from *Arthrobacter globiformis*, 10.5. I.U. mg^{-1}) were obtained from Toyo Jozo Co. Ltd. Peroxidase (horse radish, ca. 100 purpurogallin U mg^{-1}; Tokyo Kasei Kogyo Co. Ltd.), Triton X-100 (Wako Pure Chemicals Ind. Ltd.), agarose (octyl-Sepharose CL-4B; Pharmacia Fine Chemicals), and porous glass and polystyrene sheet (Amano Pharmaceutical Co.) were also required. Phosphatidyl choline was purified from egg yolk by the method of Faure [5]. A phosphatidyl choline dispersion was prepared by the method of Huang [6].

Coupling of enzymes to agarose gel

In a well-ventilated hood, 5 ml of well-washed Sepharose gel were mixed with 10 ml of water, and 0.25 g of finely divided cyanogen bromide was added at once to the stirred suspension. The pH of the suspension was maintained between 10.5 and 11.5 with 4 M sodium hydroxide solution. The reaction was complete after 10 min. After reaction, the gel was washed with a large volume of cold distilled water and carbonate buffer (pH 10, 0.1 M). To 5 ml of the mixed enzyme solution (pH 8.0, 0.05 M phosphate buffer containing 200 I.U. of phospholipase D and 200 I.U. of choline oxidase), the cyanogen bromide-activated Sepharose gel was added. The reaction mixture was stirred for 24 h at 4°C. The suspension was transferred to a Buchner funnel and washed with a large volume of 1 M sodium chloride solution and phosphate buffer (pH 8.0, 0.05 M). The immobilized enzymes were stored in the phosphate buffer at 4°C.

The amounts of unreacted enzymes were determined by the method of Warburg and Christian [7]. The gel contained 5.7 mg of enzymes (3.0 mg of choline oxidase and 2.7 mg of phospholipase D) per g of wet gel.

Coupling of enzymes to porous glass

This was carried out by the method of Weetall [8]. The porous glass (1 g), treated with γ-aminotriethoxysilane was added to 5 ml of enzyme solution (in 0.05 M phosphate buffer, pH 8.0) containing 200 I.U. of choline oxidase and 200 I.U. of phospholipase D, and the mixture stirred for 12 h at 4°C. After the reaction, the porous glass was washed by the procedure described above. The immobilized enzymes were stored in 0.05 M phosphate buffer (pH 8.0) at 4°C. The amounts of unreacted enzymes were determined as mentioned above. This reaction resulted in the glass having 5.0 mg of enzymes (2.4 mg of phospholipase D and 2.6 mg of choline oxidase) per g of dry carrier.

Coupling of enzymes to polystyrene

Polystyrene sheet (0.5 g, 0.5 × 0.5 mm^2) was added to 5 ml of γ-amino-triethoxysilane and the reaction mixture was allowed to stand for 2 min. The

polystyrene coated with γ-aminotriethoxysilane was washed with glass-distilled water and suspended in 20 ml of 1% (w/v) glutaraldehyde solution (in 0.05 M phosphate buffer, pH 7.0) for 1 h at room temperature. The sheets were washed with glass-distilled water and added to 1 ml of enzyme solution (0.05 M phosphate buffer, pH 8.0) containing 200 I.U. of choline oxidase and 200 I.U. of phospholipase D. The reaction mixture was stirred for 12 h at 4°C. After reaction, the polystyrene was washed by the procedure described above, and amount of unreacted enzyme determined as mentioned above. The reaction resulted in polystyrene having 3.5 mg of enzymes (1.7 mg of phospholipase D and 1.8 mg of choline oxidase) per g of dry carrier. The immobilized enzymes were stored in phosphate buffer at 4°C.

Immobilization of enzymes in a collagen membrane

This was done as described previously [9]. The enzyme solution (0.5 ml) containing 55 I.U. of choline oxidase and 55 I.U. of phospholipase D was added to 5 g of 1% (w/v) collagen fibril suspension (pH 4.3). The suspension was cast on a Teflon membrane and dried for 12 h at room temperature. The enzyme—collagen membrane was suspended in 0.5% (w/v) glutaraldehyde solution (in 0.05 M phosphate buffer, pH 7.0) for 1 min at room temperature and dried for 3 h at room temperature. This reaction results in a collagen membrane having 16 mg of enzymes (8 mg of phospholipase D and 8 mg of choline oxidase) per g of dry membrane. The enzyme—collagen membranes were stored in phosphate buffer at 4°C.

Enzyme assay

Unless otherwise noted, phospholipase D was determined by the method of Imamura et al. [2]. A reaction mixture (0.5 ml) of 2 mM phosphatidyl choline solution in 40 mM Tris buffer (pH 8.0, with calcium chloride and Triton X-100) containing 10 μg of native phospholipase or 0.1 g of the immobilized enzyme was shaken for 10 min at 37°C. The reaction was stopped with 0.1 ml of 0.1 M EDTA (in 1 M Tris buffer). To the reaction mixture, 0.4 ml of a solution containing 0.2 I.U. of peroxidase, 0.3 mg of 4-aminoantipyrine, 3 I.U. choline oxidase and 0.2 mg of phenol were added. The amount of quinoneimine dye produced was determined spectrophotometrically at 500 nm.

The activity of choline oxidase was determined by the method of Allain [10]; 1 μmol of hydrogen peroxide produced by the enzyme in 1 min was defined as 1 unit.

Apparatus

Figure 1 shows the schematic diagram of the sensor for phospholipid determination. The hydrogen peroxide liberated enzymatically was monitored with a voltammetric system (Model HA-101, Hokuto Denko Co., Tokyo) based on a platinum electrode ($0.5 cm^2$) at +0.60 V vs. S.C.E, and a recorder (Model SP-J5V, Riken Denshi Co., Tokyo). The immobilized enzymes (1 g, wet) were placed in a glass reactor (6 mm i.d., 3.5 cm long). The volume of the
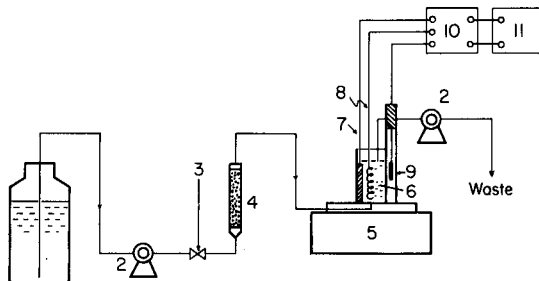
Fig. 1. Schematic diagram of the sensor for phospholipid determination. (1) buffer reservoir; (2) peristaltic pump; (3) sample inlet; (4) immobilized enzyme reactor; (5) magnetic stirrer; (6) sensing chamber (0.4 ml); (7) anode (Pt plate, 0.5 cm^2); (8) cathode (Pt wire); (9) SCE; (10) voltammetric monitoring system; (11) recorder.

cell for determination of hydrogen peroxide was 0.4 ml. A constant-temperature circulating bath was used to maintain the reaction temperature at 25°C.

Procedure for phospholipid determination

The phosphate buffer (0.02 M, pH 8.0, 0.1% in Triton X-100 and 5 μM in calcium chloride) was transferred continuously to the system by a peristaltic pump (Model SJ-1121, Mitsumi Scientific Ind.). After the baseline current became steady, a 20-μl aliquot of phosphatidyl choline dispersion or human serum was injected into the system and the current changes were recorded. The peak current was used as a measure of phospholipid concentration.

RESULTS AND DISCUSSION

Immobilization of phospholipase D and choline oxidase

Figure 2 shows the stability of native phospholipase D and choline oxidase. Both enzyme solutions (1 mg ml^{-1} in 0.05M phosphate buffer, pH 8.0) were allowed to stand at 25°C. Phospholipase D was more stable than choline oxidase, but 80% of the original activity of the former was lost after incubation for 4 days. Therefore, immobilization of both enzymes is desirable for practical analytical use of these enzymes.

Phospholipase and choline oxidase were immobilized together on octyl-Sepharose, porous glass, polystyrene and in a collagen membrane. Table 1 summarizes the activities of the immobilized enzymes; the enzymes immobilized on octyl-Sepharose showed the highest activity. Therefore, the hydrophobicity of octyl-Sepharose may play an important role for the best retention of activity. The activity of the enzymes entrapped in the collagen
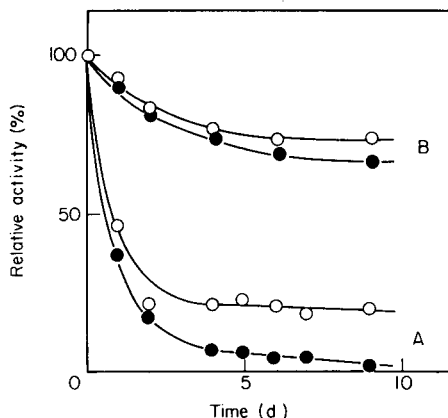
Fig. 2. Stability of phospholipase D (○) and choline oxidase (●). Curves A are for the native enzymes and curves B for the immobilized enzymes (for conditions, see text).

TABLE 1

Activities of various immobilized enzymes measured under the standard conditions

Carrier	Relative activity (%)	Specific activity [mU g^{-1} carrier]
Octyl-Sepharose[a]	100	300
Porous glass	10	30
Polystyrene	10	30
Collagen membrane	3	10

[a]Wet gel.

membrane was the lowest. This may be caused by inactivation of enzymes by glutaraldehyde. Phospholipase D and choline oxidase immobilized on octyl-Sepharose were employed for further study.

Response of the system
    Figure 3 shows typical responses obtained when various concentrations of phosphatidyl choline were used. An assay could be completed within 4 min, if the phosphatidyl choline concentration was ≤3 g l^{-1}. If at least 0.3 I.U. of phospholipase was used, a reliable assay of phosphatidyl choline in serum was obtained. The proportion of the two immobilized enzymes is an important factor in obtaining maximum reaction rate and complete reaction. When the phospholipase/choline oxidase weight ratio after immobilization was 0.9, the reaction was complete within 4 min.
    Figure 4 shows the effect of the buffer flow rate on the current. The
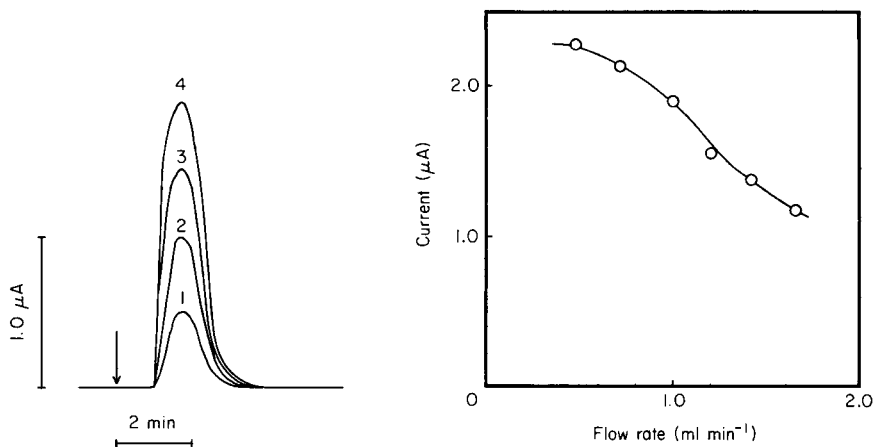
Fig. 3. Response curves for phosphatidyl choline at levels of : (1) 0.75; (2) 1.5; (3) 2.25; (4) 3.0 (all g l^{-1}). Reaction under the standard conditions except for the substrate concentrations.

Fig. 4. Effect of buffer flow rate on maximum current. Reaction under the standard conditions except for the flow rate.

current increased with decreasing flow rate. The reproducibility of the results was poor at a high flow rate because of the increased pressure drop along the column. However, the time required for assay became excessive at low flow rates and a flow rate of 1 ml min^{-1} was employed in subsequent experiments.

Effect of pH and various reagents

The effect of buffer pH is shown in Fig. 5. A broad optimum ranging from pH 8 to 10 was observed, although the optimum pH for phospholipase D was 7.0 —8.0. A shift of the optimum pH and broadening of the pH range for an enzyme after immobilization are common, and have been explained by Goldstein et al. [11]. Subsequent work was done at pH 8.0 because the pH of sera is about this value.

Because calcium ions and Triton X-100 play important roles in increasing the accuracy and the reaction rate in the enzymatic analysis of phospholipids [2], their effect on the analytical system was examined. The results obtained are shown in Figs. 6 and 7. Phospholipase D was found to be more sensitive to these species than choline oxidase. All subsequent studies were done with 50 μM calcium chloride —0.1% Triton X-100 solutions.

Calibration and application to sera

Batch analysis of phosphatidyl choline was first attempted with the apparatus described above. A sample solution (0.4 ml) was introduced and the
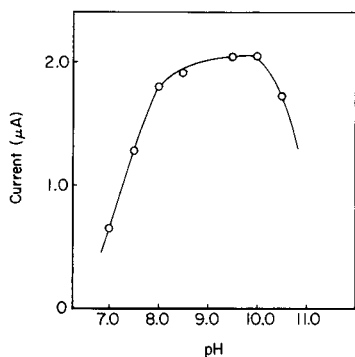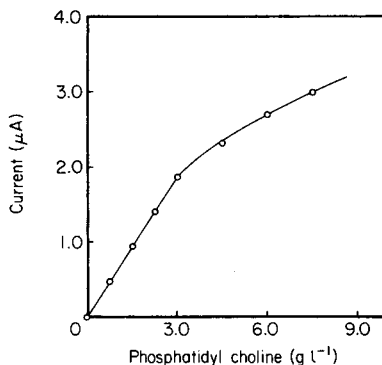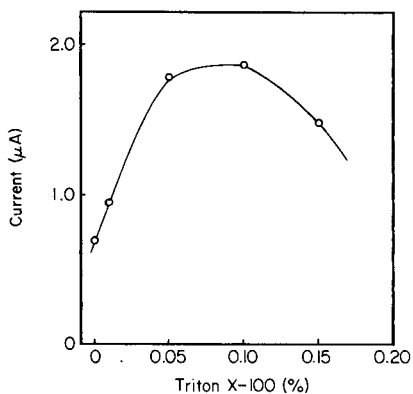
Fig. 5. Effect of buffer pH on the maximum current. Reactions under the standard conditions except for pH.
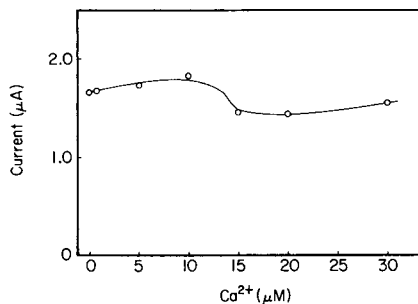
Fig. 6. Effect of calcium concentration in buffer on the maximum current. Reaction under the standard conditions except for the calcium concentration.

current was measured after incubation for 5 min. A linear relationship was found between the maximum current and the phosphatidyl choline concentration in the range 1—4 g l^{-1}, corresponding to about 2.5—11 μA. The current is greater than that given by the kinetic method, probably because the enzymatic reaction is complete. However, the time required for the assay is about 15 min for each sample. Therefore, the flow system was used for more rapid phosphatidyl choline assay. Figure 8 shows the relationship between the maximum current in the flow system and the phosphatidyl choline concentration. The calibration graph is linear up to 3 g l^{-1} for phosphatidyl choline.

Fig. 7. Effect of Triton X-100 concentration in buffer on the max. current. Reaction under the standard conditions except for the Triton X-100 concentrations.

Fig. 8. Calibration graph for flow analysis.

More concentrated sample solutions should be diluted with the buffer. The standard deviation for determination of 3 g l^{-1} of phosphatidyl choline was 0.15 g l^{-1} (50 experiments).

The phosphatidyl choline concentrations of fresh sera were determined by the proposed flow method and the conventional method [10, 11]. The results showed satisfactory agreement (correlation coefficient 0.90) for 16 assays of phosphatidyl choline in the range 1.5—3.5 g l^{-1}. This indicated that the immobilized enzymes system proposed gives an economical and reliable method for enzymatic assay of phospholipids in serum.

Stability of the immobilized enzymes

Figure 2 (curves B) shows the stability of the immobilized enzyme. A 3 g l^{-1} phosphatidyl choline solution was used; 0.1 g of immobilized enzymes (0.03 I.U.) in 0.05 M phosphate buffer (pH 8.0) was allowed to stand at 25°C. Phospholipase D was slightly more stable than choline oxidase. Both enzymes retained about 70% of their original activity after 9-d incubation. Furthermore, the immobilized enzymes were stable for 2 months when stored at 4°C. About 4% of the activity of the immobilized enzymes had been lost after 50 assays.

The activity of the reactor can be adjusted by varying the amount of immobilized enzymes placed inside the column. The rate of enzymatic catalysis can be regulated by varying the flow rate of the buffer. These, of course, control the overall reaction rate, which is very useful for enzymes having a low specific activity.

Because of these advantages, the bioelectrochemical sensor appears promising and attractive for use in the routine determination of phospholipids in biological fluids.

REFERENCES

1 B. R. Barlett, J. Biol. Chem., 243 (1959) 466.
2 S. Imamura, M. Ohno and Y. Hirouchi, J. Biochem., 81 (1977) 6.
3 M. Aizawa, I. Karube and S. Suzuki, Anal. Chim. Acta, 69 (1974) 431.
4 I. Satoh, I. Karube and S. Suzuki, Biotechnol. Bioeng., 18 (1976) 269; 19 (1977) 1095; J. Solid-Phase Biochem., 2 (1977) 1.
5 M. Faure, Bull. Soc. Chim. Biol., 32 (1950) 503.
6 C. H. Huang, Biochemistry, 8 (1969) 344.
7 O. Warburg and W. Christian, Biochem. Z., 310 (1941) 384.
8 H. H. Weetall, in K. Mosbach, (Ed.), Methods in Enzymology, Vol. 44, Immobilized Enzymes, Academic Press, New York, (1976) p. 139.
9 I. Karube, Y. Nakamoto, K. Namba and S. Suzuki, Biochim. Biophys. Acta, 429 (1976) 975.
10 C. C. Allain, Clin. Chem., 29 (1974) 470.
11 L. Goldstein, Y. Levin and E. Katchalski, Biochemistry, 3 (1964) 1913.

THE DETERMINATION OF HORSE-RADISH PEROXIDASE ACTIVITY BY ENTHALPIMETRIC AND POTENTIOSTATIC MEASUREMENTS

J. KEITH GRIME*

Department of Chemistry, University of Denver, University Park, Denver, CO 80208 (U.S.A.)

KENNETH R. LOCKHART

Department of Chemistry, University of Otago, P.O. Box 56, Dunedin (New Zealand)

(Received 9th October 1978)

SUMMARY

An enthalpimetric method is described for the determination of peroxidase activity based on the heat produced by the peroxidase-catalysed oxidation of iodide by hydrogen peroxide. Two other electron donors, hydroquinone and ascorbic acid, were found to be less suitable as substrates. The method described allows the determination of peroxidase activity in the range 2—79 IU with an r.s.d. of 3%. A potentiostatic method in which the iodide concentration is kept constant by the automatic incremental addition of sodium thiosulphate, gave activity measurements slightly less than the enthalpimetric method.

Horse-radish peroxidase (EC.1.11.1.7) is an iron-porphyrin enzyme that catalyses the oxidation of a wide variety of electron donors in the presence of hydrogen peroxide [1, 2]. The enzyme is quite stable; aqueous solutions may be stored for over a year at 5°C without significant loss in activity [3]. Peroxidase has found its primary analytical use as a secondary reagent, usually in conjunction with a chromogenic donor for the determination of substrates producing hydrogen peroxide in the primary enzymatic reaction [4]. Kits are available for the determination of glucose and galactose (Glucostat and Galactostat, Worthington Biochemical Corp.) based on coupled reactions with their respective oxidases. As an immobilized reagent, peroxidase has been used in the determination of uric acid in a coupled reaction with uricase [5], and L-phenylalanine in conjunction with L-amino acid oxidase [6]. Several inorganic ions have been determined via their inhibitory effect on peroxidase activity [7]. Thus, although the determination of peroxidase activity is not of direct physiological importance, the enzyme is important analytically.

Current methods of measuring peroxidase activity typically monitor the change of absorbance of a chromogenic donor, usually *o*-dianisidine, pyrogallol or guaiacol [4, 8]. Each has limitations. Accurate results have been obtained with *o*-dianisidine [9], but in view of its potential carcino-

genity, its use should be discouraged. Guaiacol solutions have limited stability [8] and the pyrogallol assay is time-consuming in that it contains several extraction steps [10]. In a recent report [11], the biamperostatic determination of peroxidase activity has been reported in which iodide was used as electron donor. A linear calibration graph over the range 10—150 m IU/8.5 cm^3, was obtained although the graph did not pass through the origin.

The advantages of using enthalpimetric or calorimetric procedures for enzyme assay have been discussed elsewhere [12—15]. The salient feature of this technique is the utilization of a fundamental property of all chemical reactions, the molar enthalpy of reaction. Accordingly, the primary enzymatic reaction can be monitored without recourse to complex coupling procedures. It has been shown [12] that the enzyme activity (EA), expressed in international units, can be related to the heat output of an enzymatic reaction by $EA = (1/\Delta H)(\Delta q/\Delta t) \times 10^{-6}$, where $\Delta q/\Delta t$ is the rate of heat evolution (or absorption) for an overall chemical reaction of molar enthalpy of reaction ΔH.

In the present report, the enthalpimetric determination of horse-radish peroxidase activity is described, based on the enzyme-catalysed oxidation of iodide by hydrogen peroxide. The enthalpimetric assay results are correlated with a signal-stat technique in which the rate of reaction is monitored by the rate of addition of a standard sodium thiosulphate solution necessary to maintain an effectively constant concentration of iodide ion. Delivery from the autoburette was triggered by small changes in cell potential.

Kinetic considerations

Peroxidase-catalysed reactions do not follow simple Michaelis—Menten kinetics [16] and the theory has been extended by Chance [17] to take into account the reaction of the enzyme—substrate complex (ES) with an electron or hydrogen donor (AH_2). Adopting Chance's terminology [16], the mechanism of peroxidase activity can be represented as follows:

$$E + S \underset{k_2}{\overset{k_1}{\rightleftharpoons}} ES; \ ES + AH_2 \overset{k_4}{\rightarrow} E + P$$
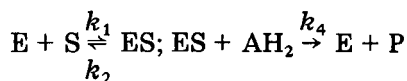
It has been shown [16] that if the hydrogen peroxide concentration (x_0) is such that $k_1 x_0 \gg k_4 a_0$, where a_0 is the donor concentration, then the rate of reaction can be represented by $k_1 = k_4 a_0$ and the kinetics are zero order if $x_0 \ll a_0$. As hydrogen peroxide is known to inhibit the reaction rate at elevated concentrations (see later), the attainment of zero-order kinetics at small values of x_0 is desirable. Clearly, the simultaneous fulfilment of the conditions $k_1 x_0 \gg k_4 a_0$ and $x_0 \ll a_0$, is not always possible because this implies that $k_1 \gg k_4$. The values of k_4 for hydroquinone and ascorbic acid have been reported as 3×10^6 mol^{-1} dm^3 s^{-1} and 2×10^4 mol^{-1} dm^3 s^{-1}, respectively, whilst the generally accepted value of $k_1(H_2O_2)$ is 9×10^8 mol^{-1} dm^3 s^{-1} [18, 19]. It should be possible, therefore, with judicious

choice of x_0 and a_0 to obtain pseudo zero-order kinetics with both substrates. In general, however, it has been observed that there is a considerable dependence of the rate of reaction on donor concentration while it is hardly affected by small changes in hydrogen peroxide concentration [8]. The expression of peroxidase activity in terms of substrate consumption per unit time is usually accompanied therefore by a statement of substrate concentration.

The general mechanism outlined for peroxidase activity does not apply for the oxidation of iodide. A rather complex mechanism involving the intermediate formation of an iron(III)-peroxidase—iodide complex has been suggested [20]. Because of the lack of a generally accepted mechanism, predictions about the reaction kinetics are not possible with this substrate.

EXPERIMENTAL

Reagents

Type 1 horse-radish peroxidase was used (lot no. 124C-9580; ca. 89 purpurogallin units/mg of solid; Sigma Chemical Co., St Louis). Stock solutions of peroxidase were prepared in distilled, deionized water. Solutions remained stable (as evidenced by their activity) for at least 4 weeks when stored at 4°C.

A 0.055 mol dm^{-3} stock solution of hydrogen peroxide (100 vol., analytical reagent-grade) was prepared and stored in dark bottles at 4°C. Working solutions were prepared as required by dilution of the stock solution and standardization by back-titration of excess of sodium arsenite with potassium iodate solution. Standardization of hydrogen peroxide solutions was done just before any series of enthalpimetric or potentiostatic measurements. The results indicated that hydrogen peroxide solutions remained stable for at least 8 h. Hydroquinone solutions were standardized by two-phase titration with potassium periodate in strong acid; excess of bromide ions was added to the titration mixture to stabilize the I^+ formed in this reaction.

Auto-oxidation of ascorbic acid solutions was minimized by storage in dark glass bottles at pH 5.0. In addition, a small amount of EDTA (1×10^{-4} mol dm^{-3}) was added to all ascorbic acid solutions, which were stored under an atmosphere of nitrogen. These solutions were standardized by direct titration with iodine.

Buffer solutions of pH 4.7 and 3.9 were prepared by adjustment of a 0.1 mol dm^{-3} sodium acetate—acetic acid mixture. Buffer solutions of pH 5.0 and 6.5 were prepared by adjustment of a 0.07 mol dm^{-3} mixture of disodium hydrogenphosphate and potassium dihydrogenphosphate. Sodium thiosulphate (0.100 mol dm^{-3}) was prepared by dilution of a Volucon concentrate. All solutions were prepared in distilled, deionized water.

Apparatus

All enthalpimetric measurements were done at 25.0°C (short-term stability ± 0.0002°C) on a Tronac calorimeter incorporating batch addition facilities. Minor modifications were made to the geometry of the mechanical stirring system to reduce heat generated by the stirring paddle. The imbalance potential engendered by temperature changes in the reaction cell was amplified by a variable-gain, null-detector microvoltmeter (Model 155, Keithley Instrument Co., Cleveland, Ohio) and recorded on a strip-chart potentiometer. Calibration heater voltages were measured with a model 3800B digital multimeter (Dana Instruments, Irvine, CA). Reagents were injected into the reaction cell through Teflon delivery lines from a gravimetrically calibrated 0.5-cm³ gas-tight syringe incorporating a Chaney adaptor. Temperature mismatch between solutions was precluded by immersion of the loaded syringe and the quasi-adiabatic reaction cell in the thermostatted water bath.

Potentiostatic measurements were made automatically with a Radiometer TTT2 automatic titrator with PHA 943 titrigraph module and titrigraph pen drive REA 300 in conjunction with a Radiometer ABU 12 autoburette. The electrode system, housed in a Radiometer M22 cell assembly, consisted of calomel and platinum electrodes (Radiometer, K401 and P101, respectively). The titrigraph was operated in the pH-stat mode with a proportional band setting of 0.05. All reagents were injected by gas-tight syringes as described earlier, and all potentiostatic measurements were made in a thermostatted cell at 25.00 ± 0.01°C.

Establishing the measurement procedure

Assignment of reaction enthalpies. The utilization of the equation for enzymatic enthalpimetry requires an assignment of the molar enthalpy of reaction for the overall enzymatic reaction, including any attendant buffer reactions. Accordingly, the enthalpy of reaction of the peroxidase-catalysed oxidation of three electron donors, hydroquinone, ascorbic acid and iodide by hydrogen peroxide was measured to ascertain the most suitable donor. In these "substrate-limiting" experiments, 0.5 cm³ of hydrogen peroxide solution, containing a 20% excess of reagent with respect to the electron donor, was injected into 15.00 cm³ of an appropriately buffered solution containing peroxidase (1.00 cm³) and donor (14.00 cm³). The resultant temperature change was monitored as the reaction proceeded to completion.

In the hydroquinone and iodide experiments, the invariance of the measured enthalpy of reaction over a range of substrate concentrations was construed as evidence that the reaction had gone to completion. After a post-reaction period (ca. 2 min), the recorder chart was calibrated in terms of heat change (in J) by activation of the Joule heating circuitry, and the reaction enthalpy (ΔH), calculated. Each donor required different conditions of pH and enzyme activity (see Table 1).

Some typical "substrate-limiting" enthalpograms are represented in

TABLE 1

Enthalpy measurements

Electron donor	Range taken (mol)	Mass of peroxidase (mg)	pH	ΔH (kJ mol^{-1})	No. of detns.
Hydroquinone	$7.4-68.3 \times 10^{-6}$	0.03	6.5	-208.6 ± 1.3	28
Ascorbic acid	$2.0-89.0 \times 10^{-6}$	1.5	5.0	-72 to -68	8
Iodide	$14.6-72.8 \times 10^{-6}$	0.06	4.7	-123.7 ± 0.7	12
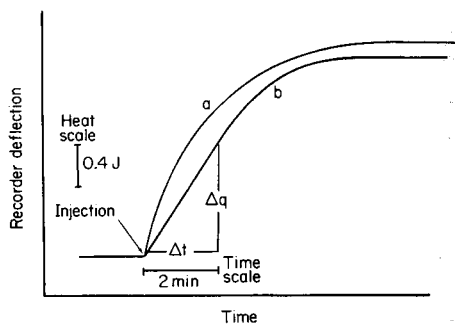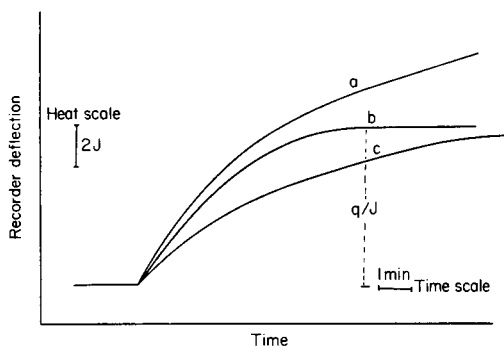
Fig. 1. Typical substrate limiting enthalpograms. (a) 100% excess of H_2O_2; (b) 20% excess of H_2O_2, hydroquinone or iodide as donor; (c) 20% excess of H_2O_2, ascorbic acid as donor.

Fig. 2. Enzyme assay enthalpograms for the initial slope method. (a) Hydroquinone as donor, (b) iodide as donor. $EA = (\Delta q / \Delta t)(1/\Delta H) 10^{-6}$ (IU).

Fig. 1. Precise enthalpy measurements were not possible in the ascorbic acid experiments because of the considerable curvature of the enthalpograms (Fig. 1, curve c). This precludes the use of ascorbic acid for the enthalpimetric assay of peroxidase activity. A common feature of all substrate-limiting enthalpograms was that a secondary heat effect was observed in the presence of a large excess of hydrogen peroxide (Fig. 1, curve a). This effect was reduced to negligible proportions by the use of a 20% excess of hydrogen peroxide (Fig. 1, curve b). Enthalpy values calculated from such enthalpograms are presented in Table 1. It is evident that, from an enthalpimetric viewpoint, hydroquinone should provide the most sensitive assay of peroxidase activity if the kinetic parameters are suitable.

It should be noted that such substrate-limiting experiments provide a convenient method of assay of either hydrogen peroxide or the electron donor. Extrapolating the enthalpy measurements observed to known sensitivity limits, it should be possible to determine hydroquinone and iodide down to a limit of 1×10^{-6} mol and 4×10^{-6} mol, respectively.

Conditions for enzyme assay. In order to assess the relationship between the substrate concentration and the measured enzyme activity, a series of

enthalpograms were recorded at a constant value of x_0 whilst varying a_0, and vice versa. In both series of experiments a constant mass of peroxidase was employed. Typical enthalpograms are represented in Fig. 2. Rate measurements were made by tangential extrapolation of the initial slope of the enthalpogram and conversion to IU after calibration in the usual manner.

Enthalpograms with hydroquinone (Fig. 2, curve a) were characterized by considerable curvature so that extrapolations of initial slope were imprecise. Clearly the magnitude of the rate constant k_4 for hydroquinone has an adverse effect on the suitability of this compound as a substrate for peroxidase assay. The observed reaction rate was shown to be independent of hydrogen peroxide concentration whilst exhibiting a first-order dependence on hydroquinone concentration up to a limiting value of 1.1 mol dm^{-3}. In contrast enthalpograms for iodide exhibited a considerable linear region, typically representing 70—80% of the total enthalpogram (Fig. 2, curve b). The dependence of the measured reaction rate on reagent concentrations is shown in Fig. 3. Evidently, maximum velocity cannot be attained and a dependence on the concentration of both hydrogen peroxide and iodide is observed. The inhibitory action of hydrogen peroxide at elevated concentrations is also apparent from Fig. 3, curve b. The construction of a Lineweaver—Burk double reciprocal plot [21] from enthalpimetric data confirmed that inhibition occurs at hydrogen peroxide concentrations of 8.3×10^{-3} mol dm^{-3}, as shown in Fig. 4. Maximum linearity of the initial slope of the enthalpogram was observed in the presence of 1.3×10^{-4} mol of iodide ions and 2.5×10^{-5} mol of hydrogen peroxide. In order to extend this technique to its sensitivity limits, a reaction rate—pH profile was constructed (Fig. 5), revealing maximum activity at pH 3.9. The above results produced a set of experimental conditions which allowed the accurate enthalpimetric assay of peroxidase activity.
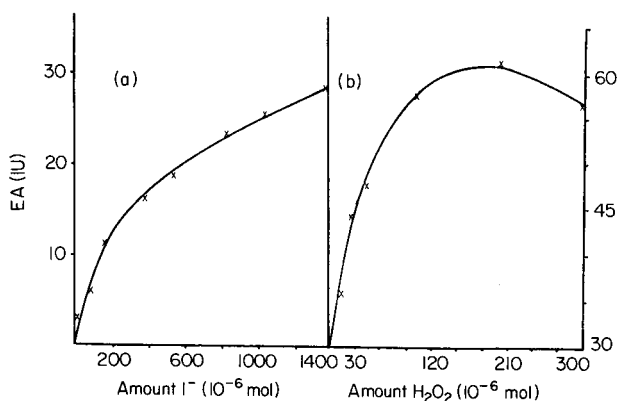

Fig. 3. Peroxidase activity vs. substrate concentration. (a) I$^-$ dependence, [H$_2$O$_2$] = 1.6×10^{-5} mol; (b) H$_2$O$_2$ dependence, [I$^-$] = 2.6×10^{-4} mol.
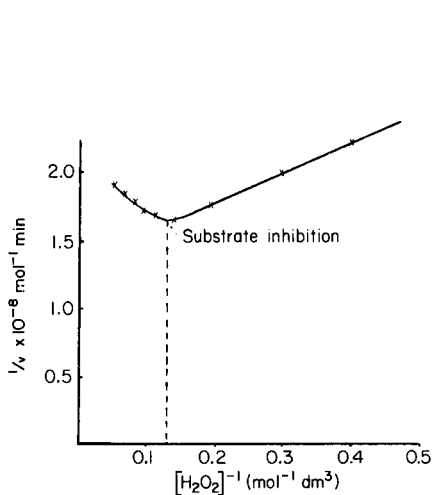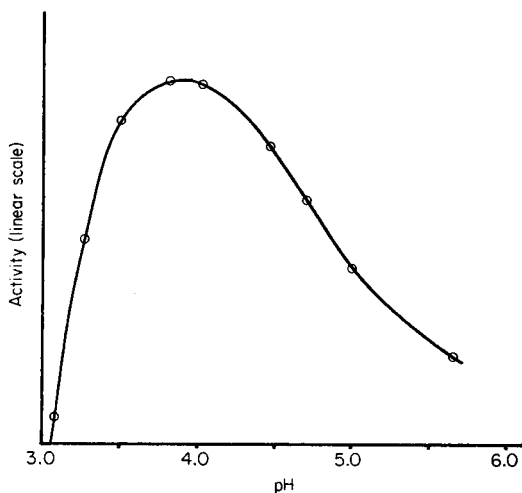
Fig. 4. Lineweaver—Burk plot showing H_2O_2 inhibition.

Fig. 5. pH profile for the H_2O_2—iodide—peroxidase reaction.

Procedures established

Enthalpimetric measurements. Enzyme assays were done by a reagent addition procedure identical to that described for the assignment of reaction enthalpies. In this case, however, the relevant data were obtained by measurement of the initial slope of the linear enthalpogram (see Fig. 2). In the experiments, 2.47×10^{-5} mol of hydrogen peroxide (0.5 cm^3) was injected into 15.00 cm^3 of a solution containing the peroxidase and iodide (1.29 $\times 10^{-4}$ mol) buffered at pH 3.9. Reagent blanks produced negligible heat effects.

Potentiostatic correlation measurements. In view of the dependence of the observed enzyme activity on substrate concentration, potentiostatic correlation analyses were done under experimental conditions identical to those described for enthalpimetric analyses. In practice, the tip of the titrant delivery line was immersed just below the surface of a buffered solution containing peroxidase and 1.29×10^{-4} mol of iodide. The stirring mechanism was activated, and the cell and its contents allowed to come to equilibrium with the thermostatted bath. The cell potential was noted and the titrigraph programmed to maintain this potential via incremental addition of 0.100 mol dm^3 sodium thiosulphate solution. Typically, potential changes of ca. 20 mV occurred before activation of the titrant delivery circuitry. Clearly the substrate concentration factors described dictate that the volume of titrant added should be minimized. The concentration of sodium thiosulphate used sufficed to ensure that the total volume of titrant added never exceeded 1 cm^3. The rate of addition of titrant was adjusted to produce a satisfactory
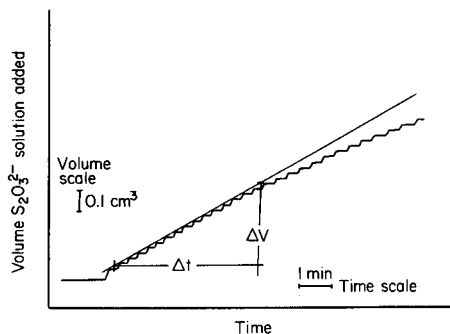
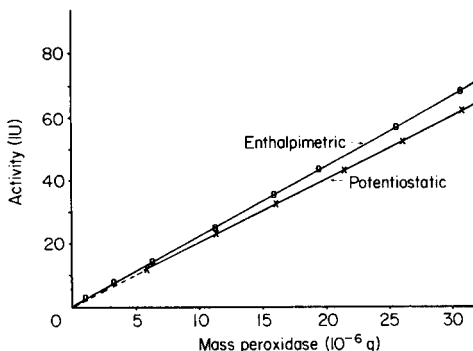Fig. 6. Typical potentiostatic progress curve.

Fig. 7. Activity determined vs. mass of peroxidase.

progress curve depending on the enzyme activity. Rate measurements were made by tangential extrapolation of the initial slope of the progress curve (Fig. 6).

RESULTS AND DISCUSSION

A plot of enzyme activity versus mass of peroxidase taken is linear over a wide range of activities (2—79 IU) for the enthalpimetric assay procedure (Fig. 7). A comparative plot for the potentiostatic procedure, included in Fig. 7, reveals a discrepancy between the two techniques which increases with increasing mass of enzyme. The precision of both techniques, however, is similar over the range 14—75 IU (Table 2). Correlation data are not presented below 14 IU as the potentiostatic curves became subject to considerable curvature at these levels making measurements of initial slope difficult. Enthalpimetric assays, however, were possible down to 2 IU (see Fig. 7). The lower activities obtained in the potentiostatic method may be related either to the decreased substrate concentration in the reaction mixture caused by titrant addition or to an inhibitory effect of thiosulphate on peroxidase activity [20] or a combination of these factors.

The enthalpimetric procedure is subject to the same kinetic limitations as most peroxidase assays. The dependence of peroxidase activity on hydrogen peroxide and iodide concentrations and the inability to achieve maximum reaction velocity dictates that both substrate concentrations must be accurately reproduced for a valid assignment of enzyme activity. Under these conditions, it is possible to determine peroxidase activity to a lower limit of 2 IU (corresponding to ca. 1 μg of Type I Sigma horse-radish peroxidase) with a relative standard deviation of ca. 3%.

The enthalpimetric procedure described, in contrast to many existing methods, provides a convenient, one-step procedure which monitors directly

TABLE 2

Correlation and precision data

Activity (IU) (enthalpimetric)	R.s.d. (%)[a]	Activity (IU) (potentiostatic)	R.s.d. (%)[a]
76.9	0.5 (4)	66.3	0.4 (4)
60.9	0.6 (4)	52.5	0.4 (4)
38.7	0.8 (4)	33.9	0.9 (4)
15.2	1.2 (4)	13.8	1.4 (4)
8.3	2.1 (3)	—	—
3.2	3.1 (3)	—	—

[a]Number of determinations in parentheses.

the rate of the primary enzymatic reaction, thus avoiding the use of complex electron donors in order to produce a measurable entity. The relatively large enthalpy of reaction and well-defined enthalpograms obtained in the "substrate-limiting" experiments suggest that this technique could be adapted easily to provide a relatively sensitive and precise determination of substrates which produce hydrogen peroxide in coupled enzyme systems.

REFERENCES

1 H. Theorell in J. B. Sumner and K. Myrback (Eds.), The Enzymes, 2 Pt.I, Academic Press, New York, 1951, p. 397.
2 B. Chance, in J. B. Sumner and K. Myrback (Eds.), The Enzymes, 2 Pt.I, Academic Press, New York, 1951, p. 428.
3 Worthington Enzyme Manual, Worthington Biochemical Corporation, 1977, p. 67.
4 G. G. Guilbault, Enzymatic Methods of Analysis, Pergamon, Oxford, 1970.
5 S. W. Kiang, J. W. Kuan, S. S. Kuan and G. G. Guilbault, Clin. Chem., 22 (1976) 1378.
6 G. Guilbault and G. Nagy, Anal. Lett., 6 (1973) 301.
7 G. G. Guilbault, P. Brignac and M. Zimmer, Anal. Chem., 40 (1968) 190.
8 J. Putter, in H. U. Bergmeyer (Ed.), Methods of Enzymatic Analysis, Academic Press, New York, 2 (1974) 685.
9 J. Putter, Habilitationsarbeit Universitat Bonn (1964).
10 Peroxidase assay data sheet, Sigma Chemical Company, P.O. Box 14508, St. Louis, Missouri, U.S.A.
11 S. Pantel and H. Weisz, Anal. Chim. Acta, 89 (1977) 47.
12 C. D. McGlothlin and J. Jordan, Anal. Chem., 47 (1975) 1479.
13 C. D. McGlothlin, J. K. Grime and J. Jordan, Enzymatic Enthalpimetry for Clinical Analysis, at Symposium of New Approaches to the Routine Determination of Serum Enzymes, Paper No. 71, American Chemical Society, New York, April, 1976.
14 K. Levin, Clin. Chem., 23 (1977) 929.
15 C. Spink and I. Wadso, in D. Glick (Ed.), Methods of Biochemical Analysis, Vol. 23, 1976, p.
16 B. Chance, in D. Glick (Ed.), Methods of Biochemical Analysis, Vol. 1, 1954, p. 408.
17 B. Chance, J. Biol. Chem., 151 (1943) 553.
18 K. G. Paul in P. D. Boyer, H. A. Lardy and K. Myrback (Eds.), The Enzymes, Vol. 8, Academic Press, New York, 1963, p. 227.
19 T. E. Barman, Enzyme Handbook, Springer Verlag, Berlin, 1 (1969) 234.
20 F. Bjorksten, Biochim. Biophys. Acta, 212 (1970) 396.
21 M. Dixon and E. C. Webb, Enzymes, Longmans, London, 1958, p. 85.

POLAROGRAPHIC STUDY: THE REACTION OF K VITAMINS WITH THIOLS AND THE CONSECUTIVE DETERMINATION OF THE K VITAMINS

KIYOKO TAKAMURA*, MIZUHO SAKAMOTO and YUMIKO HAYAKAWA

Tokyo College of Pharmacy, 1432-1 Horinouchi, Hachioji, Tokyo 192-03 (Japan)

(Received 30th August 1978)

SUMMARY

The reactions of the K vitamins and eight thiols were studied by polarography in 80% ethanol in the apparent pH range 3—10. In the absence of oxygen, thiols react with vitamin K_3 at the 3-position to form naphthohydroquinones with a thioether linkage. The general reaction mechanism was confirmed by electrochemical and spectrophotometric measurements. Vitamins K_1 and K_2 do not react. The consecutive determination of K_3 and K_1 (or K_2), whose polarographic reduction waves completely overlap, can be achieved by measurement of the total wave height, then adding excess of thioglycolic acid at pH 6.2, which results in the complete disappearance of the diffusion current of K_3. This enables K_1 (or K_2) to be determined, and hence K_3 by difference.

The biological significance of the K vitamins has become of interest in recent years [1, 2]. Since differences in their biochemical and physiological actions have been noted [2], satisfactory methods for the separation and the determination of the K vitamins from each other seem to be particularly needed.

The reaction of vitamin K_3 (abbreviated to K_3) with cysteine in alkaline solution to form a red product has been applied to the colorimetric determination of K_3 in the presence of vitamins K_1 and K_2 [3] (abbreviated to K_1 and K_2), since both K_1 and K_2 are unreactive to cysteine. In this case, the determination of K_1 and K_2 simultaneously with K_3 is impossible because of the instability of K_1 and K_2 in alkaline media.

Each K vitamin has been found to exhibit well-defined polarographic reduction waves [4—6], but their half-wave potentials are so similar that these vitamins cannot be determined simultaneously by d.c. or a.c. polarography.
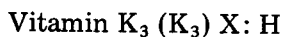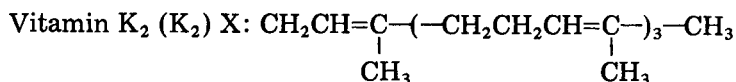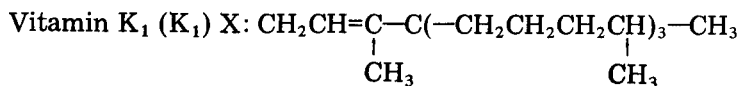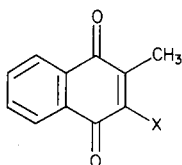
During the course of an investigation of reactions between quinones and thiols, the reaction of K_3 with some thiols in the absence of oxygen at ca. pH 7 [7] was found to produce adducts having a naphthohydroquinone-thioether structure. Such a reaction is not expected to occur for K_1 or K_2 because of the substituents at both the 2- and 3-positions.

The present paper is concerned with the reactivity of the K vitamins with several kinds of thiols, as studied by polarography, and the use of thiols in the separation and polarographic determination of the K vitamins.

EXPERIMENTAL

Reagents

Reagent-grade vitamin $K_{1(20)}$ and vitamin K_3 were obtained from Wako Pure Chemical Industries Ltd. Synthetic vitamin $K_{2(20)}$ was kindly supplied by Eizai Co. Ltd. Mercaptoethylamine was purified by sublimation. All other thiols and other chemicals used were reagent grade and used without further purification. The formulae of the K vitamins are shown below.

Vitamin K_1 (K_1) X: $CH_2CH=C-C(-CH_2CH_2CH_2CH)_3-CH_3$ with CH_3 substituents

Vitamin K_2 (K_2) X: $CH_2CH=C-(-CH_2CH_2CH=C-)_3-CH_3$ with CH_3 substituents

Vitamin K_3 (K_3) X: H

Apparatus

D.c. polarograms were recorded on a Yanako pen-recording polarograph, model P-8. The mercury flow rate and the drop time of the dropping mercury electrode (d.m.e.) used were 0.821 mg s^{-1} and 7.99 s, respectively. These values were measured in an air-free base electrolyte solution at open circuit and at 25°C. The potentials were referred to a saturated calomel electrode (s.c.e.) and all the measurements were carried out at 25 ± 0.1°C.

U.v.-visible absorption spectra were measured on a Hitachi model 323 spectrophotometer and absorbance at a constant wavelength was measured by a Hitachi Perkin-Elmer model 139 spectrophotometer at room temperature.

Preparation of solutions

Because of the extremely low solubility of the K vitamins in water, 80% ethanol/20% water (v/v) was used for the study of their reaction with thiols and for the electrochemical measurements. The pH of the solutions was adjusted with acetic acid—sodium acetate (pH 3.0—6.2) and ammonia— ammonium nitrate (pH 8—10), and the ionic strength was made 0.2 by addition of sodium perchlorate.

To make a test solution, the ethanolic stock solution of the K vitamins was diluted with the appropriate amounts of aqueous buffer solution and ethanol. Before each experiment, the concentration of the K vitamins was determined polarographically [6]. The stock solutions of thiols (0.20 M) were prepared by dissolving each thiol in water, and the concentrations were determined colorimetrically with 5,5′-dithiobis(2-nitrobenzoic acid) [8]. The stock solutions of K vitamins and thiols were stored in a dark place and in a refrigerator, respectively, and were made up fresh every week.

For the electrochemical measurements and the observation of the reaction under oxygen-free condition, dissolved oxygen was removed by bubbling pure nitrogen gas through the solution.

Measurement of equilibrium constants

The solutions of K_3 containing each thiol were allowed to stand at 25°C under oxygen-free conditions until equilbrium was reached. Then the equilibrium concentration of K_3 ($[K_3]_e$) was obtained by measurement of the diffusion current of K_3 at −0.7 V.

Assuming that the reaction between K_3 and thiol is:

(1)
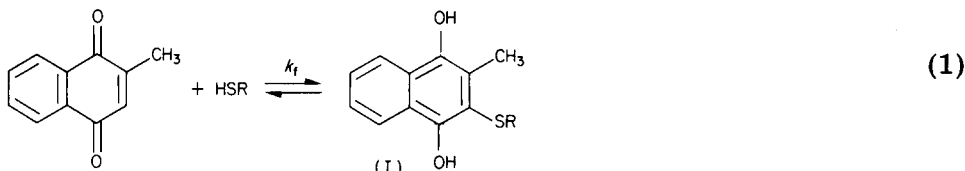
the equilibrium concentrations of thiol and reaction product (I) are given by $[HSR]_e = [HSR]_0 - ([K_3]_0 - [K_3]_e)$ and $[I]_e = [K_3]_0 - [K_3]_e$ where $[K_3]_0$ and $[HSR]_0$ are the initial concentrations of K_3 and thiol. The equilibrium constant (K) is given by $K = [K_3]_e [HSR]_e/[I]_e$.

Measurement of rate constant

After adding each thiol to the K_3 solution at a 1:1 molar ratio under oxygen-free conditions, the time-dependence of the diffusion current of K_3 during the period of the reaction was recorded, and from the results, a plot was made of the relation:

$$k_f t = \frac{a - a_e}{a(2a - a_e)} \ln \frac{a\, a_e(a - a_e) + (a - a_e)^2\, (a - x)}{(a - x - a_e)a^2}$$ (2)

where $a = [K_3]_0 = [HSR]_0$, $a_e = [K_3]_e$ and $x = [K_3]_0 - [K_3]_t$, and $[K_3]_t$ is the concentration of K_3 at time t. The rate constant (k_f) corresponding to reaction (1) was calculated from the slope of the plot of the right-hand side of eqn. (2) against t.

Consecutive determination of the K vitamins

Polarograms of K_1 (or K_2) and K_3 at pH 6.2 whose total concentration was in the range 0.1 to 1 mM were recorded in the potential region 0 to −1.0 V. The diffusion current (i_K) corresponding to both K vitamins was measured at −0.7 V. After 2.0 ml of aqueous 0.1 M thioglycolic acid solution had been added to the test solution and nitrogen bubbled for 20 min, the diffusion current (i_K') was again measured at −0.7 V, and corrected for dilution. The corrected value (i_K'') corresponds to the concentration of K_1 (or K_2). The concentration of K_3 is obtained by difference. Calibration plots for both components were obtained individually.

RESULTS AND DISCUSSION

Effect of thioglycolic acid on the polarograms of the K vitamins

Figure 1 shows the d.c. polarograms of K_1 and K_3 with and without thioglycolic acid at pH 6.2. Both K_1 and K_3 exhibit a well-defined reduction wave
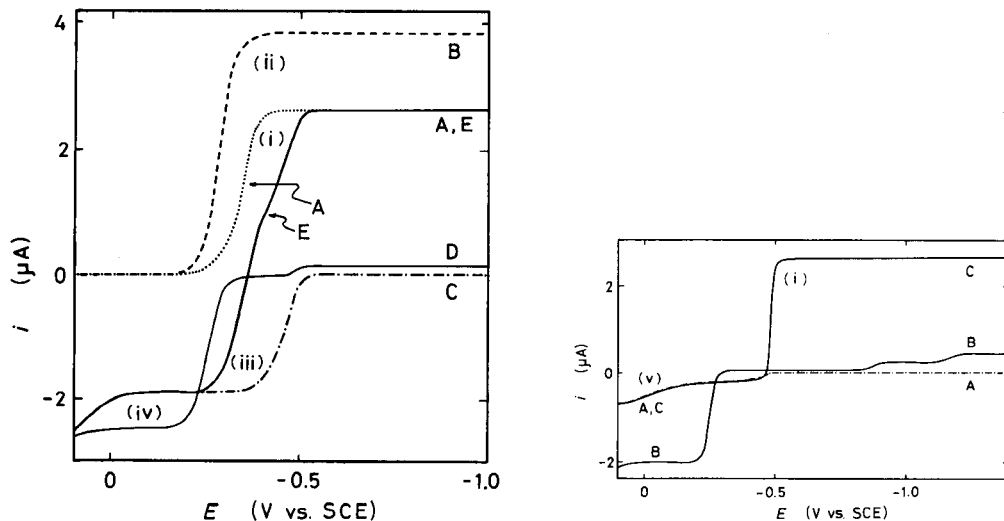
Fig. 1. Polarograms of K_1 and K_3 with and without thioglycolic acid (TGA) at pH 6.2. (A) 1.00 mM K_1; (B) 1.00 mM K_3; (C) 1.00 mM TGA; (D) 1.00 mM K_3 + 1.00 mM TGA; (E) 1.00 mM K_1 + 1.00 mM TGA. D and E were recorded after a 60-min reaction in the absence of oxygen.

Fig. 2. Polarograms of (A) 1.00 mM cysteine (cys), (B) 1.00 mM K_3 + 1.00 mM cys and (C) 1.00 mM K_1 + 1.00 mM cys. B and C were recorded after a 60-min reaction in the absence of oxygen.

(denoted as (i) and (ii) on curves A and B, respectively). The electrode reaction is
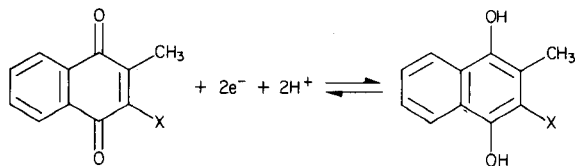
The half-wave potentials of waves (i) and (ii) are —0.34 and —0.28 V, respectively. The limiting diffusion current was directly proportional to the concentration for both the waves. The polarogram of K_2 obtained in the same medium was very similar to that of K_1.

Thioglycolic acid gives no reduction wave but there is an oxidation wave (denoted as (iii) on curve C in Fig. 1, $E_{1/2}$ = —0.45 V) corresponding to the formation of an insoluble mercury(I) complex on the mercury surface [9]. Figure 1 also shows the polarogram of a K_3—thioglycolic acid mixture recorded after a 60-min reaction time in the absence of oxygen (curve D). An increase in the thioglycolic acid concentration led to a marked decrease in the heights of both the waves (ii) and (iii) and an appearance of new oxidation wave (wave iv; $E_{1/2}$ = —0.26 V). The height of the new wave was proportional to the decrease in that of wave (ii). Curve E is the polarogram of the K_1—thioglycolic acid mixture obtained under the same conditions as curve D. In curve

E, the oxidation wave of thioglycolic acid is followed by the reduction wave of K_3. The total wave height coincides with the sum of the heights of waves (i) and (iii), indicating that there is no interaction between K_1 and thioglycolic acid. K_1 (or K_2) can be determined by measuring its diffusion current at potentials more negative than -0.5 V, even in the presence of thioglycolic acid.

Effects of other thiols on the polarograms of the K vitamins

Thiomalic and β-mercaptopropionic acids, N-acetylcysteine, 2-mercaptoethylamine and mercaptoethanol also exhibited an oxidation wave at pH 6.2 and the half-wave potentials obtained were -0.48, -0.43, -0.45, -0.46 and -0.43 V, respectively. In contrast glutathione and cysteine gave an ill-defined oxidation wave (cf. Fig. 2, wave v) whose wave height was independent of the concentration of the thiol. This behavior is typical of sulfur compounds, and is caused by the formation of adsorbed mercury(I) complexes on the mercury surface [10].

Mixtures of K_3 and the above thiols other than cysteine gave polarograms similar to curve D in Fig. 1. The polarogram of the K_3—cysteine mixture was complicated (Fig. 2, curve B). Two new reduction waves appeared ($E_{1/2} = -0.85$ and -1.2 V) as a result of the reaction between K_3 and cysteine. None of the thiols affected the reduction waves of K_1 and K_2 (see, for example, curve C, Fig. 2).

All the above results show that K_3 is reactive while K_1 and K_2 are unreactive to thiols. This finding can be applied to the consecutive determination of K_1 (or K_2) and K_3.

Reaction mechanisms

Polarograms and absorption spectra obtained for the K_3—thioglycolic acid mixture under oxygen-free condition are shown in Figs. 3 and 4, respectively.
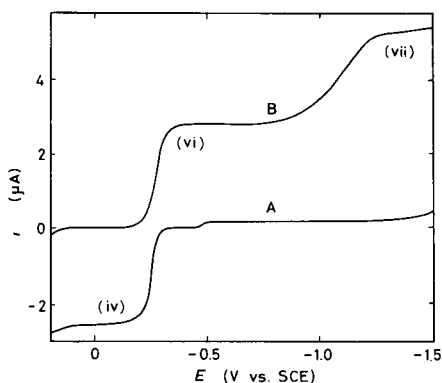

Fig. 3. Polarograms of a reaction mixture of 1.00 mM K_3 and 1.00 mM TGA. Curve A was obtained in the absence of oxygen. After (A) had been recorded, the solution was aerated for 60 min, to give curve B.
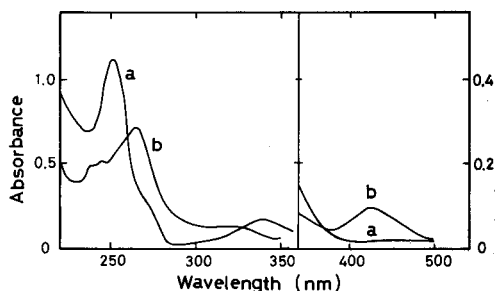
Fig. 4. U.v.-visible absorption spectra of reaction mixture of 0.050 mM K_3 and 0.050 mM TGA: spectra (a) and (b) were obtained under the same conditions as (A) and (B) in Fig. 3, respectively.

After these curves had been recorded, the solution was aerated for 60 min, as a result of which, wave (iv) disappeared completely, two reduction waves (vi) and (vii) appeared (Fig. 3), and a new absorption peak was observed at 430 nm (Fig. 4). The half-wave potential and height of wave (vi) were the same as those of wave (iv). Wave (vi) and the new absorption peak were also produced by electrolysis of the K_3—thioglycolic acid mixture at constant potential (—0.10 V). Thus, waves (iv) and (vi) are produced by a reversible redox couple and the new absorption peak is attributable to the oxidized form in the redox couple.

The peak at 430 nm can be assigned to the quinone-thioether linkage [11] so that the formation of S-(2-methyl-1,4-naphthoquinone-3-yl)thioglycolic acid (II) is evident. Then the reaction product of K_3 and thioglycolic acid is readily proved to be the reduced form of II, namely, S-(2-methyl-1,4-naphtho-hydroquinone-3-yl)thioglycolic acid (I, R = CH_2COOH) and consequently the reaction can be expressed as in eqn. (1). The waves (iv) and (vi) correspond to the oxidation and reduction directions, respectively, of the reaction I ⇌ II + 2e + 2H$^+$.

In Fig. 3, wave (vii) was assigned on the basis of its half-wave potential to the reduction of hydrogen peroxide, formed as a by-product during the air-oxidation of I.

Similar results were also obtained with all the other thiols tested except cysteine. The results for the K_3—cysteine mixture, in which two reduction waves were observed in the negative potential region (see Fig. 2), cannot be explained in detail. However, it was found by use of an excess of K_3 that approximately twice as much K_3 as cysteine was required to reach equilibrium. This suggests that subsequent reaction steps, such as reactions (3) [12] and (4) [13], must account for reaction (1).

$$(3)$$

$$(4)$$
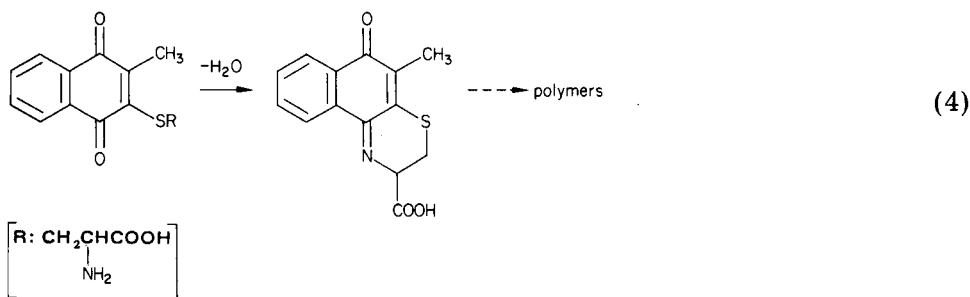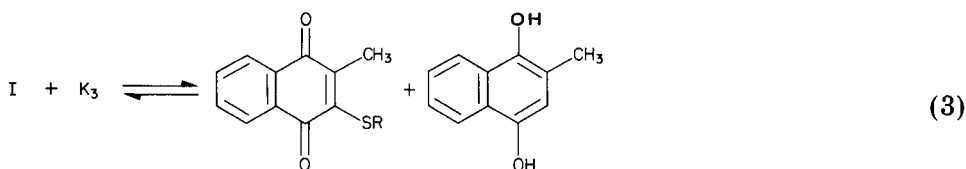
Among the K_3—thiol systems investigated, K_3—cysteine is the only case to give such results. As reaction (4) proceeds reaction (3) will be driven further to the right until 2 mol of K_3 have reacted with 1 mol of cysteine. The two

reduction waves on curve B in Fig. 2 are perhaps due to electroreduction of the thiazine derivatives resulting from reaction (4).

Analytical application: consecutive determination of vitamins K_1 (or K_2) and K_3

Based on the above experimental results, the consecutive determinations of K_1 (or K_2, both having substituent groups at the 2- and 3-positions of naphthoquinone ring) and K_3 (having no substituent group at the 3-position) can be achieved as described in the Experimental section. The reduction current observed for the sample solution without addition of thiol reflects the total concentration of the K vitamins. That part of the current corresponding to K_3 disappears when excess of thiol has been added, so that the concentration of K_1 (or K_2) is determined by measuring the remaining current. The decrease in current is a measure of K_3 concentration.

Effect of dissolved oxygen. Complete absence of dissolved oxygen during the reaction is necessary, otherwise quinone-thioether compounds produced by air-oxidation of hydroquinone-thioether compounds give a reduction wave, i.e., wave (vi), at around -0.3 V which interferes with the measurement of the reduction wave of K_1 (or K_2). The further reaction products formed in cases such as the K_3—cysteine system exhibit reduction waves (cf. curve B in Fig. 2), but they appear at such negative potentials that they cause no problems in the analysis.

Effect of pH. Complete disappearance of the diffusion current of K_3 in a short time after addition of thiol is necessary if mixtures of K vitamins are to be determined. Figure 5 shows that the diffusion current of K_3 (i_{K_3}) decreases more rapidly with increasing pH of the solution. No appreciable change is observed below pH 3. Similar results were obtained for other thiols. However, quinones, including the K vitamins, are rather unstable in alkaline media, so
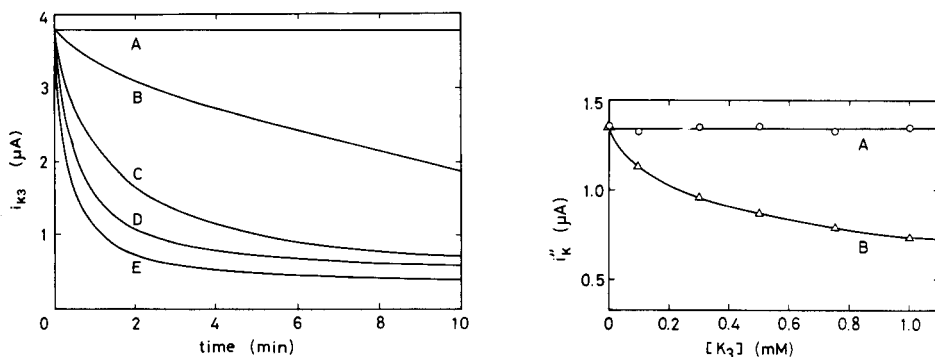

Fig. 5. i_{K_3} (at -0.70 V) vs. time curves obtained at various pH values during the reaction between K_3 and TGA in the absence of oxygen. $[K_3]_0 = 1.00$ mM; $[TGA]_0 = 1.00$ mM. (A) 1.00 mM $HClO_4$; (B) pH 4.6; (C) pH 6.2; (D) pH 8.8; (E) pH 9.8.

Fig. 6. Effect of added K_3 on i''_K obtained with (A) K_1—TGA and (B) K_1—cys mixtures. i''_K was measured after a 20-min reaction in the absence of oxygen. $[K_1]_0 = 0.500$ mM, $[TGA]_0 = 10$ mM, $[cys]_0 = 10$ mM.

that the reproducibility of the present method is invariably poor under such conditions. The pH of the solution was fixed at 6.2 in further experiments.

Reactivity of various thiols with K_3. The reactivity of five thiols with K_3 was compared in order to establish the reaction time required for the complete consumption of K_3. The equilibrium constants (K) and the rate constants (k_f) for reaction (1) were determined at pH 6.2 by the procedure described above. The results obtained are listed in Table 1. It is apparent that the values of K and k_f increase with increasing pK_a of the thiol.

In general, the increase in pK_a of the thiol gives rise to increased nucleophilicity of the thiolate ion, but also results in a decrease of the thiolate ion concentration. The results in Table 1 suggest that the nucleophilicity of the thiolate ion is the predominant factor in the reactivity of thiols with K_3.

Since thioglycolic acid is the most reactive of the five thiols, it seems to be the most effective reagent for the consumption of K_3. From the data in Table 1, the reaction time required to consume 99.8% of the initial amount of K_3 can be calculated to be 19 min in the presence of a ten-fold mole ratio of thioglycolic acid to K_3. Actually, the reduction wave of K_3 has disappeared after standing for 18 min under such conditions.

Similar treatment could not be applied to some other thiols such as mercaptoethanol, glutathione and cysteine, because of the complications arising from the subsequent reactions. However, cysteine reacts more rapidly with K_3 than the above five thiols; within 15 min wave (ii) had disappeared when ten times the amount of cysteine was added. Thus, since cysteine also showed promise as a reagent for separating the K vitamin responses, the following experiment was carried out for both thiols.

It was confirmed that neither K_1 nor K_2 reacts with thioglycolic acid or cysteine, even when the thiols are present in excess. Confirmation was needed, however, as to whether an appreciable interaction takes place between K_1 or K_2 and the product (I) in reaction (1). The polarograms of a solution containing 0.5 mM K_1 and 10 mM thioglycolic acid or cysteine in the presence of various concentrations of K_3 were recorded after reaction for 20 min. Plots of the wave height (at -0.7 V, denoted as i''_K) against the concentration of K_3 added are shown in Fig. 6, in which i''_K corresponds to the concentration of K_1 in

TABLE 1

Equilibrium and rate constants for reaction (1)

Thiol	pK_a[a]	K (M)	k_f (mM^{-1} min^{-1})
Thioglycolic acid	10.24	241	3.5×10^{-2}
Thiomalic acid	10.55	126	2.5×10^{-2}
β-Mercaptopropionic acid	10.05	99	2.0×10^{-2}
N-Acetylcysteine	9.52	47	1.5×10^{-2}
2-Mercaptoethylamine	8.27	25	2×10^{-2}

[a]Dissociation of SH group.

TABLE 2

Determination of K_2 and K_3 in admixture

[K] added (mM)		[K] found (mM)		Error (%)	
K_2	K_3	K_2	K_3	K_2	K_3
0.200	0.200	0.202	0.195	+1.0	−2.5
0.200	0.998	0.200	1.026	0	+2.8
0.400	0.499	0.398	0.500	−0.5	+0.2
0.500	0.200	0.501	0.194	+0.2	−3.0
1.000	0.998	1.007	0.987	+0.7	−1.1

the solution because of the complete consumption of K_3 by the large excess of thiol. In the case of thioglycolic acid (curve A), i_K'' is scarcely affected by the presence of up to 1.0 mM K_3. However, in the case of cysteine (curve B), a significant decrease in i_K'' is observed with increasing K_3 concentration. This suggests that the decrease in the K_1 concentration may arise from an interaction between K_1 and product I, i.e., it seems most likely that reactions similar to reactions (3) and (4) take place between K_1 and I [14]. Similar results were obtained for K_2 in place of K_1. Consequently, the use of cysteine causes serious errors in the determination of K_1 or K_2, whereas thioglycolic acid causes no such problem. Therefore, thioglycolic acid is recommended as the more suitable reagent.

Results of the determination of the K vitamins. The conditions and analytical procedure as given in the Experimental part are based on the above findings. The method was applied to the determination of the vitamins in mixed K_2–K_3 samples. The results are given in Table 2. Similar results were obtained for K_1–K_3 mixed samples. The method was accurate to ±3%.

REFERENCES

1 E. Zoch, in R. Ammon and W. Dirscherl (Ed.), Fermente, Horm., Vitam. Beziehungen Wirkstoffe Zueinander, Dritte Erweiterte Aufl., 3 (1974) 383.
2 R. A. Morton, Biol. Rev., 46 (1972) 47.
3 J. V. Scudi and R. P. Buhs, J. Biol. Chem., 144 (1942) 599.
4 H. B. Hershberg, J. Wolf and L. F. Fieser, J. Am. Chem. Soc., 62 (1940) 3516.
5 J. C. Jongkind, E. Buzza and S. H. Fox, J. Am. Pharm. Ass., Sci. Ed., 46 (1957) 214.
6 G. J. Patriarche and J. J. Lingane, Anal. Chim. Acta, 49 (1970) 241.
7 Y. Hayakawa and K. Takamura, J. Pharm. Soc. Jpn., 95 (1975) 1173.
8 J. C. Kaplan and J. C. Dreyfus, Bull. Soc. Chim. Biol., 46 (1964) 775.
9 I. M. Kolthoff and J. J. Lingane, Polarography, Vol. 2, Interscience, New York, 1952, pp. 779–791.
10 M. Brezina and P. Zuman, Polarography in Medicine, Biochemistry and Pharmacy, Interscience, New York, 1958, pp. 510–513.
11 H. Nishibayashi, N. Nakai and R. Sato, J. Biochem., 62 (1967) 215.
12 L. F. Fieser and R. B. Turner, J. Am. Chem. Soc., 69 (1947) 2335.
13 N. Nakai and J. Hase, Chem. Pharm. Bull., 16 (1968) 2334.
14 Y. Hayakawa and K. Takamura, J. Pharm. Soc. Jpn., 95 (1975) 1292.

ION-PAIR EXTRACTION OF BASIC DRUGS WITH DI(2-ETHYLHEXYL) PHOSPHORIC ACID

G. HOOGEWIJS and D. L. MASSART*

Dienst Analytische Scheikunde en Bromatologie, Farmaceutisch Instituut, Vrije Universiteit Brussel, Bosstraat, B-1090 Brussels (Belgium)

(Received 9th October 1978)

SUMMARY

Basic drugs can be quantitatively extracted from aqueous solution as ion-pair adducts, with di(2-ethylhexyl) phosphoric acid in chloroform. The effects of pH, ionic strength, and organic solvent are reported. The nature of the solvent and the pH of the aqueous solution may have a strong effect on the extraction yield. With chloroform, however, extraction is quantitative over a broad pH range.

In recent years, many new, highly sensitive quantitative techniques have been developed for the determination of drugs and drug metabolites. Preliminary steps such as the extraction process have received less attention; yet some attempts have been made to develop isolation procedures which are more effective, simpler and less time-consuming than the traditional extraction techniques.

The ion-pair extraction method, introduced mainly by Schill and coworkers [1 and references therein] is gaining increasing interest. In this method, an ionizable compound can be extracted into an organic phase as an ion pair by addition of a suitable ion with opposite charge. The degree of extraction can be improved by using as extracting agent a substance that can act both as counter-ion and as adduct-forming agent in the organic phase [1—4].

Di(2-ethylhexyl) phosphoric acid (HDEHP) is such an extracting agent. Many years ago, it was employed for the thin-layer chromatographic separation of rare earths [5], and many other workers [6] have employed it for the isolation of metals as ion-pair products. In organic analysis it has been used for the extraction or chromatography of amino alcohols and aminophenols [7—12] and for the extraction of dopamine and 5-hydroxytryptophan [13—15].

A very interesting application is in the high-pressure liquid chromatography of an HDEHP extract of metanephrine and normetanephrine [10]. The work described here was directed towards establishing the breadth of application of this extraction, and suitability of the HDEHP extractant for the quantitative isolation of basic drugs in general from aqueous solution. Indeed, HDEHP

should be a powerful extractant for amines in general, for it yields very hydrophobic counter-ions and is therefore suitable for the extraction of even very hydrophilic cationic species.

EXPERIMENTAL

Apparatus

The u.v. photometric determinations were done with a Perkin-Elmer Hitachi 200 spectrophotometer. The pH values were measured with an Ionalyser model 601 (Orion Research) and a combination glass electrode.

Chemicals and reagents

Imipramine, desipramine, procaine, cocaine, heroin, naphazoline, methapyrilene, fluphenazine, thonzylamine, promethazine and yohimbine were used as hydrochlorides, homatropine and scopolamine as hydrobromides, carbetapentane as citrate, and atropine as sulphate. They were all of pharmacopeial or equivalent purity.

Di(2-ethylhexyl) phosphoric acid (Fluka AG; Buchs, Switzerland) was used as received. All solvents and reagents were of analytical grade (E. Merck, Darmstadt) except 1-octanol ("zur synthese"). Chloroform was freed from ethanol by repeated shaking with water. Buffers of constant and low ionic strength especially developed for spectrophotometric determinations were prepared as described by Perrin [16].

Procedures

The partition experiments were carried out in centrifuge tubes. An aqueous solution (10 ml) of a salt of the basic drug was shaken during 30 min with an equal volume of an HDEHP solution in an organic solvent. Both organic and aqueous phases were equilibrated with each other before use. The tubes were shaken in a thermostated bath at 25°C. After centrifugation for 5 min (longer if emulsions were formed), the phases were separated.

The aqueous, and if possible the organic, layer was then analyzed by u.v. spectrophotometry.

Each partition experiment was carried out at least in triplicate, so that the results are the average of at least three values.

RESULTS AND DISCUSSION

HDEHP is a weak acid ($pK_A = 3.22$); it is quite viscous. Dissolved in solvents such as benzene, n-hexane, cyclohexane and carbon tetrachloride, it is predominantly dimeric, but it is monomeric in alcohols and of intermediate aggregation in acetone and chloroform [17].

Parameters influencing the extraction

Before extraction of a variety of basic drugs was investigated, some general parameters of the extraction were studied.

Solvent effect. Several solvents were tested for extraction of imipramine as test drug. The results obtained are presented in Table 1. The solvents are classified by increasing polarity, P' being the polarity index [18]; ϵ is the dielectric constant. When HDEHP is dissolved in non-polar solvents, the extraction yield is very poor. In more polar solvents ($CHCl_3$, CH_2Cl_2, $C_2H_4Cl_2$), the total amount of amine is recovered, at least if the HDEHP concentration is high enough. Ethyl acetate, however, does not permit quantitative extraction, although it has about the same polarity index as chloroform, methylene chloride and ethylene chloride.

These data suggest that the ion pairs and ion-pair adducts are better solvated in chloroform and similar solvents, most probably by hydrogen bonding. Indeed, Venable and Doyle [19] demonstrated that chloroform associates to the halide ion of ion pairs by hydrogen bonding, and Schill [20] states that in general ion pairs are better extracted by a hydrogen-donating solvent such as chloroform than by a hydrogen-accepting one, such as ethyl acetate.

Effect of the concentration of counter-ion. Figure 1 shows that there is a linear relationship between the logarithm of the distribution ratio (D = concentration of the amine in the organic phase/concentration of the amine in the aqueous phase) and the logarithm of the HDEHP concentration.

With n-heptane there is no extraction by the pure solvent, hence the slope of the plot should be equal to 1 if the extracted species is the ion pair HAX (i.e., the compound formed by the protonated amine HA^+ and the dissociated HDEHP, X^-). If the extracted species is an adduct of the HAX $\cdot$ HX type or of the HAX $\cdot$ H_2X_2 type, the slope should be 2 or 3, respectively. The slope found is 3.24, which shows that when heptane is used as the solvent, the extracted species is probably of the HAX $\cdot$ H_2X_2 type.

The slope observed depends on the solvent. For example, the slope for ethyl acetate is 0.75.

TABLE 1

Extraction of 1×10^{-4} M imipramine from aqueous solution at pH 6.1 with several solvents

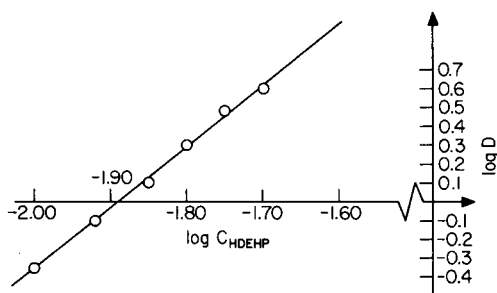| Solvent	P'	ϵ	% Extraction with			
			Pure solvent	1×10^{-3} M HDEHP	1×10^{-2} M HDEHP	1×10^{-1} M HDEHP
n-Heptane	0.0	1.003	0	4.5	11	31.5
Cyclohexane	0.0	2.023	43	23	9.5	56
l-Octanol	3.2	10.3	43.5	76	97.5	98.5
Methylene chloride	3.4	9.08	83	87.5	100	100
Ethylene chloride	3.7	10.3	70.5	78	100	100
Ethyl acetate	4.3	6.09	23	31	48	70
Chloroform	4.4	4.806	67	92	100	100

Fig. 1. Extraction of 1×10^{-4} M imipramine with HDEHP (0.010—0.020 M) in n-heptane.

Effect of ionic strength. The results of the extraction of imipramine as a function of the ionic strength are given in Table 2; ionic strength was adjusted by suitable addition of NaCl to the imipramine solution. It must be taken into account that the extraction yield is influenced by the presence of chloride ion, which can also act as counter-ion for the ion-pair extraction of amines [21]. Table 2 shows that the extraction goes through a minimum. This is probably due to two opposing effects: the ionic strength of the aqueous solution simultaneously affects the dissociation of both the amine and the acidic extractant and hence the solvation of the resulting species in the aqueous phase.

Effect of pH of the aqueous phase. The extraction of some drugs as a function of pH was investigated at constant and low ionic strength. To ensure almost complete ionization of all molecular species involved in the ion-pair formation, the pH range was chosen to fall between the pK_a values of the drugs and that of HDEHP. Preliminary experiments showed that optimum extraction was to be expected in the pH range 7.5—9.5. Consequently, this pH range was further investigated for imipramine, promethazine, procaine and thonzylamine.

When chloroform was used as the solvent, complete extraction was achieved in the pH range investigated (and even outside it, because 100% extraction of imipramine was obtained at pH 6, see Table 1). To study the pH effect, a poorer extraction solvent (n-heptane) was therefore used.

The results given in Fig. 2 prove that pH has a strong effect on the extraction. By careful choice of the pH, good extractions are therefore also possible with apolar solvents. It should be noted that according to the results of

TABLE 2

Extraction of 1×10^{-4} M imipramine as a function of ionic strength (I) at pH 6.1 with 10^{-2} M HDEHP in n-heptane or ethyl acetate

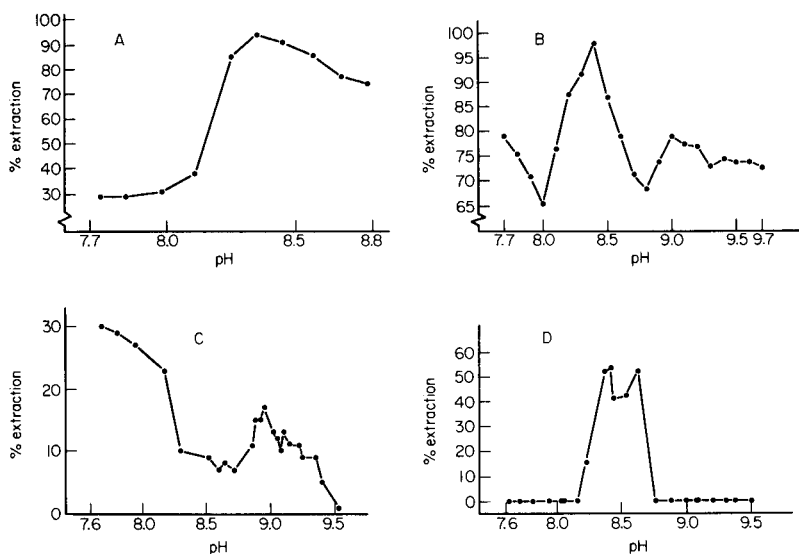| I	0	0.1	0.25	0.5	1
% Extraction					
in n-heptane	31.5	23	23.5	25.5	39
in ethyl acetate	70	67.5	68.5	70.5	76

Fig. 2. Extraction of various drugs with 0.01 M HDEHP in n-heptane as a function of pH at $I = 0.01$. (A) 1×10^{-4} M imipramine ($pK_a = 9.5$); (B) 2×10^{-4} M promethazine ($pK_a = 9.1$); (C) 5×10^{-5} M procaine ($pK_a = 9.0$); (D) 3×10^{-4} M thonzylamine ($pK_a = 8.9$).

Modin [3] and Modin and Johansson [9], the pH optimum should not depend on the properties of the amine. However, consideration of the theory leading to this statement suggests that this is true only when the concentration of the amine is much lower than that of the acidic extractant. In the present experiments, the concentration of the former is about 0.01 times the concentration of the latter; it would therefore appear that at such concentration ratios the pH optimum is no longer independent of the amine in question.

Extraction of basic drugs in general

Ten drugs with different structures were extracted with 0.1 M HDEHP in chloroform and with the pure solvent. Each drug acts as a representative sample — a probe — for a group of structurally related substances. As the extraction with chloroform as the solvent is excellent, no pH precautions are necessary and the extraction can be carried out at the pH of the aqueous solution of the drug. The results are given in Table 3. As can be seen, some drugs such as desipramine, methapyrilene and heroin are extracted to a high extent at an HDEHP concentration of 10^{-2} M; for desipramine, as little as 10^{-3} M HDEHP sufficed to obtain complete recovery. Other drugs are extracted quantitatively only at a higher (10^{-1} M) HDEHP concentration. It can be observed for instance that the extraction yield of scopolamine is only 25% with 10^{-2} M HDEHP in chloroform. It was thought that this could be due to steric hindrance in the tropane structure, hence the extraction of other tropane alkaloids (atropine, homatropine, cocaine) was studied. The results obtained are shown in the final lines of Table 3.

TABLE 3

Extraction of some amines with HDEHP in chloroform

Amine	Amine concn. (M)	% Extraction with		
		$CHCl_3$	10^{-2} M HDEHP	10^{-1} M HDEHP[a]
Procaine	5×10^{-5}	37.5	86	100
Desipramine	1×10^{-4}	57	100	100
Heroin	1×10^{-4}	46	100	100
Naphazoline	1×10^{-4}	11	77.5	100
Methapyrilene	2×10^{-4}	45	93.5	100
Scopolamine	3×10^{-3}	13.5	25	100
Fluphenazine	2×10^{-4}	85		100
Carbetapentane	5×10^{-3}	44		100
Yohimbine	1×10^{-4}	56.5		100
Thonzylamine	4×10^{-4}	22.5		100
Atropine	6×10^{-3}	0	40	100
Homatropine	5×10^{-3}	7	33	100
Cocaine	1×10^{-4}	69.5	75	100

[a]In all cases, the extraction was essentially quantitative; the approximate standard deviation to be expected is 5%.

Conclusions

It is clear that complete recovery of all the basic drugs studied is possible with 0.1 M HDEHP in chloroform. In combination with the method for direct liquid chromatography of HDEHP extracts of metanephrine and normetanephrine proposed by Eriksson et al. [10], this indicates the possibility of developing a general method for the determination of basic drugs in plasma or other biological samples.

REFERENCES

1 G. Schill, in J. A. Marinsky and Y. Marcus (Eds.), Ion Exchange and Solvent Extraction, Vol. 6, Marcel Dekker Inc., New York, 1974.
2 R. Modin and A. Tilly, Acta Pharm. Suec., 5 (1968) 311.
3 R. Modin, Acta Pharm. Suec., 8 (1971) 509.
4 R. Modin, Acta Pharm. Suec., 9 (1972) 157.
5 A. Daneels, D. L. Massart and J. Hoste, J. Chromatogr., 18 (1965) 144.
6 See, e.g., Y. Marcus and A. S. Kertes, Ion Exchange and Solvent Extraction of Metal Complexes, Wiley-Interscience, London, 1968.
7 D. M. Temple and R. Gillespie, Nature, 209 (1966) 1974.
8 J. Levine and T. D. Doyle, J. Pharm. Sci., 56 (1967) 619.

9 R. Modin and M. Johansson, Acta Pharm. Suec., 8 (1971) 561.
10 B.-M. Eriksson, J. Andersson, K. O. Borg and B.-A. Persson, Acta Pharm. Suec., 14 (1977) 451.
11 B.-A. Persson and P.-O. Lagerström, J. Chromatogr., 122 (1976) 305.
12 S. Eksborg, P.-O. Lagerström, R. Modin and G. Schill, J. Chromatogr., 83 (1973) 99.
13 M. W. McCaman, R. E. McCaman and G. J. Lees, Anal. Biochem., 45 (1972) 242.
14 M. W. McCaman, D. Weinreich and R. E. McCaman, Brain Res., 53 (1973) 129.
15 M. H. Joseph and H. F. Baker, Clin. Chim. Acta, 72 (1976) 125.
16 Perrin as cited by R. M. C. Dawson, D. C. Elliott, W. H. Elliott and K. M. Jones (Eds.), Data for Biochemical Research, Clarendon Press, Oxford, 1969, p. 502.
17 J. R. Ferraro and D. F. Peppard, Nucl. Sci. Eng., 16 (1963) 389.
18 L. R. Snyder, J. Chromatogr., 92 (1974) 223.
19 R. M. Venable and T. D. Doyle, J. Assoc. Off. Anal. Chem., 60 (1977) 52.
20 G. Schill, Separation Methods for Drugs and Related Organic Compounds, Apotekarsocieteten, Stockholm, 1978.
21 B.-A. Persson and S. Eksborg, Acta Pharm. Suec., 7 (1970) 353.

MICRODETERMINATION OF THIOBARBITURIC ACID VALUES IN MARINE LIPIDS BY A DIRECT SPECTROPHOTOMETRIC METHOD WITH A MONOPHASIC REACTION SYSTEM

P. J. KE* and A. D. WOYEWODA

Department of Fisheries and the Environment, Fisheries Management Maritimes Technology Branch, P.O. Box 550, Halifax, N.S., B3J 2S7 (Canada)

(Received 29th September 1978)

SUMMARY

A rapid direct spectrophotometric method for determining the thiobarbituric acid (TBA) value in lipids is reported. The variation in TBA value given by different reaction conditions has been investigated systematically and a monophasic TBA reaction system with incorporation of sulfite reagents has been selected for the recommended method, which can be used to determine the TBA value at levels as low as 2 nmol of malonaldehyde equivalent in 20 mg of lipids with a standard deviation of less than 8%. The procedure has been applied to some marine lipids, including highly colored or oxidized samples.

The reaction between thiobarbituric acid (TBA) and the oxidation products of unsaturated lipids, which produces a red color, was first reported by Kohn and Liversedge [1]. The spectrophotometric determination of this red compound as "TBA value" has been used to measure the degree of autoxidation of oils and lipids [2, 3] and the rancidity of various fat-containing foods [4—6]. A compound giving a red color, prepared from malonaldehyde (MA), has been identified as the reaction product given by oxidized lipids and TBA reagent [3, 7].

The TBA value has been widely adopted by oil and food technologists as a routine method for assessing the quality of lipids and food. Although several analytical improvements and modifications for determining TBA values have been published, the reproducibility of the determination with marine lipids and related oil samples, particularly for highly oxidized samples, has been less than desirable. The basic problems experienced in TBA determinations can be summarized as: the mixing of two-phase reaction systems [8, 9], the formation of a yellow pigment which interferes in the reaction [3, 9, 10], and the complexity of the carbonyls from the oxidation of polyunsaturated fatty acids [11, 12].

A rapid direct method for the micro-determination of TBA values in lipids is reported here. A monophasic TBA reaction system containing chloroform,

water and acetic acid has been found to be satisfactory with the incorporation of trichloracetic acid (TCA) and sulfite reagents. This improved TBA method gives reproducible results for some marine lipids and appears to be suitable for the routine evaluation of the oxidative rancidity of all lipids.

EXPERIMENTAL

Chemicals and instrumentation

All chemicals used were ACS grade. Lipids were extracted by Bligh and Dyer's method [13]. For the TBA stock solution (0.04 M), dissolve 2.88 g of 2-thiobarbituric acid (TBA) in 50 ml of distilled water in a 500-ml volumetric flask and dilute to volume with glacial acetic acid; vigorous stirring is required. Prepare sodium sulfite solution (0.3 M) and trichloroacetic acid (TCA) solution (0.28 M) in distilled water. For the TEP standard stock solution (0.01 M), dissolve 0.22 g of 1,1,3,3-tetraethoxypropane (TEP; K & K Laboratories, Plainview, N.Y.) in distilled water in a 100-ml volumetric flask. Prepare the TEP working standard solution (1.0×10^{-4} M) by pipetting 1 ml of TEP standard stock solution into a 100-ml volumetric flask and diluting to volume with distilled water.

A Spectronic 70 spectrophotometer (Bausch and Lomb), a clinical centrifuge (model CL, Internat. Eq. Co.) and a Vortex mixer (Fisher Scientific Co.) were used.

Recommended procedure

Prepare a TBA working solution by mixing 180 ml of TBA stock solution, 120 ml of chloroform and 15 ml of sodium sulfite reagent. This solution must be made not more than 30 min prior to analysis. The volume ratio of water: chloroform: acetic acid in the TBA working solution is important and should be kept within ± 2% variation.

For analysis, weigh accurately one drop of lipid sample (15—20 mg) into a culture tube with a Teflon-lined screw cap (20—25 ml; Kimax). Add 10 ml of TBA working solution and cap the tube tightly. To dissolve the lipids in the TBA reagent mix on a Vortex mixer for 10—15 s. Heat the tubes containing samples, blank, and 0.1 ml of TEP working standard solution for 45 min in a briskly boiling water bath. Then cool the tubes in tap water, and add 5 ml of TCA solution to each tube. After recapping and mixing by inversion, centrifuge the tubes for 6 min in a clinical centrifuge, so that the pink aqueous phase (11.2 ml) is completely separated from the chloroform layer. Measure the absorbance of the top aqueous layer at 538 nm in 10-mm cuvettes and calculate the TBA value.

For highly oxidized lipids, withdraw a portion of the separated aqueous phase and dilute it quantitatively with an appropriate amount of 55% (v/v) acetic acid in water. Use this diluted sample solution for determinations of the TBA value.

Calculation

With this procedure, a linear calibration curve is obtained for the range 1.0—40.0 nmol of malonaldehyde (MA), corresponding to 0.01—0.40 ml of TEP working standard (1.0×10^{-4} M). The molar absorptivity (ϵ; 1.90×10^5 l mol^{-1} cm^{-2}) should be carefully determined when any stock reagent solutions are changed, and also checked daily or with each set of analyses. The TBA value for a lipid sample, expressed as μmol of MA per g of lipid, can be calculated from TBA=$ADV/\epsilon W$, where A, D, and V respectively denote absorbance, dilution factor, and the total volume (l) of the aqueous phase from the TBA reaction mixture; W is the weight (g) of lipid sample. Once ϵ and V have been standardized, the calculation can be simplified to TBA= 0.0589 AD/W.

RESULTS AND DISCUSSION

Effects of TCA and sulfite

Comparisons of spectra from TBA determinations of herring lipids with and without TCA and/or sulfite reagents are shown in Fig. 1. The absorbances at 450 and 538 nm are indicative of lipid oxidation [11] but the result measured at 538 nm is relatively more stable to reaction temperature [11] and suffers less from interference from other substances [10, 14]. By using dilute sodium sulfite reagent, there are no absorption peaks at 450 and 490 nm and the absorbance at 538 nm is increased moderately. In addition, the reproducibility of TBA data is much improved for various marine lipid samples. The purpose of using TCA solution in the separation of the aqueous sample phase from the chloroform layer is mainly to eliminate traces of white precipitates and impurities carried over from the lipids after reaction with TBA. As shown in Fig. 1 (dotted curve), TCA without sulfite increases the
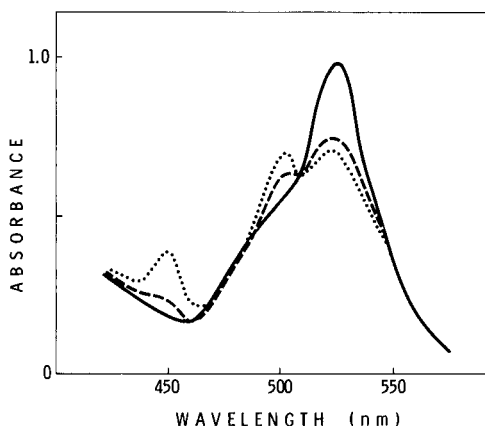

Fig. 1. Spectra given in the TBA determination of herring lipids with Na$_2$SO$_3$ and TCA (—); TCA only (···); without Na$_2$SO$_3$ or TCA (---).

absorbance at 450 and 490 nm and reduces the absorbance at 538 nm. When sulfite and TCA are both used, the spectrum obtained for a herring lipid sample (Fig. 1, solid curve) is improved and the absorbance at 538 nm is satisfactory for the microdetermination of the TBA value.

TBA reaction conditions

The variations in TBA values which arise from changes in the reaction conditions were investigated systematically in terms of the absorbance at 538 nm. The results are shown in Fig. 2. It was not possible to find conditions that guarantee attainment of the complete equilibrium. However, for practical analytical applications, the following compromise conditions can be used to give reliable TBA values for the estimation of rancidity in various lipids: the TBA reaction solution contains 0.14 nM sodium sulfite (Fig. 2A and D), 11% water (curve C, in Fig. 2A and B), 50% acetic acid (Fig. 2C), and 39% chloroform; the reaction time is 45 min at $100°C$ (Fig. 2C); 0.28 M TCA solution is added to separate the aqueous phase for the final determination (Fig. 2D).
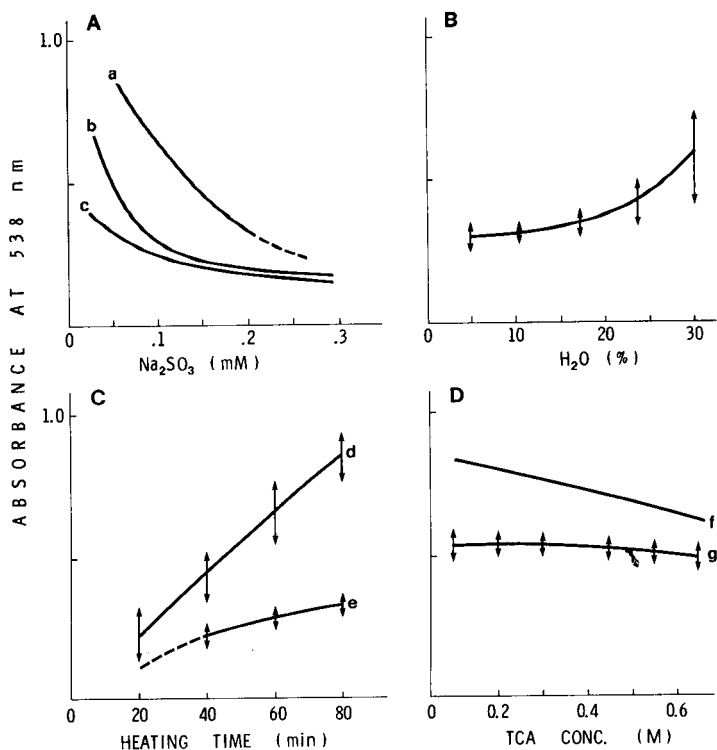
Fig. 2. Comparisons of various reaction conditions for the TBA determination on a herring lipid sample: (A) by varying the sodium sulfite content in the reaction mixture containing 25% (a), 18% (b) and 11% (c) of water; (B) by varying the water content; (C) for different reaction times with 20% (d) and 50% (e) of acetic acid in the reaction mixture; (D) by varying the TCA concentration added after TBA reaction with (g) or without (f) sodium sulfite.

These experimental conditions overcome the problems of variable reactivities with TBA [11, 12, 15], a heterogeneous reaction system [9], turbidity [7, 9], and undesirable pigments [10, 11, 14].

Recovery from TEP standard and examination of interfering substances

1,1,3,3-Tetraethoxypropane (TEP) yields malonaldehyde (MA) and was used to evaluate the TBA value; the absorbance and TL.. values for TEP standards corresponding to 0.002—0.040 μmol per g of sample are reported in Table 1. A highly reproducible linear standard graph was obtained and the molar absorptivity of TEP ($1.90 \pm 0.03 \times 10^5$) is used to calculate the TBA data. The recovery of TEP added to two lipid samples was also determined (Table 1): these data indicate that the recommended method gives lipid analyses with a recovery error of 6%.

Tests for interference from various lipid-soluble substances were carried out by adding ca. 5 mg of each compound to a 20-mg sample of herring lipids. Diverse compounds associated with lipids or lipid solubles, e.g. fatty acids (oleic and linolenic acid), amino acids (glutamine and cystine), phospholipids (lecithin and phosphatidyl ethanolamine), wax esters (from sperm whale), heme compounds (hemin and hematein), and iron(III) and copper(II) stearate, did not interfere with the TBA method, giving a relative deviation of less than 2%.

TABLE 1

Recovery by the direct method of TEP standard added to mackerel and oxidized herring oils

Lipids	TEP added (μmol)	Absorbance	TBA (μmol g^{-1})	Recovery (%)
None	0.002	0.034	0.100	—
	0.006	0.104	0.306	—
	0.010	0.170	0.501	—
	0.020	0.334	0.983	—
	0.030	0.510	1.513	—
	0.040	0.666	1.961	—
Mackerel oil	none	0.072	0.212	—
	0.010	0.248	0.731	104
	0.020	0.407	1.198	100
	0.030	0.583	1.717	99
	0.040	0.765	2.252	103
Oxid. herring oil	none	0.482	1.420	—
	0.010	0.663	1.951	106
	0.020	0.806	2.374	97
	0.030	0.998	2.948	101

Precision and application

   TBA values and relative standard deviations for six lipid samples (Table 2), determined by the proposed direct procedure, show that the method can be satisfactorily applied for the determination of TBA values in lipids, including highly oxidized samples; the method gives results with good reproducibility (r.s.d. 2—7%) and sensitivity for as little as 20 mg of sample.

   It can be concluded that the method described is simple, sensitive, and superior in reproducibility to previous methods for marine lipids. It should be readily adaptable to the determination of TBA values at levels as low as 2 nmol of MA or equivalent in 20-mg samples of lipids. This can be especially convenient for serial sampling of small amounts of oxidizing lipids, in studies of the muscle of lean fish, e.g. cod, haddock, etc., for quality control in the food industry, and for studies of secondary products from various lipid reactions.

TABLE 2

TBA values for 6 lipid samples determined by the direct method

Sample	TBA value (μmol g^{-1})	R.s.d.[a] (%)
Herring oil	0.107	5.2
Mackerel oil	0.389	2.8
Redfish oil	0.415	6.1
Capelin oil	0.621	2.2
Oxid. herring oil	2.063	7.1
Oxid. herring oil	26.49[b]	5.4

[a]Calculated from 7 determinations for each sample.
[b]Values obtained by diluting the sample 10 times.

REFERENCES

 1 H. I. Kohn and M. Liversedge, Pharmacology, 82 (1944) 292.
 2 T. C. Yu and R. O. Sinnhuber, J. Am. Oil Chem. Soc., 44 (1967) 256.
 3 T. Asakawa, Y. Nomura and S. Matsushida, Yukagaku, 24 (1975) 481.
 4 R. O. Sinnhuber and T. C. Yu, Food Technol., 12 (1958) 9; 11 (1957) 104.
 5 B. G. Tarladgis, B. M. Watts and M. T. Younathan, J. Am. Oil Chem. Soc., 37 (1960) 44.
 6 W. V. Vyncke, Fette, Seifen, Anstrichm., 77 (1975) 239.
 7 S. Patton, M. Kenney and G. W. Kurtz, J. Am. Oil Chem. Soc., 28 (1951) 391.
 8 H. Schmidt, Fette, Seifen, Anstrichm., 61 (1959) 127.
 9 A. J. DeKoning and M. H. Silk, J. Am. Oil. Chem. Soc., 40 (1963) 165.
10 T. Asakawa, Y. Nomura and S. Matsushida, Yukagaku, 24 (1975) 88.
11 R. Marcuse and L. Johansson, J. Am. Oil Chem. Soc., 50 (1973) 387.
12 P. J. Ke, R. G. Ackman and B. A. Linke, J. Am. Oil Chem. Soc., 52 (1975) 349.
13 E. G. Bligh and W. J. Dyer, Can. J. Biochem. Physiol., 37 (1959) 911.
14 W. A. Baumgartner, N. Baker, V. A. Hill and E. T. Wright, Lipids, 10 (1975) 309.
15 N. A. Porter, J. Nixon and R. Isaac, Biochim. Biophys. Acta, 441 (1976) 506.

DETERMINATION OF MERCURY BY ATOMIC ABSORPTION SPECTROMETRY WITH COLD VAPOUR AND ELECTROTHERMAL TECHNIQUES

I. KUNERT, J. KOMAREK and L. SOMMER*

Department of Analytical Chemistry, J. E. Purkyně University, 61137 Brno (Czechoslovakia)

SUMMARY

The determination of traces of mercury by the cold-vapour technique with and without previous amalgamation under various conditions with different amalgamating fillings is described. The theoretical absorbance values calculated by means of a computer program show surprisingly high coincidence with the experimental values obtained. The sensitivity of the mercury determination in graphite furnaces can be considerably increased if atomization is done from gold or silver foil instead of from the graphite surface but computations showed that there is a very significant loss of atoms during the preatomization processes at elevated temperature in graphite furnaces in all cases.

Determinations of mercury by atomic absorption spectrometry are usually based on the cold-vapour technique [1]. The extensive work in this field has been reviewed by Ure [2], and so only the earlier references important to the present theme are given in this paper. Mercury is normally generated from solution by reduction procedures with tin(II) chloride in acidic solutions, but many other reductants including stannate in alkaline medium [3] ascorbic acid [4], hydrazine sulfate [5] or sodium borohydride [6, 7] can also be used. Preliminary retention of mercury vapours by amalgamation with gold, silver, or copper wires, gold wool, etc., or by sorption on active carbon, has been widely applied for preconcentration of traces of mercury from various matrices [2, 8—13]; mercury is then easily released by heating.

The determination of mercury in a graphite furnace has only limited sensitivity, although this can be slightly improved by addition of oxidizing agents or sulfide [14—16]. Electrothermal atomization from copper, silver, or gold wires after amalgamation from solutions [17, 18] seems more promising.

In the work described here, the efficiency of the atomization process was estimated by comparing the theoretical absorbance values with the experimental values. Comparisons were made for the cold-vapour technique in the circulation mode or after previous sorption and desorption from gold-loaded asbestos wool, and for the determination of mercury in the graphite

furnace. The sensitivity of the furnace method can be considerably improved if the graphite surface is covered by gold or silver foil.

EXPERIMENTAL

Solutions and reagents

Solutions of $Hg(NO_3)_2$ and $Hg_2(NO_3)_2$ containing 1.014 g or 0.992 g of mercury per litre of 0.1 M HNO_3 were standardized by EDTA titration (xylenol orange), Hg(I) being previously oxidized by hydrogen peroxide.

Diluted mercury(II) solutions were stabilized by addition of a few drops of 5% (w/v) $KMnO_4$; 40% of the mercury was sorbed on glass vessels within 24 h from solutions containing less than 0.1 μg Hg ml^{-1} in the absence of permanganate. The sorption of mercury from dilute solutions onto glass, polyethylene and Teflon has frequently been commented on (see, e.g. [19, 20]).

All the chemicals used were analytically pure or were recrystallized or redistilled. Traces of mercury observed in analytical-grade chemicals, especially tin(II) chloride, were expelled from solutions after reduction, by passing nitrogen for 10—15 min. Activated carbon was carefully purified with hot HCl (1 + 1) and water. The silver and gold wires used were 0.5 mm in diameter and the length 2—3 mm.

Gold-coated asbestos. Asbestos fibre (3 g) was soaked in 10 ml of water containing 1 g of gold(III) chloride, dried at 100°C and reduced in a stream of hydrogen at 200°C. A 1-cm layer of this material has sufficient retention capacity for more than 300 determinations of mercury.

Silverized asbestos. Asbestos fibre (3 g) was soaked in 10 ml of water containing 1 g of silver nitrate, then plunged into 1 M sodium chloride solution, washed, dried and reduced with a solution of 10% (w/v) hydroquinone in 5% (w/v) sodium hydroxide. The treated asbestos was finally washed with water and dried at 100°C. Unless sodium chloride was used, the final product was not satisfactory.

Platinized asbestos. Asbestos fibre (3 g) was soaked in 10 ml of water containing 1 g of ammonium hexachloroplatinate, dried and ignited to a dark grey colour.

Palladized asbestos. Asbestos fibre was soaked in 10 ml of water containing 1 g of palladium chloride, dried and ignited to a brown-violet colour.

In all cases the asbestos was previously ignited to avoid excessive blanks.

Instrumentation

A Perkin-Elmer Model 306 atomic absorption spectrometer was used with a Perkin-Elmer mercury hollow-cathode lamp (lamp current 3.8 mA; λ = 253.7 nm; slitwidth, 0.7 nm) and a conventional potentiometric recorder. For the cold-vapour technique, the Perkin-Elmer Mercury Analysis System was used.
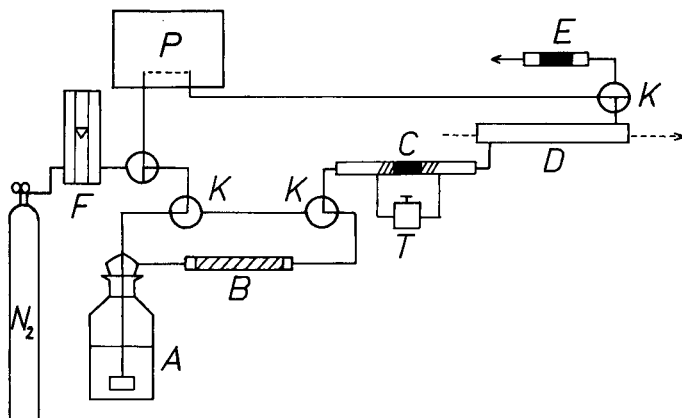
Fig. 1. Schematic diagram of the apparatus for the determination of mercury by the cold-vapour technique with previous amalgamation. (F) Nitrogen flow meter; (A) reaction bottle containing sample; (B) water absorber packed with magnesium perchlorate; (T) autotransformer; (C) amalgamation tube; (P) pump; (K) three-way stopcock; (D) optical flow cell; (E) amalgamating packing (1-cm long) which is held in the middle of a quartz tube (80 mm long; i.d. 8 mm) between two 1-cm quartz wool plugs.

Cold-vapour technique with amalgamation

Figure 1 shows the arrangement for the cold-vapour technique with amalgamation. Amalgamation was complete after a 4-min period of circulation of air containing mercury vapour at a flow rate of 0.6 l min^{-1}. The air was pumped through the sample bottle (A), the desiccant (B), the amalgamation tube (C) and then the flow cell (D). The sample bottle was then disconnected from the flow by turning the stopcocks (K) and the pump was switched off. Tube C was then heated to $500°C$ for 30 s by means of a heating coil (25 cm, 4 Ω m^{-1}, 12 V) and the mercury vapour was swept by nitrogen (1 l min^{-1}) through the flow cell and into the second amalgamation tube (E).

Modified graphite furnace HGA-74

The graphite furnace of the atomizer was lined with gold or silver foil (0.5 mm thick, 18×25 mm) for some experiments. These foils were removed and cleaned with 0.1 M HNO_3 between experiments when salt solutions had been sampled.

Calculation of theoretical absorbance vs. concentration plots

The program TEOLINE (see Fig. 2) was developed for calculation of the theoretical absorbance vs. concentration plots. It is based on the assumptions that the emission line has hyperfine structure and Gaussian shape and that the absorption line can be described by the Voigt function, both lines being shifted [21—24]. The program was written in Fortran IV; minimal core
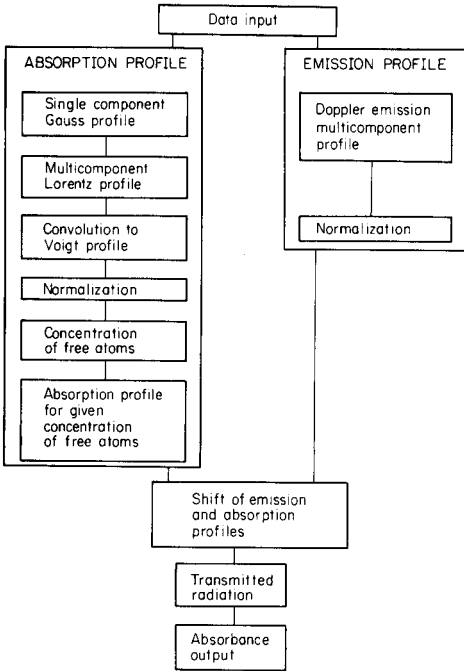
Fig. 2. Flow chart for the TEOLINE program.

storage was 120 kbytes and the computer time was about 10 min. The program is available on request from the authors. A medium-size TESLA 200 computer was used.

The input data such as the relative positions and heights of the components of the Hg 235.7 nm line, line shift, the half-width of the emission line, oscillator strength, etc., were taken from the results published by L'vov [25]. The shifted absorption profile and the transmittance are described by the following equations:

$$P'_V(u) = 8.85 \times 10^{-10} \, l \, N_{at} \, f P_V(u) \tag{1}$$

where $P_V(u)$ is the profile, described by the Voigt function resulting from the convolution product of the Doppler and Lorentz profiles; l is the length of the absorption path (cm); f is the oscillator strength of the Hg atom; and N_{at} is the concentration of free atoms per cm^3.

$$T = \int_{\infty-}^{\infty+} P_{MG}(u) \exp\left(-P'_V(u + \Delta\bar{\nu}_S)\right) du \tag{2}$$

where $(P'_V(u + \Delta\bar{\nu})_S)$ is the shifted and factorized function of the Voigt absorption profile, $\Delta\nu_S$ being the line shift; $P_{MG}(u)$ is the emission Doppler profile; $u = \nu - \nu_0$, where ν_0 is the centre of the profile; and $\Delta\bar{\nu}_S = \Delta\bar{\nu}_L/2.2$, $\Delta\bar{\nu}_L$ being the half-width of the Lorentzian profile.

The absorbance value was calculated as the negative logarithm of the transmitted radiative flux related to overlapped parts of the emission and absorption line profiles. The concentration of free atoms, N_{at} per cm^3, is

$$N_{at} = 6.023 \times 10^{17} v_1 \, sc/200.59 \, v_2 \tag{3}$$

where v_1 is the solution volume (ml); v_2 is the air volume in the device for the circulation procedure or the volume of the flow cell for the amalgamation technique; c is the Hg^{2+} concentration ($\mu g \, ml^{-1}$); and s is $[Hg]_{air}/[Hg]_{total}$, i.e. the degree of volatilization of mercury, which is $s = 0.348$ for the cold-vapour circulation procedure and $s = 1$ for the amalgamation procedure.

When graphite tubes are used with different surfaces, the number of the free atoms N_{at} is given by

$$N_{at} = 6.023 \times 10^{14} \, c \, v_1/200.59 \, v_2 \tag{4}$$

where v_1 is the volume of the sample solution (μl); v_2 is the volume of the graphite atomizer (cm^3); and c is the Hg^{2+} concentration ($\mu g \, ml^{-1}$). In this case, it was considered that the atomic vapour fills the whole hot zone of the atomizer uniformly and instantaneously at the moment of atomization.

Treatment of absorbance data

For the experimental calibration plots, A vs. c, the absorbance data were treated by the non-linear regression method with the POLYAN computer program [26] by means of a third-order polynomial. Each of 10 points was measured 5 times for a plot, and the standard deviation (s_{xy}), the sensitivity (dA/dc_M in ml μg^{-1} or l mol^{-1}) at the start of the curve, the detection limit (3 times the standard deviation of the blank divided by dA/dc_M) and the characteristic concentration ($\mu g \, ml^{-1}$ for $A = 0.004$) were also obtained from the program.

The circulation cold-vapour technique

Effects of the various reducing agents and salts on the formation of mercury atoms from Hg^{2+} solutions were studied by the following procedure.

Add 3 drops of 5% (w/v) $KMnO_4$ solution and 5 ml of 5.6 M HNO_3 to 100 ml of test solution containing 0.2—1.0 μg Hg. Remove the excess of permanganate by 5 ml of 1.5% (w/v) hydroxylammonium chloride solution and add the reducing agent. As the reductant, use 5 ml of 10% (w/v) tin(II) chloride solution in 2 M HCl with 5 ml of 9 M H_2SO_4, or 5 ml of 20% (w/v) sodium hydroxide solution with 5 ml of 10% (w/v) sodium stannate(II) solution, or 5 ml of 0.1 M ascorbic acid or 5 ml of 1 M hydrazine hydrochloride or 5 ml of 1 M formaldehyde solution.

The absorbance was measured after 30 s while air was passed at a rate of 0.6 l min^{-1}. Absorbance plots were identical for all reducing agents. The standard deviation for 1 μg Hg was lowest ($\pm 0.011 \, \mu g$; 5 measurements) when tin(II) chloride in sulphuric acid medium was used. The absorbance values calculated according to eqns. (1—3) with TEOLINE can also be used for the calibration diagram without using standard samples (cf. also Table 4).

TABLE 1

Influence of various salts at 0.01 M concentrations on the release of mercury (1 μg Hg) from solution after reduction with different reagents

Salt	SnCl$_2$		Sn(OH)$_3^-$		N$_2$H$_4$HCl		Ascorbic acid	
	s^a	A/A_0^b	s	A/A_0	s	A/A_0	s	A/A_0
—	0.348	1	0.348	1	0.348	1	0.348	1
NaSCN	0.344	0.99	0.337	0.97	0.017	0.05	0.146	0.42
NaClO$_4$	0.327	0.94	0.344	0.99	0.341	0.98	0.344	0.99
K$_2$Cr$_2$O$_7$	0.0035	0.01	0.009	0.028	0.019	0.056	0.034	0.099
KH$_2$PO$_4$	0.327	0.94	0.337	0.97	0.334	0.96	0.341	0.98
KBr	0.341	0.98	0.341	0.98	0.344	0.99	0.337	0.97
Na$_2$S$_2$O$_3$	0.0017	0.005	0.0017	0.005	0.0038	0.011	0.020	0.057
KI	0.007	0.02	0.009	0.028	0.316	0.91	0.003	0.008
Na$_2$S	0.0059	0.017	0.0017	0.005	0.003	0.002	0.0017	0.005

$^a s = [Hg]_{air}/[Hg]_{total}$.
$^b A_0$ is the absorbance of mercury vapour from the solution in the absence of salt.

RESULTS AND DISCUSSIONS

Effect of various salts on the circulation cold-vapour technique
The release of mercury vapour from solution was improved by the presence of sulfates of transition metal ions even at 0.01 M concentrations, the effect decreasing in the following order: iron(II) sulfate > copper sulfate > iron(III) sulfate > nickel sulfate > cadmium sulfate > cobalt sulfate. In the absence of tin(II) chloride, equilibrium was reached after passing air for 5 min but the mercury concentration in the gaseous phase was considerably less than after reduction within tin(II) chloride.

The concentration of mercury in the gaseous phase after the reduction was influenced by the presence of various salts even at 10^{-3} M concentrations if the salts prevented quantitative reduction of mercury or its partition equilibrium between the aqueous solution and the gaseous phase (cf. Table 1). Equilibrium was reached after air (0.6 l min^{-1}) had been passed through the sample solutions for 5 min. Chromate, thiosulfate, iodide or sulfide even at 0.01 M concentrations strongly suppressed the amount of mercury in the gas phase. The corresponding threshold concentrations were 2×10^{-7} M thiosulfate, 1×10^{-6} M sulfide, 8×10^{-6} M iodide for reduction with tin(II) chloride in acidic solution; 1.5×10^{-6} M thiosulfate, 3.5×10^{-7} M sulfide and 2×10^{-4} M iodide with alkaline stannate(II) solution; 7×10^{-4} M thiosulfate, 5×10^{-6} M sulfide and 3.5×10^{-5} M iodide with ascorbic acid; 7×10^{-5} M thiosulfate, 1.5×10^{-6} M sulfide and 4×10^{-4} M iodide with hydrazine hydrochloride; and 1×10^{-4} M thiosulfate, 1×10^{-6} M sulfide and 1×10^{-5} M iodide with formaldehyde.

Release of mercury atoms from solutions

The release of mercury atoms from solution was not quantitative for any of the reducing agents tested. For example, only 34.8% Hg was released from pure aqueous solutions containing less than 1 μg Hg, and in the presence of tin(II) chloride, $s = [Hg]_g/[Hg]_{tot} = 0.348$ at equilibrium. This s value expresses the evaporation or the actual degree of atomization of mercury, and depends on the sample solution volume, v_1, and the air volume, v_g, of the apparatus used, i.e. the volume of tubing, empty parts of bottles and the flow cell (total 293.5 ml). Since the reduction of mercury(II) to mercury is quantitative with all the reductants tested, the s value represents the partition equilibrium of elemental mercury and its solubility in water. This s value for atomic mercury did not change during five successive equilibrations between solution and gaseous phase, always with the residual amount of mercury in solution. The degree of volatilization, s, is an important input parameter in the TEOLINE 3 program for computation of theoretical absorbance values, and the partition ratio can be evaluated from it, $K = [Hg]_g v_1/[Hg]_1 v_g = 0.19$. This value is in reasonable agreement with that given by Thompson and Reynolds [27]. The release and the degree of volatilization of mercury can be strongly affected by various chemical interferences (Table 1).

The cold-vapour technique with amalgamation

Activated carbon, silver and gold wires and absorbers containing various kinds of metallized asbestos were tested for trapping mercury vapours in the circulation circuit. Maximum absorbances were achieved when gold wire, silver wire or gold asbestos was used under optimized conditions. For the other materials used, the absorbance values decreased in the order: Ag asbestos > Pt asbestos > activated carbon > Pd asbestos. The release of mercury atoms from 100—120 ml of solutions containing 0.1—1 μg Hg was quantitative after 4 min when air was passed at 0.6 l min^{-1} through the solution in a closed circuit with the amalgamation tube at room temperature. After the sorption, the amalgamating filling was pre-heated at 500—600°C for 30 s, and the mercury vapour was finally expelled by nitrogen (1 l min^{-1}) to obtain a compact atom cloud. The release of mercury was always quantitative but not always instantaneous; thus when the peak absorbance was evaluated, a $[Hg]_g/[Hg]_t$ value of unity was obtained only from gold and silver wires or gold-coated asbestos (see Table 2). The overall capacities of 1-cm layers of packing are also shown in Table 2).

The metallized asbestos allows faster entrapment of mercury vapour from the air flow during circulation than do the metal wires. The reproducibility of the amalgamation variation of the cold-vapour technique is influenced by the amalgamation time, the temperature during sorption and desorption, the flow rate of nitrogen, and by the total geometry of the amalgamation tube, flow cell and tubings. The statistical evaluation of various parameters for the different amalgamation procedures is summarized in Table 2.

TABLE 2

Evaluation of various amalgamation procedures

Amalgamation filling	Standard deviation[a] (ng Hg)	Charact. concn. (ng Hg)	Detection limit (ng Hg)	Sensitivity[b]		$\frac{[Hg]_g}{[Hg]_t}$	Capacity[c] (μg Hg)
				(ml μg^{-1})	(l mol^{-1})		
Au wire	4.5	0.3	0.9	16	3.2×10^9	1	45
Ag wire	5.2	0.3	0.8	16	3.2×10^9	1	40
Activated C	3.4	0.7	1.1	6.5	1.3×10^9	0.89	50
Au asbestos	3.4	0.3	0.8	16	3.2×10^9	1	150
Ag asbestos	4.8	0.4	1.2	10	2.0×10^9	0.90	80
Pt asbestos	5.2	0.8	1.8	6.5	1.3×10^9	0.69	50
Pd asbestos	5.6	1.0	2.2	4.2	0.8×10^9	0.45	35
None	4.5	12	13	0.35	0.07×10^9	—	—

[a]For 0.1 μg Hg. [b]For $c_M \rightarrow 0$. [c]Capacity of a 1-cm layer of packing.

Even for the amalgamation variation of the cold-vapour technique, mercury is not quantitatively released from solutions containing 0.01 M concentrations of the salts mentioned above for the method without amalgamation.

Comparison of experimental and theoretical calibration plots for the cold-vapour technique

The absorbance vs. concentration plots calculated according to eqns. (1—3) by the TEOLINE program with the input data collected in Table 3 agree with the experimental calibration plots for the cold-vapour technique with and without amalgamation (Tables 4 and 5). The differences between particular experimental and theoretical absorbance values do not exceed 0.3—8.4% for the direct circulation technique, or 0.3—7.6% (average 2.9%) for the amalgamation technique. It is therefore possible to use an absolute method for the determination of mercury without the need for standards.

The slope of the absorbance vs. concentration plots near the origin is considerably affected by the degree of volatilization s, the value of which depends on the apparatus, the volume of the sample solution and the inter-fering ions in solution. For the amalgamation method, agreement between the calculated and experimental values is guaranteed if the cloud of mercury atoms enters the flow cell at one time and the product of average atom concentration and the length of the absorption path is constant. It is difficult to estimate the true temperature of the mercury cloud in the flow cell coming from the amalgamation tube at 500°C, which corresponds to the temperature equivalent of the average kinetic energy of the mercury atoms. As the cloud travels 5 cm with the nitrogen gas flow at 1 l min^{-1} from the amalgamation tube to the flow cell during 0.15 s, the temperature of the mercury atoms was assumed to be 300°C. This parameter has little influence among the input data used for the computations, as was proved by introduction of a temperature of only 100°C.

TABLE 3

Input data for the TEOLINE program for the determination of mercury by the cold-vapour technique

Input data	Circulation	Circulation with amalgamation[a]
Hg concentration range (μg ml^{-1})	$2 \times 10^{-3} - 5 \times 10^{-2}$	$4 \times 10^{-5} - 1 \times 10^{-3}$
$\Delta \bar{\nu}_D$ (cm^{-1})	34.5×10^{-3}	47.7×10^{-3}
Absorption path (cm)	14.7	14.7
Volume of apparatus (cm^3)	393.5	—
Sample volume (cm^3)	100	100
Flow cell volume (cm^3)	21.5	21.5
Degree of volatilization (atomic yield)	0.348	1

[a]On gold-coated asbestos.

TABLE 4

Determination of mercury by the cold-vapour technique

Hg^{2+} (μg ml^{-1})	Experimental absorbance[a]	Calculated absorbance	Relative difference (%)
2×10^{-3}	0.076	0.083	8.4
4×10^{-3}	0.153	0.160	4.4
6×10^{-3}	0.228	0.231	1.3
1×10^{-2}	0.356	0.357	0.3
1.4×10^{-2}	0.458	0.464	1.3
1.8×10^{-2}	0.549	0.556	1.3
2.0×10^{-2}	0.600	0.597	0.5
2.8×10^{-2}	0.735	0.740	0.7
3.6×10^{-2}	0.856	0.860	0.5
4.4×10^{-2}	0.960	0.967	0.7
5.0×10^{-2}	1.072	1.041	2.9
Standard deviation[b]	0.011 μg/100 ml		
Detection limit	0.013 μg/100 ml		
Sensitivity	0.350 ml μg^{-1}		
	7.0×10^7 l mol^{-1}		
Characteristic concentration	0.012 μg/100 ml		

[a]Average from the method of non-linear regression.
[b]For 1 μg Hg in 100 ml from 5 measurements.

Determination of mercury in a graphite furnace

The determination of mercury in graphite furnaces is of rather low sensitivity because the reduction of mercury(II) to elemental mercury by carbon occurs almost at room temperature, and mercury volatilizes in the pre-atomization periods. Accordingly, the responses from graphite, gold and

TABLE 5

Determination of mercury by the cold-vapour technique with amalgamation on gold-coated asbestos

Hg^{2+} ($\mu g \, ml^{-1}$)	Experimental absorbance[a]	Calculated absorbance	Relative difference (%)
4×10^{-5}	0.060	0.064	6.6
8×10^{-5}	0.126	0.125	0.8
1.2×10^{-4}	0.178	0.183	2.8
1.6×10^{-4}	0.247	0.239	3.2
2.0×10^{-4}	0.299	0.292	2.3
4.0×10^{-4}	0.518	0.525	1.4
6.0×10^{-4}	0.701	0.710	1.3
8.0×10^{-4}	0.862	0.865	0.3
1.0×10^{-3}	0.930	1.001	7.6
Standard deviation[b]	$3.4 \times 10^{-3} \, \mu g/100 \, ml$		
Detection limit	$8.0 \times 10^{-4} \, \mu g/100 \, ml$		
Sensitivity	$16 \, ml \, \mu g^{-1}$		
	$3.2 \times 10^{9} \, l \, mol^{-1}$		
Characteristic concentration	$2.8 \times 10^{-4} \, \mu g/100 \, ml$		

[a]Average from the method of non-linear regression.
[b]For 0.1 μg Hg in 100 ml from 5 measurements.

silver surfaces were compared in the HGA-74 under optimized conditions. For this purpose 10-μl aliquots of mercury(II) nitrate solution in 0.01 M HNO_3 ($\leqslant 60 \, \mu g \, ml^{-1}$ for graphite and 2 $\mu g \, ml^{-1}$ for metallic surfaces) were injected into the furnace, dried at 60°C during 15 s, ashed at 100°C, 150°C or 150°C during 10 s in a nitrogen flow of 350 ml min^{-1}, and finally atomized at 700, 950 or 900°C during 10 s (under stopped flow conditions) from the graphite, gold or silver surfaces, respectively. The furnace was finally heated at 2700°C, 1050°C or 950°C, respectively, during 5 s to prevent memory effects. The use of metallic surfaces permitted higher temperatures for sample decomposition without loss of mercury, because a prior amalgamation process occurred from the sample solution and the mercury amalgam was then quantitatively decomposed. This allowed a 27-fold increase in sensitivity for the metallic surfaces compared with the graphite surface (Table 6). Strong acids, except hydrochloric acid, suppressed the absorbance signal even at moderate concentrations, especially sulfuric and perchloric acids (Table 7). There was no signal for 10 ng Hg in 1 M $HClO_4$, but 10^{-4} M concentrations of acid were without effect.

An increase in sensitivity was found in the presence of sulfide or oxidizing agents on the graphite surfaces because of decreased losses of mercury during the pre-atomization periods. The addition of 10 μl of 1 M Na_2S, 0.3 M $KMnO_4$, 1 M $K_2Cr_2O_7$ or 10% H_2O_2 to an aliquot containing 0.20 μg Hg increased the sensitivity for mercury(II), 6.5, 6 or 7 times, respectively.

TABLE 6

Evaluation of calibration plots for the determination of mercury in the HGA-74 furnace with various surfaces

	Graphite	Au foil	Ag foil
Characteristic concentration (μg ml^{-1})	0.27	0.010	0.010
Detection limit (μg ml^{-1})	0.60	0.040	0.050
Sensitivity (ml μg^{-1})	0.016	0.44	0.44
(1 mol^{-1})	3200	88000	88000
Standard deviation[a] (μg ml^{-1})	0.20	0.015	0.020

[a]For 1 μg Hg ml^{-1} with Ag and Au surfaces, and for 10 μg Hg ml^{-1} with the graphite surface ($n = 5$).

TABLE 7

Effect of mineral acids on the atomization of mercury (0.010 μg) in the HGA-74 furnace with gold and silver foils

Acid (M)	Atomic yield $[Hg]_{at}/[Hg]_{tot}$[a]							
	HCl		H$_2$SO$_4$		HNO$_3$		HClO$_4$	
	Au	Ag	Au	Ag	Au	Ag	Au	Ag
10^{-4}	0.43	0.42	0.43	0.42	0.43	0.42	0.43	0.42
10^{-3}	0.45	0.43	0.23	0.36	0.39	0.38	0.18	0.39
10^{-2}	0.47	0.47	0.14	0.41	0.37	0.47	0.03	0.28
10^{-1}	0.30	0.36	0.05	0.38	0.24	0.33	0.01	0.26
10^{0}	0.05	0.23	0.02	0.33	0.13	0.19	0	0.25

[a]Calculated from A_{exp}/A_{calc}.

The influence of various salts at concentrations of 0.1 M is summarized in Table 8 for the different surfaces; a deuterium background corrector was used. A large suppressing effect was observed for thiocyanate and perchlorate, but in general the largest effects were observed on metallic surfaces.

Very low atomic yield from graphite was found during the atomization step ($[Hg]_{at}/c_{Hg} = 0.021$) but the value was 0.40 for silver or gold surfaces, as indicated by the ratio of the slopes for the theoretical and experimental plots of absorbance vs. mercury concentration (Table 9). Thus, the atomization recorded for an uncovered graphite surface gave only about 1/50th of the theoretically possible sensitivity; when the graphite surface was covered with gold or silver foil, almost half the possible efficiency of the method was achieved. The calculated theoretical sensitivities are valid only for the particular internal volume of the HGA-74, furnace, the sample solution volume, and the heating mode used.

TABLE 8

The influence of some salt solutions (0.1 M) on the atomization of mercury from various surfaces in the HGA-74 graphite furnace[a]

Salt	$A \times 100/A_0^b$		
	Au foil	Ag foil	Graphite
$Na_2S_2O_3$	94	93	94
KI	87	99	96
KBr	89	97	90
KSCN	27	25	99
NaCl	82	65	92
$NaClO_4$	34	74	96
$ZnSO_4$	86	79	86
$CuSO_4$	70	98	79
$CdSO_4$	35	72	82
$NiSO_4$	38	62	81
$CoSO_4$	41	81	80
$Fe_2(SO_4)_3$	43	72	90

[a]0.100 μg Hg if atomized from the graphite and 0.010 μg Hg from Au or Ag foil.
[b]A_0 is the absorbance for Hg^{2+} solution in the absence of salt.

TABLE 9

Input data for the TEOLINE program for the determination of mercury in 10-μl aliquots of solution in the HGA-74 furnace

	Graphite	Au foil	Ag foil
Hg concentration range (μg ml^{-1})	0.1—60	0.1—2	0.1—2
$\Delta\bar{\nu}_D$ (cm^{-1})	62.16×10^{-3}	69.14×10^{-3}	68.25×10^{-3}
Temperature (K)	973	1223	1173
Absorption path (cm)	2.8	2.8	2.8
Atomizer volume (cm^3)	0.792	0.562	0.562

Determination of mercury in environmental samples

For the analysis of potable waters, 2 drops of 5% (w/v) potassium permanganate solution and 5 ml of 5.6 M HNO_3 were added to 100 ml of water acidified with 0.3 ml of 15.4 M HNO_3; after 15 s, 5 ml of 9 M H_2SO_4 and 5 ml of 1.5% (w/v) hydroxylammonium chloride solution was added. After decolorization, 5 ml of 10% (w/v) $SnCl_2$ solution in 2.4 M HCl were added. The mercury vapour was expelled by circulation of air for 4 min at a flow rate of 0.6 l min^{-1} and absorbed, after the gas stream had been dried with magnesium perchlorate, on gold-covered asbestos at room temperature. After release from the amalgamation tube at 500°C, the mercury vapour was swept into the flow cell by nitrogen at 1 l min^{-1} and the absorbance was recorded. The optimal concentration interval for the determination is 0.008—1.0 μg Hg in 1 l of water.

For the analysis of air, the amalgamation tube containing gold-covered asbestos was attached to the pump and air was sucked through for 2 h at a flow rate of 0.6 l min^{-1}. The tube was then fitted into the apparatus (Fig. 1), and the mercury vapour was released at 500°C from the amalgamation tube and swept into the flow cell by nitrogen at 1 l min^{-1}. The optimum concentration interval for the determination of mercury in air is 0.011—1.4 μg Hg m^{-3}.

REFERENCES

1 N. S. Poluektov, R. A. Vitkun, Zh. Anal. Khim., 18 (1963) 37.
2 A. M. Ure, Anal. Chim. Acta, 76 (1975) 1.
3 R. A. Vitkun, J. V. Zelyukova, N. S. Poluektov, Zav. Lab., 40 (1974) 949.
4 R. A. Vitkun, N. S. Poluektov and J. V. Zelyukova, Zh. Anal. Khim., 29 (1974) 691.
5 J. Y. Hwang, P. A. Ullucci and A. L. Malenfant, Can. Spectrosc., 16 (1971) 100.
6 S. D. Lyashenko and A. S. Stepanov, Zh. Anal. Khim., 31 (1976) 279.
7 R. C. Rooney, Analyst, 101 (1976) 678.
8 K. Dittrich, R. Wennrich and B. Werner, Chem. Anal., 23 (1978) 71.
9 J. W. Wimberley, Anal. Chim. Acta, 76 (1975) 337.
10 R. Woodriff, Appl. Spectrosc., 28 (1974) 78.
11 G. L. Corte and L. Dubois, Mikrochim. Acta, 1 (1975) 69.
12 J. Murphy, At. Absorpt. Newsl., 14 (1975) 151.
13 H. Nakamachi, K. Okamoto and I. Kusumi, Bunseki Kagaku, 23 (1974) 10.
14 H. J. Issaq and W. L. Zielinski, Anal. Chem., 46 (1974) 1436.
15 H. Hein and W. Schrader, Perkin-Elmer Analysentechnische Berichte, 40 (1975) 20.
16 J. F. Alder and D. A. Hickman, Anal. Chem., 49 (1977) 336.
17 M. J. Fishman, Anal. Chem., 42 (1970) 1462.
18 M. P. Newton and D. G. Davis, Anal. Lett., 8 (1975) 729.
19 C. Feldman, Anal. Chem., 46 (1974) 99.
20 H. V. Weiss, W. H. Shipman and M. A. Guttman, Anal. Chim. Acta, 81 (1976) 211.
21 H. C. Wagenar, I. Novotný and L. de Galan, Spectrochim. Acta, Part B, 29 (1974) 301.
22 H. C. Wagenar and L. de Galan, Spectrochimica Acta, Part B, 23 (1973) 157.
23 V. A. Razumov and I. S. Fishman, Zh. Prikl. Spektrosk, 10 (1969) 710.
24 B. V. L'vov, Atomno-absorpcionnyj analyz, Izd. Nauka 1966, pp. 13—58.
25 B. V. L'vov, J. Quant, Spectrosc. Radiat. Transfer, 12 (1976) 651.
26 I. Novotný and J. Horák, Scripta Fac. Sci. Nat. UJEP Brunensis, Chemia, 7 (1977) 85.
27 K. C. Thompson and G. D. Reynolds, Analyst, 96 (1971) 771.

ROOM-TEMPERATURE DISSOLUTION OF COAL FLY ASH FOR TRACE METAL ANALYSIS BY ATOMIC ABSORPTION SPECTROMETRY

DAVID SILBERMAN* and GERALD L. FISHER

Radiobiology Laboratory, University of California, Davis, California 95616 (U.S.A.)

SUMMARY

A room-temperature digestion technique with hydrofluoric acid, followed by addition of boric acid, is described for coal fly ash; 19 elements (Si, Al, Fe, Ca, Mg, K, Na, Ti, Cu, Mn, Zn, Be, Ba, Co, Cd, Cr, Ni, Pb, and Sr) can then be determined by flame and flameless atomic absorption spectrometry (a.a.s.). The technique has been applied to hopper fly ash collected from an electrostatic precipitator, aerodynamically size-fractionated stack fly ashes and National Bureau of Standards fly ash (SRM 1633). Results for ten elements (Mn, Zn, Cr, Sr, Pb, Cu, Ni, K, Co and Be) by a.a.s. were within the certified range or in good agreement with the information values for the NBS fly ash. Cadmium was 7% higher than the certified value. If the major and minor elements are present as common oxides, mass recoveries for six fly ash fractions samples were quantitative, ranging from 99.1% to 101.4%. Instrumental neutron activation analysis of the undissolved residue from SRM 1633 indicates that the dissolution technique should also be useful for a.a.s. of Sn, Mo, Sb, V, and As, but not for Se, 75% of which remains in the residue.

Coal fly ash consists primarily of fused aluminosilicates together with small quantities, generally less than 5% by weight, of incompletely oxidized carbon [1]. During the preparation of fly ash samples for quantitative analysis for trace elements, losses of volatile trace elements must be prevented. Oxidation of coal to remove carbon usually involves high-temperature ashing in a muffle furnace, low-temperature ashing in an oxygen plasma, or wet oxidation with perchloric acid. However, these techniques can result in loss of volatile trace elements and/or alteration of oxidation states, e.g. Fe(II) to Fe(III). Careful control of temperature and oxidative conditions should reduce, but not eliminate, these problems. After carbon removal, methods for dissolution of complex aluminosilicates include fusion or hydrofluoric acid dissolution. Fusion techniques involve the high-temperature dissolution of aluminosilicates in fluxes such as carbonates, hydroxides or borates of sodium, potassium or lithium [2]. Limitations of fusion dissolution include relatively high salt concentrations (which can cause non-specific absorption or molecular interferences during atomic absorption analysis), possible high reagent blanks from trace element contaminations, and exclusion of the alkali metal used in the flux from the list of analyzable elements. Also, the high temperature used to melt the flux can result in losses of volatile elements, e.g. Hg, Sn, Pb, Cd, and Se, and may affect metal oxidation states [3—5].

Methods based on hydrofluoric acid—boric acid have been used to dissolve aluminosilicate rocks, clays, glasses, cements and other siliceous materials which have low elemental or organic carbon contents [6—8]. These techniques have the advantage of providing complete dissolution at room temperature without oxidation of required components, and have been employed in combination with heat, pressure and oxidizing agents [2, 6, 9, 10]. However, incomplete dissolution can result from the presence of carbonaceous material. Previously published qualitative data for residues from dissolution studies are summarized in Table 1. These techniques employed pressure and/or heat as well as hydrofluoric acid with and without subsequent boric acid treatment. The method for coal fly ash dissolution described by Davison et al. [9] involved heating in a bomb at 110°C with a solution of aqua regia and hydrofluoric acid; boric acid was then used to complex the excess of fluoride and to dissolve insoluble metal fluorides.

The effectiveness of a modified room-temperature dissolution technique for coal fly ash with hydrofluoric acid but without oxidizing agents is described below. Atomic absorption spectrometry (a.a.s.) was the technique chosen to complete the analysis because it is highly selective and can be used to determine both percentage and trace levels; the method gives results similar to those obtained by instrumental neutron activation analysis (i.n.a.a.) [11]. The method is suitable for the analysis of size-fractionated, stack-collected coal fly ash samples, and has been checked for the well-characterized National Bureau of Standards coal fly ash (SRM 1633) [12].

TABLE 1

Summary of the elemental analyses of undissolved residues resulting from dissolution of siliceous materials

Material	Dissolution method	Element identified in residue	Analytical technique	Ref.
Diabase (igneous rock)	Covered container, 1 h at 110°C with HF	Ca, Mg, Al, Fe, Na Ti, Mn, Cu, Si	E.s.[a]	[8]
Granite (igneous rock)	Covered container, 1 h at 110°C with HF	Ca, Mg, Al, Fe, Na Ti, Mn, Cu, Zr	E.s.[a]	[8]
Coal fly ash (Indiana coal)	Bomb heating, 2 h at 110°C, aqua regia and HF followed by H_3BO_3	Ca, F, Al, C	S.s.m.s.[b]	[9]
Aluminosilicates (marine sediments)	Bomb heating, 0.5—1 h at 100°C, aqua regia and HF followed by H_3BO_3	"probably unoxidized carbon"	—	[10]

[a] Emission spectroscopy and chemical methods.
[b] Spark-source mass spectrometry.

EXPERIMENTAL

Reagents

Water was distilled, deionized, and distilled again for use in all solutions and treatments. Commercial 48% (w/w) hydrofluoric acid and boric acid were of analytical-reagent grade. Procedural blanks containing all reagents were carried through all steps of the dissolution process.

A high reagent blank for sodium (116 μg l^{-1}) in the final acidic solution was found to be due to sodium contamination in the boric acid, which was removed by batch treatment with cation exchanger. For this purification, 454 g of boric acid was dissolved in 3 l of hot water, 100 ml of AG 50W-X8 cation-exchange resin (H$^+$-form, 50—100 mesh, Bio-Rad Laboratories, Richmond, CA) was added, the mixture was kept at 80—95°C for 15 min with vigorous stirring and then vacuum-filtered through an acid-washed, glass-fiber filter, and the filtrate was cooled in a 4-l polyethylene bottle. Saturated boric acid solution was continually harvested from the bottle and water was added to replenish the saturated solution until few crystals remained; these saturated solutions gave sodium concentrations of less than 3 μg l^{-1} in the final HF/H$_3$BO$_3$ solution.

Materials

The materials studied included four stack-collected, size-fractionated coal fly ash samples [13] from a plant burning low-sulfur, high-ash coal, a sample from the hopper of the electrostatic precipitator of the same plant, and the standard reference material coal fly ash (SRM 1633). The four size-fractionated samples will be referred to as cuts 1—4; cut 0 refers to the hopper material. The volume median diameters for cuts 0 through 4 were 27, 20, 6.3, 3.2, and 2.2 μm, respectively. The NBS fly ash is a blend of ashes collected from particle emission control devices at five electric power plants.

Dissolution procedure and analysis

Up to 1 g of fly ash was transferred to a tared, screw-cap, 100-ml poly-propylene volumetric flask, and wetted with 10 ml of water to prevent the silicon losses that may occur if hydrofluoric acid is added directly to finely ground, highly siliceous material. With a plastic pipet, 10 ml of 48% hydro-fluoric acid was added and the cap was rapidly and tightly screwed down. The flask was then shaken in a reciprocating shaker overnight at low speed. After shaking, 80 ml of saturated boric acid was added and the flask replaced on the shaker for 4 h. Samples with undissolved residues were placed in an ultrasonic bath for 2 h. Samples which dissolved were transferred to polyethylene storage bottles. Samples with undissolved residue were vacuum-filtered through a 47-mm polycarbonate filter-funnel assembly fitted with a tared, HF-washed, 0.1-μm Nuclepore membrane; the collected residue was washed on the filter with water and dried at 105°C.

The filtrates were analyzed by a.a.s. with a Perkin-Elmer model 306 spectro-

photometer, equipped with a heated graphite analyzer (HGA-2000). Instrumental parameters for each element are listed in Table 2. Flame ionization of Al, Ca, Mg, K, Na, Ba, and Sr was minimized by addition of cesium. Background correction for lead (283.3 nm) was done by absorption measurement at the non-resonant 280.3-nm line. Nickel was determined at 352.5 nm to minimize non-specific absorption. The flame a.a.s. measurements reported are the averages of two 10-s integrations; flameless a.a.s. values are the averages of three measurements (strip-chart recorder). Concentrations were calculated from a standard curve derived by least-squares analysis. All standards were prepared in the HF/H_3BO_3 solution. The residue was analyzed in polyethylene containers by i.n.a.a. at the Lawrence Livermore Laboratory 3-MW pool-type reactor operating at ca. 2×10^{13} n cm^{-2} s^{-1}; γ-spectra were measured with Ge(Li) detectors coupled with 4096-channel analyzers. Spectral data were analyzed on a CDC-6600 computer with the GAMANAL code, which fits peaks with Gaussian and exponential functions and smoothed background functions [14].

RESULTS

To provide sufficient residue mass for convenient i.n.a.a., two samples of NBS fly ash (4.5 and 5.9 g) were each dissolved by addition of 50 ml of water and 50 ml of hydrofluoric acid followed by 400 ml of saturated boric acid solution. These samples yielded 3.43% and 3.47%, respectively, of the initial mass as undissolved residue. The filtrates were analyzed by a.a.s. for 19 elements and the residues were analyzed by i.n.a.a. Table 3 summarizes the results.

TABLE 2

Operating parameters for atomic absorption analysis of coal fly ash

Element	Wavelength (nm)	Oxidant (with acetylene)[a]	Element	Wavelength (nm)	Oxidant (with acetylene)[a]
Si	251.6	N_2O	Ni	352.5	air
Al[b]	309.3	N_2O	Mn	279.5	air
Fe	248.3	air	Cu	324.7	air
Ca[b]	422.7	N_2O	Zn	213.9	air
Mg[b]	285.2	N_2O	Co[e]	240.7	flameless
K[b]	766.5	air	Be	234.9	N_2O
Na[b]	589.0	air	Cr	357.9	N_2O
Ti	365.4	N_2O	Ba[b]	553.6	N_2O
Pb	283.3[c]	air	Sr[b]	460.7	N_2O
Cd[d, e]	228.8	flameless			

[a]Except for flameless a.a.s. [b]2000 μg Cs ml^{-1} (as $CsNO_3$) added. [c]Background correction at 280.3 nm. [d]Dithizone complex in 1% nitric acid (see text). [e]Deuterium-arc background correction.

TABLE 3

Elemental analysis of NBS fly ash

Element	This study[a]	Reported values	Ref.	Undissolved residue[b] (μg g^{-1} fly ash)	Undissolved[c] (%)
		———— (%) ————			
Si	22.6	21 ± 2	(14)	—	—
Al	12.7	12.7 ± 0.5	(14)	480	0.4
Fe	6.4	6.2 ± 0.3	(14)	91	0.1
Ca	4.3	4.3 ± 0.6	(14)	—	—
K	1.68	1.72	(12)[d]	—	—
Mg	1.22	1.8 ± 0.4	(14)	39	0.3
Ti	0.68	0.74 ± 0.03	(14)	440	5.9
Na	0.30	0.32 ± 0.04	(14)	1.6	0.1
		———— (μg g^{-1}) ————			
Ba	2210	2700 ± 200	(14)	310	12
Sr	1340	1380	(12)[d]	6.3	0.5
Mn	485	493 ± 7	(12)[e]	0.63	0.1
Zn	221	210 ± 20	(12)[e]	0.63	0.3
Cr	128	131 ± 2	(12)[e]	6.5	4.8
Cu	121	128 ± 5	(12)[e]	—	—
Ni	99	98 ± 3	(12)[e]	2.5	2.5
Pb	70	70 ± 4	(12)[e]	—	—
Co	42	38	(12)[d]	0.20	0.5
Be	12	12	(12)[d]	—	—
Cd	1.55	1.45 ± 0.06	(12)[e]	—	—

[a]A.a.s. of duplicate samples. [b]I.n.a.a. of duplicate samples. [c]Based on residue analysis and previously reported values. [d]NBS informational value [12]. [e]NBS certified value [12].

Except for Mg and Ba, the agreement of the a.a.s. data with previously reported values is excellent. Based on the i.n.a.a. data, better than 95% recovery is observed for all elements except Ba and Ti, for which the residue contained 12% and 5.9%, respectively, of the total elemental content. The carbon content of the residues from the NBS fly ash was 82% (±1%), determined by combustion and gravimetric analysis of carbon dioxide [15]. The concentrations of hydrogen, nitrogen and sulfur in NBS SRM 1633 are 0.1%, 0.1%, and 0.3%, respectively [16]. If these elements and the metals determined by a.a.s. exist as simple oxides, and when the undissolved residues of 3.45% are included, the average mass recovery of the NBS samples was 99.1%. Results for elements determined in the residue by i.n.a.a. but not determined in the filtrate by a.a.s. are presented in Table 4. Cl, Br, I, Hf, Zr, Ta and Lu were present in the residue at relatively high concentrations. The very high selenium content of the residue indicates the inappropriateness of the dissolution technique for this element.

Preliminary analyses for cadmium in HF/H_3BO_3 resulted in somewhat higher values than those certified by the NBS. Direct injection of eight NBS fly ash

TABLE 4

Instrumental neutron activation analysis of undissolved residues from NBS fly ash

Element	Content in residue ($\mu g\,g^{-1}$) of fly ash)	Reported values[a] ($\mu g\,g^{-1}$)	Undis-solved[b] (%)	Element	Content in residue ($\mu g\,g^{-1}$) of fly ash)	Reported values[a] ($\mu g\,g^{-1}$)	U s (
Se	7.6	10.2 ± 1.4	75	Sn	0.35	12.4 ± 0.9	2
I	0.7	2.9 ± 1.2	24	Ce	4.1	146 ± 15	2
Hf	1.9	7.9 ± 0.4	24	La	2.1	82 ± 2	2
Zr	63	301 ± 20	21	In	0.007	0.32 ± 0.10	2
Br	1.9	12 ± 4	16	Mo	0.4	18.8 ± 1.3	2
Lu	0.11	1.0 ± 0.1	11	Nd	1.2	63.8 ± 28	1
Cl	4.1	42 ± 10	10	Eu	0.04	2.5 ± 0.4	1
Ta	0.17	1.8 ± 0.3	9.8	Sc	0.28	27 ± 1	1
Yb	0.4	7 ± 3	5.7	Sb	0.06	6.9 ± 0.6	0
Th	1.1	24.8 ± 2.2	4.4	V	1.8	235 ± 13	0
W	0.18	4.6 ± 1.6	3.9	As	0.32	58 ± 4	0
Tb	0.06	1.9 ± 0.3	3.2				

[a]See reference [14].
[b]Based on residue analysis and previously reported values from fly ash analysis.

samples in HF/H_3BO_3 on two separate occasions gave results slightly higher ($1.69 \pm 0.08\ \mu g\,g^{-1}$) than the certified value ($1.45 \pm 0.06\ \mu g\,g^{-1}$). Cadmium in the HF/H_3BO_3 blank was low but difficult to quantify because of the variability of the flameless measurements. To provide better estimates of the blank, cadmium was concentrated 10-fold by dithizone extraction [17] followed by back-extraction into 1% (v/v) redistilled nitric acid. Flameless a.a.s. of the concentrated HF/H_3BO_3 blank and blank-corrected dithizone extractions of six NBS fly ash samples gave cadmium concentrations of $0.95 \pm 0.06\ ng\,ml^{-1}$ and $1.55 \pm 0.12\ \mu g\,g^{-1}$, respectively.

Analyses of size-fractionated stack fly ash (cuts 1—4) and the hopper fly ash (cut 0) indicated that the carbon contents and the undissolved residues from these samples were substantially lower than those from the NBS fly ash (Table 5). Linear regression analysis demonstrated that the carbon content of the ash and the relative mass of undissolved residue are highly correlated ($r = 0.998; p < 0.001$). Analyses for the major elements in cuts 0—4 by a.a.s. plus the undissolved residues indicated mass recoveries ranging from 100.0% to 101.4% (Table 6).

DISCUSSION

The modified HF/H_3BO_3 dissolution technique provides a simple and quantitative method for the analysis of coal fly ash. Results for the NBS fly ash by a.a.s. are mostly in excellent agreement with previously published values. The magnesium values determined by a.a.s. are substantially lower than earlier i.n.a.a. values, but the latter were the average results from two independent laboratories which differed greatly from each other [14]. Neutron activation analysis for magnesium in aluminosilicates is complicated by the

TABLE 5

Carbon content and undissolved residue of coal fly ash samples

Coal fly ash	Carbon content (% ± s.d.)[a]	Undissolved residue (% ± s.d.)[b]
NBS-1633	3.05 ± 0.05	3.45 ± 0.02
Cut 0	0.44 ± 0.01	0.63 ± 0.02
Cut 1	0.18 ± 0.02	0.22 ± 0.02
Cut 2	0.23 ± 0.03	0.20 ± 0.01
Cut 3	0.15 ± 0.06	0.21 ± 0.04
Cut 4	0.27 ± 0.02	0.27 ± 0.01

[a]Mean of 3 samples, ± 1 standard deviation, determined by CO_2 evolution from a high-temperature induction furnace.
[b]Mean of 2 samples, ± 1 standard deviation, from gravimetric analysis.

TABLE 6

Concentration (%) of major elements by a.a.s. on replicate size-fractionated (cuts 1—4) and electrostatic-precipitator-collected (cut 0) fly ash samples

Element	Cut 0	Cut 1	Cut 2	Cut 3	Cut 4
Si	29.6	29.6	28.0	27.5	26.8
Al	14.5	13.8	14.4	14.2	14.1
Fe	2.25	2.55	3.09	3.14	3.44
Ca	2.02	2.12	2.23	2.30	2.38
Mg	0.41	0.47	0.56	0.60	0.63
Na	0.99	1.19	1.75	1.83	1.85
K	0.77	0.74	0.80	0.82	0.81
Ti	0.58	0.62	0.76	0.77	0.78
S[a]	0.14	0.13	0.75	1.08	1.70
Mass[b] recovery (%)	101.4	100.7	101.1	100.4	100.0

[a]Determined by thermometric titration calorimetry; data kindly supplied by L. D. Hansen, Brigham Young University.
[b]Mass recovery calculated from undissolved residue values (Table 5) and assuming that the major elements exist as SiO_2, Al_2O_3, Fe_2O_3, CaO, MgO, Na_2O, K_2O, TiO_2, and SO_3.

interfering $^{27}Al(n, p)^{27}Mg$ reaction. The present a.a.s.—i.n.a.a. results indicate incomplete dissolution of barium, probably because of the insolubility of $BaSO_4$ in dilute acids.

Initial determinations of cadmium in the NBS fly ash gave results higher than the certified value, but inclusion of a dithizone extraction and an appropriate blank correction yielded good agreement with the certified value. The cadmium contamination was traced to the hydrofluoric acid. This work emphasizes the importance of careful determination of the cadmium contribution from the dissolution matrix.

Residue analysis indicated that 75% of the selenium was undissolved. Previous filtration studies [18] with neutron-activated fly ash (cut 4) in Tris buffer at pH 7.3 showed 30% dissolution of selenium. Other dissolution studies of selenium in cut 4 fly ash by i.n.a.a. with 0.03, 0.06, 0.09, and 0.14 M hydrochloric acid showed that 11, 38, 61, and 82%, respectively, of the total selenium content dissolved. Saturated boric acid alone or the HF/H_3BO_3 dissolution technique gave about 50% dissolution of total selenium in cut 4. These studies clearly indicate a strong pH dependence for dissolution of selenium.

Large fractions of the chlorine, bromine and iodine were associated with the undissolved residue: 9.8, 16 and 24%, respectively. These elements appear to be associated with the fly ash compounds that are resistant to dissolution by hydrofluoric acid. The group IV B elements, Ti, Zr, and Hf, had consistently high concentrations in the residue: 6, 21, and 24%, respectively, of the total elemental concentration. Langmyhr and Kringstad [8] observed titanium-containing residues from minerals dissolved with hydrofluoric acid, and zirconium and hafnium would be expected to behave in an analogous way.

Of the remaining elements which had more than 5% of their total mass in the residue (Lu, Ta and Yb), none are routinely determined by a.a.s. Values for Sn, Mo, Sb, V and As in the residues were low, indicating the suitability of this dissolution technique for subsequent a.a.s. of these elements.

Analyses of different fly ashes indicated that the mass of the undissolved residue is correlated with the carbon content of the sample. Excellent mass recoveries ranging from 99.1% to 101.4% were obtained for the six different samples tested. Analyses of five different cuts indicated a strong inverse dependence of elemental concentration on particle size for sulfur with a lesser degree of inverse dependence for Fe, Ca, Mg, Na and Ti. Silicon was the only element to display a concentration dependence directly proportional to particle size.

REFERENCES

1 G. L. Fisher, B. A. Prentice, D. Silberman, J. M. Ondov, A. H. Biermann, R. C. Ragaini and A. R. McFarland, Environ. Sci. Technol., 12 (1978) 447.
2 B. Bernas, Anal. Chem., 40 (1968) 1682.
3 R. B. Muter and L. L. Nice, in S. P. Babu (Ed.), Trace Elements in Fuel, Adv. Chem. Ser., 141, Amer. Chem. Soc., Washington, D.C., 1975, pp. 67—75.
4 L. E. Ranweiler and J. L. Moyers, Environ. Sci. Technol., 8 (1974) 152.
5 T. T. Gorsuch, Analyst, 84 (1959) 135.
6 F. J. Langmyhr and P. E. Paus, Anal. Chim. Acta, 43 (1968) 397.
7 M. L. Jackson, Soil Chemical Analysis-Advanced Course, 2nd edn., Madison, WI, 1969, p. 536.

8 F. J. Langmyhr and K. Kringstad, Anal. Chim. Acta, 35 (1966) 131.

9 R. L. Davison, D. F. S. Natusch, J. R. Wallace and C. A. Evans, Jr., Environ. Sci. Technol., 8 (1974) 1107.

10 D. E. Buckley and R. E. Cranston, Chem. Geol., 7 (1971) 273.

11 J. M. Ondov, R. C. Ragaini, R. E. Heft, G. L. Fisher, D. Silberman and B. A. Prentice, 8th Materials Research Symposium, NBS, Gaithersburg, Maryland, 1977, p. 565.

12 Certificate of Analysis, Standard Reference Material SRM 1633, Office of Standard Reference Materials, National Bureau of Standards, U.S. Department of Commerce, Washington, D.C. 20234.

13 A. R. McFarland, R. W. Bertch, G. L. Fisher and B. A. Prentice, Environ. Sci. Technol., 11 (1977) 781.

14 J. M. Ondov, W. H. Zoller, I. Olmez, N. K. Aras, G. E. Gordon, L. A. Rancitelli, K. H. Abel, R. H. Filby, K. R. Shah and R. C. Ragaini, Anal. Chem., 47 (1975) 1102.

15 J. L. Young and M. R. Lindbeck, Soil Sci. Soc. Am. Proc., 28 (1964) 377.

16 W. M. Henry, Battelle-Columbus Laboratories, personal communication.

17 E. B. Sandell, Colorimetric Determination of Traces of Metals, 3rd edn., Interscience-Wiley, New York, 1959, p. 360.

18 G. L. Fisher, D. Silberman, R. E. Heft and J. M. Ondov, Environ. Sci. Technol., in press.

COMPARISON OF ELECTROTHERMAL ATOMIC ABSORPTION SPECTROMETRY OF THE METAL CONTENT OF SEWAGE SLUDGE WITH FLAME ATOMIC ABSORPTION SPECTROMETRY IN CONJUNCTION WITH DIFFERENT PRETREATMENT METHODS

M. J. T. CARRONDO, R. PERRY and J. N. LESTER*

Public Health Engineering Laboratory, Imperial College, London SW7 2AZ (Gt. Britain)

(Received 1st September 1978)

SUMMARY

Determination of the metal content of sewage sludges is of increasing importance in order to assess the suitability of the sludge for disposal to agricultural land. The methods currently used for the determination of cadmium, chromium, copper, nickel, lead and zinc are time-consuming. A rapid electrothermal atomic absorption procedure with homogenization as the only pretreatment is compared with wet and dry pretreatment methods followed by flame atomic absorption spectrometry, in a statistically designed experiment. The precision of the rapid electrothermal atomic absorption procedure compares well with flame atomic absorption in conjunction with all pretreatment methods used. Time saved by the use of this method is substantial; the procedure could be used advantageously for routine analysis.

Although methods of metal removal exist [1], industrial wastewaters discharged to public sewers are frequently contaminated with heavy metals. During sewage treatment the heavy metals tend to be concentrated in the sludges produced [2] leaving an effluent with lower concentrations of heavy metals than the influent raw sewage.

It is desirable that these sludges should be applied to agricultural land where they may be utilized either as a conditioner or as a fertilizer [3]. As some of the "so-called" heavy metals may be phytotoxic or toxic to animals or both [4, 5], one of the main factors to be considered when evaluating the suitability of a sludge for disposal to land is its metal content [6]. It is therefore important that techniques for the estimation of the metal content of sewage sludge be suitable for routine analysis. A range of methods has been applied to the determination of heavy metals in waters, wastewaters and sewage sludges; these include neutron activation analysis [7], x-ray fluorescence [8], colorimetry [9], anodic stripping voltammetry [10] and atomic absorption spectrometry [11]. Of these methods atomic absorption spectrometry is probably the one most frequently employed for environmental samples [12—14].

When applied to samples where organic and inorganic matrices are present,

these methods generally require some form of sample pretreatment. Dry ashing followed by acid dissolution, and acid digestion are commonly used. If the analytes are present at very low concentrations, a preconcentration procedure may be needed.

Of the methods available [15, 16] a limited number has achieved general use. Dry ashing is a common procedure for the destruction of organic matter [17, 18], although some metals, particularly cadmium and to a lesser extent lead and copper, may be lost [17, 19]. It has been claimed that the addition of magnesium nitrate to some environmental samples avoids losses of cadmium and lead [20]. Perchloric acid in conjunction with nitric acid is claimed to yield high metal recoveries [13, 14]. Procedures based on the use of sulphuric and nitric acids have been recommended [9], although an extraction procedure must be included to avoid errors which would otherwise result from the precipitation of insoluble lead sulphate [13, 16]. Recently methods based on hydrogen peroxide and nitric acid have been applied to environmental samples [21, 22].

The development of flameless atomizers for atomic absorption has allowed substantial improvements in sensitivity over conventional flame techniques. Flameless atomizers allow sample pretreatment to be minimized for samples with largely organic matrices [12, 23].

The use of a rapid flameless atomic absorption method for the determination of cadmium, chromium, copper, lead, nickel and zinc in sewages and sewage effluents after homogenization, has been described [24]. Preliminary results for the analysis of sewage sludges by the same method have also been reported [25, 26]. The results presented below were obtained from a statistically designed experiment to compare the rapid flameless atomic absorption method of analysis with flame atomic absorption analysis of ashed and acid digested samples. Two digestion procedures were used, a sulphuric—nitric acid method and a nitric acid—hydrogen peroxide method. The temperature chosen for ashing was selected after optimization of the procedure and the use of magnesium nitrate as an ashing aid was also assessed.

EXPERIMENTAL

Instrumentation

A Perkin-Elmer model 305 atomic absorption spectrometer fitted with a deuterium background corrector and an HGA 72 graphite atomizer was used for all flameless analyses. The operating conditions are given in Table 1. High-purity argon was used to purge the furnace throughout.

Flame analyses were done with a Perkin-Elmer model 603 atomic absorption spectrometer equipped with deuterium background correction. The conditions for analysis were those recommended by the instrument manufacturer, except for chromium for which slit 3 (0.2 nm) was used to reduce spectral interferences [27].

TABLE 1

Instrumental operating conditions

Conditions	Cd	Cr	Cu	Ni	Pb	Zn
Wavelength (nm)	228.8	357.9	324.8	232.0	283.3	307.6
Slit width (nm)	0.7	0.2	0.7	0.2	0.7	0.7
Ashing temperature (°C)[a]	250	1100	700	800	350	450
Ashing time (s)	40	30	30	40	30	35
Atomization temperature (°C)	2100	2660	2660	2660	2300	2500
Atomization time (s)	5	5	4	5	5	5[b]

[a]In the HGA cycle, all samples were dried at 100°C for 30s.
[b]Gas stop used.

Homogenization

Approximately 250 ml of the sample diluted 50-fold and acidified to 1% (v/v) with nitric acid was homogenized in a 2-l tall-form beaker with an Ultra Turrax T45N homogenizer (Scientific Instrument Co. Ltd., London) for 5 min at 8000 rpm. To avoid contamination of the sample by chromium and nickel, the original stainless shaft, stator and rotor of the homogenizer were replaced with a replicate made of titanium. The suitability of this shaft for the homogenization of samples to be analyzed for cadmium, chromium, copper, nickel, lead and zinc has been reported previously [26].

Aliquots of 20 or 50 μl were injected into the flameless atomizer with an Eppendorf micropipette. Analysis was by direct comparison with standards in 1% (v/v) nitric acid. Results obtained by direct comparison with aqueous standards and by use of a method of standard addition were found to be in good agreement.

Reagents

Stock solutions of cadmium, nickel, lead and zinc were prepared from their nitrate salts (analytical grade). A chromium stock solution was prepared from potassium chromate (analytical grade) and a copper solution from copper wire, previously cleaned by sanding to remove oxide and by degreasing in acetone. Aristar-grade reagents were used for the treatment of the samples in order to minimize blank values.

Digestion and ashing methods

Nitric—sulphuric acid digestion. Digestions were carried out as recommended [9]; the apparatus was modified slightly by the substitution of a 500-ml flask for the original 250-ml one, permitting larger samples (50 ml) to be treated. Heat was provided by an electric isomantle.

Hydrogen peroxide—nitric acid digestion. The method used was essentially that described by Geyer et al. [21]; however, 20 ml of sample was digested

instead of the 5 ml originally proposed, thus reducing the errors involved in the estimation of the volume of thick sludges. A thermostated hot plate was used.

Destruction of organic matter by ashing. Samples were ashed in a modified Wild Barfield horizontal rectangular muffle furnace in which the flue had been enlarged to ensure an adequate natural draught through the furnace during the ashing period. Ashings were carried out at 300°C, 450°C and 550°C for 16 h in ceramic crucibles. An ethanolic 10% (w/v) solution of magnesium nitrate (analytical grade) was also used for ashing at 450°C and 550°C.

RESULTS AND DISCUSSION

A sample of mixed primary sludge (total solids 3.04%) was collected in a polythene container and acidified to 1% (v/v) nitric acid. For each of the pretreatments (ashing at various temperatures with and without magnesium nitrate, digestion and homogenization) five replicates and two blanks were undertaken. The ashed and digested samples were analyzed by flame atomic absorption spectrometry and the homogenized ones by the flameless method.

The results were treated statistically; the mean values, within-group relative standard deviation, and the results of an analysis of variance by the F-test [28] are reported. Tukey's procedure [28] was used to identify which means were statistically different at the 0.05 significance level.

A comparison of the ashing temperatures and treatments involving magnesium nitrate are presented in Table 2. Results in Table 3 relate to a similar comparison between ashing at 450°C, homogenization and the digestion procedures.

From these comparisons, it would appear that ashing at any of the temperatures tested is unsuitable when cadmium has to be determined. The values obtained for nickel when ashed at 550°C with magnesium nitrate were different at the 0.05 level of significance. However, the relative standard deviations were very low (Table 2) and this difference was probably unimportant. The ashing temperature did not seem to have any effect on the determination of copper, chromium, zinc and, perhaps more surprisingly, lead.

The data in Table 3 indicate that there were no statistically significant differences between the methods for the determination of zinc and nickel. Results for cadmium, chromium and copper by the digestion procedures and the flameless method were in good agreement, and no significant differences were identified. However, results for the ashed samples were consistently lower. Assuming the mean of the three statistically equal treatments to be 100%, the recoveries by ashing at 450°C for cadmium, chromium and copper were 71%, 85% and 92%, respectively. Results for lead by the nitric—sulphuric acid digestion procedure were significantly different from those obtained by the other pretreatment methods, recovery of lead by that method being some 83% of the mean of the other three methods.

The results presented here seem to be in agreement with data previously reported by Gorsuch [17] who found almost 100% recoveries for zinc and

TABLE 2

Comparison of metal concentrations in sewage sludges by ashing at different temperatures, with and without addition of magnesium nitrate, dissolution and flame atomic absorption spectrometry

Metal	Ashing temperature (°C)	F-test[a]	Mean conc. (mg l^{-1})	R.s.d. (%)	Recovery[b] (%)
Cadmium	300	0.01	0.128A[c]	4.2	84
	450		0.109B	13.0	71
	550		0.083C	6.3	54
	450[d]		0.092D	9.2	60
	550[d]		0.056E	4.7	37
Chromium	300	N.S.	0.76A	4.3	81
	450		0.80A	9.1	85
	550		0.80A	3.4	85
	450[d]		0.76A	2.8	81
	550[d]		0.78A	2.8	83
Copper	300	N.S.	8.7A	9.2	85
	450		9.4A	7.5	92
	550		9.5A	2.5	93
	450[d]		9.4A	5.4	92
	550[d]		9.0A	9.0	88
Nickel	300	0.05	1.67A	3.6	95
	450		1.72AB	4.9	98
	550		1.66A	1.6	94
	450[d]		1.71AB	4.5	97
	550[d]		1.79B	4.0	102
Lead	300	N.S.	17.2A	1.8	100
	450		17.5A	1.5	102
	550		17.4A	2.3	101
	450[d]		17.3A	1.1	101
	550[d]		17.0A	2.6	99
Zinc	300	N.S.	16.1A	1.7	95
	450		16.4A	1.5	97
	550		16.0A	1.6	94
	450[d]		16.2A	1.2	95
	550[d]		16.0A	1.7	94

[a]N.S. means not significant at the 0.05 probability level.
[b]Recoveries assume that the mean of the statistically equal means from the other methods (Table 3) corresponds to complete recovery.
[c]Mean concentrations obtained by different treatments which are not followed by a common letter are significantly different at the 0.05 probability level.
[d]Magnesium nitrate added as an ashing aid.

TABLE 3

Comparison of metal concentrations in sewage sludges obtained by sulphuric—nitric acid digestion, hydrogen peroxide—nitric acid digestion and ashing at 450°C and flame atomic absorption spectrometry with those obtained for homogenized samples by flameless atomic absorption spectrometry

Metal	Pretreatment	F-test[a]	Mean conc. (mg l^{-1})	R.s.d. (%)
Cadmium	H_2SO_4/HNO_3	0.01	0.161A	4.9
	H_2O_2/HNO_3		0.149A	10.0
	450°C ashing		0.109B	13.0
	Homogenization		0.150A	5.5
Chromium	H_2SO_4/HNO_3	0.05	0.97A	7.6
	H_2O_2/HNO_3		0.91A	11.0
	450°C ashing		0.80B	9.1
	Homogenization		0.93A	6.6
Copper	H_2SO_4/HNO_3	0.05	10.4A	2.1
	H_2O_2/HNO_3		10.2A	2.5
	450°C ashing		9.4B	7.5
	Homogenization		10.0A	2.6
Nickel	H_2SO_4/HNO_3	N.S.	1.68A	4.2
	H_2O_2/HNO_3		1.79A	6.9
	450°C ashing		1.72A	4.9
	Homogenization		1.82A	7.0
Lead	H_2SO_4/HNO_3	0.01	14.4A	5.0
	H_2O_2/HNO_3		17.3B	4.9
	450°C ashing		17.5B	1.5
	Homogenization		17.1B	2.4
Zinc	H_2SO_4/HNO_3	N.S.	16.9A	1.6
	H_2O_2/HNO_3		16.4A	8.3
	450°C ashing		16.4A	1.5
	Homogenization		17.7A	6.5

[a]For symbols, see footnotes to Table 2.

lead when ashing at 450°C. For cadmium, Gorsuch [17] reports 91% recovery, but only 76% in the presence of nitric acid or 78% with magnesium nitrate; these results are marginally higher than the 71% recovery observed here when ashing at 450°C or the 60% recovery obtained in the presence of magnesium nitrate. The use of magnesium nitrate as recommended [20] for biological samples did not seem to improve the recoveries of cadmium or lead. For copper, in the presence of nitric acid, recoveries of 94% [17] and 95% [18] have been reported, slightly higher than the 92% obtained here. The complete recovery for nickel reported here was expected [19]. However, the recovery for chromium, which should have been almost complete [17], was surprisingly low (85%). Chromium can be lost as chromyl chloride under strongly oxidizing

conditions [29] or as the result of the formation of oxides of low solubility in acidic conditions [29]; however, both these explanations seem improbable here. Nonetheless, low recoveries for chromium in samples of sewage sludge have been reported previously [21].

The loss of lead as a precipitate of lead sulphate in the sulphuric—nitric acid method may be expected [13, 16], although the use of ammonium acetate as recommended [9] is claimed to yield higher recoveries than those obtained here (83%). For all the other metals, this method compared well, giving rise to the lowest scatter of results as measured by the relative standard deviation.

The hydrogen peroxide—nitric acid method compares favourably in terms of recoveries, although the precision, as measured by the relative standard deviation, was generally lower than that for the other methods tested.

Flameless atomic absorption spectrometry proved to be satisfactory for the less volatile elements, chromium, nickel and copper, which is consistent with earlier studies [12, 23]. Perhaps more surprisingly, the data presented in Table 3 clearly indicate its suitability for determinations of cadmium, lead and zinc. Matrix interferences have previously been encountered [12, 23, 30] when flameless atomic absorption techniques have been applied to determinations of these elements. The lack of interferences may be entirely fortuitous, or may result from a perfect match between enhancement and suppression effects. Alternatively, synergic effects may have occurred, similar to those identified for lead and cadmium in fertilizer samples [31], which may have neutralized any interference. Undoubtedly the use of deuterium background correction is invaluable for this type of analysis, particularly for the volatile elements lead, cadmium and zinc.

Direct comparison with aqueous standards yielded accurate results for all metals in these sludge samples when analyzed by flameless atomic absorption after homogenization. For the more volatile elements (cadmium, lead and zinc) the use of a standard method of additions has been recommended [12, 32], but in some types of samples of an organic nature the use of a calibration method has yielded good results [33—35]. Similarly, in a study of direct flame atomic absorption of ultrasonically dispersed sewage sludge in a cup system, no differences between the method of standard additions and comparison with aqueous standards were found for cadmium and lead [11].

The precision of the rapid method compares well with that of the other methods with the relative standard deviations for all metals being less than 8%.

Conclusions

The rapid flameless procedure described here can be used advantageously for routine analysis. The time saved is considerable, because homogenization takes only 5 min as opposed to the 3—6 h required for a digestion. This more than compensates for the additional time (2—3 min) required for flameless analysis as opposed to flame analysis.

For every sewage treatment works, the rapid flameless method should be intially evaluated against one or more digestion procedures followed by flame analysis. If, as expected, a satisfactory agreement is achieved, the method could then be used on a routine basis. However, it should be checked, at intervals, by comparison with a standard method of additions, particularly for the volatile elements cadmium, lead and zinc.

REFERENCES

1 J. V. Rouse, J. Environ. Eng. Div. Am. Soc. Civ. Engr., 102 (1976) 929.
2 R. O. Neufeld, J. Gutierrez and R. A. Novak, J. Water Pollut. Control Fed., 49 (1977) 489.
3 Government of the United Kingdom, Department of the Environment, Report of the Working Party on the Disposal of Sewage Sludge to Land, H.M.S.O., London, 1977.
4 J. J. Dulka and T. H. Risby, Anal. Chem., 48 (1976) 640A.
5 A. L. Page, Fate and Effects of Trace Elements in Sewage Sludge when Applied to Agricultural Land — A Literature Review Study; U.S. EPA-670/Z-74-005, 1974.
6 G. A. Garrigan, J. Wat. Pollut. Control Fed., 49 (1977) 2380.
7 K. Lenvik, E. Steinnes and A. C. Pappas, Anal. Chim. Acta, 97 (1978) 295.
8 J. Smits and R. van Grieken, Anal. Chim. Acta, 88 (1977) 97.
9 Government of the United Kingdom, Department of the Environment, Analysis of Raw, Potable and Waste Waters, H.M.S.O., London, 1972.
10 J. T. Kinard, J. Environ. Sci. Health, Part A, 12 (1977) 531.
11 D. G. Mitchell, W. N. Mills, A. F. Ward and K. M. Aldous, Anal. Chim. Acta, 90 (1977) 275.
12 D. A. Lord, J. W. McLaren and R. C. Wheeler, Anal. Chem., 49 (1977) 257.
13 H. Agemian and A.S.Y. Chau, Anal. Chim. Acta, 80 (1975) 61.
14 P. Geladi and F. Adams, Anal. Chim. Acta, 96 (1978) 229.
15 T. T. Gorsuch, The Destruction of Organic Matter, Pergamon Press, N.Y., 1970.
16 N. W. Hanson, Recommended Methods of Analysis, 2nd edn., The Society for Analytical Chemistry, London, 1974.
17 T. T. Gorsuch, Analyst, 84 (1959) 135.
18 E. E. Menden, D. Brockman, H. Choudhury and H. G. Petering, Anal. Chem., 49 (1977) 1644.
19 E. C. Dunlop, in I. M. Kolthoff and P. J. Elving (Eds.), Treatise on Analytical Chemistry, Part 1, Vol. 2, Chapter 25, Interscience, New York, 1961, pp. 1055—1058.
20 M. T. Friend, C. A. Smith and D. Wishant, At. Absorpt. Newsl., 16 (1977) 46.
21 D. Geyer, P. Martin and P. Adrian, Korrespondenz Abwasser, 22 (1975) 369.
22 K. V. Krishnamurty, E. Shpirt and M. M. Reddy, At. Absorpt. Newsl., 15 (1976) 68.
23 R. B. Cruz and J. C. Van Loon, Anal. Chim. Acta, 72 (1974) 231.
24 M. J. T. Carrondo, R. Perry and J. N. Lester, Sci. Total Environ., in press. (1979).
25 J. N. Lester, R. M. Harrison and R. Perry, Sci. Total Environ., 8 (1977) 153.
26 S. Stoveland, M. Astruc, R. Perry and J. N. Lester, Sci. Total Environ., 9 (1978) 263.
27 G. F. Kirkbright and M. Sargent, Atomic Absorption and Fluorescence Spectroscopy, Academic Press. London. 1974.

28 A. H. Bowker and G. J. Lieberman, Engineering Statistics, Prentice-Hall, New Jersey, 1972.
29 W. H. Hartford, in I. M. Kolthoff and P. J. Elving (Eds.), Treatise on Analytical Chemistry, Part II Section A, Vol. 8, Interscience, New York, 1963, pp. 273—377.
30 D. Clark, R. M. Dagnall and T. S. West, Anal. Chim. Acta, 63 (1973) 11.
31 T. C. Woodis Jr., G. B. Hunter and F. J. Johnson, Anal. Chim. Acta, 90 (1977) 127.
32 F. C. Wright and J. C. Riner, At. Absorpt. Newsl., 14 (1975) 103.
33 L. A. Briese and J. P. Giesy, At. Absorpt. Newsl., 14 (1975) 133.
34 G. Lundgren, Talanta, 23 (1976) 309.
35 D. V. Brady, J. G. Montalvo Jr., G. Glowacki and A. Pisciotta, Anal. Chim. Acta, 70 (1974) 448.

DETERMINATION OF CADMIUM, COBALT, COPPER, NICKEL AND LEAD IN SOIL EXTRACTS BY DITHIZONE EXTRACTION AND ATOMIC ABSORPTION SPECTROMETRY WITH ELECTROTHERMAL ATOMIZATION

K. L. IU, I. D. PULFORD and H. J. DUNCAN*

Department of Agricultural Chemistry, University of Glasgow, Glasgow G12 8QQ (Gt. Britain)

(Received 18th September 1978)

SUMMARY

Interferences in the analysis of acetic acid, pyrosphosphate and acid oxalate extracts of soils for cadmium, cobalt, copper, nickel and lead can be overcome by extraction with dithizone in chloroform. Treatment of the extract with hydroxylammonium chloride to reduce iron(III) to iron(II) increases the percentage recovery by up to 25%. Complete recovery of the metal—dithizone complexes is ensured by using two extractions from the aqueous phase at pH 8.5 and 9.5. The metals are determined by direct injections of aliquots of the organic solution into the graphite furnace. The detection limits obtained are (in μg cm^{-3} of the extract): Cd, 0.001; Cu, 0.05; Co, 0.004; Ni, 0.02; Pb, 0.02.

A common technique in the study of trace metals in soils involves treatment with extractants specially designed to remove metals associated with a particular fraction in the soil, e.g. adsorbed, chelated, exchangeable, etc. [1—3]. The levels of certain metals extracted are often below the concentrations which can be detected by flame atomic absorption spectrometry, but can be measured by the graphite furnace procedure. In many cases, the matrix effects of the extract, which arise both from the high content of solute in the original extractant and from high levels of elements extracted from soil, lead to substantial interferences during the analysis [4, 5]. In this paper, the effects on trace metal analysis of three common soil extractants are described; two of these extractants contain high levels of dissolved material. The extractants were: (1) aqueous 0.5 M acetic acid, (2) Tamm acid oxalate (24.9 g of ammonium oxalate and 12.6 g of oxalic acid dissolved in 1 dm^3 of deionized water), and (3) aqueous 0.1 M sodium pyrophosphate.

When aliquots of the soil extracts were injected directly into the graphite furnace, multiple peaks were obtained in some cases, especially with pyrophosphate extracts, and have been reported by many workers, e.g. Dudas [6].

Various instrumental and chemical techniques employed to remove the interferences proved unsuccessful. Variation of ashing times, use of deuterium background correction, addition of equal volumes of 10% (v/v) nitric acid to the injected sample, heating of the extract to dryness with a HNO$_3$—H$_2$SO$_4$

acid mixture and redissolution of the residue in hydrochloric acid, all had no effect in removing the multiple peaks. The use of mini-flow, i.e. a reduced argon flow maintained during the atomization step, produced a single peak but with greatly reduced sensitivity.

After this lack of success by other methods, attempts were made to overcome the interferences by using solvent extraction. A similar technique based on chelation by ammonium pyrrolidinedithiocarbamate (APDC) and extraction into methyl isobutyl ketone (MIBK) has been previously used for Co, Ni, Cu, Pb and Zn [7], and such extracts have been used for cadmium with graphite furnace atomization [6]. Chelation by dithizone (diphenylthiocarbazone) is commonly used in colorimetric techniques and has been used for atomic absorption determinations of cadmium and lead in soils and plant tissue [8—10] and for trace elements in rocks and sediments [11].

The APDC—MIBK method was rejected for two reasons: (a) the metal—APDC complexes became unstable after a few hours, as has also been observed by other workers [6, 12, 13], (b) an emulsion formed at the aqueous—organic interface during extraction into MIBK, especially with pyrophosphate extracts. Neither of these aspects proved to be a problem in dithizone—chloroform extractions.

The major problem encountered in dithizone extractions has been interference from iron [10, 11]. Sandell [14] attributed this to the oxidation of dithizone by iron(III) and recommended the use of hydroxylammonium chloride to remove the interference during the colorimetric determination of metals. The same reagent was recommended by Saltzman [15] to eliminate the formation of water-soluble products which prevented complete extraction. Both the oxalate and pyrophosphate reagents are capable of extracting high levels of iron from soils [16—18].

The method described here attempts to provide maximum recoveries of five metals present in soil extracts by using a combination of techniques previously employed for other types of analysis.

EXPERIMENTAL

Reagents

Where possible analytical-grade reagents were used; deionized water was used for all solutions unless otherwise specified.

Dithizone in chloroform (0.1% and 0.05% w/v). Appropriate amounts of dithizone were dissolved in 500 cm³ of chloroform. This reagent should be stored in a refrigerator in a dark bottle and made up fresh after 3—4 days.

Ammonium citrate. Citric acid (50 g) was dissolved in not more than 30 cm³ of water, and 60 cm³ of ammonia liquor was added. The solution was left until cool and all crystals of citric acid had dissolved, and then made up to 100 cm³ with water.

Hydroxylammonium chloride. Hydroxylammonium chloride (20 g) was dissolved in 30 cm³of ammonia liquor, and then made up to 100 cm³ with water.

Procedure

The sample solution (10 cm³) was pipetted into a 100-cm³ separating funnel, followed by 5 cm³ of ammonium citrate solution and 2 cm³ of hydroxylammonium chloride solution. In the case of acid oxalate extracts, water (10 cm³) was added to prevent the formation of a precipitate. The contents of the separating funnel were well mixed and the pH adjusted to between 9 and 10 with hydrochloric acid (1 + 4) or ammonia solution (1 + 1). Dithizone in chloroform (5 cm³ of 0.1%) was then added; the funnel was shaken and the pressure was released before shaking on a reciprocating shaker for 5 min. When the two phases had separated, the organic phase was collected in a 10-cm³ volumetric flask. The pH of the aqueous phase was then adjusted to between 8 and 9 with hydrochloric acid (1 + 4) and a second extraction was carried out with 5 cm³ of 0.05% (w/v) dithizone in chloroform. The shaking procedure was repeated as before and the organic phase added to the 10-cm³ volumetric flask. If necessary, the flask was filled to the mark with chloroform. This organic phase is suitable for injecting directly into the graphite furnace.

Interferences

The effect of increasing iron concentrations (0, 100, 200 and 500 μg cm^{-3}) and the effectiveness of the hydroxylammonium chloride treatment were tested for standard 0.2 μg cm^{-3} solutions of each trace metal studied, made up in each of the three extractants. The percentage recoveries of the metals were tested in actual samples by adding 2 μg of the metal ion to aliquots of each of the soil extracts containing known quantities of each trace metal, determined by the above method.

Instrumentation

All analyses were done with a Perkin-Elmer 306 spectrophotometer and a HGA-74 graphite furnace.

To optimize the reproducibility, the sample was injected into the furnace by holding the syringe in the vertical position. The standard error of the mean based on six replicate injections of the sample adopting this method was less than ± 1.5%.

RESULTS AND DISCUSSION

Table 1 shows the influence of increasing concentrations of·iron on the analysis of standard 0.2 μg cm^{-3} solutions of the five metals studied, made up in the three extracting agents, and the increased recoveries obtained in certain cases by inclusion of treatment with hydroxylammonium chloride.

Acetic acid extracts

Without the hydroxylamine treatment, recoveries of cobalt and lead were low. It was during analyses for these two metals in the acetic acid soil extracts before treatment with dithizone in chloroform that multiple peaks were

TABLE 1

Effect of the hydroxylammonium chloride treatment on the percentage recovery of added metal ($0.2\ \mu g\ cm^{-3}$) in the three soil extractants with differing iron contents added.
(The numbers in parentheses are the standard deviations based on 3 analyses)

Fe content of solution ($\mu g\ cm^{-3}$)	Cd		Co		Cu		Ni		Pb	
	A[a]	B[b]	A	B	A	B	A	B	A	B
Acetic acid										
0	100(1.8)	100(3.2)	100(4.8)	100(4.4)	100(4.3)	100(3.2)	100(2.2)	100(2.3)	100(1.1)	100(1.0)
100	100(1.6)	100(2.0)	80(3.4)	98(7.5)	98(4.0)	103(7.8)	100(3.9)	100(1.4)	95(6.6)	100(1.5)
200	102(2.1)	100(4.3)	83(6.3)	98(5.2)	103(6.6)	105(5.6)	100(2.0)	98(4.2)	80(4.3)	100(3.0)
500	100(2.4)	102(3.7)	93(14)	100(4.3)	103(11)	103(3.7)	100(1.5)	100(7.9)	75(4.4)	97(4.5)
Oxalate										
0	100(1.0)	100(3.4)	100(4.3)	100(4.9)	100(2.4)	100(1.5)	100(7.5)	100(1.1)	100(5.9)	100(1.4)
100	107(1.9)	100(4.1)	119(7.6)	100(7.1)	105(4.0)	100(1.9)	110(1.7)	95(2.8)	105(7.6)	103(3.7)
200	105(5.4)	103(4.9)	113(4.6)	108(5.5)	105(4.5)	95(5.2)	105(4.4)	103(4.7)	120(4.5)	100(4.9)
500	97(2.8)	103(2.2)	100(4.3)	108(6.5)	110(5.5)	95(8.7)	98(4.7)	108(6.6)	150(3.9)	100(5.3)
Pyrophosphate										
0	100(3.2)	100(3.9)	100(4.6)	100(3.3)	100(6.0)	100(5.7)	100(1.9)	100(4.3)	100(5.7)	100(3.3)
100	100(2.1)	100(8.0)	100(1.6)	102(7.1)	80(4.8)	100(8.8)	100(6.3)	100(2.4)	90(5.6)	98(2.1)
200	100(2.8)	100(3.2)	103(0.4)	100(9.5)	75(4.7)	100(2.6)	100(6.8)	100(5.6)	90(4.8)	93(4.7)
500	100(1.7)	100(2.9)	95(5.1)	105(2.0)	83(3.9)	100(13)	100(3.4)	100(6.8)	93(7.6)	93(6.2)

[a] A: Without hydroxylammonium chloride [b] B: With hydroxylammonium chloride.

normally produced. Treatment of the acetic acid extracts by the full procedure gave recoveries of Cd, Co, Cu, Ni and Pb in the range 97—103% in solutions containing up to 500 μg Fe cm^{-3} (Table 1).

Acid oxalate extracts

Extraction of acid oxalate solutions by dithizone—chloroform resulted in single peaks. Inclusion of a hydroxylamine treatment did not have such an obvious effect as in the acetic acid extracts, but did, in general, result in an improvement in recovery. This diminished effect may be due to the combination of complex formation and reduction of iron by oxalate. The signal for lead was enhanced when more than 100 μg Fe cm^{-3} was present and no hydroxylamine treatment was included.

Pyrophosphate extracts

The multiple peaks produced during the analyses for all the metals studied in pyrophosphate extracts were removed by the extraction with dithizone in chloroform. Inclusion of a hydroxylamine treatment resulted in a substantial increase in the percentage recoveries for copper and lead. Overall, the treatment with hydroxylammonium chloride resulted in an improvement in the recoveries (within the ranges 100—105% for Cd, Co, Cu and Ni and 93—100% for Pb).

Table 2 shows the percentage recoveries for each metal after 2 μg had been added to aliquots of soil extracts. The recoveries lay in the range 93—108%.

TABLE 2

Percentage recoveries of 2.00 μg of metal ion added to 10-cm^3 soil extracts

Metal	Metal found in soil extract (μg)	Total recovery (μg)	Recovery (%)
Acetic acid			
Cd	0.04	2.00	98
Co	0.40	2.40	100
Cu	1.25	3.50	108
Ni	0.50	2.45	98
Pb	0.70	2.50	93
Acid oxalate			
Cd	0.04	2.00	98
Co	0.90	3.00	103
Cu	0.50	2.60	104
Ni	0.80	3.00	107
Pb	2.30	4.40	102
Pyrophosphate			
Cd	0.02	2.00	99
Co	0.05	1.95	95
Cu	1.70	3.60	97
Ni	0.50	2.30	92
Pb	0.30	2.25	98

The method has proved suitable for routine analysis of trace metals in soils. The detection limits obtained were: 0.001 μg Cd cm^{-3}, 0.05 μg Cu cm^{-3}, 0.004 μg Co cm^{-3}, 0.02 μg Ni cm^{-3} and 0.02 μg Pb cm^{-3}.

REFERENCES

1 H. H. Le Riche and A. H. Weir, J. Soil Sci., 14 (1963) 225.
2 R. G. McLaren and D. V. Crawford, J. Soil Sci., 24 (1973) 172.
3 J. L. Sims and W. H. Patrick Jr., Soil Sci. Soc. Am. J., 42 (1978) 258.
4 R. B. Cruz and J. C. Van Loon, Anal. Chim. Acta, 72 (1974) 231.
5 J. G. T. Regan and J. Warren, Analyst, 101 (1976) 220.
6 M. J. Dudas, At. Absorpt. Newsl., 13 (1974) 109.
7 T. T. Chao and R. F. Sanzolone, J. Res. U.S. Geol. Surv., 1 (1973) 681.
8 C. H. Williams, D. J. David and O. Iismaa, Commun. Soil Sci., Plant Anal., 3 (1972) 399.
9 A. M. Ure and M. C. Mitchell, Anal. Chim. Acta, 87 (1976) 283.
10 A. M. Ure, M. P. Hernandez-Artiga and M. C. Mitchell, Anal. Chim. Acta, 96 (1978) 37.
11 H. Armannsson, Anal. Chim. Acta, 88 (1977) 89.
12 R. R. Brooks, B. J. Presley and I. R. Kaplan, Talanta, 14 (1967) 809.
13 P. M. Eller and J. C. Haartz, Am. Ind. Hyg. Ass. J., 38 (1977) 116.
14 E. B. Sandell, Colorimetric determination of traces of metals, Interscience, New York, 3rd edn., 1959, p. 169.
15 B. E. Saltzman, Anal. Chem., 25 (1953) 493.
16 C. L. Bascomb, J. Soil Sci., 19 (1968) 251.
17 E. E. Gamble and R. B. Daniels, Soil Sci. Soc. Am. Proc., 36 (1972) 939.
18 M. D. Webber, J. A. McKeague, A. T. Raad, C. R. De Kimpe, C. Wang, P. Haluschak, H. B. Stonehouse, W. W. Pettapiece, V. E. Osborne and A. J. Green, Can. J. Soil Sci., 54 (1974) 293.

DETERMINATION OF NANOGRAM AMOUNTS OF BISMUTH IN ROCKS BY ATOMIC ABSORPTION SPECTROMETRY WITH ELECTROTHERMAL ATOMIZATION

JEAN S. KANE

U.S. Geological Survey, Reston, Virginia 22092 (U.S.A.)

SUMMARY

Bismuth concentrations as low as 10 ng g^{-1} in 100-mg samples of geological materials can be determined by atomic absorption spectrometry with electrothermal atomization. After HF—HClO$_4$ decomposition of the sample, bismuth is extracted as the iodide into methyl isobutyl ketone and is then stripped with ethylenediaminetetraacetic acid into the aqueous phase. Aliquots of this solution are pipetted into the graphite furnace and dried, charred, and atomized in an automated sequence. Atomic absorbance at the Bi 223.1-nm line provides a measure of the amount of bismuth present. Results are presented for 14 U.S. Geological Survey standard rocks.

Studies of the geochemistry of bismuth require an analytical method for the determination of the element in concentrations as low as 10 ng g^{-1}. Neutron-activation methods [1] allow accurate determination at this level but are not amenable to rapid analysis of large numbers of samples. Solvent extraction of the bismuth—iodide complex [2—5] into methyl isobutyl ketone (MIBK) followed by flame atomic absorption [2—4] is effective at the ng g^{-1} level. Extraction with ammonium 1-pyrrolidinedithiocarbamate (APDC) [6—9] has been adapted to graphite furnace atomic absorption determinations of bismuth that have a detection limit of 50 ng g^{-1} in a 200-mg rock sample.

This paper presents a method involving solvent extraction followed by a flameless atomic absorption spectrometric (f.a.a.s.) determination; this method lowers the detection limit to 10 ng g^{-1} for a 100-mg sample. The bismuth is separated from the major and minor elements of the rock matrix and is considerably concentrated by extraction of bismuth iodide into MIBK. The bismuth is further concentrated and the sensitivity in the graphite furnace is increased by back-extraction into aqueous ethylenediaminetetraacetic acid (EDTA). The extraction is similar to that used by Greenland and Campbell [10] in the substoichiometric radio-isotopic dilution method for the determination of bismuth. This method compares favorably with theirs in detection limit and accuracy, and eliminates the need for routine handling of radioactive chemicals.

EXPERIMENTAL

Reagents

Bismuth standards. Dissolve 1.000 g of bismuth metal in 50 ml of (1 + 9) nitric acid by overnight digestion at 100°C and quantitatively transfer to a 100-ml volumetric flask. After cooling, dilute to volume with (1 + 9) HNO_3. Dilute this standard stock solution (10.0 mg Bi ml^{-1}) weekly to 0.100 ppm, 0.050 ppm, and 0.010 ppm.

Potassium iodide solution. Dissolve 1.000 g of reagent-grade potassium iodide and 1.000 g of reagent-grade hydroxylammonium chloride in 1 l of distilled water for a 0.1% (w/v) KI solution.

EDTA solution. Dissolve 37.20 g of disodium ethylenediaminetetraacetate in 1 l of distilled water for a 1×10^{-1} M solution. Dilute to 1×10^{-5} M weekly for use in the extraction procedure.

Apparatus and operating conditions

A Perkin-Elmer 603 atomic absorption spectrometer equipped with a deuterium arc background corrector, a HGA 2100 graphite furnace, and a model 56 recorder was used.

A hollow-cathode bismuth lamp operated at 10 mA was used at a wavelength of 223.1-nm with a spectral band width of 0.2-nm to achieve resolution from the 222.8-nm absorption band. The HGA 2100 variables were: dry at 120°C for 20 s; char at 400°C for 40 s; atomize at 2700°C for 7 s. Argon was used as sheath gas at 3 l min^{-1} flow, with flow interrupted during atomization. The recorder was operated at the 1-mV pen range, i.e., with 10 × scale expansion.

Procedure

Ashing. Samples of high organic content must be ashed to destroy the organic material. Of the standard rocks, ashing is required for SGR-1, Green River Shale; SCo-1, Cody Shale; MAG-1, marine mud. Place a weighed crucible containing a weighed 1.500—2.000-g sample of rock (60—80 mesh sieve) in a cold muffle furnace and raise the temperature to 500°C in 100°C steps over 3—4 h. Ignite for 12—16 h; cool and reweigh the crucible. Calculate the percentage of ash.

Sample decomposition and extraction. Weigh 100 mg of rock or ash into a Teflon beaker. Add 3 ml of 72% perchloric acid and 10 ml of 40% hydrofluoric acid. Prepare a blank and five standards in the 2—50-ng range with the same acid additions. Digest all samples for at least 18 h at 115—120°C, taking the samples to dryness. Dissolve the digestion residue in 2 ml of 72% perchloric acid with a minimum of heating and add 5 ml of water to complete the dissolution. Cool to room temperature and transfer to 60-ml separatory funnels. Add 1 ml of aqueous 1% (w/v) hydroxyammonium chloride to reduce iron(III); then add 5 ml of MIBK. Begin mixing of the phases with an air stream as described by Greenland and Campbell [11]; add 5 ml of the 0.1% potassium iodide solution. Continue mixing the phases for 2—3 min.

Discard the aqueous phase. Wash the MIBK layer with 5 ml of 0.05% (w/v) iodide solution, mix for 1—2 min and again discard the aqueous phase. Strip twice with 1-ml aliquots of 10^{-5} M EDTA, mixing for 2—3 min each time. Collect and combine the two stripping aliquots. Inject 20 μl into the HGA 2100 for the final measurement. Plot peak height vs. ng Bi in standards and determine ppb Bi in rocks from the analytical curve. Using the percentage of ash, correct the ppb Bi in ash to ppb in rock for ashed samples.

Extractions were carried out in groups of 18: 1 blank, 12 rocks, 5 standards. Complete extraction and f.a.a.s. of a group requires 4 h.

RESULTS AND DISCUSSION

Sample decomposition

The sample decomposition procedure used is essentially that of Greenland and Campbell [10]. This decomposition does not completely destroy organic matter from SGR-1, SCo-1, or MAG-1. Ashing to destroy the organic material, coupled with digestion at 115—120°C until samples were dry, gave full dissolution of the sample and 100% extraction of the bismuth into MIBK with iodide.

Extraction

Bismuth iodide can be extracted completely into MIBK. Several extractions followed with radioactive tracer all yielded between 97% and 100% bismuth. Solubility of MIBK in water, volatility of MIBK in the air-bubbler system of phase mixing, and partial extraction of the residual volume of perchloric acid from the digestion step all contribute to a highly variable extraction volume. Additionally, the f.a.a.s. measurement of bismuth that has been extracted from the digestion medium provides a very much lower sensitivity and higher detection limit than that of undigested bismuth standard solutions carried through the same extraction. All of these factors make direct use of the MIBK phase unsuitable.

Perchloric acid, even at 1:10 dilution by the reagents used in the extraction, does extract to some extent into MIBK. At the 100°C digestion temperature recommended by Greenland and Campbell [10], a variable residual volume of 0.2—2.5 ml of perchloric acid remained after digestion periods exceeding 36 h. At the lowest residual volumes, unpredictable bismuth losses ranging from 10% to 50% were sometimes encountered when two wash steps were used as in the Greenland—Campbell procedure [10]. The highest residual volumes decreased the completeness of the EDTA stripping step by as much as 25%. Also, they introduced a volume error, as the EDTA stripping aliquot removes that portion of the extracted perchloric acid not removed by washing.

By digesting to dryness at 115—120°C and picking the residue up in 2 ml of perchloric acid and 5 ml of water, a constant volume is assured. One stripping aliquot, however, does not give a constant enough yield, the variation being from 60% to 80%. Combining two 1-ml stripping aliquots gives a constant 85—90% yield.

TABLE 1

Bismuth content (ng g⁻¹) of 14 USGS Standard Rocks[a]

Rock	Split	This work Bismuth (ppb)				Mean (ppb)	S.d. (ppb)	R.s.d. (%)	F Ratio	Other investigators Greenland and Campbell [10] (Mean ppb Bi ± s.d.)	Laul et al. [1]
AGV-1	2/13	35	80	54	58	51.9	17	32	0.407 (0.95)	55.5 ± 5.0	56
	14/18	55	35	55	45						
	111/14	47	45	72	25						
	52/21	50	55	40	80						
BCR-1	80/7	45	20	30	40	44.1	12	27	2.398 (0.95)	49.6 ± 4.9	47
	19/29	65	60	50	48						
	67/32	45	37	40	45						
	46/18	70	25	40	45						
BHVO-1	12/8	15	(5)	10	15	13.9	6	46	1.480 (0.95)	18.8 ± 2.7	
	4/1	25	10	(5)	(5)						
	31/5	15	15	10	15						
	50/14	23	20	25	10						
DTS-1	4/27	(5)	(5)	(5)	(5)	< 10	—	—	—	5.1 ± 3.4	4.8
	40/16	10	(5)	(5)	20						
	39/13	(5)	10	(5)	(5)						
	4/4	15	(5)	(5)	(5)						
G-2	56/4	25	35	20	40	32.6[b]	11	32	0.489 (0.95)	41.0 ± 4.9	38
	75/8	55	40	37	20						
	16/23	30	34	45	20						
	116/7	41	30	25	25						
GSP-1	39/20	30	25	25	30	31.7	7		5.838 (0.99)	36.7 ± 4.3	
	65/11	30	20	15	25						
	38/23	32	45	50	38						
	55/5	45	40	32	25						

Sample									F ratio		
MAG-1	**26/6**	**305**	**405**	**365**	**310**	**331**	**35**		1.168 (0.95)	384 ± 16	
	38/3	350	280	310	280						
	31/5	350	305	330	340						
	12/27	300	365	375	335						
PCC-1	39/26	(5)	(5)	30	(5)	<10	—	—	—	5.7 ± 3.2	8
	36/8	(5)	(5)	(5)	(5)						
	39/16	(5)	(5)	(5)	(5)						
	25/27	10	20	(5)	(5)						
QLO-1	9/24	48	80	70	50	63.3	14	22	0.076 (0.95)	66.3 ± 4.4	
	2/20	48	62	90	60						
	39/15	65	70	80	45						
	17/23	70	60	55	60						
RGM-1	13/7	260	295	240	275	279	31	11	0.504 (0.95)	283 ± 19.7	
	55/4	265	340	270	300						
	48/31	270	320	250	270						
	54/15	270	245	325	265						
SCo-1	55/23	470	420	370	360	389	49	13	1.849 (0.95)		
	26/3	340	420	415	320						
	68/3	325	370	340	370						
	40/15	480	425	340	460						
SDC-1	119/4	340	300	255	285	278	52	19	0.566 (0.95)	276 ± 12.5	
	97/12	325	215	200	335						
	61/24	300	340	295	235						
	76/15	300	205	300	210						
SGR-1	25/23	910	1070	945	960	1030	95	9	0.911 (0.95)		
	4/12	985	960	1050	1150						
	33/19	1020	1060	950	1150						
	28/3	1070	930	1250	1070						
STM-1	45/30	140	155	75	75	110	29	26	1.280 (0.95)	250 ± 62	
	21/27	110	130	150	115						
	21/26	82	80	80	110						
	41/10	140	150	82	100						

[a] S.d. indicates the within-bottle standard deviation; r.s.d. the relative standard deviation. For the F ratio, the bracketed numbers indicate the significance level. [b] A value of 51 ± 8.5 ppb has also been reported [9].

Generally, procedural blanks contained 2—3 ng Bi which is identical to the 2—3 ng Bi in the reagent blank reported by Greenland and Campbell [10]. Blanks containing more bismuth (5—7 ng) were obtained with some packages of graphite tubes; the major portion of the bismuth is attributable to the tube. No amount of prefiring appears to remove this bismuth. Determination of, and correction for, blanks are therefore essential.

Bismuth content of USGS standard rocks

Fourteen U.S. Geological Survey (USGS) standard rocks were analyzed in random sequence. Four 100-mg samples from each split (bottle) were used as follows: 4 splits each of AGV-1 (andesite), BCR-1 (basalt), BHVO-1 (basalt), DTS-1 (dunite), G-2 (granite), GSP-1 (granodiorite), MAG-1 (marine mud), PCC-1 (peridotite), QLO-1 (quartz latite), RGM-1 (rhyolite), SCo-1 (shale), SDC-1 (mica schist), SGR-1 (shale), and STM-1 (nepheline syenite) for a total of 224 determinations. Table 1 gives data for each of the 224 extractions; grand means for each rock; F ratios; and analytical error, the square root of the mean sum of squares variance within bottles. Also shown are the results of other investigators for these rocks.

Except for DTS-1 and PCC-1, the means in the Table are given to three significant figures; however, the analytical error indicates two significant figures, and the user may wish to round the means.

For DTS-1 and PCC-1, essentially all individual extraction values are at the detection limit of 5—10 ng Bi g^{-1} in 100-mg samples, and the means are reported as <10 ng g^{-1}, without statistical treatment. This agrees well with the results of Greenland and Campbell [10] and Laul et al. [1]. Analytical error at the detection limit is expected to be ± 100%.

Bismuth contents of SCo-1, and SGR-1 are reported only in this paper. All remaining USGS standard rocks have been investigated for bismuth by Greenland and Campbell [10]. With the exception of STM-1, excellent agreement of mean ppb Bi exists between this work and theirs. Of the standard rocks reported here, only G-2 has also been reported for the APDC extraction—graphite furnace method [9]. On the basis of that one comparison, this method gives similar accuracy for low bismuth levels.

Experimental deviations of 10—12% for MAG-1, RGM-1, SCo-1, and SGR-1 are close to those reported for the substoichiometric isotopic dilution method [10]. Deviations for SDC-1 and STM-1 are higher; these rocks should not be used as standards for bismuth determinations by this method. With the exception of these two rocks, precision for bismuth determinations above 150 ppb by the proposed method is better than the 15—25% error reported for bismuth in most rocks determined by the APDC extraction [9].

The experimental deviations reported here for AGV-1, BCR-1, BHVO-1, G-2, GSP-1, and QLO-1 range from 6 to 17 ng g^{-1} absolute and from 20 to 55% relative. All of these rocks have bismuth levels only slightly above the detection limit, which accounts for the large error. If high accuracy is needed in this range, replicate analyses and/or an increase in sample size to 250—500 mg becomes necessary.

One-way analysis of variance applied to the data demonstrated that bismuth contents were homogeneous among bottles. Except for GSP-1, the mean sum of squares for bottles was not significantly greater than the within-bottle variation of the 95% confidence level. The variation for GSP-1 was not significant at the 99% confidence level.

REFERENCES

1 J. C. Laul, D. R. Case, F. Schmidt-Bleek and M. E. Lipschutz, Geochim. Cosmochim. Acta, 34 (1970) 89.
2 C. L. Luke, Anal. Chim. Acta, 39 (1967) 447.
3 J. B. Headridge and J. Richardson, Analyst, 95 (1970) 930.
4 J. G. Viets, Anal. Chem., 50 (1978) 1097.
5 R. C. Rooney, Analyst, 90 (1965) 545.
6 H. K. Y. Lau, H. A. Droll and P. F. Lott, Anal. Chim. Acta, 56 (1971) 7.
7 M. E. Hofton and D. P. Hubbard, Anal. Chim. Acta, 62 (1972) 311.
8 K. E. Burke, Analyst, 97 (1972) 19.
9 W. H. Ficklin and F. N. Ward, U.S. Geol. Surv. J. Res., 4 (1976) 217.
10 L. Paul Greenland and E. Y. Campbell, Anal. Chim. Acta, 60 (1972) 159.
11 L. Paul Greenland and E. Y. Campbell, Anal. Chim. Acta, 67 (1973) 29.

SUBSTOICHIOMETRIC PRECONCENTRATION IN RADIOANALYTICAL METHODS

V. I. SHAMAEV

Mendeleev Institute of Chemical Technology, 9 Miusskaja Square, Moscow A-47 (U.S.S.R.)

(Received 27th February 1978)

SUMMARY

   The application of substoichiometric (with respect to interfering elements) separation as a method of preliminary concentration is suggested in order to decrease the contents of interfering elements to permissible levels in the methods of determination. The equations for the calculations of enrichment factors and isolated fractions of test elements are derived and the corresponding dependences are plotted. The combination of substoichiometric concentration with some new radioanalytical methods allows comparatively simple determinations of micro amounts of one element to be made in the presence of macro amounts of other elements with similar chemical properties.

   The application of analytical reagents in substoichiometric quantities sharply increases the selectivity of determinations in isotope dilution [1, 2] and radiometric correction [3] methods. For example, direct determinations of hafnium by substoichiometric precipitation with phosphate ions are possible if the concentration of zirconium is 60—70% that of hafnium, and determinations of cesium by substoichiometric extraction with sodium tetraphenylborate (TPB) into nitrobenzene are possible in the presence of equimolar quantities of potassium, etc.

   In some new radioanalytical methods [4—6], the upper limit of the permissible quantities of interfering elements is 50—200 times higher than in the substoichiometric variants of isotope dilution and radiometric correction methods. Further improvements in selectivity can be reached by combining these methods with preliminary substoichiometric concentration.

THEORETICAL

   Substoichiometric concentration means the preliminary isolation of a fraction of the test element to be determined with a quantity of reagent that is substoichiometric with respect to the sum of the test element and an interfering element: $h_0 = m_R/nm_0$ where $m_0 = m_M + m_B$; m_M is the molar quantity of the test element (labelled with its radioisotope); m_B is the molar quantity of interfering element; m_R is the molar quantity of reagent; and n is the stoichiometric ratio, i.e. the number of moles of reagent interacting with one mole of the labelled element.

The losses of the labelled element in this operation are taken into account by means of the radiometric correction equation [7]:

$$m_M = (m_M)_{is}/(1 - \alpha) \tag{1}$$

where $(m_M)_{is}$ is the quantity of the isolated fraction of the labelled element. $\alpha = A_{nis}/A_{in}$, and $(1 - \alpha) = A_{is}/A_{in}$; here A_{in}, A_{is} and A_{nis} are the initial (total) radioactivity of the labelled element and the radioactivities of its isolated and non-isolated fraction, respectively.

The preliminary substoichiometric concentration can be applied not only in radioanalytical methods, but in any method of analysis.

The value of α can be calculated theoretically in accordance with the equation derived previously [4]:

$$\alpha = d + [d^2 + 4m_M \cdot (m_0 - m_R/n) \cdot (\beta - 1)]^{\frac{1}{2}}/2 \cdot m_M \cdot (\beta - 1) \tag{2}$$

where $d = (\beta - 1)(m_M - m_R/n) - m_0$, and β is the exchange constant, i.e. the ratio of the equlibrium constants for both elements in the process applied.

When $m_B \gg m_M$, eqn. (2) simplifies to

$$\lim \alpha_{(m_M \to 0)} = \alpha_0 = \lambda - 1/[\lambda + (\beta - 1)] \tag{3}$$

where $\lambda = 1/h_0 = nm_0/m_R$. Correspondingly the degree of isolation of a micro amount of a labelled element is $(1 - \alpha_0) = \beta/[\lambda + (\beta - 1)]$.

If Y_0 is used to denote the initial molar ratio of unlabelled and labelled element, then $Y_0 = m_B/m_M$ or, if $m_B \gg m_M$, $Y_0 = m_0/m_M$. The ratio of the quantities of these elements in the isolated fraction is denoted by $Y' = (m_B/m_M)_{is}$. When $m_B \gg m_M$, then

$$Y' = m_R/nm_M (1 - \alpha_0) \tag{4}$$

Substitution in eqn. (4) of the value of α_0 from eqn. (3) gives, after some manipulation,

$$Y' = [1/\beta m_M][m_0 - (m_R/n)(1 - \beta)] \tag{5}$$

The enrichment factor for a single-stage substoichiometric isolation is then

$$X = Y_0/Y' = (1 - \alpha_0)/h_0 = \beta/[1 + h_0 (\beta - 1)] \tag{6}$$

In accordance with eqns. (3) and (6), the enrichment factors and the values of the isolated fractions of a labelled element can be calculated for the different values of β and the different quantities of reagent used (for the cases $m_B \gg m_M$). The results have been shown in Fig. 5 of a previous paper [6]. Figure 1 of the present paper shows theoretically calculated values of $(1 - \alpha)$ and enrichment factors for different relative amounts of a labelled element for $\beta = 10$. It can be seen that when Y_0 decreases the isolated fraction of a labelled element also decreases whereas the enrichment factor increases. For small values of β, these changes are relatively small but are more essential for bigger values of β. The data represented in Fig. 5 of ref. 6 can be used to calculate X and $(1 - \alpha)$ values at intervals from $Y_0 = \infty$ to $Y_0 = 10$ to 20.
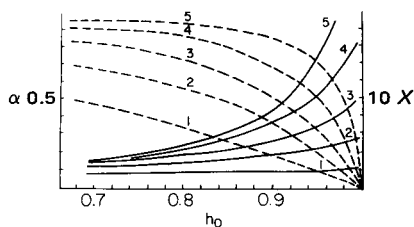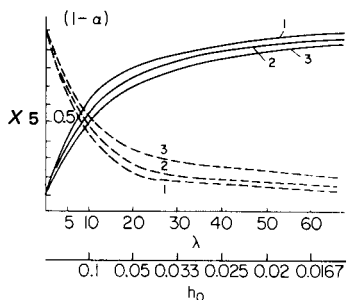
Fig. 1. The dependences of the enrichment factor (unbroken lines) and isolated fractions of a labelled element (dotted lines) on the substoichiometric fraction of a reagent and on Y_0 (for $\beta = 10$). Curve (1) $Y_0 = 10$; (2) $Y_0 = 20$; (3) $Y_0 = 100$.
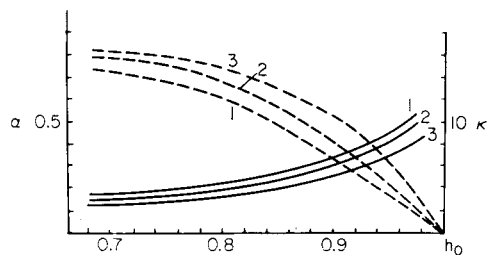
Fig. 2. The dependences of enrichment factors (unbroken lines) and isolated fractions of a labelled element (dotted lines) on the substoichiometric fraction of a reagent for $\beta < 1$ and $m_B \gg m_M$. Curve (1) $\beta = 0.5$; (2) $\beta = 0.2$; (3) $\beta = 0.1$; (4) $\beta = 0.05$; (5) $\beta = 0.02$.

For multistage substoichiometric concentrations, the total enrichment factor is equal to the product of the enrichment factors for each stage of concentration: $X_{total} = X_1 \cdot X_2 \cdot X_3 \ldots X_i$. The theoretical calculations and the experimental results show that the replacement (at each stage of concentration) of a single process of isolation by several successive isolations (each with smaller amounts of reagent) does not lead to any essential improvement in the enrichment factor or isolated fraction of a test element.

The method of substoichiometric concentration is quicker and more effective than ion-exchange chromatograpy and even can be compared favourably with extraction chromatography for the separation of micro amounts of one element from macro amounts of other elements with similar chemical properties. The method also has the advantage that the value of m_0 in the resultant solution can be found from the amount of reagent used in the last stage of the substoichiometric concentration. This value must be known for the determination of the labelled element by most selective radioanalytical methods [4—6].

EXPERIMENTAL CONFIRMATION

Preconcentration of cesium

Equations (3) and (6) and the theoretically calculated relationships represented in Fig. 5 of ref. 6 were verified experimentally for the preconcentration of cesium in the presence of rubidium and potassium ions by substoichiometry extraction with sodium tetraphenylborate (TPB) into nitrobenzene. Known amounts of potassium (rubidium) and cesium (labelled by ^{137}Cs) were extracted with known quantities of TPB. After radiometric determination of the interphase distribution of cesium, the alkali metals were re-extracted into 1 M

hydrochloric acid. The excess of acid was removed by evaporation and the next stage of cesium concentration was carried out with corresponding quantities of TPB. If necessary, before the second or the third stage of concentration, the solution was additionally labelled by carrier-free ^{137}Cs.

The enrichment factor was calculated as follows. First, the amount of cesium extracted into the organic phase was calculated from the initial quantity of cesium taken and the interphase distribution of radioactivity found:

$$(m_{Cs})_{org} = (m_{Cs})_{in} \cdot (1 - \alpha) = (m_{Cs})_{in} \cdot A_{org}/A_{in}$$

Secondly, the amount of rubidium (or potassium) in the organic phase was calculated from the quantity of reagent used minus the quantity of reagent consumed in the extraction of cesium: $(m_{Rb, K})_{org} = m_{TPB} - (m_{Cs})_{org}$. From these data the new ratio of the two elements in the organic phase (Y') and the enrichment factor ($X = Y_0/Y'$) can be calculated.

The experimental and theoretical data for the system Cs—Rb—TPB—nitrobenzene (Table 1) show good agreement for the values of X and $(1 - \alpha)$. Table 1 also shows that after a three-stage extraction with substoichiometric quantities of TPB, the relative quantity of rubidium has decreased by more than 40-fold. In the resultant solution, the amount of rubidium is only 10-fold greater than the amount of cesium; at such a ratio, direct determinations of cesium are possible by extracting with different quantities of TPB into nitrobenzene [5].

The experimental and theoretical data for the substoichiometric concentration of cesium in presence of potassium by TPB extraction into nitrobenzene also agree well (Table 2). As it is possible to determine cesium in a 50-fold excess of potassium by extraction with different quantities of TPB [5], Table 2 shows that a single-stage concentration is enough for a 500-fold amount of potassium; a two-stage concentration suffices even for a 5000-fold amount.

Systems with $\beta < 1$

Substoichiometric concentration can also be carried out for systems in which an interfering element forms more stable compounds with the reagent

TABLE 1

Preconcentration of cesium in presence of rubidium by substoichiometric extraction

	m_{TPB} (mmol)	h_0 (%)	$(1-\alpha)$ exp.	$(1-\alpha)$ theor.	$Y' = \left(\frac{m_{Rb}}{m_{Cs}}\right)_{is}$	X exp.	X theor.
For $m_{Cs} = 6 \times 10^{-4}$ mmol; $m_{Rb} = 10^{-1}$ mmol; $Y_0 = 166$; $\beta = 5$							
1st extn.	1.47×10^{-2}	15	0.41	0.46	60.2	2.76	3.12
2nd extn.	2.23×10^{-3}	15	0.48	0.45	18.9	3.18	3.12
For $m_{Cs} = 1.2 \times 10^{-3}$ mmol; $m_{Rb} = 5 \times 10^{-1}$ mmol; $Y_0 = 417$; $\beta = 5$							
1st extn.	2.02×10^{-2}	4	0.18	0.173	93.5	4.46	4.32
2nd extn.	9.97×10^{-4}	5	0.17	0.205	27.2	3.44	4.20
3rd extn.	1.99×10^{-4}	20	0.56	0.555	10.0	2.72	2.78

TABLE 2

Preconcentration of cesium in presence of potassium by substoichiometric extraction

m_{TPB} (mmol)	h_0 (%)	$(1-\alpha)$ exp.	$(1-\alpha)$ theor.	$Y' = \left(\dfrac{m_K}{m_{Cs}}\right)_{is}$	X exp.	X theor.
For $m_{Cs} = 8.9 \times 10^{-4}$ mmol; $m_K = 2.82 \times 10^{-2}$ mmol; $Y_0 = 30$; $\beta = 25$						
1st extn. 1.47×10^{-3}	5.4	0.50	0.505	2.31	12.9	13.0
For $m_{Cs} = 6.7 \times 10^{-4}$ mmol; $m_K = 2.68 \times 10^{-2}$ mmol; $Y_0 = 40$; $\beta = 25$						
1st extn. 1.47×10^{-3}	5.3	0.51	0.51	3.31	12.2	12.2
For $m_{Cs} = 5.4 \times 10^{-3}$ mmol; $m_K = 2.68 \times 10^{-1}$ mmol; $Y_0 = 50$; $\beta = 25$						
1st extn. 1.47×10^{-3}	5.3	0.54	0.53	4.05	12.2	12.0
For $m_{Cs} = 1.31 \times 10^{-3}$ mmol; $m_K = 5.24 \times 10^{-1}$ mmol; $Y_0 = 400$; $\beta = 25$						
1st extn. 2.63×10^{-2}	5.0	0.62	0.57	32.4	12.3	11.4
2nd extn. 1.31×10^{-3}	5.0	0.43	0.51	1.98	16.2	12.9
For $m_{Cs} = 3.66 \times 10^{-4}$ mmol; $m_K = 1.44$ mmol; $Y_0 = 3935$; $\beta = 25$						
1st extn. 7.24×10^{-2}	5.0	0.58	0.57	341.0	11.5	11.4
2nd extn. 3.62×10^{-3}	5.0	0.46	0.57	37.1	9.2	11.4
3rd extn. 1.81×10^{-4}	5.0	0.54	0.51	2.43	15.2	12.5

used than does the element to be determined, i.e. for systems, with $\beta < 1$, where the preconcentration of the labelled element occurs in its non-isolated fraction.

The limiting value (at $m_M \rightarrow 0$) of the non-isolated fraction of a labelled element is calculated similarly to the previous case, according to eqn. (3). The new ratio of the two elements in the non-isolated fraction:

$$Y' = (m_B/m_M)_{nis} = (m_B - m_R/n)/m_M \cdot \alpha_0 = (1/\alpha_0) \cdot (Y_0 - m_R/nm_M) \qquad (7)$$

Substituting the value of α_0 from eqn. (3) gives

$$X = \lambda/[\lambda + (\beta - 1)] \qquad (8)$$

Figure 2 gives the results of calculations of enrichment factors and fractions of a labelled element in the resultant solutions (i.e. non-isolated fractions of a labelled element) as a function of the relative quantities of reagent used. The effective preconcentration of a labelled element can be realized only if the substoichiometric fraction of a reagent is high enough. The region of optimum values of h_0 shifts in the direction of bigger values with decrease in the exchange constant: for $\beta = 0.2$, $(h_0)_{opt} \cong 0.8-0.9$; for $\beta = 0.02$, $(h_0)_{opt} \cong 0.94-0.98$.

The curves of Fig. 2 were plotted on the assumption that the substoichiometric quantity of the reagent had reacted completely. For systems with $\beta < 1$, where the optimum relative quantities of a reagent are close to its stoichiometric quantities, the possibility of deviation of the values of α_0 and X from their calculated values must be considered [8]. The value of α_0 increases and the optimum value of h_0 also increases. If the deviations are big enough, the utilization of a superstoichiometric quantity of reagent can be recommended ($h_0 > 1$).

The shortcoming of systems with $\beta < 1$ is the fact that the determination of m_0-values in the resulting solution demands (unlike the previous case) a knowledge of the value of β. However, from the experimentally found value of α, Fig. 2 can be used to determine the value of h_0, from which the m_0-value in the resultant solution can be calculated from the equation.

$$m_0 = (m_R/n)(1/h_0 - 1) \tag{9}$$

Another shortcoming of systems with $\beta < 1$ is the difficulty of determining the optimum substoichiometric quantity of the reagent.

For systems with $\beta > 1$, the good effects of concentration are achieved with large increases of reagent (differing by more than one order of magnitude), but for systems with $\beta < 1$ the limiting optimum quantities of the reagent differ from each other only by about 20—30%. To choose the optimum value of h_0 in such a case, preliminary isolation from an aliquot of a labelled solution with an arbitrary amount of reagent is recommended. After that, use of Fig. 2 and the experimentally found value of α (for the given exchange constant) gives the value of h_0, and the value of m_0 can be calculated from eqn. (9). It is then easy to choose the optimum quantity of reagent.

Figure 3 shows the dependence of the non-isolated fraction of a labelled element and the enrichment factor on values of h_0 for different relative amounts of interfering ions (for $\beta = 0.1$). Calculations show that the enrichment factor increases with increase in the relative amount of a labelled element, but this increase is relatively small.

Substoichiometric concentration from multicomponent systems

The preliminary substoichiometric concentration allows comparatively simple analyses of many complicated systems to be made by radioanalytical methods. If a solution contains several ions capable of reaction with the reagent used, then the ions forming the most stable compounds react preferentially and those ions forming less stable compounds do not react.

If the substoichiometric fraction of a reagent is low enough, two- or three-stage concentration reduces a multicomponent system to a two-component system comprising the test element and the element with the closest chemical

Fig. 3. The dependence of enrichment factors (unbroken lines) and isolated fractions of a labelled element (dotted lines) on the substoichiometric fraction of a reagent for $\beta = 0.1$. Curve (1) $Y_0 = 4$; (2) $Y_0 = 9$; (3) $Y_0 = \infty$.

properties. Such two-component systems can be easily analysed by special radioanalytical methods [4—6].

Theoretical calculations of the fractions of each component isolated at each stage of the process are complicated mathematically. By means of Fig. 5 of the earlier paper [6], Figs. 1—3 of the present paper, and the corresponding theoretical calibration curves [4], it is possible to carry out approximate calculations.

Consider the following example: the analyzed solution contains 1000 μmol of element A, 100 μmol of element B and 1 μmol of element M (test element). The exchange constants are $\beta_{A/B} = 5$, $\beta_{M/B} = 10$ and $\beta_{M/A} = 50$. For the first stage of substoichiometric concentration, if the quantity of reagent is m_R/n = 50 μmol ($h_0 = 0.05$), the resultant solution after re-extraction will have the following composition: element A, 33.3 μmol; element B, 16 μmol; element M, 0.67 μmol. For the second stage of concentration, if $m_R/n = 2.5$ μmol, then the solution resulting from re-extraction will have the following composition: element A, 0.32 μmol; element B, 1.76 μmol; element M, 0.42 μmol. Such a small relative amount of element A does not prevent the determination of element M by special radioanalytical methods [4—6].

These considerations were checked experimentally for the preconcentration of cesium from solutions containing large quantities of sodium, potassium and rubidium. The ratios of the alkali metals in the initial solution were Na:K:Rb:Cs = 1380:460:53:1. The solution for analysis was divided into two aliquots, of which one was labelled with ^{137}Cs and the other with [86]Rb. Extraction with a nitrobenzene solution of TPB was carried out from both aliquots under the same conditions and with the same quantity of the reagent. The amounts of rubidium and cesium isolated were calculated from their initial amounts and the interphase distribution of radio-activity by means of eqn. (1). The amount of potassium isolated was calculated from the amount of reagent taken minus the extracted amounts of rubidium and cesium. The interaction of sodium with TPB for such relative quantities of TPB and alkali metals was disregarded ($\beta_{Cs/Na} = 2500$) [9]. The results (Table 3) show that after two successive extractions the complicated system analysed is reduced to a two-component

TABLE 3

Preconcentration of cesium in mixtures of alkali metals. The compositions of the resulting solutions after each stage of substoichiometric concentration are given.

Element	Composition of initial mixture (μmol)	After 1st extn. (μmol) ($h_0 = 5\%$)	After 2nd extn. (μmol) ($h_0 = 4\%$)	After 3rd extn. (μmol) ($h_0 = 20\%$)
Na	4350	0	0	0
K	1140	35.4	0.28	0
Rb	165	41.2	2.6	0.538
Cs	3.14	2.0	0.386	0.254

system. The residual amount of potassium does not interfere in the determination of cesium, and the relative amount of rubidium is much lower than the upper limit permissible for the determinaton of cesium by the method of isolation with different quantities of a reagent [5].

REFERENCES

1 J. Růžička and J. Stary, Talanta, 8 (1961) 288.
2 J. Růžička and J. Stary, Substoichiometry in Radiochemical Analysis, Pergamon Press, Oxford, 1968.
3 V. I. Shamaev, Zh. Anal. Khim., 22 (1967) 1310.
4 V. I. Shamaev, Zh. Anal. Khim., 27 (1972) 48.
5 V. I. Shamaev, J. P. Korchagin and T. V. Tchudinovskich, Zh. Anal. Khim., 33 (1978) 286.
6 V. I. Shamaev, Anal. Chim. Acta, 104 (1979) 327.
7 V. I. Shamaev, Zh. Anal. Khim., 22 (1967) 988.
8 V. I. Shamaev, Zh. Anal. Khim., 32 (1977) 1293.
9 M. Kyrs, Dissertation, Institute of Nuclear Research, Prague, 1974.

NITRATE ION-SELECTIVE ELECTRODES BASED ON COMPLEXES OF 2,2'-BIPYRIDINE AND RELATED COMPOUNDS AS ION EXCHANGERS

T. L. HWANG and H. S. CHENG*

Institute of Chemistry, Tsing Hua University, Hsinchu (Taiwan)

(Received 11th September 1978)

SUMMARY

Nickel complexes of 2,2'-bipyridine and its dimethyl and diphenyl derivatives as well as biquinoline and dipyridyldisulphide were tested as ion exchangers in liquid membranes for nitrate-selective electrodes. The selectivity of these electrodes for nitrate increased with increasing size of the exchange site. Of the five ion exchangers tested, the 4,4'-diphenyl-2,2'-bipyridine complex showed the best responses; the limit of detection of nitrate was about 10^{-6} M and responses were stable in the pH range 2—8.2.

Various kinds of nitrate-selective electrodes have been studied and some are commercially available [1]. The liquid ion-exchange membranes of these electrodes contain a cationic metal chelate or bulky quaternary ammonium ion dissolved in a suitable organic solvent. The metal chelate type of ion exchanger has been limited to substituted 1,10-phenanthroline chelates of nickel or iron [2—5]. This paper reports the properties of nickel chelates with 2,2'-bipyridine (bipy), which is constitutionally similar to 1,10-phenanthroline, and the related compounds, 4,4'-dimethyl-2,2'-bipyridine (Me₂ bipy), 4,4'-diphenyl-2,2'bipyridine (Ph₂ bipy), 2-2'-dipyridyldisulphide (PS) and 2,2'-biquinoline (biq), dissolved in 2-nitro-*p*-cymene. The relation between their structure and selectivity for common anions is discussed qualitatively.

EXPERIMENTAL

Chemicals
2,2'-Bipyridine (Wako), 4,4'-dimethyl- and 4,4'-diphenyl-2,2'-bipyridine (G. Frederick Smith), and 2,2'-dipyridyldisulphide and 2,2'-biquinoline (Aldrich) were used. All the other chemicals were of reagent grade. 2-Nitro-*p*-cymene (Aldrich) was used without further purification. Deionized water was used throughout.

Preparation of ion-exchange materials
Nitrate salts of the nickel complexes, Ni(bipy)₃(NO₃)₂ · 6H₂O [6],

Ni(Me$_2$bipy)$_3$ (NO$_3$)$_2$ · 5H$_2$O [7], Ni(Ph$_2$bipy)$_3$ (NO$_3$)$_2$ · 5H$_2$O [7], Ni-biq(NO$_3$)$_2$ · 2H$_2$O [8], and Ni—PS(NO$_3$)$_2$ [9] were prepared from nickel nitrate and the appropriate chelating reagent as described in the literature. All these compounds were twice recrystallized. Anhydrous salts were obtained by heating at 80°C in vacuo, and were stored over phosphorus pentoxide. The purity of these salts was checked by chemical analysis for nickel, and was found to be satisfactory.

Electrode assembly

Saturated solutions of the ion exchangers were prepared in 2-nitro-*p*-cymene by warming and stored in air-tight bottles. The ion-exchanger reservoir of an Orion 93-07 nitrate-selective electrode sensing module, which had been thoroughly cleaned with acetone and ether, and dried, was immersed in those saturated solutions for more than 1 h. The electrode was then re-assembled, and when the membrane became wetted with the organic solvent, the electrodes were immersed in 10^{-3} M sodium nitrate solution. Electrodes were ready for use, when steady potentials were reached for about 30 min. In some cases, the internal reference solution used was 0.01 M sodium nitrate— 0.01 M potassium chloride instead of the original Orion reference solution. There was no difference in the electrode potential whichever internal solution was used.

Measurements

The e.m.f. measurements were made with a Radiometer PHM62 pH meter at 25.0 ± 0.1°C. The reference electrode was an Orion 90-02 double-junction type. The position of the electrodes in the sample solutions was kept constant and steady-state potentials were recorded. Duplicate measurements were made in each case.

RESULTS AND DISCUSSION

The responses to nitrate ion activity of the ion-selective electrodes with the five types of liquid ion-exchange membranes are shown in Fig. 1. Two electrodes of each type were tested; the results agreed within experimental error (± 0.5 mV). The slopes of the linear parts of the response curves for most of the electrodes were close to the theoretical value of 59.16 mV per decade change in nitrate activity. Ni(Ph$_2$bipy)$_3$ (NO$_3$)$_2$ and Ni—biq(NO$_3$)$_2$ showed linear response down to 10^{-4} M; for the latter electrode, the curve broke abruptly below this level, whereas the former electrode could detect about 10^{-6} M nitrate. The range of linear response for the other three membranes was much narrower.

When the liquid ion-exchange membranes containing Ni(Ph$_2$bipy)$_3$ (NO$_3$)$_2$, Ni—biq(NO$_3$)$_2$ and Ni(Me$_2$bipy)$_3$(NO$_3$)$_2$ were transferred from one solution to another, e.g. from 10^{-2} to 10^{-3} M nitrate, the response time was very short; normally 20—30 s was needed to reach steady potential values, the
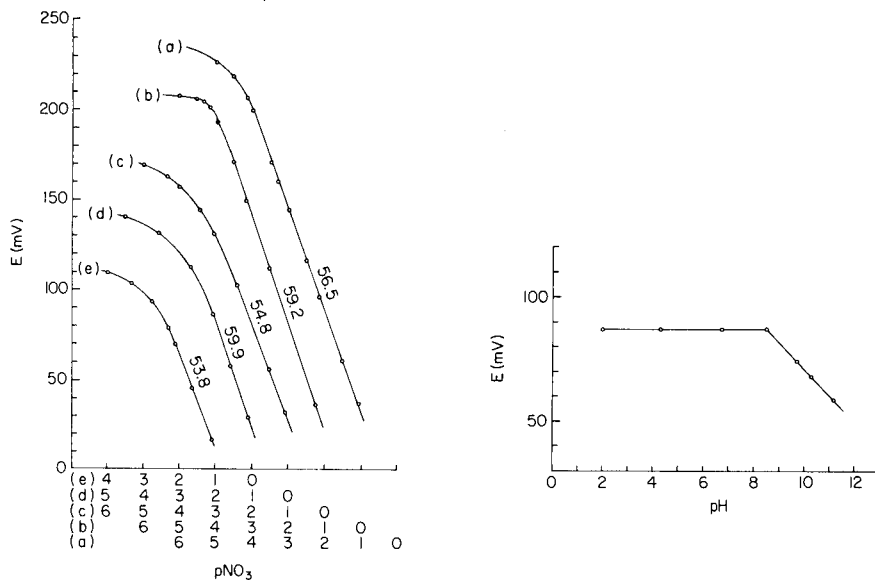
Fig. 1. Response curves for various liquid-membrane electrodes in pure nitrate solutions. The numbers on the curves are the experimentally observed slopes, and the abscissa refers to the activity; for clarity, the pNO_3 values for each electrode are displaced by 1 unit. Ion exchangers: (a) $Ni(Ph_2\ bipy)_3^{2+}$; (b) $Ni-biq^{2+}$; (c) $Ni(Me_2\ bipy)_3^{2+}$; (d) $Ni(bipy)_3^{2+}$; and (e) $Ni-PS^{2+}$.

Fig. 2. Effect of pH on the response of the membrane with the $Ni(Ph_2\ bipy)_3^{2+}$ exchanger.

response time increasing in the order mentioned. Longer response times were observed for the other electrodes: 2 min for $Ni(bipy)_3\ (NO_3)_2$ and 5 min for $Ni-PS(NO_3)_2$.

Selectivity

Selectivity ratios (K_{12}, or $K_{NO_3,\ X}$ where X = Cl^-, Br^-, I^-, NO_2^- and SO_4^{2-}) for nitrate were determined by Method III of Srinivasan and Rechnitz [10]; their computational method was preferred to their graphical method. In the case of bromide and iodide ions, for which the selectivity ratios were large, sodium salts of these ions (0.5 and 10^{-2} M, respectively) were added with constant increment of volume to 10^{-2} and 10^{-3} M sodium nitrate solutions. With chloride, nitrite and sulphate ions, for which selectivity ratios were small, 10^{-1} M sodium nitrate solution was added to the solution containing both nitrate (10^{-2} and 10^{-3} M) and 5—30 times as much interfering ion.

The selectivity ratios at initial nitrate concentrations of 10^{-2} and 10^{-3} M, are summarized in Table 1. Since 10^{-3} M nitrate was beyond the linear Nernstian range for the $Ni(bipy)_3\ (NO_3)_2$ and $Ni-PS(NO_3)_2$ electrodes, their selectivity ratios were determined only at the 10^{-2} M nitrate level. Moreover,

because the selectivity ratio with sulphate was very small for the other three electrodes, only 10^{-3} M nitrate solutions were studied. The precision (relative error) of the average values listed in Table 1 was normally better than 10%. For comparison, the data for the Orion 93—07 electrode determined in this study are also included in Table 1; these are very close to the values given for this electrode [3].

Table 1 shows that the selectivity of these electrodes for anions is in the general sequence $I^- > NO_3^- > Br^- > NO_2^- > Cl^- > SO_4^{2-}$, which is the order generally found for such electrodes. It also shows that, except for iodide, the interference of a given secondary ion increases with decreasing size of the exchange site. For 1:3 NiL (L=ligand) complexes, the nitrate selectivity decreases in the order of decreasing size of the site, i.e., $Ni(Ph_2 bipy)_3^{2+} > Ni(Me_2 bipy)_3^{2+} > Ni(bipy)_3^{2+}$, and for the 1:1 complexes $Ni-biq^{2+} > Ni-PS^{2+}$. These trends can be elucidated qualitatively as follows.

According to the theory of Sandblom et al. [11], the selectivity ratio, K_{12}, of a liquid membrane of complete dissociation type is given by $K_{12} = u_2 k_2 / u_1 k_1$. When the membrane is of strong association type, the experimentally observed selectivity ratio, T_{12}, can be regarded to a good approximation as the weighted average of the two selectivity ratios, P_{12} and Q_{12} [11—14]:

$$T_{12} \simeq (1-\tau) P_{12} + \tau Q_{12}$$

where $P_{12} = (u_2 + u_s)k_2 / (u_1 + u_s)k_1$, $Q_{12} = u_{2s} k_2 K_{1s}/u_{1s} k_1 K_{2s}$, and $\tau = u_s(u_{2s}/K_{2s} - u_{1s}/K_{1s})/(u_1 + u_s) u_{2s}/K_{2s} - (u_2 + u_s) u_{1s}/K_{1s}$. In these equations the subscripts $1s$ and $2s$ refer to the ion-site pairs; u represents the mobility in the membrane, k the ionic partition coefficient between water and the solvent

TABLE 1

Selectivity ratios, $K_{NO_3, X}$ for the various liquid membrane electrodes. (A) $Ni(Ph_2bipy)_3$-$(NO_3)_2$; (B) $Ni(Me_2 bipy)_3 (NO_3)_2$; (C) $Ni(bipy)_3 (NO_3)_2$; (D) $Ni-biq(NO_3)_2$; (E) $Ni-PS(NO_3)_2$ in 2-nitro-p-cymene; (F) Orion 93-07

X	$[NO_3^-]$ (M)	A	B	C	D	E	F
SO_4^{2-}	10^{-2}	—	—	0.17	—	0.23	—
	10^{-3}	1.5×10^{-4}	6.0×10^{-3}	—	1.8×10^{-3}	—	1.4×10^{-4}
Cl^-	10^{-2}	3.3×10^{-3}	1.8×10^{-2}	0.22	3.6×10^{-2}	0.24	6.0×10^{-2}
	10^{-3}	2.0×10^{-3}	1.3×10^{-2}	—	2.1×10^{-2}	—	5.2×10^{-2}
NO_2^-	10^{-2}	4.3×10^{-2}	0.25	0.26	0.21	0.92	6.1×10^{-2}
	10^{-3}	6.7×10^{-2}	0.31	—	0.13	—	7.4×10^{-2}
Br^-	10^{-2}	0.11	0.17	0.28	6.1×10^{-2}	0.92	0.11
	10^{-3}	0.11	0.40	—	8.1×10^{-2}	—	0.13
I^-	10^{-2}	15	21	19	17	72	18
	10^{-3}	17	15	—	15	—	15

in the membrane, and K_{1s} and K_{2s} the dissociation constants of the ion pairs.

K_{12} and P_{12} depend only on the properties of the solvent, whereas Q_{12} depends on the solvent and on the site. As the same solvent was used throughout, only the effect of site on Q_{12} needs consideration. For a given interfering ion, the ratio k_2/k_1 can be regarded as constant because the solvent is the same. If it is assumed that $u_{2s} = u_{1s}$, then Q_{12} is chiefly governed by the ratio of K_{1s}/K_{2s}. According to Yamamoto et al. [15], dissociation of the ion pair in an organic solvent increases with increasing size of the pair. Thus, for a given interfering ion, the selectivity for nitrate should decrease in the order of decreasing size of the exchange site, i.e. $Ni(Ph_2bipy)_3^{2+} >$ $Ni(Me_2bipy)_3^{2+} > Ni(bipy)_3^{2+} > Ni—biq^{2+} > Ni—PS^{2+}$. The present results show that the selectivity ratios with $Ni—biq(NO_3)_2$ are quite similar to those obtained with $Ni(Me_2bipy)_3(NO_3)_2$. This may be due to the pseudo-octahedral structure of the former compound [8], leading to screening of the nickel charge by the ligand comparable to that with the octahedral 1:3 complexes.

That the values of $K_{NO_3^-, I^-}$ are almost constant at around 18 for most of the membranes suggests that the mechanism involves complete dissociation because of the large size of the ion-site pair. The value of 72 for the $Ni—PS(NO_3)_2$ membrane cannot be regarded as significant because the 0.01 M nitrate solutions used lie almost at the end of the linear response range and the accuracy must therefore be suspect.

The $Ni(Ph_2bipy)_3(NO_3)_2$ complex in 2-nitro-p-cymene exhibited excellent properties as a liquid membrane, hence the effect of pH on this electrode was further studied. Nitric acid was diluted by water to pH 2.0 and then the pH was increased by adding sodium hydroxide solution. The electrode potential was constant up to pH 8.2 (Fig. 2). The Orion electrode has a tolerable pH range of 2—12 but the range pH 3—10 is normally recommended. To test the durability and reproducibility, three electrodes were constructed; all showed good response for at least 6 months.

REFERENCES

1 J. Koryta, Anal. Chim. Acta, 61 (1972) 329; 91 (1977) 1, and references cited therein.
2 J. W. Ross, Can. Patent 816,843, July 1 (1969).
3 J. W. Ross, Solid-State and Liquid Membrane Ion-Selective Electrode, in R. A. Durst (Ed.) Ion-Selective Electrodes, Nat. Bur. Stand. Spec. Publ., 314 (1969).
4 J. Růžička, C. G. Lamm and J. Chr. Tjell, Anal. Chim. Acta, 62 (1972) 15.
5 R. E. Reinsfelder and F. A. Schultz, Anal. Chim. Acta, 65 (1973) 425.
6 P. Pfeiffer and U. Fr. Tappermann, Z. Anorg. Allgem. Chem., 215 (1933) 273.
7 W. Wichopas and R. S. Drago, J. Am. Chem. Soc., 90 (1968) 6946.
8 G. H. Faye and J. L. Wood, Can. J. Chem., 55 (1967) 2335.
9 M. Keeton and B. P. Lever, Inorg. Chem., 10 (1971) 47.
10 K. Srinivasan and G. A. Rechnitz, Anal. Chem., 41 (1969) 1203.

11 J. Sandblom, G. Eisenman and J. L. Walker, Jr., J. Phys. Chem., 71 (1967) 3862.
12 G. Eisenman, Anal. Chem., 40 (1968) 310.
13 C. Fabiani, P. R. Danesi, G. Scibona and B. Scuppa, J. Phys. Chem., 78 (1974) 2370.
14 G. Fabiani, Anal. Chem., 48 (1976) 865.
15 Y. Yamamoto, E. Sumimura, K. Miyoshi and T. Tominaga, Anal. Chim. Acta, 64 (1973) 225.

THE QUANTITATIVE ELECTROCHEMICAL GENERATION OF BROMINE IN ACETIC ACID

T. J. PASTOR*, V. J. VAJGAND, V. V. ANTONIJEVIĆ and Z. VELIČKOVIĆ

Department of Chemistry, Faculty of Sciences, University of Belgrade (Yugoslavia)

(Received 2nd August 1978)

SUMMARY

The quantitative electrochemical generation of bromine at a platinum electrode in acetic acid is described. Coulometric methods for the determination of hydroquinone and 2-methylhydroquinone are reported. The best results are obtained with 0.7—1.1 M potassium acetate solutions as supporting electrolyte, and biamperometric end-point detection. The effects of water and acetic anhydride on the accuracy of titrations are discussed. Determination of the formal redox potential of the Br_2/Br^- system in a 0.9 M potassium acetate solution in acetic acid showed that bromide is oxidized directly to bromine at a platinum electrode with 100% current efficiency.

Aqueous solutions of bromine are unstable and are rarely used as titrants in quantitative chemical analysis [1, 2]. Many of the difficulties can be overcome by using coulometric titrations with electrochemically generated bromine. Szebellédy and Somogyi [3] in their early work in which they described the basic principles of coulometric titrations, determined thiocyanate, hydrazine and hydroxylamine with bromine. In later studies, bromine has been widely used in coulometric titrations of many inorganic compounds, organic substances and pharmaceutical products in aqueous media [2, 4—10].

Although the higher stability of bromine solutions in acetic acid makes it possible to determine many substances volumetrically in non-aqueous solvents [2, 11—16], coulometric titrations in such solvents have received very little attention. Macero and Janeiro [17] have reported briefly on coulometric titrations with bromine in 90% acetic acid solutions. However, the electrochemical oxidation of halides in non-aqueous solvents has been extensively investigated [18—29], and so it seemed of interest to study the conditions for quantitative generation of halogens. The mechanism of bromide oxidation to bromine at a platinum electrode in acetic acid is simple [26]. The present studies were therefore directed towards establishing suitable conditions for the generation of bromine with 100% current efficiency, and then coulometric redox titration methods for the determination of small amounts of substances in acetic acid solvent.

EXPERIMENTAL

Apparatus and chemicals

The coulometric titration apparatus with biamperometric end-point detection has already been described [30]. The current—potential curves at the anode in solutions of suitable composition were recorded by the bridge method. In some cases, the potential difference between the working electrode and the mercury—mercury (I) acetate reference electrode was measured with a Radiometer PHM 26 voltmeter. The redox potential of the Br_2/Br^- system was measured with this voltmeter in conjunction with a platinum electrode and the mercury—mercury(I) acetate reference electrode.

All the chemicals used were of analytical-reagent grade. Anhydrous acetic acid was prepared by distillation of glacial acetic acid, the fraction boiling at 118°C being used as solvent. When acetic anhydride was distilled, the fraction boiling at 140°C was collected. Commercial anhydrous potassium acetate, sodium acetate, sodium perchlorate and potassium bromide were dried at 120°C before use.

The catholytes tested were 0.3—1.3 M potassium acetate, 0.6—1.0 M sodium acetate and 0.2 M sodium perchlorate solutions in acetic acid, as well as 0.9 M potassium acetate solutions in 9+1, 7+3 and 1+1 mixtures of acetic acid and acetic anhydride. The anolyte was prepared by saturating the relevant supporting electrolyte with potassium bromide; the bromide concentration in the anolyte was determined by potentiometric titration with a standard solution of silver nitrate.

The indicators used were dissolved in acetic acid. Solutions of hydroquinone and 2-methylhydroquinone in acetic acid were prepared by accurate weighing.

Procedures for the determination of hydroquinone and 2-methylhydroquinone

Method A. The catholyte was poured into the narrower compartment of the vessel to cover the sintered-glass disc. A suitable volume of the solution to be analyzed was measured into the larger compartment of the titration vessel and 15—20 ml of the anolyte was added. After immersion of the electrodes, the levels of the solutions in the two compartments were equalized by adding the appropriate solution to the cathode compartment. The reagent was generated continuously at constant current (1—5 mA) until end-point was reached.

Method B. Here, the solution of the substance to be determined was added to the anolyte after 50—90% of the necessary amount of the reagent had been generated; the titration was then completed by continuous generation of the reagent. In practice, the appropriate solutions were poured into the cathode and anode compartments up to the same level, the electrodes were immersed then added to the anode compartment, the solution levels were equalized again, and the reagent was generated until the end-point was reached.

Method C. The sample solution was added to the anolyte after 90—95% of the necessary amount of bromine had been generated, and the titration was completed by discontinuous generation of the reagent in small amounts for 3—5 s each time at a current of 1—5 mA, until the end-point was reached. The general procedure was the same as in Method B.

Formal redox potential of the Br$_2$/Br$^-$ system

A definite volume of the anolyte containing a known amount of potassium bromide was measured, and bromine was generated in different known amounts. The potential of the platinum electrode in solution was measured at several definite concentration ratios of the components of the redox pair. The values of the redox potential, plotted against the logarithm of the ratio of the concentrations of bromine and bromide in solution, gave a straight line in accordance with the Nernst equation. The intersection of this line with the ordinate at the point log [Ox]/[Red] = 0 gives the formal redox potential of the system. The number of electrons (n) involved in the reaction is determined from the slope of the straight line.

RESULTS AND DISCUSSION

Current—potential curves

The oxidation potentials of bromide and of the test substances at the platinum anode were established by recording the current—potential curves in a 0.9 M potassium acetate solution in acetic acid, before and after addition of potassium bromide and the test substances. As expected bromide is oxidized at a much more negative potential than the acetate of the supporting electrolyte (Fig. 1), so that the basic condition for quantitative electrochemical generation of bromine in acetic acid is satisfied. Hydroquinone and 2-methylhydroquinone are oxidized at still more negative potentials (Fig. 1), which indicates the possibility of their oxidation at the anode in coulometric titration by Method A. This may lead to inaccurate results if the products of the chemical and electrochemical oxidation of test substances are different.

Generation of bromine in acetic acid

On the basis of earlier experience of coulometric redox titration methods with electrically generated lead(IV) acetate and manganese(III) acetate in acetic acid [30,31], initial investigations were done with a 0.9 M potassium acetate solution. A preliminary estimate of the current efficiency for the oxidation of bromide at the platinum electrode was obtained by generating bromine for a definite time at constant current, and titrating the bromine formed with a standard solution of hydroquinone [30] to a biamperometric end-point. The obtained results justified detailed investigations of this and other supporting electrolytes.
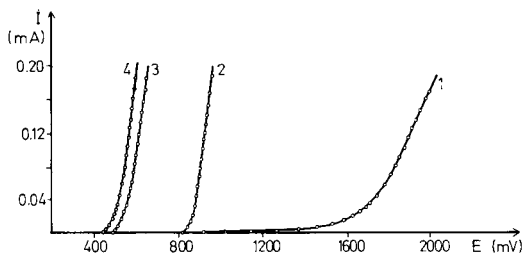
Fig. 1. The current—potential curves for 0.9 M potassium acetate in acetic acid (curve 1), and for saturated potassium bromide (curve 2), 0.01 M hydroquinone (curve 3) and 0.01 M 2-methlhydroquinone (curve 4) in the same electrolyte.

Coulometric titrations with electrically generated bromine

Coulometric determination of hydroquinone with electrically generated bromine was examined in detail. All the three procedures gave good results for titrations of 0.3—1.1 mg of hydroquinone in 0.9 M potassium acetate solution (Table 1). The shape of the recorded titration curves obtained for Method A indicates the presence of two reversible systems in the solution (Fig. 2a), i.e. under these conditions hydroquinone is oxidized to quinone, as expected [11,12]. The pronounced current minimum indicates the titration end-point. When about 0.3 mg of hydroquinone was determined at a current of 2.5 mA, the biamperometric curve was more diffuse, and detection of the

TABLE 1

Coulometric titrations of hydroquinone and 2-methylhydroquinone in acetic acid by Methods A, B and C

Taken (mg)	Recovery (%)			I (mA)	Supporting electrolyte
	A	B	C		
Hydroquinone					
1.116	98.8 ± 0.4	100.0 ± 0.3	100.1 ± 0.5	5.00	0.9 M CH_3COOK
0.556	98.4 ± 0.5	99.8 ± 0.3	99.3 ± 0.6	5.00	0.9 M CH_3COOK
0.280	97.3 ± 0.7	99.3 ± 0.3	99.0 ± 0.9	2.50	0.9 M CH_3COOK
0.544	98.6 ± 0.6	98.7 ± 0.2	98.8 ± 0.2	5.00	0.7 M CH_3COOK
0.544	98.6 ± 0.4	98.8 ± 0.3	99.8 ± 0.9	5.00	1.1 M CH_3COOK
0.544	98.8 ± 0.6	101.2 ± 0.4	101.8 ± 0.5	5.00	1.3 M CH_3COOK
1.086	98.9 ± 0.5			5.00	0.3 M CH_3COOK
1.086	98.9 ± 0.1			5.00	0.5 M CH_3COOK
1.123			99.6 ± 0.1	5.00	0.6 M CH_3COONa
1.123			100.6 ± 0.7	5.00	1.0 M CH_3COONa
2-Methylhydroquinone					
1.283	100.2 ± 0.4	100.8 ± 0.3	100.1 ± 0.7	5.00	0.9 M CH_3COONa
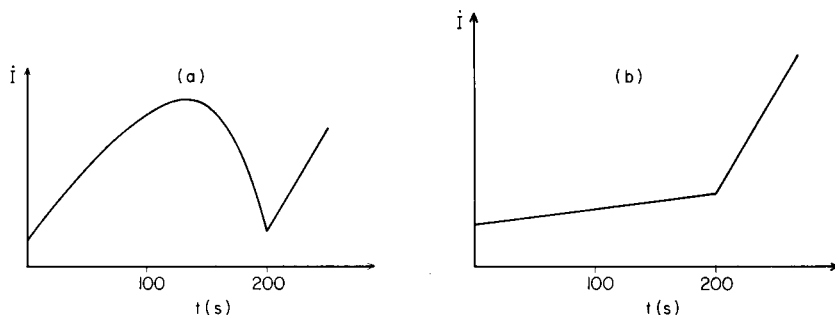
Fig. 2. The shapes of the biamperometric titration curves obtained by Method A on addition of hydroquinone solution, before the generation of bromine, to (a) 0.9 M potassium acetate solution, and (b) 0.5 M potassium acetate solution.

end-point became difficult (Table 1). It is interesting that when Method B was used, when up to 75% of the necessary amount of bromine was previously generated, the current minimum indicated the end-point of the titration, whereas under other conditions the current in the indicator circuit increased slowly until the end-point was reached (Fig. 2b). It should, however, be emphasized that the shape of the titration curves also depends on the preliminary treatment or history of the electrode. For example, after several successive ignitions of the same indicator electrodes, curves of the shape shown in Fig. 2(a) were obtained only in the first titrations. Only when Method C was used, did a current minimum appear under all working conditions at the titration end-point.

The amounts of bromine which can be generated with 100% current efficiency in a 0.9 M potassium acetate solution saturated with potassium bromide were then determined by titrating different amounts of hydroquinone by Method C. It was found that with 20 ml of the anolyte, generation was complete only if the amount of electricity consumed did not exceed 2.5 coulombs.

Photometric methods based on the indicators methyl orange, methyl red, crystal violet and benzidine—the last of which was used successfully in coulometric titrations with lead(IV) acetate and manganese(III) acetate in acetic acid [30] could not be supplied successfully for end-point detection in bromine titrations. The colour of the solutions in the presence of these indicators changed only after a rather large amount of reagent had been added after the true end-point.

Changes in the concentration of potassium acetate in the supporting electrolyte from 0.7 to 1.3 M affected neither the shape of the titration curves nor the accuracy of the results obtained (Table 1). In more dilute solutions (0.3—0.6 M) of potassium acetate, titration curves of the shape shown in Fig. 2(b) were obtained; precise evaluation of the end-point was then more difficult.

It is known that sodium acetate exerts a positive effect on the solubility of potassium bromide in acetic acid [32]. The possibilities of coulometric titrations with bromine in 0.6—1.0 M sodium acetate solutions were therefore examined. The titration curves obtained were of the same shape as in more dilute solutions of potasium acetate (Fig. 2b). The results of determinations by Methods A and B were 4—5% lower than the theoretical values, but good results were obtained by Method C (Table 1).

In solutions of sodium perchlorate, the reaction of hydroquinone with bromine is slow. Thus, with Method A, there was a sudden increase in current in the indicator circuit after several seconds of generation of the reagent. Since it is known that mercury(II) catalyzes oxidation processes with bromine [7], some mercury(II) acetate was added to the sample solutions; there was only a slight acceleration of the reaction. Changes in the acidity of the titrated solutions by adding perchloric acid or sodium acetate or pyridine and other bases, did not achieve the desired effect.

The effect of water on the accuracy of the results obtained was examined. It was expected that water would not affect the current efficiency for bromine generation as much as that found in generation of lead(IV) acetate or manganese (III) acetate [30]. When 0.0—10.0% of water was added to the anolyte prepared in 0.9 M potassium acetate before generation of bromine, and hydroquinone was titrated by Methods A and C, the results showed that the accuracy was not affected by the presence of up to 4% water in the anolyte. On further increase of the water content (to 10%), the recovery of hydroquinone increased to 107%, as in pure water. Accordingly, the negative effect of water should not be explained by a decrease in the current efficiency of bromine generation, but rather by the fact that the bromine formed is consumed in other reactions, e.g. substitution of bromine in the benzene nucleus.

The reactions in a 0.9 M potassium acetate solution prepared in 9 + 1, 7 + 3 and 1 + 1 mixtures of acetic acid and acetic anhydride were also studied. Higher concentrations of acetic anhydride were not tested because of the limited solubility of potassium acetate. In the titration of hydroquinone by Method A, the results obtained were up to 13% lower than the theoretical results, depending on the present amount of acetic anhydride in solution and the time of determination. This is probably due to reaction of hydroquinone with acetic anhydride; this was confirmed by the results obtained in the same solvent after previous generation of about 95% of the necessary amount of the reagent (Table 2).

A supporting electrolyte of 0.9 M potassium acetate solution in acetic acid was also used in titrations of 2-methylhydroquinone by all the procedures. This compound is quickly and quantitatively oxidized with the consumption of one mole of bromine; the results obtained are good and reproducible (Table 1).

The formal redox potential of the Br_2/Br^- system in a 0.9 M potassium acetate solution was determined as described under Experimental. A linear

TABLE 2

Coulometric titrations of hydroquinone in a 0.9 M potassium acetate solution in mixtures
of acetic acid and acetic anhydride by Methods A, B and C at a constant current of 5.00 mA

Taken (mg)	Recovery (%)			HAc:Ac$_2$O
	A	B	C	
0.590	97.2 ± 0.3	99.7 ± 0.1	101.2 ± 0.8	9:1
1.087	94.8 ± 1.5	101.1 ± 0.5	101.1 ± 0.5	7:3
1.112	91.8 ± 0.8	102.0 ± 0.5	100.1 ± 1.0	1:1

dependence was obtained between the measured values of the redox potential
and the logarithm of the ratio of the concentrations of the bromine and bromide
in solution. The slope of the straight line obtained was 57.5 mV, which corres-
ponds to a one-electron transition; this is yet another proof of direct oxidation
of bromide to bromine at the platinum electrode in acetic acid, and confirms
that the current efficiency for bromine generation is close to 100%. The value
of the formal redox potential was found to be 952 mV, which shows that
bromine in the given supporting electrolyte is a strong oxidizing agent. Coulo-
metric determinations of other reducing compounds with this reagent in acetic
acid therefore seem possible.

REFERENCES

1 I. M. Kolthoff and R. Belcher, Volumetric Analysis, Vol. III, Interscience, New York,
   1957, p. 564.
2 A. Berka, J. Vulterin and J. Zyka, New Redox Methods in Analytical Chemistry,
   Pergamon, Oxford.
3 L. Szebellédy and Z. Somogyi, Fresenius Z. Anal. Chem., 112 (1938) 385, 391, 400.
4 A. P. Zozulya, Kulonometricheskii Analiz, Khimiya, Leningrad, 1968, p. 59—75.
5 E. Bishop, Mikrochim. Acta, (1960) 803.
6 A. F. Krivis, E. S. Gazda, G. R. Supp and P. Kippur, Anal. Chem., 35 (1963) 1955.
7 E. C. Olson, Anal. Chem., 32 (1960) 1545.
8 S. Bruckenstein and D. C. Johnson, Anal. Chem., 36 (1964) 2186.
9 R. P. Buck and R. W. Eldridge, Anal. Chem., 37 (1965) 1242.
10 V. J. Jennings, A. Dodson and A. Harrison, Analyst, 99 (1974) 145.
11 O. Tomiček and A. Heyrovský, Collect. Czech. Chem. Commun., 15 (1950) 977.
12 O. Tomiček and J. Valcha, Collect. Czech. Chem. Commun., 16 (1951) 113.
13 J. V. L. Longstaff and K. Singer, Analyst, 78 (1953) 491.
14 L. Erdey, T. Meisel and Gy. Rády, Acta Chim. Acad. Sci. Hung., 26 (1961) 71; Chem.
   Abstr., 55 (1961) 24368f.
15 C. O. Huber and J. M. Gilbert, Anal. Chem., 34 (1962) 247.
16 J. Vulterin and J. Zýka, Talanta, 10 (1963) 891.
17 D. J. Macero and R. A. Janeiro, Anal. Chim. Acta, 27 (1962) 585.
18 I. M. Kolthoff and J. F. Coetzee, J. Am. Chem. Soc., 79 (1957) 1852.
19 A. I. Popov and D. H. Geske, J. Am. Chem. Soc., 80 (1958) 1340, 5346.
20 R. T. Iwamoto, Anal. Chem., 31 (1959) 955.

21 I. V. Nelson and R. T. Iwamoto, J. Electroanal. Chem., 7 (1964) 218.
22 T. Iwasita and M. C. Giordano, Electrochim. Acta, 14 (1969) 1045.
23 G. Durand and B. Trémillon, Anal. Chim. Acta, 49 (1970) 135.
24 R. Guidelli and G. Piccardi, Anal. Chem., 43 (1971) 1639.
25 L. Sereno, V. A. Macagno and M. C. Giordano, Electrochim. Acta, 17 (1972) 561.
26 M. Mastragostino, G. Casalbore and S. Valcher, J. Electroanal. Chem., 44 (1973) 37.
27 F. Magno, G. A. Mazzocchin and G. Bontempelli, J. Electroanal. Chem., 47 (1973) 461.
28 B. Lopez, T. Iwasita and M. C. Giordano, J. Electroanal. Chem., 47 (1973) 469.
29 G. Casalbore, M. Mastragostino and S. Valcher, J. Electroanal. Chem., 68 (1976) 124; 77 (1977) 373.
30 T. J. Pastor, V. J. Vajgand and Z. Kićović, Mikrochim. Acta, (1976 II) 525.
31 T. J. Pastor, V. J. Vajgand and V. V. Antonijević, Mikrochim. Acta, (1978) 131.
32 E. Griswold, M. M. Jones and R. K. Birdwhistell, J. Am. Chem. Soc., 75 (1953) 5701.

A NEW CATALYTIC DETERMINATION OF ULTRATRACE AMOUNTS OF IRON WITH *p*-ANISIDINE AND *N, N*-DIMETHYLANILINE

TAKUJI KAWASHIMA* and YOSHIHIRO KOZUMA

Chemical Institute, College of Liberal Arts, Kagoshima University, Korimoto, Kagoshima 890 (Japan)

SHIGENORI NAKANO

Chemical Institute, Faculty of Education, Tottori University, Koyama-cho, Tottori 680 (Japan)

(Received 21st March 1978)

SUMMARY

A new sensitive catalytic method for the determination of iron(II) and iron(III) is proposed. *p*-Anisidine reacts with *N,N*-dimethylaniline to form *N*-(*p*-methoxyphenyl)-*N',N'*-dimethyl-*p*-phenylenediamine (MDP). In the presence of hydrogen peroxide, iron(III) catalyzes the oxidation of MDP to a blue compound (λ_{max} = 735 nm). Iron(II) is also determined, being oxidized by hydrogen peroxide. Working curves are linear in the approximate range 6—20 ng Fe ml^{-1}; as little as 10^{-7} M iron can be determined easily. The method is applicable to the analysis of pure ammonium and alkali metal salts containing 10^{-4}—10^{-5}% iron.

The most commonly used spectrophotometric reagents for iron(II) are 1,10-phenanthroline and 2,2'-bipyridine [1]; more recently various substituted nitrosophenols have been proposed [2, 3]. Catalytic methods are generally much more sensitive than spectrophotometric methods based on stoichiometric reactions [4, 5]. Catalytic determinations of iron have been based on the oxidation of methyl orange [6] or iodide [4, 7] by hydrogen peroxide, and of *p*-phenetidine by periodate in the presence of 2,2'-bipyridine [8]. Hirayama and Sawaya [9] have proposed a sensitive kinetic procedure for iron(III) based on the catalytic oxidation of Bindschedler's Green (4,4'-bis (dimethylamino)diphenylamine). Erdey and Szabadváry [10] and Kreingold and Sosenkova [11] have reported a kinetic method for iron(III) based on oxidation of variamine blue B base (*N*-(*p*-methoxyphenyl)-*p*-phenylenediamine) by hydrogen peroxide; but even pure variamine blue B is light-sensitive and turns blue, thus causing high blanks [12].

The present paper describes the analytical application of the catalytic effect of iron on the reaction of *p*-anisidine with *N,N*-dimethylaniline in the presence of hydrogen peroxide. By using the reactants separately and replacing aniline with *N,N*-dimethylaniline, blank values can be kept low, the decomposition and the oxidation of the product in storage being avoided. Ultratrace amounts of

iron(II) and iron(III) can be determined. Some pure chemicals containing trace amounts of iron were analyzed to test the method.

EXPERIMENTAL

Reagents

Deionized distilled water was used. Stock solutions of iron(II) and iron(III) (1 mg ml^{-1}), prepared from ammonium iron(II) sulfate hexahydrate (3.51 g) or iron(III) chloride hexahydrate (2.42 g) in 500 ml of 0.1 M hydrochloric acid, were standardized by titration with EDTA. Working solutions were prepared by suitable dilution with 0.1 M hydrochloric acid. *p*-Anisidine and *N,N*-dimethyl-aniline were purified by vacuum sublimation and vacuum distillation, respectively. *p*-Anisidine (2.5 × 10^{-2} M) and *N,N*-dimethylaniline (8.0 × 10^{-2} M) solutions were prepared in 0.1 M hydrochloric acid. Aqueous hydrogen peroxide (1.3% w/v) solutions were used. These solutions, except for iron(III) solutions, were prepared daily. All chemicals used were of analytical grade.

Apparatus

A Hitachi Perkin-Elmer Model 139 spectrophotometer with 10-mm glass cells was used for absorbance measurements; absorption spectra were obtained with a Shimadzu UV-200 double-beam spectrophotometer with 10-mm glass cells. A Beckman Model SS-2 pH meter and Taiyo Model C-550 circulating thermostated bath were also used.

Recommended general procedure

To 20—23 ml of sample solution (about 0.1 M in hydrochloric acid) containing not more than 1 μg of iron in a 100-ml beaker, add 5 ml of 2 M acetic acid solution and adjust the pH to ca. 3.5—3.7 with 2 M sodium acetate solution (pH meter). Transfer the solution to a 50-ml volumetric flask, add a mixture of 4 ml of 2.5 × 10^{-2} M *p*-anisidine and 8.5 ml of 8.0 × 10^{-2} M *N,N*-dimethylaniline (or 5 ml of 2.5 × 10^{-2} M anisidine and 7 ml of 8.0 × 10^{-2} M dimethylaniline) and finally 5 ml of 1.3% hydrogen peroxide solution. Dilute to the mark with water, mix well, and heat to 50°C in a thermostat. Exactly 60 min after the initiation of the reaction, pipette ca. 5 ml of the reaction mixture into a dry test tube immersed in an ice bath to quench the reaction. Then measure the absorbance at 735 nm in 10-mm cells preferably within 50 min, against a distilled water reference.

RESULTS AND DISCUSSION

p-Anisidine reacts with *N,N*-dimethylaniline to form *N*-(*p*-methoxyphenyl)-*N',N'*-dimethyl-*p*-phenylenediamine (MDP). Iron(III) seems to affect the condensation reaction; the absorption spectrum of a mixture of the reactants

changed on addition of milligram amounts of iron(III), whereas it did not change without iron(III) even on heating for 60 min at 50°C. MDP is probably oxidized to a blue compound, N,N-dimethyl-N'-(p-methoxyphenyl)-1,4-quinonediiminonium ion (DMQ) by trace amounts of iron(III) in the presence of hydrogen peroxide in the same way as in the case of variamine blue B base [12].

The blue compound, DMQ, has an absorption maximum at 735 nm (Fig. 1). As expected, the reagent blank shows little absorbance at this wavelength.

Effect of reaction variables

The effect of pH on the color development for the catalytic reaction was examined for a constant time of 60 min at 50°C. The color development was at a maximum and almost constant in the pH range 3.5—3.7, decreasing quite rapidly on both sides of this range.

The effect of temperature on the catalytic reaction was examined at 45°, 50° and 55°C (Fig. 2). The reaction of iron(II) at 50°C is also shown in Fig. 2. As can be seen, the mode of coloration by iron(II) is the same as that of iron(III), presumably because iron(II) is oxidized to iron(III) by hydrogen peroxide. The reaction is faster at higher temperatures, but the decomposition of blue compound becomes more extensive above 55°C. For the sake of high sensitivity and reproducibility, a heating time of 60 min at 50°C was chosen for the recommended procedure. The absorbance of the reaction mixture remains unchanged for at least 50 min so long as the mixture is kept in an ice bath.

The color development was examined at three different concentrations of p-anisidine with different N,N-dimethylaniline concentrations (Fig. 3). For anisidine concentrations of 2.0×10^{-3} and 2.5×10^{-3} M the absorbance remains constant over the ranges 1.3×10^{-2}—1.44×10^{-2} M and 1.0×10^{-2}—1.2×10^{-2} M
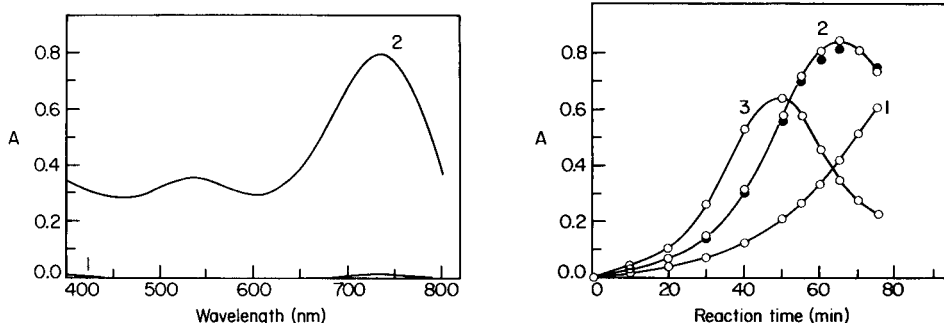
Fig. 1. Absorption spectra of DMQ. (1) Reagent blank; (2) 0.8 μg of iron(III) per 50 ml. 2.0×10^{-2} M p-anisidine; 1.36×10^{-2} M N,N-dimethylaniline; pH 3.5—3.7; 50°C for 60 min.

Fig. 2. Effect of temperature on color development of 0.8 μg of iron(III) (○) and iron(II) (●). Reaction temperature: (1) 45°; (2) 50°; (3) 55°C. Other conditions as in Fig. 1.

dimethylaniline, respectively, whereas with 1.5×10^{-3} M anisidine, the absorbances are much lower.

The effect of hydrogen peroxide concentration was also examined. The color development was almost constant in the hydrogen peroxide concentration range 0.052—0.20% (w/v), and 5 ml of hydrogen peroxide (1.3%) was used for the reaction volume of 50 ml.

Calibration graphs

Typical working curves over the range 0—1.0 μg of iron(III) per 50 ml by the recommended procedure are shown in Fig. 4: the linear range decreases with increasing anisidine concentration. Working curves for iron(II) are almost identical to those for iron(III) within experimental error. The curvature of the calibration plots might be attributed to decomposition of the blue DMQ compound at very low concentrations.

The results of the determination of iron(II) and iron(III) in composite samples are shown in Table 1. As can be seen, the sensitivity of the proposed method is high and the reproducibility satisfactory.

Effect of diverse ions

The effect of diverse ions on the determination of 0.60 μg of iron(III) was examined. No interferences were found up to at least the following concentrations: 100 μg of Al(III), As(III), As(V), Ba(II), Ca(II), Cd(II), Co(II), Mn(II),
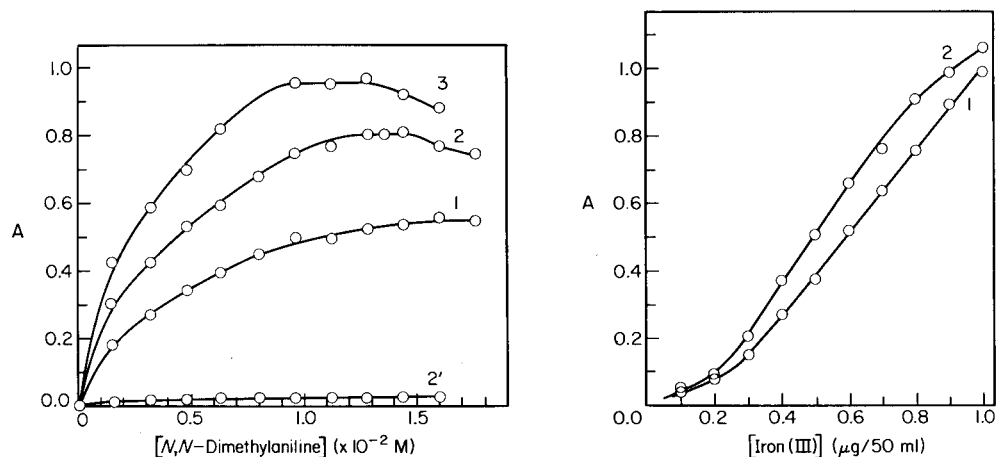
Fig. 3. Effect of *p*-anisidine and *N,N*-dimethylaniline concentrations. *p*-Anisidine: (1) 1.5 $\times 10^{-3}$ M; (2) 2.0×10^{-3} M; (2') reagent blank; (3) 2.5×10^{-3} M. Iron(III): 0.8 μg per 50 ml. pH 3.5—3.7. All at 50°C for 60 min.

Fig. 4. Working curves for iron. *p*-Anisidine: (1) 2.0×10^{-3} M; (2) 2.5×10^{-3} M. *N,N*-Dimethylaniline: (1) 1.36×10^{-2} M; (2) 1.12×10^{-2} M. pH 3.5—3.7. All at 50°C for 60 min.

TABLE 1

Determination of total iron (Fe(II) + Fe(III)) by the recommended procedure

Fe(II) added (μg)	Fe(III) added (μg)	Fe found (μg)	Fe(II) added (μg)	Fe(III) added (μg)	Fe found (μg)
0	0.60	0.600, 0.595, 0.605	0.30	0.30	0.600
0	0.80	0.803, 0.800, 0.785	0.50	0.30	0.790
0.70	0	0.688, 0.701, 0.705	0.20	0.40	0.601
0.40	0.20	0.610	0.20	0.50	0.700
0.50	0.20	0.690	0.50	0.50	0.975

Mo(VI), Ni(II), Pb(II), Sr(II), Te(IV), Zn(II); 10 μg of Se(IV), W(VI); 100 μg of I$^-$, Br$^-$, PO$_4^{3-}$, ClO$_4^-$; 20 mg of ammonium chloride, ammonium sulfate, potassium chloride, sodium chloride, sodium nitrate.

Interfering ions are listed in Table 2. Copper(II) catalyzes the reaction in the same way as iron(III), although the sensitivity for copper(II) is about one fifth that for iron(III): the absorption maximum of DMQ and the pH dependence of the reaction are similar to those obtained for iron(III). The interference of copper(II) can be eliminated by reduction with a mixture of zinc and silver granules in a Jones-type reductor column [13] (Table 2). There are positive interferences from cerium(IV), chromium(VI) and vanadium(V); these ions also seem to catalyze the color development. Negative interferences are observed from tin(II) and tin(IV); in the presence of tin(II) or tin(IV), the reaction rate is retarded, possibly because of adsorption of the reactants and of iron(III) on the hydrolyzed species of tin.

TABLE 2

Effect of interfering ions on the determination of 0.60 μg of iron(III) by the recommended procedure

Ion added	Amount added (μg)	Fe(III) found (μg)	Ion added	Amount added (μg)	Fe(III) found (μg)
Ce(III)	10	0.570	Sn(II)	100	0
Ce(IV)	10	>1		10	0.380, 0.370, 0.163
Cr(III)	100	0.530		1	0.590, 0.614, 0.611
	10	0.570, 0.585	Sn(VI)	10	0.214, 0.205, 0.211
	1	0.580		1	0.556, 0.557, 0.544
Cr(VI)	100	0.635, 0.600	V(V)	100	0.757, 0.740
	10	0.645, 0.655		10	0.635
Cu(II)	10	>1		1	0.630
	1	0.915, 0.871, 0.922	F$^-$	100	0.385
	1[a]	0.613, 0.607, 0.576		10	0.570

[a]Treated by the reduction procedure as in the text.

TABLE 3

Determination of iron in pure reagent chemicals

Compound[a]	Sample taken (mg)	Fe added (μg)	Fe found (μg)	Fe corrected for addition	
				(μg)	(%)
NH$_4$Cl	200	0	0.28	0.28	1.40×10^{-4}
	200	0.53	0.86	0.33	1.65×10^{-4}
KCl	200	0	0.22	0.22	11.0×10^{-5}
	200	0.53	0.71	0.18	9.0×10^{-5}
	200	0.60	0.73	0.13	6.5×10^{-5}
NaCl	200	0	0.15	0.15	7.5×10^{-5}
	200	0	0.19	0.19	9.5×10^{-5}
	200	0.53	0.70	0.17	8.5×10^{-5}
	200	0.60	0.79	0.19	9.5×10^{-5}
NaNO$_3$	200	0	<0.05	<0.05	$<2.5 \times 10^{-5}$
	200	0	<0.05	<0.05	$<2.5 \times 10^{-5}$
	200	0.53	0.51	—	—
	200	0.60	0.65	0.05	2.5×10^{-5}

[a]Analytical grade; iron contents given by manufacturer on certificate of guarantee are below 3×10^{-4}% for each compound.

Application to some pure chemicals

The iron contents of some analytical-grade chemicals such as ammonium chloride, potassium chloride, sodium chloride and sodium nitrate were determined with the results shown in Table 3. Recovery of added iron was found to be quantitative and the reproducibility was satisfactory.

REFERENCES

1 E. B. Sandell, Colorimetric Determination of Traces of Metals, Interscience, New York, 3rd edn., 1959, p. 537.
2 T. Korenaga, S. Motomizu and K. Tôei, Anal. Chim. Acta, 65 (1973) 335.
3 K. Tôei, S. Motomizu and T. Korenaga, Analyst, 100 (1975) 629; 101 (1976) 974.
4 K. B. Yatsimirskii, Kinetic Methods of Analysis, Pergamon Press, Oxford, 1966.
5 P. R. Bontchev, Talanta, 17 (1970) 499.
6 V. V. Budanov, Izv. Vyssh. Uchebn. Zaved., Khim. Khim. Tekhnol., 5 (1962) 47; Chem. Abs., 58 (1963) 2338a.
7 K. B. Yatsimirskii and G. A. Karacheva, Zh. Neorg. Khim., 3 (1958) 352; Chem. Abs., 52 (1958) 19364d.
8 I. F. Dolmanova, V. I. Rychkova and V. M. Peshkova, Zhur. Anal. Khim., 28 (1973) 1763.
9 K. Hirayama and T. Sawaya, Nippon Kagaku Kaishi, (1976) 1401.
10 L. Erdey and F. Szabadváry, Mikrochim. Acta, (1959) 424.
11 S. Kreingold and L. I. Sosenkova, Zhur. Anal. Khim., 26 (1971) 332.
12 L. Erdey, Chemist-Analyst, 48 (1959) 106.
13 G. H. Ayres, Quantitative Chemical Analysis, Harper and Row, New York, 2nd edn., 1969, p. 390.

Short Communication

FLAME ATOMIC ACOUSTIC SPECTROMETRY — A NEW TECHNIQUE APPLIED TO THE DETERMINATION OF SODIUM

A. G. HOWARD* and D. A. GREENHALGH

Department of Chemistry, University of Southampton, Southampton, Hampshire (Gt. Britain)

When sodium atoms in a premixed flame are excited by a pulsed source of laser radiation, audio sound waves are produced [1, 2]. This communication describes the preliminary application of this phenomenon to the determination of sodium.

Following resonant absorption of visible radiation by sodium atoms in an air—acetylene flame, rapid collisional quenching of the electronically excited state and energy transfer to the flame gases give rise to localized heating and production of a pressure wave which can readily be detected. In preliminary experiments an instrument has been constructed, based on a narrow bandwidth flash-lamp-pumped tunable dye laser, to measure the amplitude of the sound waves which are produced and to assess the analytical potential of the technique in trace metal determinations.

Instrumentation

A schematic diagram of the instrument is given in Fig. 1. Sample solutions were aspirated into a nebulizer-burner system from a Varian-Techtron AA1100 atomic absorption spectrometer. Sodium atoms were excited by tuning a Chromatix CMX-4 flashlamp-pumped dye laser to either of the 3^2P—3^2S transitions of the sodium atom. With a methanol—water solution of rhodamine 6G at a repetition rate of 25 Hz, pulses 2 μs long and with a bandwidth of 0.1 cm^{-1} were obtained over the range 575 to 610 nm. Output energies varied with the wavelength of operation but were in the range 0.5—4.0 mJ per pulse. Alternatively, excitation was effected by an "in-house" dye laser pumped with the second harmonic of a Nd/YAG laser (J. K. Lasers unstable resonator giving 150 mJ at 1.06 μm and 40 mJ at 532 nm). With a solution of rhodamine B in methanol, an output of 4 mJ per pulse at 30-Hz repetition rate was achieved at approximately 590 nm. The pulse width of the Nd/YAG pumped dye laser was 6 ns with a bandwidth of 0.2 cm^{-1}.

The acoustic signal was detected by a Knowles CA2856 microphone positioned 5 cm from the flame. The microphone signal was processed with a Brookdeal 9415/9425 boxcar signal averager, triggered by a photodiode sensing
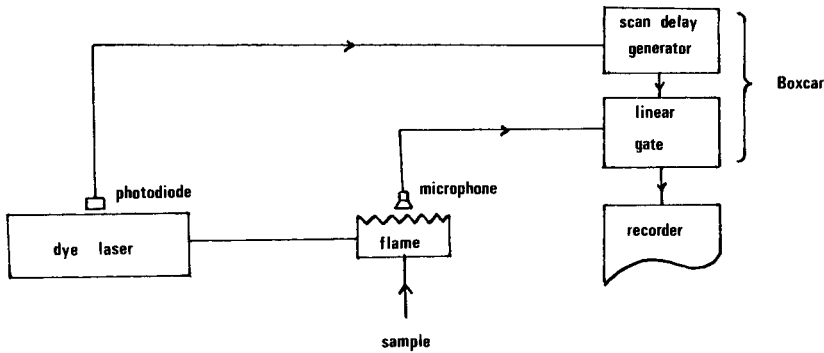
Fig. 1. Schematic diagram of a flame atomic acoustic spectrometer.

the dye laser output. Output from the signal averager was displayed on a Servoscribe chart recorder or a Techtronix 585A oscilloscope fitted with a type-86 fast-rise preamplifier.

Results

The acoustic signal is obtained only when the laser is tuned to a suitable absorption line. With strong aqueous sodium solutions (1 mg Na ml^{-1} as sodium chloride), tuning of the laser to the appropriate wavelength can readily be achieved by ear.

Oscilloscope traces of the microphone output are presented in Fig. 2. The signal is positive for only the first 50 μs of the trace and the boxcar gate was set to sample for only the central 2 μs of this positive pulse (a delay of approximately 1.3 ms after the laser pulse). A narrow gate was chosen in these preliminary experiments because of the noisy laboratory environment. In future experiments acoustic isolation of the sample region will be used to allow more of the pulse to be used. The initial microphone pulse length is significantly longer than the laser pulse, irrespective of excitation pulse length (2 μs from the CMX-4 or 6 ns from the Nd/YAG pumped dye laser). The pulse profiles
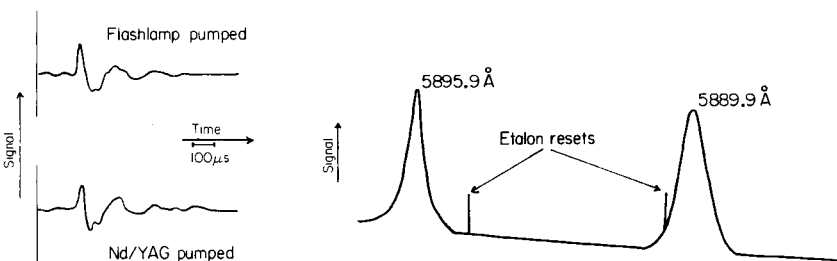
Fig. 2. Oscilloscope traces of microphone response to laser-induced acoustic signal.

Fig. 3. Sodium D lines doublet spectrum obtained by acoustic detection.

are identical for the two experiments and close to the limiting detector response of 10 kHz. Thus the initial high frequency component in Fig. 2 is the microphone response to the initial shock wave whilst the lower frequency component following this (ca. 4 kHz) is probably the microphone ringing at, or close to, its peak response frequency of 3.3 kHz. In a recently reported similar experiment with a faster-responding microphone (140 kHz), the initial pulse was again detector limited [1]. Clearly, in order to monitor the relaxation processes following the laser pulse, a very fast pressure transducer is required.

A typical spectrum, obtained by optoacoustic detection of the sodium 3^2P—3^2S doublet, is given in Fig. 3. Detector response was found to be linear with sodium ion concentration over the studied range of 1—100 μg ml^{-1} of sodium solution aspirated into the flame. The response of 10 μg Na ml^{-1} solutions was unaffected by the presence of 100-fold amounts of lithium or potassium ions.

Discussion

Acoustic detection of atoms offers great potential in both analytical and fundamental spectrometry. By making use of narrow bandwidth laser excitation sources, it is possible to obviate the need for monochromators. Without monochromators, spectral line overlap and stray light problems associated with the more common forms of atomic spectrometry become less pronounced and more reliable analytical information is to be expected.

For analytical purposes, pulse-to-pulse stability, dye lifetime and output power of most flashlamp-pumped dye lasers are poor, and Nd/YAG (or similar) pump lasers are preferable. However, with narrow bandwidth, short pulse length, high peak power lasers, saturation can occur. For sodium atoms under the flame conditions reported in this work, saturation is expected to occur at approximately 1 MW cm^{-1} [3]. In an analytical experiment, saturation is to be avoided since its effect is to reduce considerably the gross amount of laser energy transferred by absorption to the metal atoms and hence to an acoustic signal. In the case of the CMX-4, this corresponds to a beam diameter of 1—3 mm. However, to avoid saturation with the Nd/YAG pumped dye laser an area of several cm^2 is required. In the present experiments, beam expansion sufficed to avoid saturation but much of the laser energy was lost since it did not pass through the flame. Tailoring of the expansion optics to the flame geometry should considerably improve the situation.

The preliminary experiments reported here have demonstrated the potential of the acoustic detection of atoms. Flame atomic acoustic spectrometry appears to be insensitive to the ionization interferences which cause severe problems in atom detection by the measurement of flame conductivity [4]. The technique should be readily applicable to other elements and, with suitable instrumentation, high sensitivity and selectivity should be attainable.

REFERENCES

1 J. E. Allen, Jr., W. R. Anderson and D. R. Crosley, Opt. Lett., 1(4) (1977) 118.
2 W. R. Anderson, J. E. Allen, Jr., T. D. Fansler and D. R. Crosley, Preliminary Program and Abstracts for 10th Materials Research Symposium on Characterization of High Temperature Vapours and Gases, September, 1978, National Bureau of Standards, Gaithersburg, Maryland, pp. 88—89.
3 B. L. Sharp and A. Goldwasser, Spectrochim. Acta, Part B, 31 (1976) 431.
4 G. C. Turk, J. C. Travis and J. R. De Voe, Anal. Chem., 50(6) (1978) 817.

Short Communication

SPECTROPHOTOMETRIC AND DIFFERENTIAL PULSE POLAROGRAPHIC DETERMINATIONS OF SULPHAGUANIDINE BY REACTION WITH HYPO-CHLORITE AND PHENOL

A. G. FOGG* and N. M. FAYAD

Chemistry Department, University of Technology, Loughborough, Leics. LE11 3TU (Gt. Britain)

A procedure for the colorimetric determination of sulphanilamide by an indophenol reaction has already been reported [1]. Although other sulphona-mides studied did not interfere, sulphaguanidine gave a green-yellow colour in contrast to the blue indophenol colour given by sulphanilamide. The inter-action of sulphaguanidine with hypochlorite and phenol has now been studied in more detail, and colorimetric and differential pulse polarographic deter-minations of sulphaguanidine have been developed. In the earlier method for sulphanilamide [1], the indophenol derivative is formed by heating the aqueous sample solution at 60°C for 40 min with phenol, sodium hypochlorite and sodium nitroprusside in strong alkaline solutions; the nitroprusside acts as a catalyst, as in the analogous reaction with ammonia [2]. Detailed studies of the reaction of sulphaguanidine showed that there is no need for nitroprusside, which is advantageous because nitroprusside gives an appreciable blank owing to the formation of nitropentacyanoferrate(II) [3]; the optimum conditions are different from those required for sulphanilamide and the colour formed (yellow in the absence of nitroprusside) is less stable.

Recently, indophenol derivatives formed from ammonia, sulphanilamide and *p*-aminophenol at the 1×10^{-7} M level have been determined by differen-tial pulse polarography (d.p.p.) [4]. The coloured product formed in the re-action of sulphaguanidine with hypochlorite/phenol also gives a well-defined polarographic wave, and the reaction conditions for the d.p.p. test of sul-phaguanidine are now reported. The composition of the solution is the same as that prepared for colorimetry except that some ethanol is included, in order to avoid the appearance of an adsorption pre-wave.

Experimental

Sodium hypochlorite solution. Dilute 20 ml of commercial sodium hypo-chlorite solution (10—14% available chlorine) to 500 ml with distilled water.

Standard sulphaguanidine solution, 2.8 × 10⁻⁴M. Dry sulphaguanidine to constant weight at 105°C, dissolve 0.600 g in a little dilute hydrochloric acid and dilute the solution to 100 ml with water in a volumetric flask. Two further dilutions (10 ml → 100 ml) gave a 2.8 × 10⁻⁴M sulphaguanidine solution.

Colorimetric Procedure. To a 50-ml volumetric flask add, in the following order, 1 ml of 10 M sodium hydroxide solution, 5 ml of aqueous 3% (w/v) phenol solution, up to 5 ml of sample or standard sulphaguanidine solution containing less than 0.4 mg of sulphaguanidine (add water to make the volume added to 5 ml) and 10 ml of sodium hypochlorite solution. Heat the flask in a water bath at 45°C for 10 min, cool, dilute to 50 ml with water, and immediately measure the absorbance at 450 nm in 1-cm cells.

Calibration graphs obtained by this procedure were rectilinear and corresponded to a molar absorptivity of 1.65×10^4 l mol⁻¹ cm⁻¹ for the coloured product, assuming a 1:1 molar conversion from the sulphaguanidine. The coefficient of variation (eight determinations) at the 2.8×10^{-5}M level in the measured solutions was 1%.

The alkalinity of the solution is critical: the addition of 2 ml of 10 M sodium hydroxide gives an apparent molar absorptivity of only 1.21×10^4 l mol⁻¹ cm⁻¹. The concentrations of phenol and hypochlorite are less critical but the volumes added should be controlled quite closely. Calibration graphs should be prepared for each new batch of hypochlorite reagent solution. The colour intensity decreases rapidly for heating times greater than 10 min (e.g. apparent $\epsilon = 1.48$ and 0.75×10^4 l mol⁻¹ cm⁻¹ after 15 and 25 min respectively). Loss of colour intensity after cooling to room temperature is much slower (e.g. apparent $\epsilon = 1.35 \times 10^4$ l mol⁻¹ cm⁻¹ after heating for 10 min followed by a standing period of 35 min).

Polarographic procedure. A PAR 174 polarographic analyser (Princeton Applied Research Corp.) was used in the differential pulse mode with a 0.5-s forced drop time and a scan rate of 5 mV s⁻¹. The dropping mercury electrode was used with a saturated calomel electrode and a platinum auxiliary electrode.

The procedure is the same as the colorimetric procedure except that 5 ml of ethanol is added after the heating step and before dilution to 50 ml. Deoxygenation is effected by passing nitrogen through the solution for 7 min. The d.p.p. curve is then immediately recorded between −0.4 and −0.8 V.

Typical differential pulse polarograms show very well-defined peaks ($E_p = 0.63$ V), and calibration curves are rectilinear over the range 0.5—4μg ml⁻¹. The coefficient of variation at the 2-μg ml⁻¹ level is 2.4% (10 determinations).

The polarographic method was applied to the determination of sulphaguanidine in a sample of Guanimycin Suspension Forte kindly supplied by Allen and Hanburys Ltd. The sample (1 g) was weighed into a 50-ml beaker and mixed well with 20 ml of water and 2 ml of concentrated hydrochloric acid. The mixture was transferred to a 100-ml volumetric flask, diluted to volume with water and filtered through a sintered glass crucible; 10 ml of the filtrate was diluted to 100 ml in a volumetric flask. Further dilutions (10 ml → 100 ml followed by 20 ml → 100 ml) were made, and aliquots (5 ml)

of the final solution were used for the determination. The sulphaguanidine equivalent in the final solution was found to be 2.15 μg ml^{-1} with a coefficient of variation of 6%. This corresponds to 2.1 g of sulphaguanidine in 15 ml of Guanimycin Suspension Forte compared with the 1.98 g nominal content. Naturally the procedure could be applied more appropriately to the determination of trace amounts of sulphaguanidine.

Behaviour of other sulphonamides

The behaviour of several other sulphonamides under the recommended reaction conditions was studied. None of these reacted at the same low levels as sulphaguanidine. For sulphanilamide at the 10^{-3} M level, the blue indophenol colour and the polarographic reduction peak at -0.33 V [4] were observed but the extent of reaction was much less than would be the case with nitroprusside present. Sulphadiazine at the 10^{-3} M level gave the yellow colour and a polarographic wave ($Ep = -0.63$ V); the absorbance and peak currents obtained were consistent with about 10% of the sulphadiazine reacting. Two other pyrimidine sulphonamides, sulphamerazine and sulphadimidine, and also sulphapyridine give a slight reaction at the 10^{-2} M level indicating about 1% reaction. No colour reactions or polarographic waves were observed for sulphathiazole, sulphasomidine, sulphaphenazole, sulphamethizole, guanidinium chloride or benzene sulphonamide.

Discussion

The colorimetric and polarographic procedures described are reasonably selective for sulphaguanidine, and could be applied advantageously for identification as well as determination. Good precision is possible if the reaction conditions and heating times are properly controlled, so that the procedures may be of value even though the clinical use of sulphaguanidine is declining.

The nature of the yellow species is not known: the colour remains yellow on acidification. When oxidized with hypochlorite under acidic conditions followed by reaction with phenol in alkali, sulphaguanidine gives the blue species ($\epsilon = 1.07 \times 10^4$ l mol^{-1} cm^{-1} at 625 nm) obtained with other sulphonamides and many other compounds [5].

REFERENCES

1 C. T. H. Ellcock and A. G. Fogg, Lab. Pract., 23 (1974) 555.
2 W. F. Davis, J. W. Graab and E. J. Merkle, Talanta, 18 (1971) 263.
3 J. H. Swinehart, Coord. Chem. Rev., 2 (1967) 385.
4 A. G. Fogg and Y. Z. Ahmed, Anal. Chim. Acta, 101 (1978) 211.
5 D. R. Davis, A. G. Fogg, D. T. Burns and J. S. Wragg, Analyst, 99 (1974) 12.

Short Communication

NEUTRAL LIPID SENSOR BASED ON IMMOBILIZED LIPASE AND A FLOW-THROUGH pH ELECTRODE

IKUO SATOH, ISAO KARUBE* and SHUICHI SUZUKI

Research Laboratory of Resources Utilization, Tokyo Institute of Technology, 4259 Nagatsuta-cho, Midori-ku, Yokohama, 227 (Japan)

KATSUAKI AIKAWA

TOA Electronic Co., 1-chome, Takadanobaba, Shinjuku-ku, Tokyo 160 (Japan)

(Received 18th July 1978)

Many enzyme electrodes have been developed for clinical analysis [1]. A few reports have been published on enzyme electrodes for lipid determination [2—4]. Lipoprotein lipase hydrolyzes neutral lipids in serum to glycerol and fatty acids. The fatty acids can be determined with a pH electrode, so that neutral lipids can be determined indirectly by lipoprotein lipase and a pH electrode. A neutral lipid sensor with a reactor containing a lipase—collagen membrane and a combined glass electrode, for determinations in serum has been described [3]. However, the time required for each determination was 30 min, because of the low activity of the immobilized lipase. In this report, lipoprotein lipase is covalently bound to polystyrene sheets coated with γ-aminopropyltriethoxysilane, and a new flow-through pH electrode is described as the sensor.

Experimental

Materials. Lipase (glycerol ester hydrolase; EC. 3.1.1.3., from *Pseudomonas* sp., twice recrystallized, 2000 I.U. mg^{-1}; Amano Pharmaceutical Co.). Glyceryl trioleate (olein; Tokyo Kasei Kogyo) was distilled under reduced pressure (152°C at 0.5 mm Hg), and used as the standard triglyceride. Polystyrene sheet (Amano Pharmaceutical Co.), human serum (Japanese Red Cross Central Blood Center, Shibuya, Tokyo) were used. Other solvents and reagents were analytical- or laboratory-grade materials. Glass-distilled water was used.

Preparation of the immobilized enzyme. Polystyrene sheet (thickness, 0.5 mm) was cut into slices of 1—4 mm², which were suspended in γ-aminopropyltri-ethoxysilane for 10 min and washed with distilled water. The slices were treated with 1.0% (w/v) glutaraldehyde solution (in 0.1 M phosphate buffer, pH 7.0) for 1 h at room temperature and packed into a silica tube (0.6 cm i.d., 4 cm long). The aqueous enzyme solution (20 ml of 15 mg ml^{-1} solution in 0.1 M phosphate buffer, pH 7.0) was passed through the column and

recycled for 1 h at room temp. This enzyme reactor contained 0.6 I.U. of lipase.

Enzyme and lipid assay. Lipase activity was determined by the method of Dole [5], with *p*-nitrophenyl acetate as substrate. Neutral lipids were determined by the acetylacetone method [6].

Apparatus. The flow system used for determination of neutral lipids is illustrated in Fig.1. Figure 2 shows the flow-through pH electrode (specially constructed by TOA Electronics Co.). The electrode system consisted of a tubular glass responsive membrane electrode and a saturated calomel electrode, connected via a ceramic junction (2-mm diameter) at the bottom of the tubular electrode. The resistance of the tubular electrode was 10 MΩ; its total internal volume of the electrode was 110 μl.

Procedure for determination of lipids in serum. The serum (200 μl) was added to 3 ml of isopropanol in a 15-ml centrifuge tube, 0.7 g of adsorbent (silicic acid) was added, mixed for 5 min and then centrifuged at 2000 G for 5 min. The supernatant liquid obtained was injected into the system. Tris—HCl buffer (0.5 $\times$ 10^{-3} M, pH 7.0) solution was continuously transferred to the system during measurements. The concentration of Tris—HCl buffer was so low that the buffer action of the solution was very weak, and pH changes could be measured in the presence of the buffer.

Results

Figure 3 shows the electrode responses for various amounts of olein. The potential of the glass electrode increased with time until a maximum was reached. The time required to reach the maximum was 1 min; the potential returned to its initial level within 3 min.

The relationship between the logarithm of the concentration of the olein and the potential difference is linear, changing by 8 mV over the range 5—50 μM.
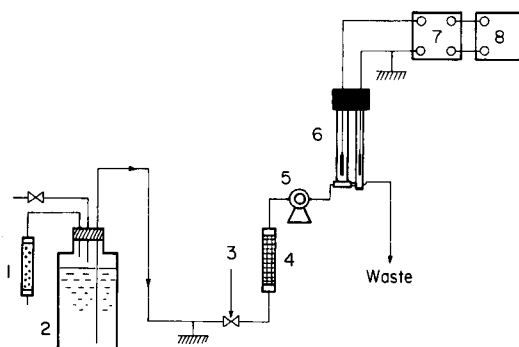
Fig. 1. Schematic diagram of neutral lipid sensor: 1 soda lime, 2 buffer reservoir, 3 sample inlet, 4 immobilized lipase reactor, 5 peristaltic pump, 6 flow pH electrode, 7 electrometer, 8 recorder.
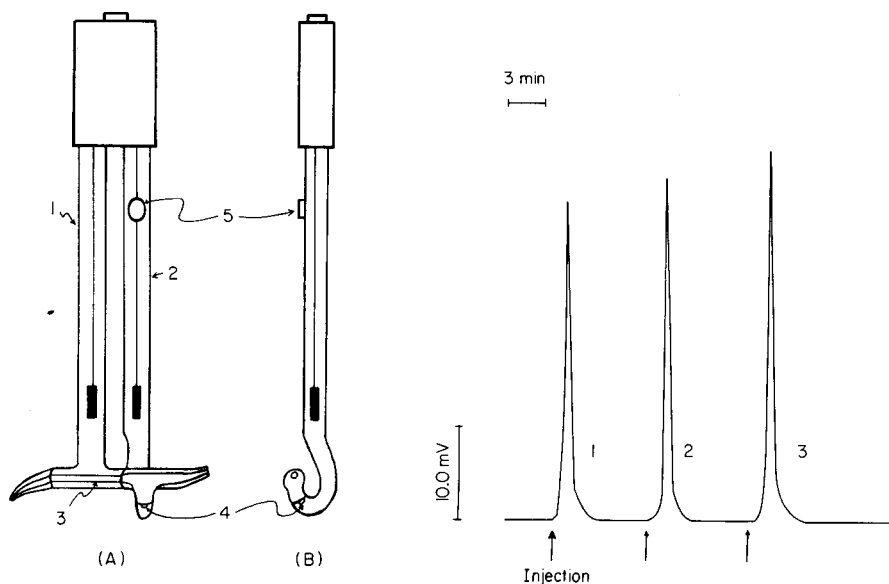
Fig. 2. Schematic diagram of flow-type pH electrode. (A) Front view; (B) side view. (1) Glass electrode (7 mm o.d., 9 cm long); (2) SCE; (3) tubular responsive glass membrane; (4) junction; (5) saturated KCl inlet.

Fig. 3. Response curves for glyceryl trioleate (olein). (1) 15.5 μM; (2) 30.0 μM; (3) 43.5 μM, at 20°C and pH 8.30; flow rate 72 ml h^{-1}.
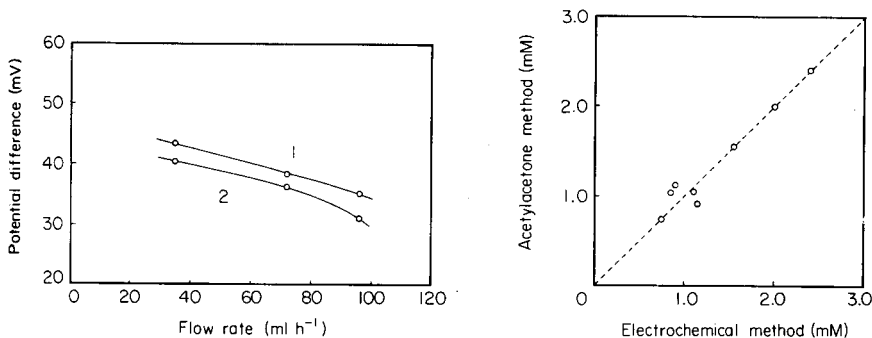
Fig. 4. Relationship between flow rate and potential difference for: (1) 43.5 μM; (2) 30.0 μM olein (standard conditions at 20 ± 0.1°C).

Fig. 5. Comparison of electrochemical and acetylacetone methods.

Figure 4 shows the effect of flow rate on the response of the electrode to two lipid concentrations. A decrease in the potential difference with increase in flow rate was observed. If the flow rate was < 70 ml h^{-1}, the immobilized lipase had sufficient time measurably to hydrolyze cholesterol esters. There-

fore, a flow rate of 72 ml h^{-1} is recommended for lipid determinations if cholesterol esters are present.

The re-usability of the sensor was examined with various concentrations of the trioleate. Lipid determinations were done 20—25 times a day, and no decrease in the response was observed over a 10-day period. The potential difference was reproducible to within 5%.

Neutral lipids were isolated from various human sera with isopropanol as described above, and determined by the conventional acetylacetone method and the electrochemical method. The results, compared in Fig. 5, show a good correlation. Therefore, the sensor can be used for the determination of neutral lipids in human sera.

Discussion

The lipase used in this study was a lipoprotein lipase with properties very similar to, if not identical with, those of the lipoprotein lipase of postheparin plasma and other animal tissues in regard to substrate selectivity and response to specific inhibitors such as sodium taurocholate, sodium lauryl sulfate, sodium dodecylbenzene sulfate and copper(II) sulfate [7].

Neutral lipids in serum are solubilized as lipoproteins and remain mainly as chyromycron and low-density lipoproteins. The immobilized lipase hydrolyzes the neutral lipids in serum to glycerol and fatty acids. As fatty acids are partly dissociated, the activity of hydrogen ion in the solution is proportional to fatty acid concentration in the sample solution. Thus the measured maximum potential difference is proportional to the logarithm of the lipid concentration, i.e. $\Delta E = k \log C$, where ΔE is the difference between the initial and maximum potentials, C is the lipid concentration and k is a constant.

In these studies, the lipase was immobilized covalently on the surface of the polystyrene slice. The activity of the immobilized lipase (1.2 I.U. per g of polystyrene) was 10 times higher than that reported previously (0.12 I.U. per g collagen) [3]. It is well known that the composition of each human serum is quite different. Proteins and various ions in serum affect the potential determined by the glass electrode. Therefore, the neutral lipid fraction was extracted with isopropanol. As a result, the total analysis time was only 4 min. The results obtained the lipid sensor were in good agreement with those obtained by the conventional method. A rapid and continuous determination of lipid is possible with the lipid sensor.

REFERENCES

1 G. G. Guilbault, in G. Svehla, (Ed.), Wilson and Wilson's Comprehensive Analytical Chemistry, Vol. VIII, Elsevier, Amsterdam, 1977, p. 1.
2 I. Satoh, I. Karube and S. Suzuki, Biotechnol. Bioeng., 19 (1977) 1095.
3 I. Satoh, I. Karube and S. Suzuki, J. Solid-Phase Biochem., 2 (1977) 1.
4 H. Huang, S. S. Kuan and G. G. Guilbault, Clin. Chem., 23 (1977) 671.
5 V. P. Dole, J. Clin. Invest., 35 (1956) 150.
6 M. J. Fletcher, Clin. Chim. Acta, 22 (1968) 393.
7 T. Narasaki and A. Kondo, Tech. Bull. Fac. Agric. Kagawa Univ., 24 (1973) 137.

Short Communication

DETERMINATION OF DIBUTYL AND MONOBUTYL PHOSPHATES IN TRIBUTYL PHOSPHATE KEROSENE MIXTURES BY SOLVENT EXTRACTION AND GAS CHROMATOGRAPHY

YANG-CHIH LEE* and GANN TING

Institute of Nuclear Energy Research, Atomic Energy Council, P.O. Box 3, Lung-Tan (Taiwan)

Tributyl phosphate (TBP) undergoes degradation when it is exposed to acids, heat or radiation, with the formation of dibutyl phosphate (DBP), monobutyl phosphate (MBP) and phosphoric acid [1—3]. The amounts of MBP and phosphoric acid formed under certain conditions are very small, but the amount of DBP formed is significant. As several cations, e.g. UO_2^{2+}, $Th(NO_3)_2^{2+}$, and $Zr(OH)_2^{2+}$ form organic-soluble complexes with DBP, the effect of the degradation is a progressive reduction in the efficiency of removal of fission products, with loss of uranium and thorium to waste effluent streams, and emulsification or precipitation within the contactors.

As reported by previous workers [4, 5] the degradation products in recycled solvents may be removed by washing with sodium carbonate solution or repeated alkali and acid washing. To control the efficiency of this solvent-recovery procedure and the composition of the fresh and recycled solvent, a procedure for determining DBP and MBP in TBP—kerosene mixtures is required.

The impurities from TBP in kerosene and recovery solvents for the Purex and Thorex systems have been expressed indirectly by solvent activities and β, γ-decontamination factors [6, 7]. The extraction of $ZrO(NO_3)_2$ is proportional to the total molar concentration of MBP and DBP, and the partition of $Zr(SO_4)_2$ is proportional to the molar concentration of MBP [8]. The best method for the direct simultaneous determination of DBP and MBP in TBP is g.l.c. [9]. The acidic components contained in the TBP—dodecane system were determined [10, 11] by g.c.—m.s. and g.l.c. was used [12] to determine 2—10% DBP and 0.6—3.2% MBP in various solvents containing TBP. G.l.c. cannot be used when TBP is diluted by a mixture of hydrocarbons because the large hydrocarbon peaks overlap the small MBP and DBP peaks [8]. Ertel et al. [13] reported the separation of DBP from TBP by carbonate—fluoride stripping, re-extraction into chloroform and determination by g.l.c. On the basis of these previous studies, a new extraction-separation and gas chromatographic determination of DBP and MBP in 30% TBP—kerosene has been established.

Experimental

Materials. TBP (Merck) and DBP, MBP and *p*-tolylsulphonyl methylnitros-amide (Tokyo Kaisei Chemical Industries Ltd., Japan) were used. Kerosene was obtained from Chinese Petroleum Corporation. All other chemicals were analytical grade.

A Shimazu GC-5A chromatograph with f.i.d. and a minigrator (Spectra Physica) were used for quantitative analysis. A glass column (3 m × 2.6 mm i.d.) packed with 60—80 mesh Chromosorb W (AW DMCS) coated with 15% (w/w) of Carbowax 20 M was used for the separation of the alkyl esters. A 5-μl microsyringe (SGE-5A-RN-GP) was used.

Procedure. The separation procedure for determining DBP and MBP in 30% TBP—kerosene is shown in Fig. 1. A known amount of commercial DBP (mixture of DBP and MBP) was dissolved in 30% TBP—kerosene; the DBP and MBP were extracted into the aqueous phase as NaDBP and Na$_2$MBP. The separated aqueous solution, acidified with dilute hydrochloric acid to convert the sodium salts to DBP and MBP, was extracted with ether, carbon tetra-chloride, chloroform or n-amyl alcohol to find the best solvent. To compare the recovery yields, the separation scheme was repeated several times. The extracted DBP and MBP were converted with diazomethane to volatile methyldibutyl phosphate (MDBP) and dimethylbutyl phosphate (DMBP)
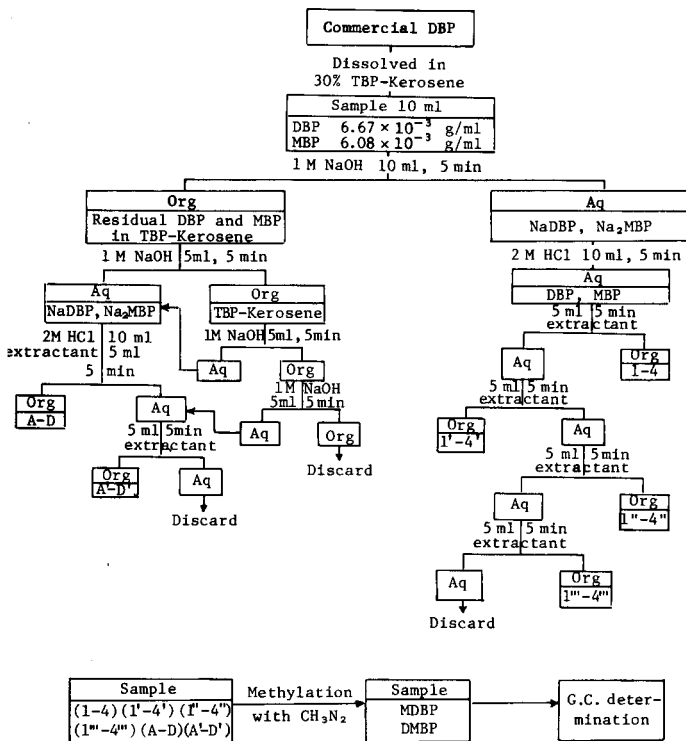
Fig. 1. Separation scheme for extraction of DBP and MBP.

respectively; the diazomethane was prepared by treating *p*-tolylsulphonyl methylnitrosamide with alcoholic potassium hydroxide [8]. Finally, MDBP and DMBP were determined by g.l.c. The optimum shaking time and extractants are discussed below.

Results and discussion

The simplest way to determine DBP and MBP in 30% TBP—kerosene is to analyze the mixtures, without separation, by g.l.c. but Table 1 shows that the overlapping and interference problem is serious; prior separation of the DBP and MBP is required for the determination of small amounts of DBP and MBP in 30% TBP—kerosene. Commercial DBP (a mixture of DBP and MBP) was titrated with sodium hydroxide solution and back-titrated with hydrochloric acid. The results indicated that the rate of reaction was as fast as that of a strong acid. On the basis of these reactions, attempts to separate DBP and MBP from kerosene—TBP mixtures were made with ethyl ether, carbon tetrachloride, chloroform and n-amyl alcohol as extractants. A typical gas

TABLE 1

The retention times of kerosene, DMBP, MDBP and TBP under various experimental conditions with an injection temperature of 210°C

Column conditions	Retention time (min)			
	Kerosene	DMBP	MDBP	TBP
180°C	0—20	6.3	11.0	16.5
70°C (2 min) 70—180°C (4°C min^{-1}) 180°C (25 min)	0—51	27.0	33.4	41.4
70°C (2 min) 70—180°C (4°C min^{-1}) 150—170°C (2°C min^{-1}) 170°C (30 min)	0—58	33.2	41.3	52.8
80°C (2 min) 80—140°C (4°C min^{-1}) 140°C (20 min) 140—180°C (2°C min^{-1}) 180°C (8 min)	0—65	33.4	49.2	55.1
80°C (2 min) 80—130°C (4°C min^{-1}) 130°C (28 min) 130—170°C (1°C min^{-1}) 170°C (6 min)	0—85	42.0	66.2	83.1
70°C (2 min) 70—140°C (4°C min^{-1}) 140—170°C (1°C min^{-1}) 170°C (20 min)	0—70	33.2	45.7	65.1
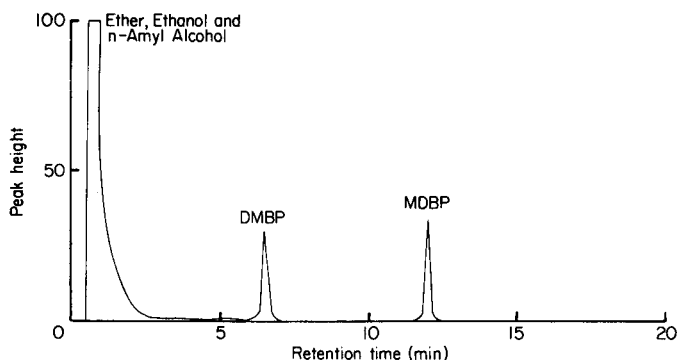
Fig. 2. Gas chromatogram of solution separated from 30% TBP—kerosene mixtures.
Injection temperature, 210°C; column temperature, 180°C.

chromatogram of the separated organic phase (Fig. 2) shows that no interference is present and the separation of DBP and MBP from the 30% TBP—kerosene mixture, is satisfactory. The results (Table 2) indicate that the efficiency of separation of DBP and MBP with either ethyl ether or carbon tetrachloride as extractant is not satisfactory, in agreement with previous studies [14, 15]. The results for chloroform extractant are also shown in Table 2; chloroform is a good extractant for the separation of DBP from 30% TBP—kerosene mixtures. Stewart and Crandall [14] reported that the distribution coefficients of DBP and MBP between n-amyl alcohol and water are ca. 1000 and 2.9, respectively, and Table 2 shows that n-amyl alcohol is the best extractant for the separation of DBP and MBP from TBP—kerosene mixtures. Systematic studies of the extraction of DBP and MBP with n-amyl alcohol at different shaking times (5—30 min), summarized in Table 3, suggest that n-amyl alcohol is a very good extractant for the separation of DBP and MBP from 30% TBP—kerosene mixtures. The accuracy of this analytical technique was obtained by adding different concentrations of DBP (15—1270 μg ml^{-1}) and MBP (14—1121 μg ml^{-1}) to 30% TBP—kerosene solutions. The average recovery for a single extraction (stages 1—4, Fig. 1) for DBP and MBP is 97.84 ± 3.00% and 61.76 ± 2.65%, respectively. The average error for the determination of DBP is 2.51%. The approximate limits for the determination of DBP and MBP in TBP—kerosene mixtures is ca. 10 μg ml^{-1}. The time required for one determination is ca. 1 h but this can be reduced if a large number of samples is involved.

This method has been used to study the levels of DBP and MBP in recycled solvents; the standard deviation for concentrations of ca. 10 μg ml^{-1} is ± 1.41 μg ml^{-1} and ± 1.24 μg ml^{-1} for DBP and MBP, respectively. This analytical procedure is a rapid and convenient method for determining the composition of fresh and recycled solvents; it can also be used to indicate the efficiency of the solvent recovery procedure for TBP—kerosene extractants.

TABLE 2

The extraction of DBP and MBP with ethyl ether, carbon tetrachloride, chloroform and n-amyl alcohol with a shaking time of 5 min

Extractant	Component	Recovery (%) from stages (Fig. 1)						Total recovery	K_d
		1–4	1'–4'	1"–4"	1'''–4'''	A–D	A'–D'		
Ethyl ether	DBP	85.09 ± 2.29	7.69 ± 0.80	2.63 ± 0.67	0.89 ± 0.21	1.55 ± 0.15	0.32 ± 0.10	98.17 ± 2.53	7.59
	MBP	11.05 ± 0.70	2.97 ± 0.50	2.70 ± 0.90	1.03 ± 0.08	2.88 ± 0.92	0.58 ± 0.04	21.21 ± 1.55	0.12
Carbon tetrachloride	DBP	83.55 ± 3.15	11.86 ± 2.17	2.96 ± 0.08	1.71 ± 0.71	1.50 ± 0.37	0.42 ± 0.27	102.00 ± 3.92	5.64
	MBP	4.96 ± 0.36	3.88 ± 1.61	1.23 ± 0.34	—	—	—	10.07 ± 1.69	0.05
Chloroform	DBP	95.79 ± 1.72	2.86 ± 0.33	0.33 ± 0.03	—	0.94 ± 0.17	0.11 ± 0.02	100.03 ± 1.76	30.03
	MBP	0.67 ± 0.04	0.29 ± 0.02	0.23 ± 0.06	—	—	—	1.19 ± 0.07	0.01
n-Amyl alcohol	DBP	98.07 ± 2.43	0.89 ± 0.26	0.11 ± 0.02	—	0.78 ± 0.23	0.18 ± 0.11	100.03 ± 2.46	98.07
	MBP	60.53 ± 1.69	23.05 ± 0.27	9.80 ± 0.51	9.66 ± 0.15	2.52 ± 0.13	1.12 ± 0.03	99.68 ± 1.80	1.70

TABLE 3

Studies of the extraction of DBP and MBP with n-amyl alcohol at different shaking times

Component	Shaking time (min)	Recovery (%) from stages (Fig. 1)						Total recovery
		1—4	1'—4'	1"—4"	1'''—4'''	A—D	A'—D'	
DBP	5	96.71	0.69	0.56	0.19	1.39	0.21	99.75
	10	97.72	1.61	0.26	0.17	2.61	0.17	102.54
	20	98.64	1.33	0.80	0.29	1.33	0.20	102.59
	30	96.62	0.78	0.35	0.15	1.68	0.05	99.93
MBP	5	62.50	23.30	7.94	2.54	1.94	1.68	99.90
	10	61.60	22.67	8.65	3.25	2.35	0.41	98.93
	20	60.93	23.96	7.91	1.01	2.42	1.50	97.73
	30	63.67	22.17	7.27	2.58	2.04	1.04	98.77

REFERENCES

1 L. L. Burger and E. D. McClanahan, Jr., USAEC Report HW-52943 (1957).
2 J. D. Goode, USAEC Report ORNL-2287 (1957).
3 A. T. Gresky, USAEC Report ORNL-1518 (1953).
4 R. H. Ellerhorst and R. K. Klopfenstein, USAEC Report NLCO-744 (1958).
5 R. K. Klopfenstein, J. H. Krekeler and D. E. Richards, USAEC Report NLCO-815 (1960).
6 W. Davis, Jr., USAEC Report ORNL-2848 (1960).
7 D. W. Brite, USAEC Report HW-30463 (1954).
8 A. H. Kibkey and W. Davis, Jr., USAEC Report ORNL-TM-2289 (1968).
9 C. J. Hardy, J. Chromatogr., 13 (1964) 372.
10 R. Becker and L. Stieglitz, KFK-1373 (1973).
11 B. G. Brodda and E. Merz, Fresenius Z. Anal. Chem., 273 (1975) 2.
12 A. Brignocchi, G. M. Gasparini and M. Pizzichini, AEC-TR-7587 (1973).
13 D. Ertel, P. Groll, G. Knittel and W. Thesis, J. Radioanal. Chem., 32 (1976) 297.
14 D. C. Stewart and H. W. Crandall, J. Am. Chem. Soc., 73 (1951) 1377.
15 C. J. Hardy and D. Scargill, J. Inorg. Nucl. Chem., 10 (1959) 323.

Short Communication

SPECTROPHOTOMETRIC AND TITRIMETRIC METHODS FOR THE DETERMINATION OF VITAMIN C BASED ON ITS REACTION WITH THE FERRICINIUM CATION

M. M. ALY

Chemistry Department, Faculty of Science, Assiut University, Assiut (Egypt)

Interest in the versatile chemistry of ferrocene stems from the ease with which an electron can be removed from the iron(II) atom to produce the ferricinium cation [1, 2] which in turn may behave as a strong electron acceptor under appropriate conditions. The intermediate formation of the ferricinium cation and its subsequent reduction to ferrocene by a hydrogen atom has been suggested to account for the isolation of ring-substituted ferrocenes from the reaction of diazonium salts with ferrocene [3—6]. This mechanism prompted the present investigation of the reaction of the ferricinium cation with ascorbic acid (which can provide two hydrogen atoms) and its analytical applications.

Experimental
Chemicals and equipment. Spectroscopic-grade solvents, de-ionized water, B.D.H. chemicals and Hopkin and Williams buffers were used. Ferricinium trichloroacetate was prepared by dissolving ferrocene (0.027 mol) in a solution of trichloroacetic acid (0.27 mol) in carbon tetrachloride (150 ml). The solution was saturated with oxygen and left for 2 days. The precipitated crystalline reagent was filtered off, washed with carbon tetrachloride and dried under vacuum over phosphorus pentoxide. This salt was characterized [2] as $(C_5H_5)_2Fe^+(HB)^-(HB)_2$ in the solid state (HB = trichloroacetic acid); $(HB)^-$ converts to B^- in water. Freshly prepared stock solutions of ferricinium trichloroacetate (1.6063 g in 250 ml of water) and ascorbic acid (1.1019 g in 500 ml of water) were prepared. Electronic spectra were measured with a Unicam SP800 spectrophotometer.
Spectrophotometric determination of ascorbic acid. A suitable aliquot of the ascorbic acid solution was added to a mixture containing the ferricinium trichloroacetate solution (10 ml), buffer (10 ml) and chloroform (10.0 ml), and the resulting solution was shaken for 2 min. The absorbance of the filtered yellow chloroform layer was measured at 440 nm against a chloroform blank.
Titrimetric determination of ascorbic acid. A suitable aliquot of ascorbic acid solution was added to the buffer solution (10 ml) followed by chloroform

(10 ml); this solution was titrated with the violet-red solution of ferricinium trichloroacetate, which acts as its own indicator. The end-point is indicated by a faint blue colour. End-point detection is facilitated by extraction of the ferrocene formed from the aqueous layer into chloroform.

Blank analyses were run and the values obtained were subtracted, as appropriate, from the absorbance or from the volume of titrant required. Benzene or tetrachloromethane could replace chloroform as the non-aqueous layer in either method. The formation of ferrocene in the non-aqueous layer in the spectrophotometric method and the consumption of the ferricinium salt in the titrimetric method were almost instantaneous when the pH values of the reaction solutions were above 2. At pH values of 2 and 1, the reaction was slower, so that solutions had to be shaken for 5 min. In some experiments, ferrocene was identified in the chloroform layer by its electronic spectrum (two peaks at 440 and 325 nm); in others, the chloroform was evaporated, the residue was sublimed, and the sublimate was characterized as ferrocene by melting points and electronic spectrum. The aqueous layer in the titrimetric method gave negative tests for iron(III) with thiocyanate or acetylacetone.

Results and discussion

The spectrophotometric and titrimetric data are shown in Tables 1 and 2, respectively. The ratio $B/A = 2$ with an average error of $\pm 4\%$. Accordingly, the reaction of ascorbic acid with ferricinium trichloroacetate is

$2(C_5H_5)Fe^+CCl_3CO_2^-(CCl_3CO_2H)_2$ + Ascorbic acid → 2 Ferrocene + Dehydroascorbic acid + 6 CCl_3CO_2H.

TABLE 1

Spectrophotometric determination of ascorbic acid based on its reaction with ferricinium trichloroacetate at different pH values

pH	Ascorbic acid added (A) ($\times 10^{-6}$ mol)	Ferrocene detected (B) [a] ($\times 10^{-6}$ mol)	B/A	% Error
3	2.504	5.19 (0.052)	2.073	+3.65
	6.26	12.97 (0.130)	2.072	+3.60
	12.52	24.25 (0.243)	1.937	−3.15
	18.78	38.32 (0.384)	2.040	+2.00
	25.04	49.50 (0.496)	1.977	−1.15
2	2.504	5.090	2.033	+1.65
	6.26	13.07	2.088	+4.4
1	2.504	5.190	2.073	+3.65
	6.26	12.97	2.072	+3.60

[a]Calculated from the ferrocene absorption peak at 440 nm ($\epsilon = 100.2$ l mol^{-1} cm^{-1}). Absorbances are given in parenthesis for experiments carried out at pH 3 (1.0-cm cell). The amoun of ferrocene formed in the absence of ascorbic acid decreases from 6.19×10^{-5} mol at pH 7 to 2.495×10^{-5} mol at pH 4, 3.0×10^{-6} mol at pH 3.0, and 2.0×10^{-6} mol at pH 2.0.

TABLE 2

Titrimetric determination of ascorbic acid with ferricinium trichloroacetate at pH 1—6

pH	Ascorbic acid added (A) ($\times 10^{-6}$ mol)	Ferricinium compound required $(B)^a$ ($\times 10^{-6}$ mol)	B/A	% Error
6	2.292	4.481	1.955	−2.25
	4.584	9.260	2.020	+1.00
	11.469	23.599	2.058	+2.90
	22.922	44.082	1.923	−3.85
	57.304	120.485	2.103	+5.15
5	2.292	4.523	1.973	−1.35
	11.469	23.898	2.084	+4.20
4	2.292	4.780	2.086	+4.30
	11.469	23.690	2.066	+3.30
3	2.292	4.730	2.064	+3.20
	11.469	23.599	2.058	+2.90
	22.922	45.804	1.998	−0.10
2	2.292	4.481	1.955	−2.25
	11.469	23.898	2.084	+4.20
1	2.292	4.580	1.998	−0.10
	11.469	23.699	2.066	+3.30

^{a}Calculated from the faint blue end-point to the titrations.

A linear relationship is obtained on plotting the absorbance of the ferrocene formed at pH 3 (Table 1) against the molar concentration of the added ascorbic acid. The ferricinium cation decomposes to ferrocene and other products in neutral or slightly acidic solutions (footnote, Table 1). The cation is, however, stable at pH 2—3 and the spectrophotometric determination of ascorbic acid is possible under these acidic conditions. This limitation does not apply to the titrimetric method, apparently because the preferred reaction of the added ferricinium cation is with ascorbic acid and the ferrocene formed impedes the decomposition of the cation. This explanation accords with the facts that the blue solution produced at the end-point is stable for several hours and that the results are reproducible. The slower rate of reaction of the cation with ascorbic acid at pH 2 and 1, compared with other acidic conditions is compatible with the observed stability of the cation in highly acidic solution.

The results shown in Tables 1 and 2 indicate that as little as 0.6 mg of the vitamin can be determined by this reaction. The method has some advantages over some known methods. Thus, the preparation of the stable ferricinium salt does not involve elaborate chemical preparations, and aqueous solutions are fairly stable. Iron(II) does not interact with the ferricinium salt, and so does not interfere with the determination, which is an advantage over both the B.P. method [7] (titration with ammonium cerium(IV) sulphate) and the

U.S.P. method [8] (titration with 2,6-dichlorophenolindophenol). The stability of the non-aqueous extract of the ferrocene formed in the spectrophotometric determination for several days, and the use of the blue ferricinium salt as its own indicator, enhance the applicability of the methods compared to other published procedures. Thus, the colour formed in the reaction of diazotized 4-methoxy-2-nitroaniline fades after 10 min ⌊9⌋. The coupling of dehydroascorbic acid (obtained by the oxidation of ascorbic acid) with 2,4-dinitrophenylhydrazine does not provide a specific method for the determination of the vitamin, because 2,3-diketogulonic acid (a decomposition product of ascorbic acid in pharmaceutical preparations) reacts similarly [10]; the necessary modification is a time-consuming process that involves three separate determinations [11]. In the direct titration of ascorbic acid with cerium(IV) sulphate and ferroin indicator, results tend to be high unless phosphoric acid is added, but this addition retards the direct reaction between ascorbic acid and cerium(IV) and accurate pH adjustment is essential [12]. The proposed method has a clear advantage over the method of Eldawy et al. [13] which is based on some uncharacterized coloured reaction product obtained from the reaction of dimethoxydiquinone with ascorbic acid. The method involves the tedious preparation of the diquinone, and the reddish-violet colour produced with ascorbic acid is stable only in the dark.

No interferences were observed, in either the spectrophotometric or the titrimetric determinations, on using suitable portions of a mixture containing ascorbic acid (50 mg) and any of the following compounds; vitamin B_1 (2 mg), vitamin B_2 (3 mg), vitamin B_6 (1 mg), vitamin B_{12} (1 μg), folic acid (0.02 mg), nicotinamide (20 mg), calcium pantothenate (10 mg), biotin (0.02 mg), vitamin E (5 mg), iron(II) sulphate (15 mg), copper(II) sulphate (0.33 mg), manganese sulphate (0.33 mg), magnesium sulphate (2 mg), potassium sulphate (2 mg), zinc sulphate (2 mg), calcium fluoride (1 mg), sodium molybdate (1 mg), DL-methionine (20 mg), aspartic acid (20 mg), glutamic acid (25 mg), ethinyl estradiol (1 mg), methyl testosterone (2 mg), fructose (100 mg), glucose (200 mg), mannose (200 mg), sucrose (200 mg), starch (100 mg), lactose (150 mg) and dehydroascorbic acid (20 mg).

The ascorbic acid added could be determined in such mixtures, which were of composition similar to that of multivitamin preparations, with an average error of about 4%. It is suggested, therefore, that the proposed methods are suitable for routine determinations of vitamin C either alone or in commercial multivitamin preparations. The methods are very simple, rapid, and sufficiently sensitive.

REFERENCES

1 M. M. Aly, R. Bramely, J. Upadhyay, A. Wasserman and P. Wooliams, Chem. Commun., (1965) 404.
2 M. M. Aly, D. V. Banthorpe, R. Bramely, R. E. Cooper, D. W. Jopling, J. Upadhyay, A. Wasserman and P. Wooliams, Monatsh. Chem., 98 (1967) 887.

3 M. Rosenblum, W. G. Howells, A. K. Banerjee and C. Bennett, J. Am. Chem. Soc., 84 (1962) 2726.
4 W. F. Little and A. K. Clark, J. Org. Chem., 25 (1960) 1979.
5 A. L. Beckwith and R. J. Leydon, Tetrahedron Lett., 6 (1963) 385.
6 W. F. Little, K. Lyna and R. Williams, J. Am. Chem. Soc., 85 (1963) 3055.
7 British Pharmacopoeia 1968, p. 65.
8 U.S. Pharmacopeia, 18th Revision, Mack Co., Easton, Pa., 1970, p. 52.
9 M. Schmall, C. W. Pifer and E. G. Wollish, Anal. Chem., 25 (1953) 1486.
10 J. H. Roe and C. A. Kuether, J. Biol. Chem., 147 (1943) 399.
11 J. H. Roe, M. B. Mills, M. J. Oesterling and C. M. Damron, J. Biol. Chem., 174 (1948) 201.
12 G. G. Rao and G. S. Sastry, Anal. Chim. Acta, 56 (1971) 335.
13 M. A. Eldawy, A. S. Tawfik and S. R. Elshabouri, Anal. Chem., 47 (1975) 461.

Short Communication

DETERMINATION OF THORIUM IN NATURAL WATERS AFTER EXTRACTION WITH ALIQUAT-336

M. COSPITO* and L. RIGALI

CAMEN, S. Piero a Grado, Pisa 56010 (Italy)

(Received 29th September 1978)

The thorium content of natural waters is usually at the ppb level, so that its determination requires a preliminary concentration step. Among the methods available, co-precipitation of thorium oxalate with calcium as the carrier [1] is frequently used and forms the basis of an ASTM standard method for thorium in waters and waste waters [2]. This co-precipitation, however, does not eliminate most of the substances which interfere in the available colorimetric methods for thorium. A separation step is therefore required.

In the method described below, co-precipitation is followed by a selective extraction with Aliquat-336 dissolved in xylene; thorium is finally determined spectrophotometrically with arsenazo-III. Aliquat-336, an aliphatic quaternary ammonium salt, has been used to separate thorium from low-grade ores [3] and provides a valuable separation from many interfering elements, e.g. zirconium, hafnium, molybdenum, titanium and rare earths, which unavoidably follow thorium during the co-precipitation with calcium oxalate.

Experimental

Standard thorium solution (1µg Th ml⁻¹). Dilute an aliquot of stock solution of thorium chloride (2.0 mg Th ml⁻¹) suitably with 8 M hydrochloric acid. Prepare working standards daily.

Aliquat-336 solution. Dissolve 50 g of Aliquat-336 (tricaprylmethylammonium chloride; technical grade, General Mills) in xylene and dilute to 1 l. Shake three times in a separatory funnel with 250-ml portions of 4 M nitric acid to convert the quaternary ammonium salt to the nitrate form.

All reagents were of good reagent-grade quality. Twice-distilled water was used.

Collection and pretreatment. Collect the water samples in plastic bottles and filter through Millipore 0.45-µm filters as soon as possible. Add 25 ml of concentrated nitric acid per litre of water to give pH ≤ 0.5. Conserve in plastic bottles. Analyse as quickly as possible.

Coprecipitation. To 1.025 l of the acidified water in a 2-l beaker, add 10—15 ml of calcium nitrate solution (20 mg Ca ml⁻¹ in 0.5 M nitric acid).

Add 10 ml of 36% (w/v) hydrogen peroxide solution and 50 ml of 4.0% (w/v) ammonium oxalate solution in 0.5 M nitric acid (25 mg $C_2O_4^{2-}$ ml^{-1}). If any precipitate forms, add concentrated nitric acid dropwise until it disappears. Add ammonia liquor dropwise with vigorous stirring until the pH is 1.8 ± 0.1 (pH meter). Heat to 70—80°C. Allow to stand for about 3 h, without further heating. Check the completeness of precipitation by adding 1 ml of the 4% ammonium oxalate solution to the supernatant liquid. Remove the supernate by suction with a tube fitted with a porous sintered glass filter. Transfer the wet precipitate to a centrifuge tube, centrifuge at 5,000 rpm, wash with oxalate wash solution (1% w/v ammonium oxalate adjusted to pH 1.8 ± 1 with nitric acid), and transfer the precipitate to the original 2-l beaker. Dissolve the precipitate in (1 + 1) nitric acid. Evaporate twice almost to dryness and finally dissolve in 30 ml of 4 M nitric acid.

Solvent extraction. Transfer to a 200-ml separatory funnel. Extract twice with 30-ml portions of Aliquat-336 solution. Discard the aqueous phase, combine the organic extracts, wash with 40 ml of 4 M nitric acid and finally strip with two 50-ml portions of 3 M hydrochloric acid. Centrifuge to obtain good phase separation. A period of 6 min suffices to attain equilibrium in all cases. Combine the acid extracts in a 200-ml beaker and discard the organic phase. Evaporate almost to dryness on a sand-bath, and then to dryness, carefully avoiding carbonization of any organic matter. Add two successive portions of 3 ml of concentrated hydrochloric acid, boil and again evaporate to dryness. Dissolve the residue in 5 ml of 8 M hydrochloric acid. If any opalescence appears, repeat the treatment with concentrated hydrochloric acid.

Determination. Transfer the solution to a 10-ml standard flask. Add 0.4 ml of arsenazo-III solution (aqueous 0.5 mg ml^{-1}, freshly prepared and filtered) and dilute to 10.0 ml with 8 M hydrochloric acid. Mix well and measure the absorbance in a 2-cm absorption cell at 665 nm against a reagent blank. Determine the thorium content by reference to a calibration curve.

Discussion and results

The conditions adopted in the precipitation step favour precipitation of thorium oxalate rather than calcium oxalate. Precipitation at pH 4 [2] usually gave poor recoveries of thorium. At pH 1.8, thorium was quantitatively recovered, while precipitation of calcium oxalate was incomplete; 8—15 mg Ca l^{-1} were found in the supernatant liquid. Standing of precipitates for about 3 h usually proved adequate. The oxalate precipitation from homogeneous solution at pH 2 by adding methyl oxalate [4] was also tried. The method was effective but required a longer time.

The oxalate precipitation did not produce significant elimination of foreign ions which might be present in micro amounts, particularly zirconium, titanium and rare earth elements, which are coprecipitated to some extent and interfere in the arsenazo-III method. Calcium itself, however, when present in high concentrations, seriously interferes in the same determination [5].

An effective separation of thorium from these elements was accomplished

by extraction with Aliquat-336 solution (5% w/v). Maximum extraction coefficients for thorium ($E_a^o \simeq 50$) are obtained in the 2—5 M nitric acid concentration range [6]. Other tetravalent actinides (U, Pu, Np) are well extracted, but they are unlikely in natural waters. Uranium(IV) can be oxidized to uranium(VI) before the co-precipitation.

The purification of thorium was considerably enhanced by the stripping step. Hydrochloric acid exhibits a strong salting-out action towards many elements [8], which therefore remain in the organic phase while thorium is stripped into the aqueous phase ($E_a^o \simeq 2 \times 10^{-3}$). Uranium(VI), for instance, was partially extracted by Aliquat-336 from 4 M nitric acid solution ($E_a^o \simeq 0.5$), but was only very slightly stripped into 3 M hydrochloric acid.

The destruction of residual nitrate before the spectrophotometric determination was a delicate step. Provided that carbonization of traces of organic matter from the extractant was avoided, the total oxidation of organic matter was neither necessary nor useful.

Table 1 reports the results of a series of tests to check the recovery of thorium and the precision of the method.

Interferences. No interference was found from ions commonly present in natural waters in centigram amounts, such as magnesium, sodium, potassium, silicon, sulfate and phosphate. Calcium, which has an extraction coefficient below 10^{-2}, was present to a slight extent in the final solution, but this did not interfere in the spectrophotometric determination. Metal ions dissolved in natural waters at ppm levels were also considered. No interferences were found from aluminum, chromium(III), cobalt, copper, nickel, zinc, cadmium or vanadium(V) at the 1-ppm level, or from iron(III) and manganese(II) at the 5-ppm level.

Special care was taken over some elements which are usually present in water at ppb levels, like thorium, and interfere strongly with the arsenazo-III method. A series of tests was run with solutions containing thorium (0.95 μg l^{-1}) to which the other element was added at the 100 μg l^{-1} level. The

TABLE 1

Recovery of thorium from 1-l samples of deionized water containing known amounts of thorium

Th added (μg)	Th recovered (μg)	No. of detns.	Relative error (%)	Standard deviation (μg)
4.75	4.86	4	+ 2.3	0.048
2.85	2.88	6	+ 1.0	0.126
1.90	1.88	6	−1.1	0.082
0.95	0.95	6	0.0	0.120
0.48	0.51	6	+ 6.2	0.059
0.95[a]	0.97	6	+ 2.1	0.051

[a] 2-l samples, calcium carrier 0.2 g l^{-1}.

amounts of thorium recovered were essentially quantitative in the presence of zirconium(IV) (0.99), molybdenum (0.96), uranium(VI) (0.94), titanium(IV) and cerium(IV) (0.93) and lanthanum(III) (0.95); the values in parentheses are the thorium recoveries ($\mu g \, l^{-1}$, mean of 3 analyses) in each case.

The decontamination from zirconium is especially attractive because it is effective enough to allow the determination of thorium without adding oxalic acid to mask zirconium. This addition of oxalic acid has been recommended to eliminate the interference of zirconium [7], but was found to decrease the absorbance of the thorium—arsenazo-III complex unless the absorbance was measured immediately.

Application of the method. The method was applied to the analysis of Italian water samples. Table 2 reports the results for samples from the Monti Cimini Area (North Lazio). The results are in good agreement for spiked and unspiked samples.

TABLE 2

Results of determinations of thorium in spring water samples from the Monti Cimini Area (Italy) collected on June 8, 1978

Geographical origin	Content found ($\mu g \, l^{-1}$)[a]		
	A	B	C
Veiano	0.30	1.25	2.28
Lago di Vico (1st source)	0.34	1.35	2.31
Lago di Vico (2nd source)	0.46	1.40	2.44
Ronciglione	0.78	1.70	2.79
Vetralla	0.30	1.27	2.30

[a]A=unspiked. B, C = after addition of a spike of 1.0 μg (B) and 2.0 μg (C).

REFERENCES

1 A. E. Taylor and R. T. Dillen, Anal. Chem., 24 (1952) 1624.
2 American Society for Testing and Materials, ASTM D2333-68 (Reapproved 1974).
3 M. Cospito and L. Rigali, Anal. Chim. Acta, 57 (1971) 107.
4 M. K. Carron, D. L. Skinner and R. E. Stevens, Anal. Chem., 27 (1955) 1058.
5 S. Abbey, Anal. Chim. Acta, 30 (1964) 176.
6 P. Gerontopulos and L. Rigali, Radiochim. Acta, 3 (1964) 122.
7 S. B. Savvin, Talanta, 8 (1961) 673.
8 USAEC Report ORNL, 3785 (1965).

Short Communication

SPECTROPHOTOMETRIC DETERMINATION OF *N*-SUBSTITUTED
AND *N*-UNSUBSTITUTED NITROIMIDAZOLES

DAVID W. FINK* and ALLEN FOX

*Merck Sharp and Dohme Research Laboratories, P.O. Box 2000, Rahway, New Jersey
07065 (U.S.A.)*

The nitroimidazoles are of wide pharmaceutical interest; even the simplest of them, 2-nitroimidazole, is the antibacterial azomycin [1]. Among the numerous analytical methods to which these compounds are amenable is a sensitive colorimetric technique, first introduced in an application to a nitro-thiazole drug [2], in which alkaline hydrolysis yields nitrite ion; this is used to generate a diazonium cation which is coupled with an aromatic amine to produce a diazo chromophore. A later study of these reactions demonstrated that nitroimidazoles bearing *N*-substituents react more readily than the *N*-unsubstituted compounds [3]; analytical conditions have been described for the former compounds only. The present communication demonstrates that this method has more general applications and that it can be used under appropriate conditions for measuring *N*-unsubstituted as well as *N*-substituted nitroimidazoles.
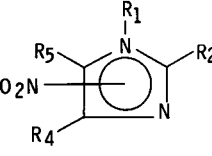
Experimental
Reagents and solutions. The drugs 2-isopropyl-1-methyl-5-nitroimidazole (Ipronidazole, I; see Table 1), (1-methyl-5-nitroimidazol-2-yl)methyl carbamate (Ronidazole, II) and 1,2-dimethyl-5-nitroimidazole (Dimetridazole, III), were obtained as purified analytical reference standards from Hoffmann-La Roche, Merck and Salsbury Laboratories, respectively. 2-Nitroimidazole (Azomycin, IV), 4(5)-nitroimidazole (V), and 2-methyl-4(5)-nitroimidazole 99%, (VI) (all from Aldrich Chemical Co.) were used without further purification.

All other chemicals were analytical-reagent grade unless otherwise specified. An aqueous solution (1.0 mg ml^{-1}) of *N*-(1-naphthyl)ethylenediamine dihydrochloride (Matheson Coleman and Bell) was prepared fresh daily. A solution (0.80 mg ml^{-1}) of *p*-aminobenzoic acid (Matheson Coleman and Bell) was prepared in 2.40 M HCl. Copper sulfate (Merck) was dissolved in the appropriate concentration of sodium hydroxide immediately prior to use to give a concentration of 0.25 mg ml^{-1}.

Procedure. Earlier general procedures [3—5] were followed. To an aqueous solution (10.00 ml) of the nitroimidazole, add 5.00 ml of the alkaline CuSO$_4$

TABLE 1

Spectrophotometric response of nitroimidazoles[a]

Compound	R_1	R_2	NO_2 Position	Relative sensitivity[b]
N-Substituted				
I	CH_3	$CH(CH_3)_2$	5	0.93
II	CH_3	$CH_2O\overset{O}{\overset{\|}{C}}NH_2$	5	0.83
III	CH_3	CH_3	5	1.00
N-Unsubstituted				
IV	H	NO_2	2	0.08
V	H	H	4(5)	0.78
VI	H	CH_3	4(5)	0.86

[a]$R = H$ for all undesignated substituents. [b]For reaction conditions, see text.

solution and hydrolyze the sample in a closed (vented) vessel at 100°C for 2—5 h. After cooling to room temperature, add 1.0 ml of a suitable hydrochloric acid or sodium hydroxide solution to adjust $[OH^-]$ to 0.4 M. From this point, the sample is treated as described previously [5]. Place the hydrolyzate in an ice bath for 10 min, add 5.00 ml of 0.08% (w/v) *p*-aminobenzoic acid solution, and allow the diazotization to take place. After 2 min, add 1.0 ml of aqueous 0.1% (w/v) *N*-(1-naphthyl) ethylenediamine; after the coupling reaction has run for 20 min, add 3 g of sodium chloride and extract the diazo chromophore into butanol. Measure the absorbance at 550 nm and establish the concentration from a previously prepared calibration line. In addition to a reagent blank, it is convenient to measure an unhydrolyzed portion of the sample as a check on unidentified sources of nitrite which may be present in the solution [5].

Results and discussion
    Source of nitrite. Cockerill et al. [6] found that the decomposition of *N*-substituted nitroimidazoles by hydroxide ion causes ring opening so that the generation of nitrite from the ring nitrogens is feasible. When the present technique was applied to imidazole and 1-methylimidazole in solutions covering the concentration range 0.3—0.7 M sodium hydroxide, neither of these imidazole yielded any measurable nitrite; this suggests that, independent of *N*-substitution, the nitro substituent is the active functional group in this technique.

Effect of N-substitution. Each of the six nitroimidazoles examined (three *N*-substituted and three *N*-unsubstituted) yielded nitrite as a hydrolysis product under appropriate conditions. Figure 1, which presents absorbance normalized relative to the maximum yield obtained from each compound, shows the effect of hydroxide concentration on the liberation of nitrite. For each substrate, absorbance increases over a range of 1—2 pOH units and remains constant with higher alkalinity. Thus *N*-substitution facilitates the nitrite-generating reaction: compared to the *N*-substituted substrates, the unsubstituted compounds require a hydroxide concentration more than ten times greater for the reaction to proceed.

In their study of the mechanism of the alkaline degradation of antiparasitic nitroimidazoles in aqueous solution, Cockerill et al. [6] concluded that the site of the nucleophilic attack by the hydroxide ion is a carbon of the heteroaromatic ring and that the identity of the *N*-substituent has a marked effect on the decomposition rate. In these molecules, reactivity towards nucleophiles is enhanced by the electron-withdrawing effect of the nitro group [7] and by
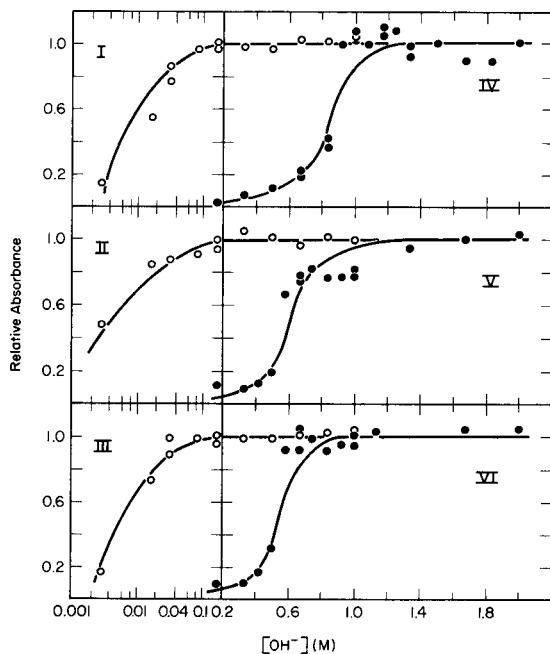
Fig. 1. Effect of hydroxide concentration on the alkaline hydrolysis of nitroimidazoles. *N*-substituted nitroimidazoles (○): (I) 2-isopropyl-1-methyl-5-nitroimidazole; (II) (1-methyl-5-nitroimidazol-2-yl)-methyl carbamate; (III) 1,2-dimethyl-5-nitroimidazole. *N*-unsubstituted nitroimidazoles (●): (IV) 2-nitroimidazole; (V) 4(5)-nitroimidazole; (VI) 2-methyl-4(5)-nitroimidazole. Each compound (12 μg) was hydrolyzed for 2 h at 100°C except IV, for which 120 μg was hydrolyzed for 5 h, with twice the copper catalyst concentration described in the text.

copper catalysis [8]: when II and V were hydrolyzed at 100°C for 1.5 h in 0.5 and in 0.67 M hydroxide, both in the presence and in the absence of copper, the nitrite yield was reduced two- to fourfold when the catalyst was excluded.

Compounds IV—VI would be even less prone to nucleophilic attack than I—III because they exist in the anionic conjugate base form in the reaction medium (i.e., pK_a = 7.15 and 9.20 for IV and V, respectively [9], and 9.67 for VI [10]). N-Substituted nitroimidazoles decompose in 0.5 M sodium hydroxide after 24 h at room temperature although N-unsubstituted derivatives are stable under these conditions [11, 12]; other workers have also noted that imino dissociation decreases ring reactivity to nucleophilic attack [8, 13]. A nitro group in a nitroimidazolate anion is more difficult to reduce electrochemically than in its neutral (or N-substituted) species [11, 12]; N-substitution inhibits electrophilic attack by diazonium cations [4, 14] by decreasing the availability of ring electrons for resonance [14] in accord with the enhanced reactivity of I—III relative to IV—VI in the present reaction.

Positional isomers. To estimate the relative sensitivity of this technique toward these nitroimidazoles, compounds I—VI were each hydrolyzed for 5 h at 100°C with twice the copper concentration prescribed above; a 1.33 M hydroxide medium was selected to optimize the reaction for each nitroimidazole (Fig. 1). The results (Table 1) show that, under these conditions, 2-nitroimidazole (IV) yields significantly less nitrite than its isomer, V. Because the products of this irreversible reaction are the same, these data reflect the relative rates of reaction of the nitroimidazoles. A stoichiometric yield of nitrite can be realized by this reaction [3] so that longer hydrolysis times could be used to provide increased sensitivity for compound IV.

A previous study of the effect of the 2-substituent has demonstrated that hydroxide attack does not occur between the nitrogen atoms [6], and other investigations have established that proximity to the unshared electron pair in its sp^2-hybridized orbital on nitrogen has an important influence on the chemical properties of the nitro group. In an investigation of the decomposition of III and of its 4-nitro isomer in 5% sodium hydroxide solution [7], no reaction was observed for the latter compound in which the nitro group is bonded in the position a- to N(3) and its unshared electron pair; in another study, an N-substituted compound containing a nitro group in the 5-position decomposed photolytically to nitrite in alkaline solution much more rapidly than a similar 2-nitroimidazole [4]. In addition, 4-nitroimidazoles generally degrade more slowly in 0.5 M NaOH than 5-nitroimidazoles, and nitro groups near the lone pair are more difficult to reduce electrochemically than those in their isomers [11, 12].

In the anionic form, the nitro group in IV is flanked by two electronegative hetero-atoms and their unshared electron pairs; this would further tend to inhibit nucleophilic attack at this position. In contrast, the 4-nitro group in V is adjacent to only one of the unshared pairs. The isomer effect would also contribute to the difference between the unsubstituted and N-substituted substrates in this study: the nitro groups are each bonded in the β-position to N(3) in I—III and in the α-position to an unshared pair in the anions of IV—VI.

Conclusions

Previous applications of this method to the determination of 60—100 ppm of nitroimidazoles in medicated feeds [5, 15, 16] and of lower concentrations in biological fluids [4] have illustrated the sensitivity of the approach. With stoichiometric nitrite yield, the calibration plots of all nitroimidazoles will be identical. Accuracy and precision have also been demonstrated previously: relative errors and relative standard deviations of less than 5% can be realized [5]. Simultaneous determinations in mixtures of *N*-substituted and *N*-unsubstituted nitroimidazoles by electrochemical and spectrophotometric techniques have been of interest [11, 12] and the present results show that photometric measurement can also be used for this application. For example, hydrolysis in 1.5 M sodium hydroxide will yield total nitroimidazole, and use of 0.1 M hydroxide will reflect only the *N*-substituted component. These results show that the photometric technique is more generally applicable than previously reported, and indicate its satisfactory application to *N*-unsubstituted hetero-aromatic compounds.

REFERENCES

1 P. N. Preston, Chem. Rev., 74 (1974) 279.
2 C. R. Szalkowski, J. Assoc. Off. Agric. Chem., 42 (1959) 245.
3 E. P. K. Lau, C. Yao, M. Lewis and B. Z. Senkowski, J. Pharm. Sci., 58 (1969) 55.
4 J. A. F. de Silva, N. Munno and N. Strojny, J. Pharm. Sci., 59 (1970) 201.
5 C. R. Szalkowski and J. Kanora, J. Assoc. Off. Anal. Chem., 52 (1969) 101.
6 A. F. Cockerill, R. C. Harden and D. N. B. Mallen, J. Chem. Soc. Perkin Trans. 2, (1972) 1428.
7 V. Sunjić, T. Fajdiga, M. Japelj and P. Rems, J. Heterocycl. Chem., 6 (1969) 53.
8 J. Miller, Aromatic Nucleophilic Substitution, Elsevier, Amsterdam, 1968, pp. 236—237, 258—260.
9 G. G. Gallo, C. R. Pasqualucci, P. Radaelli and G. C. Lancini, J. Org. Chem., 29 (1964) 862.
10 D. Dumanović, J. Ćirić, A. Muk and V. Nikolić, Talanta, 22 (1975) 819.
11 D. Dumanović, S. Perkučin and J. Volke, Talanta, 18 (1971) 675.
12 D. Dumanović and J. Ciríc, Talanta, 20 (1973) 525.
13 G. Doddi, P. Mencarelli and F. Stegel, J. Chem. Soc. Chem. Commun., (1975) 273.
14 J. E. Stambaugh and R. W. Manthei, J. Chromatogr., 31 (1967) 128.
15 D. W. Fink, J. V. Pivnichny, J.-S. K. Shim and J. W. Tolan, J. Assoc. Off. Anal. Chem., 61 (1978) 1523.
16 Analytical Methods Committee, Analyst, 103 (1978) 509.

Short Communication

FLOW INJECTION ANALYSIS WITH A FLUORIMETRIC DETECTOR FOR DETERMINATIONS OF GLYCINE AND ALBUMIN

JOY L BRAITHWAITE and J. N. MILLER*

Department of Chemistry, Loughborough University of Technology, Loughborough, Leicestershire LE11 3TU (Gt. Britain)

Flow injection analysis (f.i.a.) was introduced in 1975 by Růžička and Hansen [1] as a simple and convenient approach to continuous flow automatic analysis. The essential feature of the method is the rapid and reproducible injection of small volumes of sample into an unsegmented carrier stream. Successive discrete slugs or zones of sample are carried by the stream to an appropriate detector. A major advantage of this approach is its flexibility: by varying the experimental conditions, a wide range of sample zone concentration gradients can be achieved, and sample dispersions can be made suitable for different types of measurements [2]. Other advantages include the small sample requirements, high sampling rates, simplicity of the equipment, and economy in the use of reagents.

Many of the applications of f.i.a. so far described utilize spectrophotometric detection [3, 4], though other detectors have also been used [2]. Fluorimetric methods are well known to offer greater sensitivity than absorptiometric methods, often permitting analyses at ng ml^{-1} and pg ml^{-1} levels. These advantages are frequently utilized in a wide variety of clinical, toxicological and other analyses, and many fluorimetric assays have been successfully automated [5]. This communication describes the use of f.i.a. in conjunction with a fluorimetric detector. Analyses for fluorescent label molecules, as well as analyses based on the intrinsic fluorescence of the samples, demonstrate the validity of the approach.

Experimental

In all experiments the carrier stream was pumped through polyethylene autoanalyzer tubing (2.5 mm i.d: Altec Ltd., Alton, Hampshire) by a Quickfit Instruments peristaltic pump. Samples were injected manually from disposable syringes with standard hypodermic needles (thickness 0.5 mm, length 10 mm, B—D Plastipac) into a perspex injection block of the type described by Růžička and Hansen [1]. Fluorescence was detected with a Perkin-Elmer Model 1000 fluorimeter modified to hold a glass flow cell of 45-μl capacity: excitation wavelengths (selected using interference filters) and fluorescence

wavelengths (selected by using a continuous interference wedge) are given below. A Bryans Ltd., (Mitcham, Surrey) model 27000 recorder was used.

For the determination of glycine (see below), fresh o-phthalaldehyde (OPT; Sigma Chemical Company) reagent solutions were prepared daily; these contained 0.8 g of OPT, 10 ml of ethanol and 200 μl of 2-mercaptoethanol made up to 1 l in 0.1 M sodium borate buffer, pH 10.4. For the determination of albumin, the sodium salt of 8-anilino-1-naphthalene sulphonic acid (ANS; Sigma) was used at a concentration of 15 mg l^{-1} at pH 7. Pure human serum albumin and standard human serum were obtained from Hoechst (U.K.), London. Electroimmunoassay was done on "Cellogel" cellulose acetate membranes [6] with Dakopatts purified antibodies (Mercia Brocades Ltd., West Byfleet, Surrey). All other reagents were of analytical or equivalent grade.

Results and discussion

Quinine sulphate. For preliminary studies an intrinsically fluorescent solute was used: solutions of quinine sulphate in 0.05 M sulphuric acid (0.1—0.5 ml) were injected into a carrier stream of the same acid. The fluorimeter excitation and emission wavelengths were 337 and 450 nm, respectively. For a given sample volume, the maximum fluorescence recorded for a sample, i.e. peak height on the recorder trace, was proportional to the solute concentration up to a level of 2 μg ml^{-1}. As expected, increasing the line length (distance between the sample injection point and the detector), and increasing the carrier stream flow rate, reduced the maximum fluorescence because of increased diffusion of the sample zones. However, these effects were relatively small: doubling the line length from 195 to 390 nm produced mean fluorescen intensity reductions of 9.7%, and increasing the flow rate from 2.5 to 3.5 ml min^{-1} reduced the peak heights by 11.0% on average. The half-wash time [1] at a line length of 19.5 cm was found to be 1.55 s and sampling rates of up to 270 per hour were readily attainable. Even 1 ng ml^{-1} solutions of quinine sulphate could be detected, even though the excitation filter used did not exactly match the optimum excitation wavelength of this solute (350 nm). The precision of analysis (coefficient of variation, 2.0%) was also satisfactory (Fig. 1) though automatic injection methods would probably produce even better results.

m-Hydroxybenzoic acid. This compound fluoresces at pH 13, but not at neutral pH [7]. It was therefore used to study the many potential applications of f.i.a. in which a pH change would bring about the desired fluorescence signal: neutral aqueous solutions (0.1—0.4 ml) of m-hydroxybenzoic acid were injected into a KC1—NaOH solution of pH 13. Excitation and emission wavelengths on the fluorimeter were 337 nm and 410 nm, respectively. The fluorescence generated was studied at a number of different carrier stream flow rates and line lengths, as well as at various solute concentrations in the range 0.05—10.00 μg ml^{-1}. (A linear relationship between fluorescence intensity and concentration was found over this range.) The results obtained for a
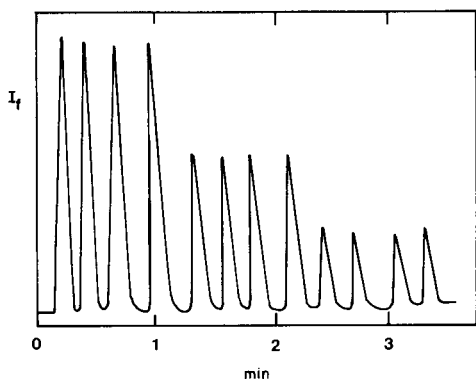
Fig. 1. Recorder chart trace showing the f.i.a. of quinine sulphate solutions. 200 μl samples were injected into a carrier stream moving at 2.5 ml min^{-1}. The line length was 39 cm.

TABLE 1

Fluorescence signals (peak heights) generated in flow injection analysis for m-hydroxybenzoic acid

Flow rate (ml min^{-1})	Line length (mm)		
	165	300	500
2	3.46	3.85	3.65
2.5	3.44	3.96	3.85
3.0	3.45	4.05	4.00

10 μg ml^{-1} solution (Table 1) are typical. In this application diffusion of the sample zone is necessary if the solute is to attain an alkaline pH. Increasing the flow rate thus enhances the fluorescence signal (though the effect is not apparent at short line lengths); increasing the line length first causes increased fluorescence but then the signal falls again, presumably because of excessive dispersion of an already-fluorescent zone.

Glycine. The determination of this amino acid is of some importance, because it is frequently added to dietetic soft drinks to mask the bitter after-taste of saccharin. Coppola and Hanna [8] determined glycine, using fluorescamine as a fluorescent label. In the present work, o-phthalaldehyde (OPT) was used as the label: this non-fluorescent compound is water-soluble and rapidly generates fluorescent derivatives of primary amines and amino acids [9]. Glycine-containing samples (100 μl) were injected into a carrier stream of the OPT reagent described above. Excitation and emission wavelengths were 337 nm and 455 nm, respectively. In this analysis the development of the optimum fluorescence signal depends on the time allowed for the fluorigenic reaction to take place. Thus, decreasing the flow rate from 3.5 to 2.0 ml min^{-1}, and increasing the line length from 30 cm to 134 cm both increased the fluorescence

signals. The response of the system was linear for pure glycine standards in
the range 0—8 μg ml^{-1}, but concentrations as low as 2 pg ml^{-1} were detectable.
The method was tested by analyzing two brands of low-calorie orange juice
and one brand of dietetic cola. The results were checked by the manual
method of Coppola and Hanna [8], the agreement between the two methods
being excellent (Table 2). The glycine contents of all the drinks were in the
expected range. With the flow-injection method, sampling rates of 180 per
hour could be readily achieved. The method could be extended to other assays
in which OPT is used as a fluorophor, e.g. determination of histamine [10].

Serum albumin. Analyses for serum albumin levels are frequently required
in clinical chemistry, dye-binding methods being most widely used. Certain
acidic dyes are non- or weakly-fluorescent in aqueous solution, but strongly
fluorescent when bound to albumin [11]. In this work albumin levels were
determined by injecting diluted solutions (50 μl) into a carrier stream of ANS.
The fluorescence of the resulting albumin—ANS complex was measured at
excitation and emission wavelengths of 370 nm and 470 nm, respectively.
Flow rates in the range 2.0—3.5 ml h^{-1} and line lengths of 15—50 cm all
produced very similar fluorescence signals from a given albumin solution.
Seven serum samples (A—G) were analyzed at a 1:100 dilution, and the
albumin concentrations determined by flow injection were compared with
those determined by a manual ANS-binding method (A—C) and by electro-
immunodiffusion (D—G). For samples A—C, pure albumin solutions were
used as standards, for the remainder a standard serum was used. The results
(Table 3) show good agreement between methods, except in cases F and
G. These two serum samples were several weeks old and exhibited considerable
turbidity. In view of the large spectral bandwidth of the fluorimetric detector
(ca. 35 nm) it seems very likely that increased light scattering caused the
spuriously high signal in these cases. When fresh samples are used, however,

TABLE 2

Determination of glycine (in g dl^{-1}) in dietetic drinks

Samples	Dilution for analysis	F.i.a. method	Coppola and Hanna [8] method
Low-calorie orange juice	1:150	0.33	0.34
Low-calorie orange juice	1:150	0.41	0.43
Dietetic cola	1:50	0.17	0.15

TABLE 3

Determination of serum albumin concentrations

Sample	A	B	C	D	E	F	G
F.i.a. result	4.1	3.9	4.0	3.7	3.9	4.9	5.2
Comparison result	4.0	3.9	3.8	4.1	3.5	3.7	3.7

the precision of the method (coefficient of variation 1.8%) and the high sampling rate (at least 180 samples per hour) make it very suitable for routine use.

The analyses described above demonstrate the additional sensitivity obtained when fluorimetry is used as the detection technique for f.i.a. They also demonstrate the simplicity and flexibility of the f.i.a. method; all the modifications necessary to change from one analysis to another could be completed in a few minutes. Somewhat surprisingly, use of a thermostated bath to maintain constant temperature in the system had no significant effect on any of the results reported here, though such a precaution would be necessary if the fluorescence intensity were highly temperature-dependent.

The simplicity, precision and sensitivity of the flow-injection method make it highly suitable for many other analyses, including automatic homogeneous fluoroimmunoassays and nephelometric, enzymatic and chemiluminescence assays. Such methods are currently under study in this laboratory.

REFERENCES

1 J. Růžička and E. H. Hansen, Anal. Chim. Acta, 78 (1975) 145.
2 J. Růžička and E. H. Hansen, Anal. Chim. Acta, 99 (1978) 37.
3 J. Růžička and J. W. B. Stewart, Anal. Chim. Acta, 79 (1975) 79.
4 J. Růžička, J. W. B. Stewart and E. A. Zagatto, Anal. Chim. Acta, 81 (1976) 387.
5 P. Froehlich, in E. L. Wehry (Ed.), Modern Fluorescence Spectroscopy, Vol. 2, Heyden, London, 1976.
6 V. J. Bowman, Ph.D. Dissertation, Loughborough University, 1975.
7 G. A. Thommes and E. Leininger, Anal. Chem., 30 (1958), 1361.
8 E. D. Coppola and J. G. Hanna, J. Assoc. Off. Anal. Chem., 57 (1974) 1265.
9 M. Roth, Anal. Chem., 43 (1971) 880.
10 R. Hakanson, A. L. Rönnberg and K. Sjölund, Anal. Biochem., 47 (1972) 356.
11 G. Weber and D. J. R. Lawrence, Biochem. J., 56 (1954) xxxi.

Short Communication

SPECTROPHOTOMETRIC DETERMINATION OF LANTHANIDES WITH CALMAGITE

HARRY G. BRITTAIN*

Department of Chemistry, Ferrum College, Ferrum, VA 24088 (U.S.A.)

(Received 18th September 1978)

Commonly used reagents for the spectrophotometric determination of lanthanides include arsenazo-I [1], arsenazo-III [2], 1-(2-pyridylazo)-2-naphthol [3], 4-(2-pyridylazo)-resorcinol [4], eriochrome black T [5], xylenol orange [6] and chlorophosphonazo dyes [7]. Recently, hydroxy naphthol blue alone [8] and in conjunction with EDTA [9] was used for the spectrophotometric microdetermination of alkaline earths and lanthanides, although its instability in basic solution and tendency to bind to many different metal ions weaken its effectiveness.

In the present work, the interaction of lanthanide elements with the calcium-binding dye 1-(1-hydroxy-4-methyl-2-phenylazo)-2-naphthol-4-sulfonic acid (calmagite) is investigated. Calmagite, originally prepared and developed as a stable substitute for eriochrome black T [10], is widely used as an indicator in the EDTA titration of alkaline earths and in the spectrophotometric determination of calcium [11] and magnesium [11—14]. Solutions of this azo dye are stable for months; the present procedure is not compromised by reagent instability, and excellent metal ion sensitivities may be obtained.

Experimental

Reagents and Stock Solutions. Calmagite (G. Frederick Smith Chemical Company) was used as received; recrystallization of the starting material did not affect the results. A 6.0×10^{-5} M stock solution of calmagite was prepared by dissolving 0.022 g of dye in 1 l of doubly distilled water. Ammonia buffer of final pH 10.0 was prepared by mixing 32.1 g of NH_4Cl and 22.4 g of KCl with 227 ml of ammonia liquor and then diluting to 1.0 l. Stock solutions of lanthanide ions, made by dissolving the 99.9% chlorides (Alfa Inorganics) in doubly distilled water, were standardized gravimetrically [15].

Procedure. Prepare the reagent solution by mixing 1.0 ml of the ammonia buffer with 2.0 ml of the calmagite stock solution in the spectrometer cuvette. Pipette small quantities of metal ion solution (0.01—0.10 ml) directly into the cuvette; add a corresponding quantity of water into a second

---

*Present address: Department of Chemistry, Seton Hall University, South Orange, N.J. 07079, U.S.A.

cuvette containing calmagite reagent. Place the solutions in the sample and reference beams of a double-beam spectrophotometer and scan from 450 to 800 nm. The change in absorbance may be read as an increase at 530 nm or a decrease at 610 nm.

Calibration curves. Linearity of calibration curves was maintained until the lanthanide ion concentration reached approximately 3×10^{-5} M; this upper limit did not depend appreciably on the identity of the metal used. Higher concentrations may be determined, but the calibration curves are not linear at metal concentrations much above 3×10^{-5} M. The lower limits of detection were dependent on the smallest change in absorbance detectable by the apparatus used (0.002 absorbance units).

Apparatus. A Beckman 25 UV/VIS recording spectrophotometer with expanded scale facilities was used. The pH of the mixed solutions was checked on a Fisher Accumet 144 pH meter with a standard glass combination electrode inserted directly into the spectrophotometer cuvette.

Results and discussion

At pH 10.0, 98.2% of the calmagite is present [10] as the monoprotonated blue form (λ_{max}, 610 nm): Ca^{2+} or Mg^{2+} forms a red complex (λ_{max}, 530 nm). The addition of lanthanides to a solution of calmagite at pH 10.0 gave identical spectral changes. The metal complexes absorb only slightly at 610 nm, so that the decrease in calmagite absorbance measured at this wavelength when lanthanide ions are added is directly related to their concentration.

Various lanthanide ions displayed approximately the same sensitivity toward calmagite (Table 1) but the dye is most sensitive toward elements at the beginning of the lanthanide series; maximum sensitivity was noted for Pr^{3+}. The lower limits of detection are ca. 20% better than those obtained with hydroxy naphthol blue [8]. The determination of lanthanide ions with calmagite is more sensitive than with the arsenazo-III method [2] and about as sensitive as the xylenol orange technique [6].

Job's method of continuous variation was used to determine the stoichiometry of the lanthanide—calmagite complexes; a 1:1 complex formed with all the metals studied; equilibrium constants were calculated from $K = [CAL-Ln]/[CAL][Ln]$, where $[CAL-Ln]$ is the concentration of metal-complexed dye, $[CAL]$ is the concentration of uncomplexed dye at equilibrium, and $[Ln]$ is the concentration of uncomplexed lanthanide ion. Formation constants, calculated from the spectrophotometric data, are shown in Table 1.

The determination of lanthanide ions with hydroxy naphthol blue [8] is complicated by its tendency to bind tightly to first-row transition metal ions [16] which cannot be masked with cyanide as the resulting complexes bind equally well with this dye [16]. Transition metal ions also interfere in the determination of lanthanide ions with calmagite, but small quantities (less than 20 mg l^{-1}) of Al, Co, Cu, Fe, and Ni can be masked with cyanide.

TABLE 1

Lower limits of detection and formation constants obtained in the reaction of calmagite with various lanthanide elements[a]

Metal	Limit ($\times 10^{-7}$ M)	Limit (ng ml^{-1})	log K
La^{3+}	2.59	36.0	4.244
Pr^{3+}	1.92	27.1	4.683
Nd^{3+}	2.06	29.7	4.538
Sm^{3+}	2.13	32.0	4.393
Eu^{3+}	2.20	33.4	4.329
Gd^{3+}	2.27	35.7	4.264
Tb^{3+}	3.59	57.1	4.200
Dy^{3+}	4.03	65.5	4.084
Ho^{3+}	4.34	71.6	4.036
Er^{3+}	4.63	77.4	3.988
Yb^{3+}	5.25	90.8	3.822

[a]Data obtained in solutions of 0.3 M total ionic strength.

Alkaline earths, Cd, Pb, Mn and Zn also interfere with the determination of lanthanides; these cannot be masked with cyanide and should be separated before attempting to determine the concentration of a lanthanide ion with calmagite.

REFERENCES

1 H. Onishi and C. V. Banks, Talanta, 10 (1963) 399; J. S. Fritz, M. J. Richard and W. J. Lane, Anal. Chem., 30 (1958) 1776; S. Shibata, F. Takeuchi and T. Matsumae, Anal. Chim. Acta, 21 (1959) 177.
2 S. B. Savvin, Talanta, 8 (1961) 673.
3 S. Shibata, Anal. Chim. Acta, 28 (1963) 388.
4 L. Sommer and H. Novotna, Talanta, 14 (1967) 457; K. N. Munshi and A. K. Dey, Microchem. J., 8 (1964) 152.
5 M. K. Akhmedli, P. B. Granovskaya and R. A. Neimatove, Zh. Anal. Khim., 28 (1973) 278.
6 V. Svoboda and V. Chromy, Talanta, 13 (1966) 237; W. J. de Wet and G. B. Behrens, Anal. Chem., 40 (1968) 200.
7 J. W. O'Laughlin and D. F. Jensen, Talanta, 17 (1970) 329; T. Taketatsu, M. Kaneko and N. Kono, Talanta, 21 (1974) 87.
8 H. G. Brittain, Anal. Chim. Acta, 96 (1978) 165.
9 H. G. Brittain, Anal. Chem., 49 (1977) 969.
10 F. Lindstrom and H. Diehl, Anal. Chem., 32 (1960) 1123.
11 F. Ingman and R. A. Ringbom, Microchem. J., 10 (1966) 545.
12 H. Flaschka and P. Sawyer, Talanta, 9 (1962) 249.
13 F. H. Harrison, Metalurgia, 70 (1964) 251.
14 A. Hofer and R. Heidinger, Z. Anal. Chem., 230 (1967) 95.
15 J. Clinch and E. A. Simpson, Analyst, 82 (1957) 258.
16 H. G. Brittain, Anal. Lett., 11 (1978) 355; 10 (1977) 1105.

Short Communication

RAPID DETERMINATION OF MERCURY IN AIR WITH GOLD-COATED QUARTZ WOOL AS COLLECTOR

ZENKO YOSHIDA* and KENJI MOTOJIMA

Japan Atomic Energy Research Institute, Tokai-mura Naka-gun, Ibaraki-ken (Japan)

(Received 22nd June 1978)

Mercury may be present in air as a vapor or adsorbed on dust, or as volatile mercury compounds. Because the contents of mercury may vary from a few ng m^{-3} in urban air [1] to 10 μg m^{-3} near chlor-alkali plants [2], the analytical system must be capable of handling wide ranges. Of the many possible methods, flameless atomic absorption spectrometry (a.a.s.) has been most frequently applied. For the collection of mercury from air, scrubbing solutions such as potassium permanganate [3, 4] and iodine monochloride [5] are suitable when the mercury content is high, but with less than 100 ng Hg m^{-3}, contamination from the chemicals used, variable blank levels, and instability of mercury in the solution may cause serious problems. Moreover, long times, e.g. 10 h, may be needed to collect enough mercury, and liquid collectors are vulnerable during transport. Solid collectors such as activated charcoal [6—8], silver [9—12], and gold [13—17] in various shapes have been used; with these, blanks can be reduced by preheating, and the mercury collected can be determined accurately by volatilization techniques which give sharp and reproducible a.a.s. peaks.

For rapid and efficient collection of mercury, the solid collector should have a large surface area. This communication describes the use of gold-coated quartz wool which has a very large surface area, and is suitable for the rapid collection of mercury from air even in urban areas.

Experimental

Equipment. A schematic diagram of the apparatus is shown in Fig. 1. The collector tube (8) is heated to 800°C in an electric furnace (5) controlled by a temperature programmer (6). The mercury analyzer (Hiranuma Sangyo Co. HG-1) is based on flameless a.a.s.

Preparation of collector tube. Several different methods were employed for the preparation of gold-coated quartz wool. In method (i), quartz wool (0.1 g; 1—5 μm diameter), was immersed in gold paste (Engelhard Industries) containing 0.5—5 mg of gold; after drying, the wool was ignited in a nitrogen stream at 650°C for 2 h. In method (ii), quartz wool (0.1 g) was treated with 5 ml of gold(III) chloride solution containing 5 mg of gold(III) at 120°C
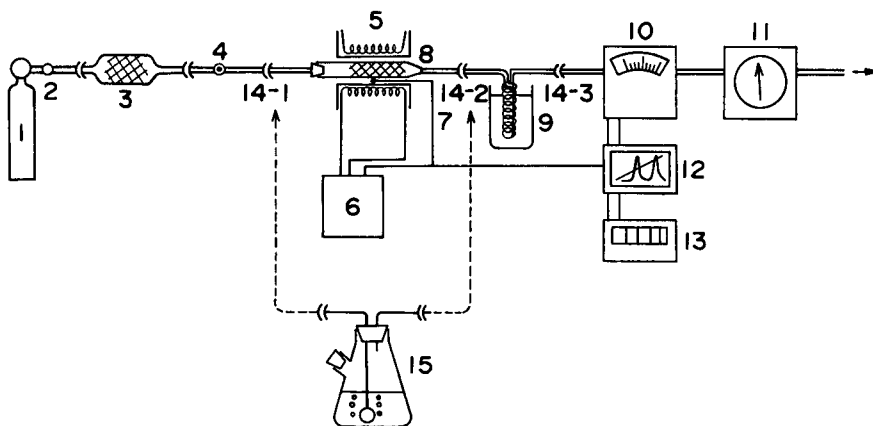
Fig. 1. Diagram of the general apparatus. (1) Nitrogen; (2) needle valve; (3) gold-coated quartz wool in a quartz tube (15 mm i.d., 100 mm long); (4) injection port; (5) heater; (6) temperature programmer; (7) thermocouple; (8) collector tube; (9) heat exchanger; (10) mercury analyzer; (11) gas flow meter; (12) two-pen recorder; (13) electronic integrator; (14-1, 2, 3) ball joints; (15) reduction—aeration vessel.

until all water evaporated, and then the wool was ignited at 650°C for 15 min in the nitrogen stream (500 ml min^{-1}). In method (iii), colloidal gold was used instead of gold(III) solution in method (ii). In other preparations, attempts were made to improve the adhesion on the quartz wool by reducing gold(III) with tin(II), and asbestos was used instead of quartz wool in method (ii). Method (i) was found to be best in terms of collection efficiency, rapid thermal release of mercury, and homogeneous distribution and tight adhesion of the gold particles. The gold-coated quartz wool was packed in a quartz tube as shown in Fig. 2; the additional layer of quartz wool (4') traps any gold removed from the gold-coated layer. The utility of the stainless steel gauze (3) is discussed below.

   Chemicals. For the standard mercury(II) stock solution (1 mg ml^{-1}), reagent-grade mercury(II) chloride dried for 24 h in a desiccator containing concentrated sulfuric acid was dissolved in water. Working solutions were prepared daily by suitable dilution.
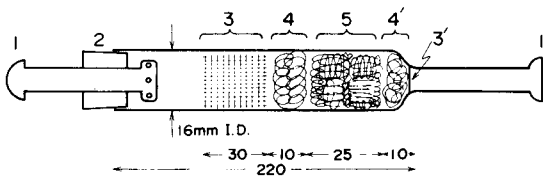
Fig. 2. Collector tube. (1) Ball joint; (2) silicone rubber cap; (3, 3') stainless steel gauze; (4, 4') quartz wool; (5) gold-coated quartz wool.

All chemicals were of reagent grade used without further purification. Deionized, twice-distilled water was used.

Recommended procedure. Draw the sample air through the collector at a rate of 15 l min^{-1} for 1—2 h with a diaphragm pump; a Millipore filter is attached in front of the collector. After collection, seal both ends of the tube by ball joint caps for storage as required. For analysis, attach the collector tube as shown in Fig. 1, and pass purified nitrogen through the system at 2.0 l min^{-1}. Heat the collector at 650°C, and determine the amount of mercury from peak-area measurements. Before entry to the mercury analyzer, the hot nitrogen containing mercury is cooled by passing through a spiral tube immersed in warm water (65°C) to prevent condensation of mercury.

Results and discussions

Calibration method. A normal reduction—aeration method of mercury(II) with tin(II) [18] with some modifications, was employed to prepare standard amounts of mercury (100—500 ng). For the preparation of less than 100 ng of mercury, the method of Long et al. [9] and Scaringelli et al. [6] was used, in which air is saturated by mercury vapor at a definite temperature. The peak-area measurements were directly proportional to the amounts of mercury produced by these methods down to 2 ng; the relative standard deviation was less than 3%, if the content of mercury vapor in the carrier gas (2.0 l min^{-1}) was less than 1000 ng l^{-1}.

Efficiency of mercury collection. The efficiency of collection of mercury by different forms of gold was investigated. The collector tube was placed in position (8, Fig. 1) and a known amount of mercury was introduced by the reduction—aeration method. After aeration for 5 min, the reduction—aeration vessel was detached and mercury on the collector was determined by heating. The collection efficiencies found are shown in Table 1. Analogous tests for less than 100 ng of mercury were made by using the saturated mercury vapor injection method (Table 1).

A gold-coated quartz wool collector should not be used more than ten times, especially when the amount of mercury is large. For example, the collection efficiency of gold (1 mg)-coated quartz wool decreased to 80% for 2500 ng of mercury after a dozen measurements. A study of the effect of the flow rate of carrier gas on the collection efficiency of gold (5 mg)-coated quartz wool showed that there was no significant difference at flow rates between 2.0 and 20 l min^{-1}.

Thermal evaporation of mercury from the collector. Collected mercury (500 ng) was evaporated by heating up to 650°C at a temperature increase of 20°C min^{-1} and fed into the mercury analyzer. With gold wire (6 g) a sharp absorption peak was obtained (Fig. 3, curve a) at about 250°C, which agrees well with that reported previously for gold plate [19]. Similar experiments with gold-coated quartz wool in tubes of various diameter (Fig. 3, curves b—d) showed that the peak temperature increases and peak broadening becomes serious as the tube diameter increases. With diameters greater than 15 mm,

TABLE 1

Collection efficiency of different types of gold

Collector	Hg taken (ng)	Efficiency (%)	Collector	Hg taken (ng)	Efficiency (%)
Gold wire[a]	100	105	Quartz wool	100	105
	200	98	(0.1 g) with	200	101
	500	96	1 mg Au	500	98
	2500	87		2500	97
	5000	72		5000	92
Gold wool[b]	250	67,71	Quartz wool	100	99
	500	68,69	with 5 mg Au	200	100
				500	101
				2500	100
				5000	100
				9	110
				18	108
				54	102

[a]Gold wire (6 g; 1 mm diameter, 5 mm long) in a quartz tube (8 mm i.d.).
[b]Gold wool (0.5 g) in a quartz tube (4 mm i.d.).
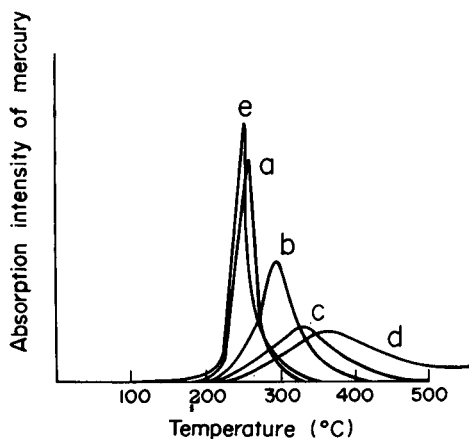
Fig. 3. Thermal evaporation of mercury from collector tubes of various diameter (T-Hg curves). (a) Gold wire (6 g) in a 4-mm i.d. glass tube; (b—e) gold (5 mg)-coated quartz wool (0.1 g) in quartz tubes of (b) 8 mm, (c) 12 mm (d) 15 mm i.d. without stainless steel gauze, and (e) 15 mm i.d. with stainless steel gauze.

mercury was not released completely even at 750°C. This effect is due to slow heating in the collector tube because of poor thermal conductivity of quartz wool and can be eliminated by placing a tightly rolled stainless steel gauze in

TABLE 2

Mercury content of air samples

Sampling location and conditions	Hg content (ng m⁻³)	Sampling location and conditions	Hg content (ng m⁻³)
Research Laboratory not using mercury or its compounds		In pine woods near the ocean far from mercury industries	
Feb. 21, 18°C (45%)[a]	104	Mar. 3, 6°C (40%)	21
Feb. 22, 22°C (48%)	90	Mar. 4, 2°C (65%)	30
		Mar. 9, 20°C (55%) (windy)	37
Polarographic Laboratory		May 6, 23°C (68%)	12
Jan. 25, 15°C (40%)	165	Aug. 30, 26—28°C (77%)	14, 11, 11
May 6, 22°C (53%)[b]	568, 409, 815		

[a]Percentages in parentheses indicate humidity.
[b]Laboratory unventilated for 7 days.

front of the gold-coated quartz wool; this gauze serves to preheat the carrier gas. With the gauze, the peak shape was greatly improved (Fig. 3, curve e) and the peak temperature was again about 250°C.

Stability of mercury collected on gold-coated quartz wool. After known amounts of mercury (22, 100 or 500 ng) had been trapped, and the collectors had been capped with ball joints, they were allowed to stand for various periods of time before determination of mercury by the normal procedure. Standing times up to 72 h made no difference to the results.

Analytical results. Table 2 shows typical mercury concentrations found in different environments.

The advantages of this collector are its high collection efficiency, and large capacity because of the large surface area of the quartz wool. Interferences from SO_2 or NO_2 were not observed even when their concentrations in air were 25 ppm and 14 ppm (the threshold values of both are 5 ppm). It is difficult, however, to determine mercury in compounds such as sulfide or halide; further investigations of this problem are in progress.

REFERENCES

1 R. S. Foote, Science, 17 (1972) 513.
2 G. A. Neville, Can. Chem. Educ., 3 (1967) 4.
3 Mercury Analysis Working Party of BITC, Anal. Chim. Acta, 72 (1974) 37.
4 D. Gardner, Anal. Chim. Acta, 82 (1976) 321.
5 A. L. Linch, R. F. Stalzer and D. T. Lefferts, Am. Ind. Hyg. Ass. J., 29 (1968) 79.
6 F. P. Scaringelli, J. C. Puzak, B. I. Bennett and R. L. Denny, Anal. Chem., 46 (1974) 278.
7 A. Sugimae, Bunseki Kagaku, 22 (1973) 1350.
8 H. Nakamachi, K. Okamoto and I. Kusumi, Bunseki Kagaku, 23 (1974) 10.

9 S. J. Long, D. R. Scott and R. J. Thompson, Anal. Chem., 45 (1973) 2227.

10 K. Imaeda, K. Ohsawa and M. Wako, Bunseki Kagaku, 26 (1977) 651.

11 P. E. Trujillo and E. E. Campbell, Anal. Chem., 47 (1975) 1629.

12 S. C. Wroblewski, T. M. Spittler and P. R. Harrison, J. Air Pollut. Control Assoc., 24 (1974) 778.

13 D. H. Anderson, J. H. Evans, J. J. Murphy and W. W. White, Anal. Chem., 43 (1971) 1511.

14 J. Olafsson, Anal. Chim. Acta, 68 (1974) 207.

15 C. M. Baldeck, G. W. Kalb and H. L. Crist, Anal. Chem., 46 (1974) 1500.

16 K. Kato, A. Ando and T. Kishimoto, Bunseki Kagaku, 21 (1972) 1057.

17 S. Nishi, Y. Horimoto and N. Nakano, Bunseki Kagaku, 23 (1974) 386.

18 Z. Yoshida and M. Takahashi, Mikrochim. Acta, (1977) 459.

19 Z. Yoshida and S. Kihara, J. Electroanal. Chem., 86 (1978) 167.

Short Communication

FACTORS AFFECTING PEAK SHAPE IN COLD-VAPOUR ATOMIC
ABSORPTION SPECTROMETRY FOR MERCURY

D. C. STUART

*Slowpoke Nuclear Reactor, Trace Analysis Research Centre, Dalhousie University,
Halifax, Nova Scotia B3H 4J1 (Canada)*

The most commonly employed technique for the sensitive determination
of mercury in various matrices is based on cold-vapour atomic absorption
spectrometry. The reduction/aeration method with a flow-through absorption
cell has been evaluated with radiotracers [1]. In this method, reproducible
results can be obtained only if the pattern of release of the mercury from the
test solution, and hence the mercury absorption peak shape, are always the
same. A number of publications on the method have noted that inconsisten-
cies in peak shape do occur. The BITC paper [2] noted that chloride, bromide
and iodide can diminish the absorbance of the mercury peaks, and also that
these ions cause a major decrease in the speed of the reduction of mercury by
tin(II) chloride. Fawkes et al. [3] noted some erratic results related to the
reduction of potassium permanganate. Jacobs et al. [4] found considerable
variability in blood analyses which could be reduced greatly by basing
estimates on the approximate peak area rather than the peak height. Stuart
[5] noted such effects in fish samples subjected to partial digestion tech-
niques.

It is well established by now that the presence of substances which form
strong associations with mercury will cause problems which must be guarded
against, but it is not always clear which reagents should be avoided,
especially if they are introduced as part of the sample matrix.

This paper describes two types of interference on the peak shape, categor-
izes several commonly employed reagents which cause these effects, and
discusses methods of detecting and correcting for some of the interferences.

Experimental

Equipment. The apparatus used consisted of an a.a.s. unit with a kit for
conversion to allow use of the reduction/aeration cold-vapour mercury analysis
technique [1]. A photon counting readout [6] was utilized to allow measure-
ment of rapid signal changes, for accurate timing, and for convenience and
simplicity in the numerical integration of peak areas.

Procedure. After the normal peak shape had been established with mercury standard solutions, as well as the expected effect of changes in carrier gas flow rate, variations induced by the addition to the test solution of several reagents were investigated. In particular, these included the addition of small amounts of hydroxylammonium chloride, 1-octanol, and cysteine hydrochloride. In addition, fish samples which had been labelled with radiotracer mercury and had been wet-ashed by partial digestion techniques [5] were analyzed.

Use of an amalgamation-collection step for the mercury was also investigated. Collection on and release from copper and silver wires and a column of powdered copper were studied by means of radiotracer [197] Hg.

Results and discussion

Absorbance peak shape and area. The shape of the absorbance peak is determined by the rate of release from the test solution, which is first order in mercury concentration under the conditions used (excess of reductant). Hence the shape is exponential (Fig.1, curve A), once conditions of steady flow and mixing of the solution by aeration have been established. The absorbance peak area is summed from the beginning of absorbance up to the point at which the absorbance has fallen to 20% of the peak height. This is convenient in practice and represents about nine tenths of the total area.
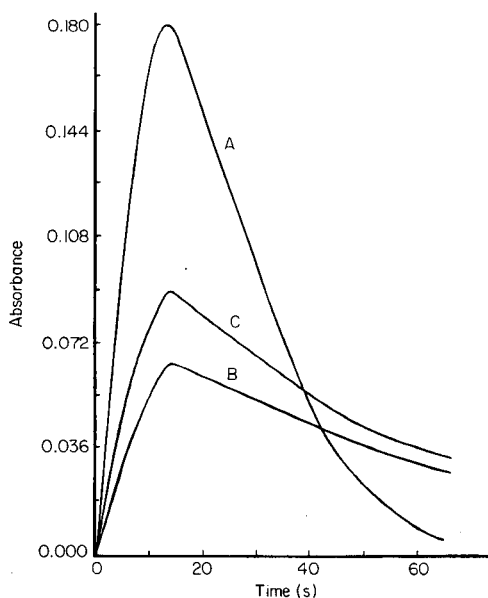
Fig. 1. Shape of mercury absorbance curves. (A) 7.6×10^{-6} g mercury standard; (B) as (A) with 0.2 ml of 1% cysteine hydrochloride added; (C) fish sample with the partial digestion method of wet ashing.

Hold-back effects on peak shape. Hydroxylammonium chloride (or sulfate) is used in many procedures [1—5, 7—14] often with imprecise instructions to add a sufficient amount to make the solution clear and colourless. Data given in Table 1 show that small excesses of this reagent result in severe reductions in both peak height and peak area and that any variability of the amount added between samples may indeed give erratic results.

This "hold-back" effect was also observed in the analysis of fish samples which had been labelled in vivo with radiotracer methylmercury chloride [5].

Since part of the mercury is held in solution in this type of interference and cannot be aerated, the analysis yields low results and the estimation of peak area will not correct the error. Furthermore, the hold-back effect will generally not be detected. Therefore, it is necessary to avoid reagents which cause this effect. Oxalic acid might be used in place of hydroxylammonium chloride [15], and the sulfate form of reagents such as tin(II) should be preferred to the chloride form [3, 5, 7, 11]. A complete sample digestion procedure is essential [5].

Effect on peak shape of reduction in rate of release of mercury from solution. Many chemicals have been found to slow the rate of release of mercury from the test solution. Table 2 and Fig. 1 (curve B) show data for cysteine hydrochloride, the results being typical for this type of interference; the peaks become more drawn out as the amount of cysteine is increased. The presence of reagents containing a sulfhydryl group has previously been observed to make analysis for mercury in urine more difficult [16]. Such compounds are components of biological matrices, and will give trouble, especially with partial digestion techniques [5]. It has been suggested that cysteine be added to dilute mercury solutions to help stabilize them [17]. Such solutions would not be suitable for the present type of analysis.

Similar interfering effects were observed for the addition of the anti-foaming agent, 1-octanol suggested by Fawkes et al [3] and with partially ashed fish samples [5] (Fig. 1, curve C). The absorbance peak is again drawn out in time, resulting in a greatly reduced peak height. In these cases, satisfactory correction for the interference may be obtained by using peak area rather than peak height, as is demonstrated in Table 2.

It is noteworthy that this effect occurs quite commonly, as pointed out above, and can therefore be a major source of error with this technique. Other ways around this interference are to use continual cycling of the aeration gas,

TABLE 1

Effect of addition of hydroxylammonium chloride on the mercury absorbance peak

Amount added (ml)[a]	0.00	0.01	0.02	0.05	0.10	0.20	0.30
Peak height (%)	100	97	98	85	60	34	13
Peak area (%)	100	98	98	83	65	36	11

[a] 5 g of hydroxylammonium chloride in 10 ml of water.

TABLE 2

Effect of cysteine hydrochloride (added as a 1% w/v solution) on the mercury absorbance peak

Amount added (ml)	Peak height (%)	Peak area (%)	Peak width (s)
0.00	100	100	41
0.02	100	100	40
0.05	94	95	42
0.10	67	104	62
0.20	36	96	104

as did Hatch and Ott [18], or to apply an amalgamation collection technique [19].

Amalgamation collection. The highest sensitivity is achieved if all the mercury is put through the absorption cell at once, giving a very sharp peak. A step may be added to the procedure to collect all the mercury in the test solution by amalgamation on an appropriate material. The mercury is subsequently released all at once by rapid heating of the collector. Variability in rate of release will, of course, still strongly affect results based on peak height.

Amalgamation collection from the sample solution was attempted onto copper and silver wire collectors with an applied voltage, as outlined by Brandenberger and Bader [20]. However, this method was unsuccessful when ashing solutions were used with radiotracer mercury added, as no conditions could be found such that the collection efficiency was complete, or even consistent.

Complete collection of added radiotracer could be readily obtained by passing the solution through a small column packed with powdered copper, in a simplified version of the method suggested by Dogan and Haerdi [21]. The tracer mercury was collected very near the top of a well-packed column. Unfortunately, the copper column was difficult to dry thoroughly, and the powder tended to disperse into the aeration system. Furthermore, on heating, the radiotracer mercury was never completely released, either from the copper powder or from the previously mentioned wires. Vaughn and McCarthy have noted a similar problem with platinum foil [22]. This type of amalgamation collection was therefore abandoned. Watling has recently described an amalgamation collection method with which good precision was obtained, though recoveries were typically low by 7—11% [23].

REFERENCES

1 D. C. Stuart, Anal. Chim. Acta, 101 (1978) 429.
2 Bureau International Technique du Chlore, Anal. Chim. Acta, 84 (1976) 231.
3 J. Fawkes, M. Folson and E. O. Oswald, Anal. Chim. Acta, 82 (1976) 55.
4 M. B. Jacobs, S. Yamaguchi, L. J. Goldwater and H. Gilbert, Am. Ind. Hyg. Assoc. J.,
  21 (1960) 239.
5 D. C. Stuart, Anal. Chim. Acta, 96 (1978) 83.
6 J. F. Skene, D. C. Stuart, K. Fritze and T. J. Kennett, Spectrochim.
  Acta, Part B, 29 (1974) 339.
7 J. F. Uthe, F. A. J. Armstrong and M. P. Stainton, J. Fish. Res. Bd. Can., 27 (1970)
  805.
8 G. Lindstedt, Analyst, 95 (1970) 264.
9 G. Lindstedt and I. Skare, Analyst, 96 (1971) 223.
10 I. Skare, Analyst, 97 (1972) 148.
11 M. R. Hendzel and D. M. Jamieson, Anal. Chem., 48 (1976) 926.
12 R. K. Munns and D. C. Holland, J. Assoc. Off. Anal. Chem., 54 (1971) 202.
13 D. Gardner, Anal. Chim. Acta, 82 (1976) 321; 93 (1977) 291.
14 A. A. El-Awady, R. B. Miller and M. J. Carter, Anal. Chem., 48 (1976) 110.
15 R. F. Milton and J. L. Hoskins, Analyst, 72 (1947) 6.
16 I. M. Weiner and O. H. Müller, Anal. Chem., 27 (1955) 149.
17 H. V. Weiss, W. H. Shipman and M. A. Guttman, Anal. Chim. Acta, 81 (1976) 211.
18 W. R. Hatch and W. L. Ott, Anal. Chem., 40 (1968) 2085.
19 S. J. Long, D. R. Scott and R. J. Thompson, Anal. Chem., 45 (1973) 2227.
20 H. Brandenberger and H. Bader, Helv. Chim. Acta, 50 (1967) 1409; At. Absorpt.
  Newsl., 6 (1967) 101; At. Absorpt. Newsl., 7 (1968) 53.
21 S. Dogan and W. Haerdi, Anal. Chim. Acta, 84 (1976) 89.
22 W. W. Vaughn and J. H. McCarthy, U.S. Geol. Surv. Prof. Paper 501-D D 123 (1964).
23 R. J. Watling, Anal. Chim. Acta, 99 (1978) 357.

Announcements

Chemical Society Analytical Division SAC 80

The internationally popular series of triennial SAC Conferences, organised by the Analytical Division of the Chemical Society (formerly the Society for Analytical Chemistry, "SAC") will be continued at the University of Lancaster from July 20th to 26th, 1980.

The scientific programme will follow the successful pattern of previous Conferences held at the Universities of Nottingham, Durham and Birmingham, and will include sessions of specialized interest, bringing the most recent developments on analytical chemistry to the attention of delegates. This will be coupled with a range of workshop sessions, an extensive trade exhibition, and specialist discussions, with, of course, the traditional programme of social events.

Plenary lectures will be given by internationally-known authorities, and contributed papers are invited for lecture and poster sessions devoted to all aspects of analytical chemistry. Abstracts (about 200 words) of papers and poster presentations should be submitted by November 30th, 1979.

Further information from: The Secretary, SAC 80, Analytical Division, Chemical Society, Burlington House, London WV1 0BN, England.

International Winter Conference 1980 on Developments in Atomic Plasma Spectrochemical Analyses

An international conference dealing with inductively coupled, microwave, and d.c. plasma discharges will be held on January 6—11, 1980, in San Juan, Puerto Rico. Papers describing original work on applications, fundamentals and instrumentation developments of atomic plasmas in spectrochemical analyses are invited. Authors of solicited papers for general and specialized symposia are requested to submit the title of their contribution and a 50—100 word preliminary abstract prior to June 1, 1979. Poster session papers will also be accepted.

Submit abstracts or direct questions for further information to: Winter Conference 1980, ICP Information Newsletter, Chemistry—GRC Tower I, University of Massachusetts, Amherst, Massachusetts 01003, U.S.A. Telephone: 413-545-2294.

Prize Biochemical Analysis 1980

The German Society for Clinical Chemistry awards the prize Biochemical Analysis every two years at the conference "Biochemische Analytik" in Munich.

The prize of DM 10,000 is donated by Boehringer Mannheim GmbH for outstanding and novel work in the field of biochemical analysis or bio-

chemical instrumentation or for significant contributions to the advancement of experimental biology especially relating to clinical biochemistry.

Competitors for the prize 1980 (conference 28th April—2nd May, 1980) should submit papers concerning one theme, either published or accepted for publication between October 1st 1977 and September 30th 1979, in triplicate before November 15th 1979 to: Prof. Dr. Dr. I. Trautschold, Secretary of the prize Biochemical Analysis, Medizinische Hochschule Hannover, Karl-Wiechert-Allee 9, 3000 Hannover 61, G.F.R.

EXPOCHEM '79

EXPOCHEM '79, an international exposition of analytical instruments for the industrial and biomedical fields, will be held at the Astrohall in Houston, Texas on October 22—25, 1979. This scientific exhibition is expected to be the largest and most all-embracing of its kind ever presented in the U.S.

In addition, a technical program will be arranged so that each morning session will begin with a plenary lecturer who will present the state-of-the-art and current developments in a particular area. The remaining speakers will include leading authorities from throughout the world. Among the topics to be included are: automation, data-handling, gas, liquid, gel permeation, and thin-layer chromatography, mass spectrometry, atomic absorption, air pollution, water analysis, biochemical analysis, pharmaceutical analysis, ion selective electrodes and surface characterization. Intensive short courses on the following subjects will also be available on the weekend prior to the exposition: Capillary Gas Chromatography; Gas Chromatography-Mass Spectrometry; Quantitative Thin-Layer Chromatography; High-Performance Liquid Chromatography; Maintaining and Troubleshooting Chromatographic Systems Laboratory; Analysis of Industrial Effluents for Toxic Pollutants; Thermal Methods of Analysis; Practical Electroanalytical Chemistry; Simplex Optimization in Research and Development; Analog and Digital Electronics for Laboratory Scientists.

Inquiries regarding exhibition space, presentation of papers or short courses should be directed to: Dr. A. Zlatkis, Chemistry Department, University of Houston, Houston, Texas 77004 or phone: (713) 749-2623.

Computer-based Analytical Chemistry — 20th FECHEM Conference

This FECHEM Conference will be held during 24—28th September, 1979, at Portorož, Yugoslavia. The main topics will be: fundamentals of computerization of analytical laboratories; principles and problems of computer-based instruments and networks; analytical information systems (storage, retrieval and computer-based interpretation of instrumental data); special topics in computer-based analytical procedures.

Further information from: Dr. Jure Zupan, Boris Kidrič Institute of Chemistry, P.O. Box 380, 61001 Ljubljana, Yugoslavia.

AUTHOR INDEX

Short Communications

CONTENTS